Université Paris Cité

Ecole doctorale Bio Sorbonne Paris Cité (BioSPC) 562

Réponses Moléculaires et Cellulaires aux Xénobiotiques (RMCX)
Unité de Biologie Fonctionnelle et Adaptative (CNRS UMR 8251)

Molecular effects of the anticancer drug cisplatin on the protein tyrosine phosphatase 1B (PTP1B) and structural impact of PTP1B cancer-associated mutations

Par Rongxing LIU

Thèse de doctorat de PHYSIOLOGIE ET PHYSIOPATHOLOGIE

Dirigée par Fernando RODRIGUES-LIMA

Présentée et soutenue publiquement à Paris le 19/07/2022

Devant le jury compose de:

Professeur Bertrand FRIGUET, Sorbonne Université	Rapporteur
Professeur Dominique LEDOUX, Université Sorbonne Paris Nord	Rapporteur
Professeur Valérie SERRE, Université Paris Cité	Examinatrice
Professeur Christine CHOMIENNE-THOMAS, Université Paris Cité	Examinatrice
Docteur Fabien GUIDEZ, Université de Bourgogne	Examinateur
Professeur Fernando RODRIGUES-LIMA, Université Paris Cité	Directeur de thèse

Titre: Effets moléculaires de l'anticancéreux cisplatine sur la protéine tyrosine phosphatase 1B (PTP1B) et étude de mutants oncogéniques

Résumé: La protéine tyrosine phosphatase 1B (PTP1B) est un régulateur majeur de différentes cascades de signalisation telles que la voie de l'Epidermal Growth Factor Receptor (EGFR). L'importance biologique de PTP1B est notamment soulignée par des études de souris knock-out et l'identification de mutations/délétions récurrentes de PTP1B liées à des altérations métaboliques et oncogéniques. L'activité de PTP1B dépend d'un résidu cystéine catalytique conservé qui rend l'enzyme sensible à l'oxydoréduction. L'oxydation et l'inhibition réversibles de PTP1B par les espèces réactives de l'oxygène sont considérées comme un mécanisme physiologique critique dans l'activation et le contrôle redox de la signalisation comme observé pour la voie de EGFR. Le cisplatine est l'un des médicaments anticancéreux les plus efficaces et les plus utilisés en clinique. Il est couramment admis que le mécanisme d'action du cisplatine repose principalement sur la formation d'adduits stables de l'ADN sur la guanine, qui entraînent des dommages à l'ADN et finalement la mort cellulaire. Cependant, plusieurs études indiquent que le cisplatine pourrait également avoir un impact sur d'autres processus biologiques tels que la réparation de l'ADN et la signalisation cellulaire, notamment la voie de EGFR. De plus, le cisplatine pourrait exercer, au moins en partie, ces effets biologiques en se liant à des peptides ou à des protéines conduisant à des altérations structurales et/ou fonctionnelles. Dans cette thèse, nous montrons que PTP1B est une cible du cisplatine. Les études mécanistiques indiquent que le cisplatine inhibe PTP1B de manière irréversible en se liant de manière covalente au résidu cystéine catalytique de l'enzyme. En accord avec ces données, les expériences menées sur des cellules et des souris exposées au cisplatine ont montré une inhibition de la PTP1B endogène et une augmentation concomitante de la phosphorylation sur tyrosine de l'EGFR. Ces résultats sont cohérents avec des études précédentes montrant une activation de la voie de l'EGFR par le cisplatine et avec des travaux récents suggérant que l'inhibition de PTP1B par des complexes de platine pourrait représenter un nouveau mécanisme anticancéreux. Notre travail permet de

mieux comprendre le réseau complexe de voies subissant une modulation lors de l'administration de cisplatine, réseau allant au-delà de l'effet génotoxique bien établi du cisplatine. Parallèlement à ces travaux, nous avons étudié plus avant l'impact fonctionnel et structural de trois mutations faux-sens identifiées chez des patients atteints de lymphome à cellules B (V184D, R221G et G259V). Nous avons constaté que ces mutations conduisent à des variantes de PTP1B altérées et dépourvues d'activité tyrosine phosphatase. Comme attendu, la surexpression de ces mutants conduit à une phosphorylation accrue de l'EGFR, un substrat physiologique de PTP1B. Bien que la cristallisation de ces mutants n'ait pas été possible, des approches biochimiques et de modélisation moléculaire suggèrent que ces mutations ont un impact sur la structure et/ou la dynamique de boucles importantes de l'enzyme et que certaines mutations (V184D et G259V) peuvent conduire à l'instabilité et à l'agrégation de l'enzyme.

Mots clefs: PTP1B, cisplatine, signalisation EGFR, activité enzymatique, mutation oncogénique, lymphome à cellules B

Title: Molecular effects of the anticancer drug cisplatin on protein tyrosine phosphatase 1B (PTP1B) and structural impact of PTP1B cancer-associated mutations

Abstract: Protein tyrosine phosphatase 1B (PTP1B) is a critical regulator of different signaling cascades such as the EGFR pathway. The biological importance of PTP1B is further evidenced by knockout mice studies and the identification of recurrent mutations/deletions in PTP1B linked to metabolic and oncogenic alterations. PTP1B activity depends upon a conserved catalytic cysteine residue that renders the enzyme redox sensitive. Reversible oxidation and inhibition of PTP1B by reactive oxygen species (ROS) is considered as a critical physiological mechanism in the activation and the redox control of tyrosine kinase signaling as observed in the EGFR pathway. Cisplatin is one of the most successful and widely used anticancer drug. The mechanism of action of cisplatin is thought to rely mainly on the formation of stable DNA adducts on guanine that lead to DNA damaging events and ultimately to cell death. However, several studies indicate that cisplatin could also impact other biological processes such as DNA repair and cell signaling, most notably the EGFR pathway. In addition, cisplatin could exert, at least in part, these biological effects through binding to peptide or proteins with subsequent structural and/or functional alterations. In this thesis, we report that PTP1B is a target of cisplatin. Mechanistic studies show that cisplatin inhibits PTP1B in an irreversible manner and binds covalently to the catalytic cysteine residue of the enzyme. Accordingly, experiments conducted in cells and mice exposed to cisplatin show inhibition of endogenous PTP1B and concomitant increase in tyrosine phosphorylation of EGFR. These findings are consistent with previous studies showing tyrosine phosphorylation-dependent activation of the EGFR pathway by cisplatin and with recent studies suggesting that PTP1B inhibition by platinum complexes could represent a novel anticancer mechanism. Our work provides a better understanding of the intricate network of pathways undergoing modulation upon cisplatin administration and that goes beyond the well-established genotoxic effect of cisplatin. In parallel to this work, we further studied the functional and structural impact of three missense mutations identified in B

cell lymphoma patients (V184D, R221G and G259V). We found that these mutations lead to impaired PTP1B variants that are devoid of tyrosine phosphatase activity. In line with this, expression of these mutants lead to increased tyrosine phosphorylation of EGFR, a well-known prototypic substrate of PTP1B. While crystallization of these mutants was not possible, biochemical approaches and molecular modelling suggest nonetheless that these mutations impact the structure and/or dynamics of important loops of the enzymes and can lead to protein instability and aggregation.

Keywords: PTP1B, cisplatin, EGFR signaling, enzyme activity, oncogenic mutation, B cell lymphoma

ACKNOWLEDGEMENTS

How time flies! When I started writing this part, I suddenly realized that my PhD career in Paris is going to end. I still remember the day when I arrived in Paris. It was in the morning of the 12/09/2018. I was so excited because it was my first time traveling abroad. Everything was new and exotic to me. I took three big luggage and it was hard for me to get to the RER B platform. Luckily, a gentleman came and helped me to take my luggage to the platform. I was so thankful for his kindness. With the great longing, my new study in Paris started.

After near four years practice in the laboratory of "Molecular and Cellular Responses to Xenobiotics (RMCX)" and in the unit of "Functional and Adaptive Biology (BFA)", I learned a lot about structural biology and epigenetics, which could be great helpful to my research career. Thanks for the providing of the platform.

First, I would like to thank Professor Jean Marie Dupret, the head of our group, who welcomed me warmly. Really he is an experienced Professor with good-smelling perfume. Also, I would like to thank my supervisor, Professor Fernando Rodrigues-Lima, who takes care of me a lot no matter in my experiments or in my live. He is easy-going and talkative, equipped with rich knowledge. He set a good example that I want to be in the future. Without his encouragement and guidance, my study here would not go so smoothly. Besides, I want to thank Professor Christine Chomienne, for her referring me to Professor Fernando Rodrigues-Lima.

Life in Paris is passionate because I have many lovely colleagues. I would like to thank my neighbor, named Roseline. She treats me very kindly, though sometimes she talked to her friends too often on the phone. Another neighbor, named Jean-luc, likes talking to himself. Also, he likes music, motorcycle and shopping. And thanks for his kind help when I moved my office. I would like to thank Qing, who tought me how to do the *p*NPP assay and gave me a lot of suggestions when I arrived here. Also, I want to thank Monsieur Zhang, he is always motivated and passionate to scientific research. Now he gets the opportunity to study in USA, hoping he could publish a "Nature" paper. I would like to thank Monsieur Berthelet. He is smart, like a genius. When I am

in trouble or in need some suggestions, he always tries his best to help me, such a warm guy. Madame Christina is the real colleague of mine because we enrolled in the same year. She is nice and elegant every day with a lot laughing, even I could hear her laughing in my office. But that's good. Also I have to thank her a lot because she really helped me a lot. I would like to thank Madame Linh, she is an expert of RP-UFLC as well as RT-qPCR. She is pretty gentle. Thanks for her suggestions when I choose the mutuelle. Madame Justine, the dance queen, is nice and thanks for her help in RP-UFLC. I would like to thank Madame Louise for her kind help when I have trouble with the doctor. I would like to thank Monsieur Florent, for his help in designing primers. I would like to thank Madame Fredrique, for her kind providing of antibodies as well as explanation of the process and attentions of CRISPR-Cas9 assay.

I would like to thank Monsieur Emile for his teaching of transfection. Besides, I would like to thank all the other members of the RMCX team: Madame Francoise (gentle and responsible), Olja (gentle and friendly), enviable couple of Pascal and Valentina (talkative, gentle and friendly)…

I would like to thank Monsieur Ahmed, Monsieur Patrick and Monsieur Cedric in Pasteur Institute for their help in protein crystallization.

I would like to thank French CAF, for their kind providing of housing assistance.

I would like to thank China Scholarship Council (CSC), for its supporting to study here.

I would like to thank my friends (Xingcheng, Wengen, Youwei, Quanquan, Jingjing, Bingbing, Mingyang, Yunliang, Xiaoyu, Weige……). Thanks all of you. Without you, I would be alone.

I would like to thank my parents, for their support and encouragement. In the Covid year, they worried me a lot. They always remind me to take care of myself, giving selfless love. Here I want to say, I love you. Now it's my turn to care of you.

The last one that I want to thank is myself. It's hard for a foreigner to study alone abroad, but I have to. I have to get used to the French culture, French language…… But everything is fine when it starts. With the spread of epidemic Covid-19, my life seems getting tough, especially the lockdown period (03/2020-05/2020). I lived alone

and I did not see my friends for near 3 months. I think this is the worst time in my life. But I “survived”. With good dreams of living and studying here, I start continuing my research. Now everything is in rejuvenation. Lastly and importantly, I wish myself a good job and a good future, in order to live up to these years of hard work.

Rongxing LIU

20/05/2022

TABLE OF CONTENTS

BACKGROUND AND MAIN RESULTS 11
LIST OF PUBLICATIONS 18
ABBREVIATIONS 19
LIST OF FIGURES 22
LIST OF TABLES 24
1 INTRODUCTION 25
1.1 Background 25
1.2 Cisplatin 25
1.2.1 History of cisplatin 25
1.2.2 Action of cisplatin 27
1.2.2.1 Formation of cisplatin-DNA adduct 27
1.2.2.2 Cisplatin induced oxidative stress 28
1.2.2.3 Other molecular mechanisms of cisplatin 29
1.2.3 Clinical use of cisplatin 29
1.2.4 Side effects of cisplatin 30
1.2.4.1 Nephrotoxicity 30
1.2.4.2 Ototoxicity 30
1.2.4.3 Cisplatin-induced leukemia 31
1.2.4.4 Drug resistance 32
1.2.5 Conclusion and prospect of cisplatin 33
1.3 Protein phosphorylation 34
1.3.1 Phosphorylation sites 35
1.3.2 Phosphorylation regulation 35
1.3.2.1 Protein kinases 36
1.3.2.2 Protein phosphatases 37
1.4 Protein tyrosine phosphatases (PTPs) 38
1.4.1 Receptor protein tyrosine phosphatases (RPTPs) 40
1.4.2 Non receptor protein tyrosine phosphatases (NRPTPs) 40
1.5 Protein tyrosine phosphatase 1B (PTP1B) 44
1.5.1 PTP1B expression in different tissues 44

1.5.2 PTP1B involved gene ontology (GO) 45
1.5.3 PTP1B in cell signaling pathway 47
1.5.3.1 PTP1B in insulin pathway 47
1.5.3.2 PTP1B in leptin pathway 48
1.5.3.3 PTP1B in integrin pathway 48
1.5.3.4 PTP1B in ErbB pathway 49
1.5.4 PTP1B in diseases 50
1.5.4.1 PTP1B in T2DM and obesity 50
1.5.4.2 PTP1B in cancers 51
1.5.4.3 PTP1B in neurodegenerative disease 54
1.5.4.4 PTP1B in hematopoietic malignancies 56
1.5.5 PTP1B structures 59
1.5.5.1 PTP1B regulatory domains 60
1.5.5.1.1 N-terminal catalytic domain of PTP1B 60
1.5.5.1.2 Proline rich domain of PTP1B 62
1.5.5.1.3 C-terminal ER targeting domain of PTP1B 63
1.5.5.2 PTP1B functional loops 63
1.5.5.2.1 pTyr loop 64
1.5.5.2.2 E loop 65
1.5.5.2.3 WPD loop 66
1.5.5.2.4 S loop 68
1.5.5.2.5 P loop 68
1.5.5.2.6 Q loop 69
1.5.6 Difference between PTP1B and TCPTP 70
1.5.7 PTP1B catalytic mechanism 72
1.5.8 PTP1B mutations 73
1.5.8.1 PTP1B mutations in pan-cancer 74
1.5.8.2 PTP1B mutations in hematopoietic malignancies 75
1.5.9 PTP1B inhibitors 76
1.5.9.1 Allosteric PTP1B inhibitors 77
1.5.9.2 Multiple aryl phosphorylation sites inhibitors of PTP1B 78
1.5.9.3 PTP1B mRNA inhibitors 80

2 OBJECTIVES 82
3 RESULTS 83
3.1 Result 1 83
3.2 Result 2 116
3.3 Result 3 143
4 CONCLUSION 175
5. REFERENCES 178
6. PUBLICATIONS 197

BACKGROUND AND MAIN RESULTS
CONTEXTE ET RÉSULTATS PRINCIPAUX

Mes travaux de recherche de doctorat sont principalement centrés sur l'enzyme humaine PTP1B (Protein Tyrosine Phosphatase 1B). Je me suis intéressé d'une part aux effets du cisplatine, un anticancéreux majeur, sur l'activité enzymatique de PTP1B et, d'autre part, sur l'impact moléculaire et fonctionnel de mutations de PTP1B identifiées dans des lymphome B humains.

La phosphorylation des résidus tyrosine par les protéines tyrosine kinases (PTK) est un mécanisme ubiquitaire de signalisation cellulaire qui joue un rôle important dans de nombreux processus biologiques tels que la prolifération, la différenciation, la migration et l'apoptose [1]. La phosphorylation des tyrosines est régulée négativement par l'action opposée des protéines tyrosine phosphatases (PTPs) qui déphosphorylent les résidus de phosphotyrosine (pTyr). Les PTPs sont donc des acteurs clés de la signalisation et des réponses cellulaires [2, 3]. Il n'est donc pas surprenant que des activités aberrantes des PTPs soient impliquées dans différentes maladies telles que le diabète, les troubles immunitaires et le cancer [4-6]. PTP1B est une tyrosine phosphatase intracellulaire prototypique non réceptrice, ubiquitaire et abondante, reconnue comme un régulateur négatif majeur de nombreuses cascades de signalisation d'intérêt métabolique et/ou oncogène, telles que les voies de l'insuline ou de l'epidermal growth factor (EGF) [6, 7]. Le rôle biologique critique de PTP1B est mis en évidence par l'identification de mutations/délétions récurrentes de PTP1B dans certains cancers et par des modèles de souris knock-out présentant des altérations métaboliques et oncogènes [8-11]. L'activité enzymatique de PTP1B dépend d'un résidu cystéine catalytique conservé qui rend l'enzyme sensible à l'oxydoréduction [12, 13]. L'oxydation et l'inhibition réversibles du PTP1B par les espèces réactives de l'oxygène (ROS) sont considérées comme un mécanisme physiologique critique dans l'activation et le contrôle redox de la signalisation de la tyrosine kinase, comme observé dans la voie de l'EGFR [14]. En outre, il a été démontré que la modification chimique de la cystéine du site actif de PTP1B par des électrophiles

environnementaux (tels que les quinones ou les métaux lourds) inactive l'enzyme et entraîne une phosphorylation tyrosine et une signalisation aberrantes de l'EGFR [15, 16].

Le cisplatine, également appelé cis-dichlorodiamine platine (II) (CDDP), a été synthétisé pour la première fois en 1845. Barnett Rosenberg a alors découvert que les produits de l'électrolyse des électrodes de platine pouvaient inhiber la division cellulaire [17]. Il a donc orienté ses recherches vers les tumeurs et a prouvé que le cisplatine avait de puissants effets anticancéreux in vivo et in vitro [18]. Le cisplatine a été autorisé par la Food and Drug Administration (FDA) en 1978. La découverte du cisplatine a stimulé le développement des complexes métalliques dans le domaine médical et a eu une importance révolutionnaire pour le traitement du cancer au cours des décennies suivantes. Sur la base de sa structure simple et de son fort effet anticancéreux, une série de dérivés avec des indications correspondantes ont été proposés, notamment le carboplatine (2e génération) ou l'oxaliplatine (3e génération). Il est démontré que le cisplatine induit la mort cellulaire. Plus précisément, la mort des cellules cancéreuses induite par le cisplatine est médiée par une série d'effets biochimiques et de mécanismes moléculaires qui incluent la formation d'adduits à l'ADN, l'induction d'espèces réactives de l'oxygène (ROS) ainsi que d'autres voies [19].

Le cisplatine peut avoir un impact sur chacune des phases du cycle cellulaire (G1, S, G2, M) et sur l'état de repos (G0) de manière à inhiber la croissance tumorale en trois étapes. La première étape est l'absorption par les cellules. Des données indiquent que la façon dont le cisplatine peut pénétrer dans les cellules est une combinaison de diffusion passive et de transport actif. La deuxième étape est l'activation hydrolytique. Brièvement, un chlore est remplacé lentement par une molécule d'eau pour former $[PtCl(H_2O)(NH_3)_2]^+$, où la molécule d'eau est facilement relarguée de sorte que le platine se coordonne avec une base de l'ADN. Ensuite, l'autre chlore est également relargué pour former $[Pt(H_2O)_2(NH_3)_2]^+$. La troisième étape est l'interaction avec l'ADN. Le platine se lie aux doubles brins (liaison transversale inter-brins) ou à deux points d'un simple brin (intrastrand) d'ADN afin de stopper la réplication de l'ADN

des cellules cancéreuses et conduisant ainsi à l'apoptose des cellules [20].

Les cellules cancéreuses présentent un métabolisme élevé et des concentrations élevées d'espèces réactives de l'oxygène (ROS) qui contribuent à la prolifération cellulaire. Les ROS peuvent affecter des protéines qui sont impliquées dans les voies de signalisation cellulaire comme les kinases ERK1/2, des récepteurs tyrosine kinases, le facteur nucléaire NF-κB ou la phosphatidylinositol-3 kinase (PI3K) [19, 21]. Il a été démontré que le cisplatine génère des ROS directement ou indirectement par l'intermédiaire des mitochondries [22]. Il est connu que l'équilibre redox des cellules est maintenu par des molécules contenant des groupements sulfhydryles (cystéine, glutathion réduit) qui peuvent réagir avec les ROS. Si le niveau de ROS est excessif, les cellules peuvent être endommagées et mourront sous l'effet du stress oxydatif. Après avoir pénétré dans les cellules, le cisplatine réagit avec le système enzymatique antioxydant et contribue à la libération de ROS, conduisant à la peroxydation lipidique, augmentant la production de malondialdéhyde (MDA), réduisant le niveau de glutathion réduit, endommageant l'ADN, activant des facteurs pro-inflammatoires et pro-apoptotiques et déclenchant finalement l'apoptose [23]. En parallèle, le stress oxydatif entraine la libération par les mitochondries d'une grande quantité de cytochrome C, ainsi que le relarguage de calcium du réticulum endoplasmique (RE), ce qui pourrait favoriser la libération de cytochrome C, l'amplification de la réaction en cascade et finalement l'apoptose des cellules [24].

En plus des mécanismes décrits ci-dessus, une étude récente a montré que l'efflux de calcium du RE pouvait réguler l'apoptose induite par le cisplatine dans les cellules cancéreuses du col de l'utérus humain par l'activation de la caspase 3 [25]. Des travaux ont également montré que les lésions de l'ADN induites par le cisplatine entraînent l'activation de la famille des protéines kinases activées par des agents mitogènes (MAPK), notamment MAPK/ERK [26], c-jun N-terminal kinase (JNK)/protéine activatrice-1 (AP-1) [27], p38 MAPK [26] et p53 [28]. Le cisplatine active également la voie de signalisation sérine-thréonine protéine kinase B (AKT)/cible mammalienne de la rapamycine (mTOR) ainsi que les voies du récepteur du facteur de croissance épidermique (EGFR), Src et PI3K [29].

Dans l'ensemble, l'action de la mort des cellules cancéreuses induite par le cisplatine est médiée par une série de mécanismes, notamment la formation d'adduits de l'ADN, l'induction d'espèces réactives de l'oxygène et d'autres altérations aberrantes des voies de signalisation.

Comme indiqué précedemment, le cisplatine est l'un des médicaments anticancéreux les plus efficaces et les plus utilisés. il est admis que le mécanisme d'action du cisplatine repose principalement sur la formation d'adduits stables de l'ADN sur la guanine, qui entraînent des dommages à l'ADN et finalement la mort cellulaire [30, 31]. Cependant, comme décrit précedemment plusieurs études indiquent que le cisplatine pourrait également avoir un impact sur d'autres processus biologiques tels que la réparation de l'ADN et la signalisation cellulaire, notamment la voie de l'EGFR [31-33]. En outre, le cisplatine pourrait exercer, au moins en partie, ces effets biologiques en se liant à des peptides ou à des protéines, ce qui entraînerait des modifications structurelles et/ou fonctionnelles [34]. En particulier, il a été rapporté que les fonctions de certaines enzymes cellulaires sont inhibées par le cisplatine par le biais de la liaison au groupe thiol des cystéines sensibles au redox [35, 36].

Mes travaux de thèse montrent aux niveaux moléculaire, cellulaire et in vivo que le cisplatine inhibe les fonctions enzymatiques de la tyrosine phosphatase PTP1B. Dans des expériences mécanistes et cinétiques utilisant la PTP1B humaine recombinante purifiée nous montrons que l'inhibition est irréversible et implique la formation d'un adduit covalent de cisplatine avec la cystéine catalytique redox-sensible de l'enzyme. Des expériences complémenaites menées dans des cellules et chez la souris indiquent que le traitement par le cisplatine entraîne l'inhibition irréversible de l'enzyme PTP1B endogène et l'activation concomitante de la signalisation de l'EGFR. Dans l'ensemble, mes travaux identifient la PTP1B comme une cible du cisplatine et suggèrent que l'inhibition de PTP1B par le cisplatine pourrait contribuer, au moins en partie, aux effets pharmacologiques et/ou toxicologiques du cisplatine, notamment via l'activation aberrante des voies de signalisation dépendantes de PTP1B. Plus largement, mon travail permet de mieux comprendre le réseau complexe de voies qui

subissent une modulation lors de l'administration de cisplatine et qui va au-delà de l'effet génotoxique bien établi du cisplatine.

En parallèle à mes recherches sur les effets du cisplatine sur PTP1B, je me suis également intéressé à l'étude de l'impact moléculaire et cellulaire de mutations ponctuelles oncogéniques affectant PTP1B et identifiées chez des malades atteints de lymphome médiastinal primaire à cellules B (PMBCL). Cette pathologie maligne est un sous-type rare de lymphome agressif à cellules B qui dériverait des cellules B thymiques [37]. Bien que le PMBCL soit considéré comme distinct des autres sous-types de lymphomes non hodgkiniens à cellules B, il présente des caractéristiques qui se chevauchent avec le lymphome hodgkinien [37]. Les cellules malignes expriment des marqueurs de cellules B (CD19, CD20, CD22) et des facteurs de transcription de cellules B tels que PAX5, OCT2, BCL6 [38]. On sait que la pathobiologie du PMBCL repose sur l'altération de différentes voies moléculaires. En particulier, il a été démontré que différentes cascades de signalisation cellulaire, telles que les voies JAK/STAT et le facteur nucléaireκB (NF-κB), sont déréglées dans le PMBCL, entraînant une augmentation de la phosphorylation de la tyrosine protéique [39, 40]. Récemment, des mutations récurrentes du *PTPN1* (codant pour PTP1B) ont été décrits dans les PMBCL et les lymphomes hodgkiniens, confirmant ainsi les évidences précédentes de l'implication de PTP1B dans la lymphomagenèse [9, 41]. En outre, un variant d'épissage inactif de PTP1B a été identifiée dans des cellules de lymphome hodgkinien et il a été démontré que l'expression de ce variant augmentait la signalisation la phosphorylation de tyrosines des protéines de la voie JAK/STAT [42]. D'autres études sur des modèles de souris ont également indiqué que l'absence de PTP1B induit un néoplasme myéloprolifératif et peut conduire au développement d'une leucémie aiguë [10, 11].

Il a été montré que PTP1B joue un rôle central dans la modulation des voies de signalisation oncogènes telles que les cascades EGFR et JAK/STAT via la déphosphorylation de tyrosines présentes sur plusieurs protéines effectrices [43, 44]. Il est intéressant de noter que des défauts génétiques ayant un impact sur ces voies et/ou une signalisation aberrante sont connus dans les lymphomes [45, 46].

Comme toutes les PTPs, PTP1B partage un mécanisme catalytique commun basé sur une cystéine nucléophile et d'autres résidus invariants importants situés dans un certain nombre de boucles hautement conservées qui forment le site actif (comme la boucle pTyr, la boucle WPD, la boucle P et la boucle Q) [47]. La structure, la flexibilité et la dynamique de ces boucles du site actif (notamment la boucle WPD, résidus 177-188) mais aussi des résidus adjacents sont essentielles pour la catalyse et la modulation de l'activité de PTP1B [48, 49]. De plus, il est maintenant connu qu'il existe également un réseau de régulation (réseau allostérique) impliquant différents résidus de l'enzyme (tels que Arg56, Ala69, Tyr153 ou Asn193) qui contribuent à l'activité de PTP1B notamment en influençant les mouvements de la boucle WPD [48, 49].

Comme indiqué précedemment, des mutations somatiques récurrentes de PTP1B dans les PMBCL ont été récemment identifiées chez l'Homme. Bien que ces mutations soient présentes sur l'ensemble de la séquence de PTP1B, la majorité d'entre elles se trouvent néanmoins dans le domaine catalytique de l'enzyme (couvrant les résidus 1-321) [9]. L'analyse de l'activité tyrosine phosphatase de ces mutants dans des lysats cellulaires a indiqué que certaines mutations peuvent conduire à des variants de PTP1B dont l'activité est significativement réduite, alors que d'autres mutations ont peu d'impact [9]. Il est intéressant de noter que trois mutations ponctuelles ont été trouvées dans la boucle WPD (V184D), la boucle P (R221G) et la boucle Q (G259V) chez des patients atteints de PMBCL. Bien qu'il ait été démontré que la mutation V184D réduit l'activité tyrosine phosphatase globale des lysats cellulaires surexprimant le mutant V184D de PTP1B, l'impact moléculaire et enzymatique de ces trois mutations de PTP1B n'a pas été étudié [9]. Au cours de ma thèse, j'ai étudié aux niveaux moléculaire et enzymatique trois mutations de PTP1B identifiées chez des patients PMBCL et situées dans la boucle WPD (V184D), la boucle P (R221G) et la boucle Q (G259V) [9, 47]. A l'aide de protéines recombinantes purifiées, j'ai pu montrer que les mutants PTP1B présentaient une activité phosphatase extrêmement faible. De même, l'expression des trois mutants de PTP1B dans des cellules conduit à des variants enzymatiques ayant une très faible activité tyrosine

phosphatase intrinsèque et à une augmentation concomitante de la phosphorylation de l'EGFR, un substrat connu de PTP1B. D'autres approches biochimiques et de dynamique moléculaire ont montré que ces mutations de PTP1B ont un impact sur la stabilité globale de la protéine, sa dynamique et la flexibilité des boucles du site actif, notamment la boucle WPD, la boucle P et la boucle Q. Cette partie de mes travaux de thèse montre donc que les mutants PTP1B (V184D, R221G et G259V) identifiés dans des lymphomes B humains ont une activité tyrosine phosphatase fortement altérée susceptible de conduire à des mécanismes de signalisation cellulaire aberrants.

LIST OF PUBLICATIONS

(1) **Rongxing LIU**, Wenchao ZHANG, Panhong GOU, Jérémy BERTHELET, Qing NIAN, Guillaume CHEVREUX, Véronique LEGROS, Gautier MOROY, Linh-Chi BUI, Li WANG, Jean-Marie DUPRET, Frédérique DESHAYES and Fernando RODRIGUES LIMA. Cisplatin causes covalent inhibition of protein-tyrosine phosphatase 1B (PTP1B): molecular, cellular and *in vivo* mice studies. (Submitted, see section "3.1" of the thesis)

(2) **Rongxing LIU**, Yujie SUN, Jérémy BERTHELET, Linh-Chi BUI, Ximing XU, Jean-Marie DUPRET, Mireille VIGUIER, Frédérique DESHAYES and Fernando RODRIGUES LIMA. Biochemical, enzymatic and computational characterization of recurrent somatic mutations of the human protein tyrosine phosphatase PTP1B in primary mediastinal B cell lymphoma. (Submitted, see section "3.2" of the thesis)

(3) **Rongxing LIU**, Cécile MATHIEU, Jérémy BERTHELET, Wenchao ZHANG, Jean-Marie DUPRET and Fernando RODRIGUES LIMA. Human protein tyrosine phosphatase 1B (PTP1B), from structure to clinical inhibitor perspectives. (Submitted, see section "3.3" of the thesis)

(4) Zhang W, Berthelet J, Michail C, Bui LC, Gou P, **Liu R**, Duval R, Renault J, Dupret JM, Guidez F, Chomienne C, Rodrigues Lima F. Human CREBBP acetyltransferase is impaired by etoposide quinone, an oxidative and leukemogenic metabolite of the anticancer drug etoposide through modification of redox-sensitive zinc-finger cysteine residues. Free Radic Biol Med. 2021 Jan;162:27-37. doi: 10.1016/j.freeradbiomed.2020.11.027. Epub 2020 Dec 2. PMID: 33278510.

(5) Xu X, Zhang W, Berthelet J, **Liu R**, Michail C, Chaffotte AF, Dupret JM, Rodrigues-Lima F. From transglutaminases (TGs) to arylamine N-acetyltransferases (NATs): Insight into the role of a spatially conserved aromatic amino acid position in the active site of these two families of enzymes. Biochem Biophys Res Commun. 2020 Apr 30;525(2):308-312. doi: 10.1016/j.bbrc.2020.02.082. Epub 2020 Feb 20. PMID: 32089267.

(6) Nian Q, Berthelet J, Zhang W, Bui LC, **Liu R**, Xu X, Duval R, Ganesan S, Leger T, Chomienne C, Busi F, Guidez F, Dupret JM, Rodrigues Lima F. T-Cell Protein Tyrosine Phosphatase Is Irreversibly Inhibited by Etoposide-Quinone, a Reactive Metabolite of the Chemotherapy Drug Etoposide. Mol Pharmacol. 2019 Aug;96(2):297-306. doi: 10.1124/mol.119.116319. Epub 2019 Jun 20. PMID: 31221825.

(7) Nian Q, Berthelet J, Parlato M, Mechaly AE, **Liu R**, Dupret JM, Cerf-Bensussan N, Haouz A, Rodrigues Lima F. Structural characterization of a pathogenic mutant of human protein tyrosine phosphatase *PTPN2* (Cys216Gly) that causes very early onset autoimmune enteropathy. Protein Sci. 2022 Feb;31(2):538-544. doi: 10.1002/pro.4246. Epub 2021 Nov 27. PMID: 34806245; PMCID: PMC8820110.

ABBREVIATIONS

AD: Alzheimer’s disease

ADP: adenosine diphosphate

AKT: serine-threonine protein kinase B

AP-1: activator protein-1

APL: acute promyelocytic leukemia

ASOs: antisense oligonucleotides

ATP: adenosine triphosphate

BCR: B cell receptor

CDDP: cis-dichlorodiamine platinum (II)

CGAP: cancer genome atlas project

CK1: cell kinase 1

CML: chronic myeloid leukemia

CR: complete remission

Ctr1: calcitonin receptor 1

DD: dose-dense

DLBC: diffuse large B-cell lymphoma

DSK: dual-specificity kinase

ECM: extracellular matrix

EGFR: epidermal growth factor receptor

EMT: epithelial–mesenchymal transition

ER: endoplasmic reticulum

ERK: extracellular-regulated kinase

FAK: focal adhesion kinase

FCR: Fc receptor

FDA: Food and Drug Administration

GEPIA: gene expression profiling interactive analysis

GO: gene ontology

Grb2: growth factor receptor-bound protein 2

GSH: glutathione

H_2O_2: hydrogen peroxide

HCD: higher-energy c-trap dissociation

HMGB1: high mobility group protein B1

HSC: hematopoietic stem cell

HSCT: hematopoietic stem cell transplantation

IR: insulin receptor

JAK-2: janus kinase 2

JNK: c-jun N-terminal kinase

MAPK: mitogen-activated protein kinase

MDA: malondialdehyde

mTOR: mammalian target of rapamycin

NF-ƙ: nuclear factor kappa

NGS: new generation sequencing

NLS: nuclear localization sequence

NRPTP: non receptor protein tyrosine phosphatase

ObR: leptin receptor

OCT2: octamer-binding protein 2

PARP1: poly [adp-ribose] polymerase 1

PCNA: proliferating cell nuclear antigen

PD: Parkinson’s disease

PDB: protein data bank

PI3K: phosphatidylinositol-3 kinase

PKC: protein kinase C

PMBCL: primary mediastinal B cell lymphoma

PPM: metallo-dependent protein phosphatase

PPP: phosphoprotein phosphatase

PSC: pluripotent stem cell

PTK: protein tyrosine kinase

PTM: post-translational modification

PTP: protein-tyrosine phosphatase

PTP1B: protein tyrosine phosphatase 1B

ROS: reactive oxygen species

RPTP: receptor protein tyrosine phosphatase

RTK: receptor tyrosine kinase

SH2: Src homology 2

STAT3: signal transducer and activator of transcription 3

STE: sterile kinase

STK: serine/threonine kinase

T2DM: type 2 diabetes mellitus

t-AML: therapy-related acute myeloid leukemia

TCR: T cell receptor

TK: tyrosine kinase

TKL: tyrosine kinase-like

TSC: totipotent stem cell

USC: unipotent stem cell

LIST OF FIGURES

Figure 1: Cellular interactions of CDDP……..…27

Figure 2: Formation of cisplatin-DNA adduct……..…28

Figure 3: The targets and mechanisms of cisplatin…….…….34

Figure 4: Phosphorylation regulation networks……...36

Figure 5: Classification of PTPs…….....39

Figure 6: Alignment of PTP catalytic domain sequences of 17 non-receptor PTPs…42

Figure 7: Phylogenetic tree of PTP catalytic domain of 17 non-receptor PTPs……...43

Figure 8: PTP1B protein expression in different tissues……..……44

Figure 9: PTP1B mRNA expression in different tissues……..……45

Figure 10: Gene/protein linked to PTP1B function from GO analysis……46

Figure 11: Signaling pathway involving PTP1B……..…47

Figure 12: Schematic representation of the “two faces” of PTP1B in cancer, with its substrates and effects respectively……53

Figure 13: Relative expression of PTP1B and corresponding survival plots in GBM, LUAD and PAAD respectively……53

Figure 14: Pathways affected by neuronal PTP1B activation in Alzheimer's disease progression……...…55

Figure 15: Schematic diagram of PTP1B in IFN-γ-induced neuroinflammation and 6-OHDA-induced neuronal death……55

Figure 16: Biomarker targets for CAR therapy in hematological malignancies…..…58

Figure 17: Relative expression of PTP1B and corresponding survival plots in LAML and DLBC……..…59

Figure 18: Schematic representation of the domain structures of PTP1B full length..60

Figure 19: Oxidized status of PTP1B……..……62

Figure 20: Overall structure and functional loops of PTP1B……64

Figure 21: pTyr loop of PTP1B with corresponding residues……..……65

Figure 22: E loop of PTP1B with corresponding residues……66

Figure 23: WPD loop of PTP1B with corresponding residues……..…67

Figure 24: S loop of PTP1B with corresponding residues……68
Figure 25: P loop of PTP1B with corresponding residues……69
Figure 26: Q loop of PTP1B with corresponding residues……..…..…70
Figure 27: Schematic representation of the structures of PTP1B and TCPTP and their respective substrates linked to cancer……..….71
Figure 28: Schematic representation of the different key domains of TCPTP and 3D structural alignment of TCPTP and PTP1B……...…72
Figure 29: The two steps catalytic mechanism of PTP1B dephosphorylation…….….73
Figure 30: *PTPN1* gene mutation in pan-cancer from COSMIC database……..74
Figure 31: *PTPN1* mutations type in PMBCL and HL……..…75
Figure 32: Multiple PTP1B binding sites……..…79

LIST OF TABLES

Table 1: Information of platinum-included drugs……26

Table 2: Subfamilies of protein kinases……...…37

Table 3: Categories of protein phosphatases……38

Table 4: PTP catalytic domain of 17 non-receptor PTPs……..……41

Table 5: PTP catalytic domain identity of 17 non-receptor PTPs……43

Table 6: GO of PTP1B related genes……...…46

Table 7: Involvement of PTP1B in diseases……50

Table 8: Amino acid replacement and corresponding base change of *PTPN1* missense substitution in PMBCL and HL……76

Table 9: Allosteric inhibitors and corresponding allosteric binding site of PTP1B….77

Table 10: Categories of PTP1B inhibitors that bind to A, B, C and D sites……..…80

Table 11: The two ASOs sequences of PTP1B mRNA inhibitors……81

1 INTRODUCTION

1.1 Background

Hematopoietic malignancies are a series of blood related cancers that usually originate in the bone marrow and result in high numbers of abnormal blood cells. Until now, the pathogenesis of hematopoietic cancers are still unclear, but at least, a combination of genetic factors and non-inherited factors (like smoking, chemical exposure…) are believed to contribute to the development of hematopoietic malignancies [50].

Cisplatin is a therapeutic drug, which is indicated for the treatment of several cancers including leukemia and lymphoma. Meanwhile, numerous studies pointed out that the treatment of primary malignancies with cisplatin could induce treatment-associated cancers. Unfortunately, the exact mechanisms of those secondary malignancies are still poorly understood. Cancers have many causes, but ultimately involve oncogenes that display roles for the carcinogenic process. Altered cell signaling is a hallmark of several cancers. Dysregulation of tyrosine kinases and tyrosine phosphatases have been shown to be essential in carcinogenesis [51]. In this thesis, we focused on PTP1B tyrosine phosphatase regulated by cisplatin. Also we carried out experiments on PTP1B mutants since this enzyme has been shown to be mutated notably in certain hematopoietic malignancies [9, 42]. In addition, we summarized the specific PTP1B inhibitors since it is a potential target to many diseases.

1.2 Cisplatin

1.2.1 History of cisplatin

Cisplatin, which is also named cis-dichlorodiamine platinum (II) (CDDP), was firstly synthesized in 1845, and Barnett Rosenberg then discovered that electrolysis products from platinum electrodes could inhibit cell division [17]. Therefore, he turned the research direction into tumors, and proved that cisplatin had strong anticancer effects *in vivo* and *in vitro* [18]. Cisplatin has been allowed by Food and

Drug Administration (FDA) to be used in clinics in 1978. The discovery of cisplatin has driven the development of metal complexes in the medical field and has revolutionary significance for cancer treatment in the following decades. Based on its simple structure and strong anticancer effect, a series of derivatives with corresponding indications have been put forward, including carboplatin (2nd generation), oxaliplatin (3rd generation) and so forth (Table 1).

Generation	Name	Molecular formula	Indications	Side effects
1st	Cisplatin	$Cl_2H_6N_2Pt$ 	Sarcomas, lymphoma, malignant epithelial tumor, testicular cancer…	Low blood counts, kidney toxicity, ototoxicity, nausea and vomiting…
2nd	Carboplatin	$C_6H_{12}N_2O_4Pt$ 	Ovarian cancer…	Bone marrow suppression, kidney toxicity, neurotoxicity, nausea and vomiting…
	Nedaplatin	$C_2H_{10}N_2O_3Pt$ 	Head and neck cancer, small and non-small cell lung cancer, esophageal and ovarian cancer…	Bone marrow suppression, kidney toxicity, anaphylactic shock…
3rd	Oxaliplatin	$C_8H_{14}N_2O_4Pt$ 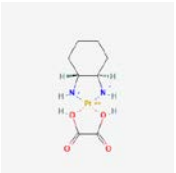	Metastatic testicular cancer, colorectal cancer…	Neurotoxicity, nausea and vomiting, blood system…
	Lobaplatin	$C_9H_{18}N_2O_3Pt$ 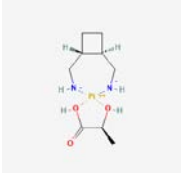	Breast cancer, small cell lung cancer, chronic myeloid leukemia...	Blood toxicity, gastrointestinal toxicity…

Table 1: Information of platinum-included drugs.

1.2.2 Action of cisplatin

Cisplatin is shown to induce cell death. More precisely, cisplatin-induced cancer cell death is mediated through a series of biochemical effects and molecular mechanisms that include the formation of DNA adducts, induction of reactive oxygen species (ROS) as well as some other pathways [19] (Figure 1).

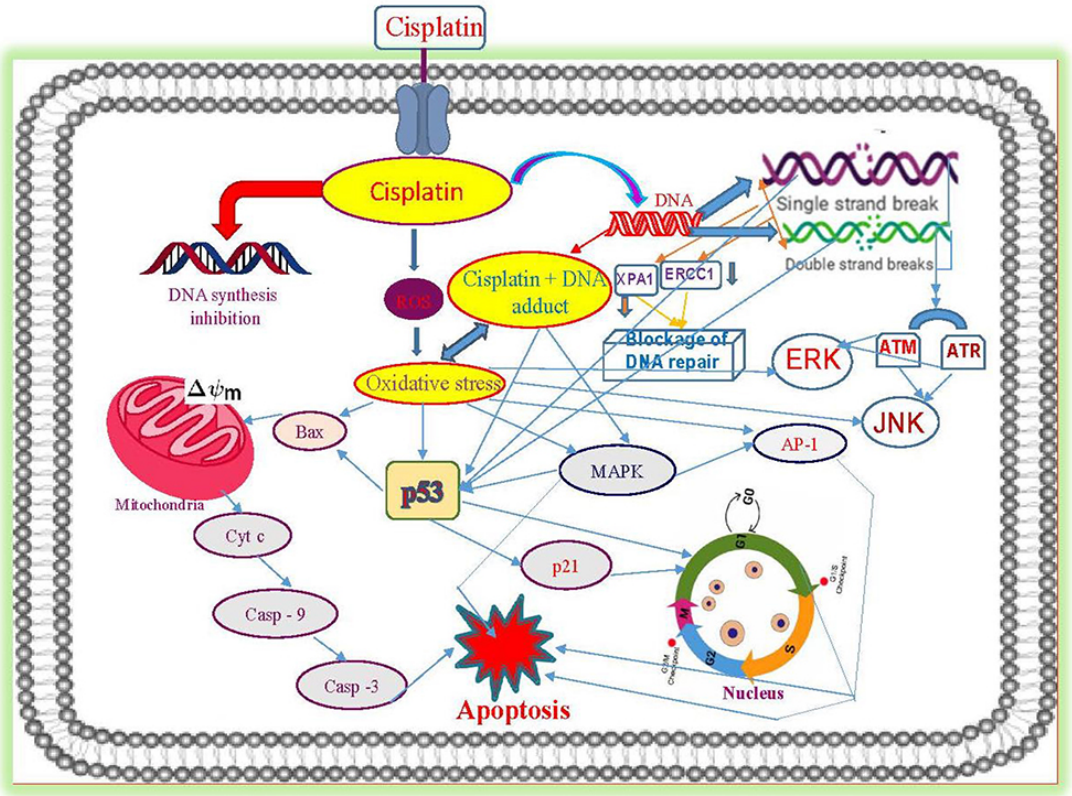

Figure 1: Cellular interactions of CDDP [19]

1.2.2.1 Formation of cisplatin-DNA adduct

Cisplatin can impact each phase of cell proliferation cycle (G1, S, G2, M) and resting state (G0) so as to inhibit tumor growth within three steps (Figure 2). The first step is uptake by cells. Evidence indicated that the possible way that cisplatin enter cells is a combination of passive diffusion [52] and active transport [53]. The second step is hydrolytic activation. Briefly, a chlorine is replaced slowly by water molecule to form $[PtCl(H_2O)(NH_3)_2]^+$, where the water molecule is easily detached so that

platinum coordinates with one site of the DNA base. Then the other chlorine is also detached to form $[Pt(H_2O)_2(NH_3)_2]^+$. The third step is interaction with DNA. Platinum cross-links with double strands (interstrand crosslink) or two points of a single strand (intrastrand) of DNA in order to stop the DNA replication of cancer cells and then cause them undergo apoptosis [20, 54].

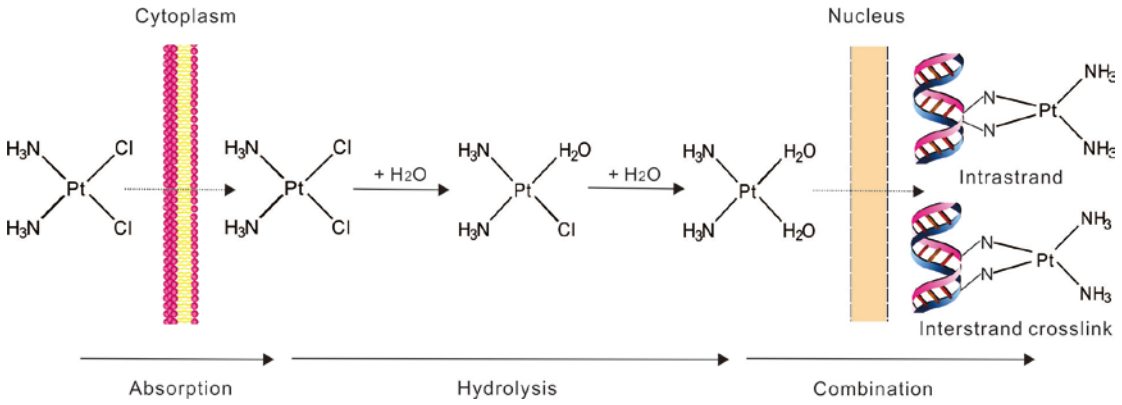

Figure 2: Formation of cisplatin-DNA adduct.

1.2.2.2 Cisplatin induced oxidative stress

Cancer cells exhibit high metabolism and elevated reactive oxygen species (ROS) concentrations to facilitate their propagation. ROS could affect key signaling proteins that are involved in biochemical pathways for cell biological functions, like extracellular-regulated kinase 1/2 (ERK1/2), ligand independent receptor tyrosine kinases (RTKs), nuclear factor kappa-light-chain-enhancer of activated B cells (NF-κB) or phosphatidylinositol-3 kinase (PI3K) [19, 21]. Cisplatin has been shown to generate ROS directly or indirectly through mitochondria [22, 55]. Briefly, redox balance in cells is maintained by molecules containing sulfhydryl groups (-SH), which can react with ROS. If the ROS level is out of balance, cells will be damaged and will die under oxidative stress. After entering cells, cisplatin reacts with the antioxidant enzyme system and triggers the release of reactive oxygen free radicals, inducing lipid peroxidation, increasing malondialdehyde (MDA) production, reducing GSH level, damaging DNA, activating pro-inflammatory and pro-apoptotic factors and eventually

triggering apoptosis [23, 56]; meanwhile, the oxidative stress response in the intracellular cascade causes the mitochondria to release a large amount of cytochrome C, as well as open calcium pool of endoplasmic reticulum (ER) which could positively promote the release of cytochrome C, promoting further amplification of the cascade reaction and finally causing cells apoptosis [24].

1.2.2.3 Other molecular mechanisms of cisplatin

Apart from the known mechanism of cisplatin by forming adduct with DNA and inducing ROS, cisplatin could also target other proteins. A recent study has shown that calcium efflux from the ER could regulate cisplatin-induced apoptosis in human cervical cancer cells through caspase 3 activation [25]. Studies have also shown that cisplatin-induced DNA damage results in the activation of mitogen-activated protein kinases (MAPK) family, involving MAPK/ERK [26], c-jun N-terminal kinase (JNK)/activator protein-1 (AP-1) [27, 57, 58], p38 MAPK [59] and p53 [28]. Cisplatin also activates serine-threonine protein kinase B (AKT)/mammalian target of rapamycin (mTOR) signal pathway as well as epidermal growth factor receptor (EGFR), Src and PI3K pathways [29].

As a whole, the action of cisplatin-induced cancer cells death is mediated by a series of mechanisms, including the formation of DNA adducts, induction of reactive oxygen species, and other aberrant altering of signal pathways.

1.2.3 Clinical use of cisplatin

Due to its high efficiency, cisplatin has been put into clinical use for many years. It has been used against many types of cancer, including bladder, ovarian, head and neck, esophageal, small and non-small cell lung, breast, cervical, stomach, prostate, sarcomas as well as lymphomas (https://chemocare.com/chemotherapy/drug-info/cisplatin.aspx). Importantly, it is also the first-line drug for testicular cancer, especially for testicular cancer that has metastasized, in which the cure rate of patients increased from 10% to 85% [60] (https://www.can-cer.gov/about-cancer/treatment/

drugs/cisplatin).

1.2.4 Side effects of cisplatin

Cisplatin is not specific for tumor DNA, so the battle between cisplatin and tumor cells is a classic one, maintaining a balance between killing tumor cells without affecting healthy cells too much. However, platinum is a heavy metal that will accumulate in our body, resulting in interference with normal physiological activities as well as damage to different tissues. The most common side effects are nausea, vomiting, diarrhea, hiccups as well as severe nephrotoxicity, ototoxicity, neurotoxicity, bone marrow suppression and drug resistance.

1.2.4.1 Nephrotoxicity

Most of the residual cisplatin is excreted by kidney. Due to its reabsorption by renal tubules and collecting ducts, cisplatin largely accumulates in kidney [61], greatly enhancing the toxicity of cisplatin to kidney by the evidence of tubular damage and dysfunction, leading to decrease in glomerular filtration and necrosis [62]. Also cyst formation and interstitial fibrosis are found following damages with long-term cisplatin treatment [63]. Mechanisms of cisplatin induced nephrotoxicity include high expression of calcitonin receptor 1 (Ctr1) and its localization to the basolateral membrane of the proximal tubule, suggesting that Ctr1 plays an important role in cisplatin uptake [64]. Another investigation showed that knockout of the octamer-binding protein 2 (OCT2) significantly reduced urinary cisplatin excretion and nephrotoxicity [65]. At present, clinically, hydration therapy is mainly used to reduce nephrotoxicity caused by cisplatin, by giving a lot of fluids to shorten the residence time of cisplatin and reduce the concentration of cisplatin in kidney so as to allow accumulated cisplatin be excreted from the body as soon as possible.

1.2.4.2 Ototoxicity

Cisplatin-induced ototoxicity affects up to 93% of the patients who are treated by

cisplatin [19]. The lesions are mainly concentrated in cochlear hair cells and spiral ganglion cells, resulting in the symptoms of progressive and irreversible sensorineural hearing loss [66]. Numerous hypothesis have been proposed. First, cisplatin stimulates the potassium channels of epithelial cells to cause potassium outflow from the cells, which changes the ion concentration and osmotic pressure in the cells, thus activating the apoptotic enzymes in cells [67]. Second, in the cochlea, if the level of ROS is no longer quenched by the intracellular antioxidant system, excessive ROS can trigger a series of reactions to disrupt cell structure, such as DNA damage, oxidative modification of proteins, and increased lipid peroxidation of cell membranes, eventually leading to cells apoptosis [68]. Third, several other factors have been studied to understand the pathophysiology of cisplatin-induced ototoxicity, like copper transporters, organic cation transporters, transient receptor potential channel family, calcium channels, multidrug resistance-associated proteins [69] as well as receptor-interacting protein (RIP) kinase 3-dependent necroptosis [70]. Enhancing the antioxidant protection system and inhibiting the apoptosis pathway are considered as two mainstream protective measures to reduce the ototoxic side effects caused by cisplatin. But in clinics, low-dose systemic medication or topical medication are adopted, as well as monitoring and maintaining the renal function of patients.

1.2.4.3 Cisplatin-induced leukemia

Similarly to alkylating agents and topoisomerase inhibitors, cisplatin can cause bone marrow suppression [71, 72], which is manifested as a decrease in white blood cells, granulocytes, and platelets. Among them, the reduction of white blood cells is the most obvious, even if red blood cells are also affected in severe cases. Cisplatin-induced bone marrow dysfunction is accompanied by an acute nerve injury in the bone marrow, resulting in sensory and autonomic neuropathy [73]. Patients that have previously received cisplatin treatment show irreversibly chronic bone marrow failure, leading to the impairment of hematopoietic stem cells (HSCs) and bone

marrow regeneration [72, 74].

The mechanism of cispltin induced leukemia is still poorly understood. It is concluded that several hypothesizes are pointed out. First, cisplatin could damage DNA both in cancer and normal cells. It can simply select or create conditions to enhance the existing proto-leukemia cells that have a tendency to develop into acute leukemia. Once the cytotoxic chemotherapy eradicates other clones, the leukemia clone is revealed [75]. Second, radiotherapy, chemotherapy, etc. can further impair body immune function, causing tumor cells to proliferate and increasing the susceptibility to tumorigenesis [76]. Third, similarly to myelodysplastic syndrome, therapy-related acute myeloid leukemia (t-AML) shares specific genetic mutations [77]. Due to the non-specific mechanism of cisplatin on cells, bone marrow suppression is inevitable. In clinics, combination low-dosage of cisplatin with other drugs or replacement of cisplatin by other platinum based drugs with less risk of bone marrow suppression are recommended.

1.2.4.4 Drug resistance

Nonetheless with the massive use of cisplatin and the ability of cells to repair the damaged DNA, different drug resistance mechanisms occur, including decreased drug uptake [78], increased efflux [79, 80], increased detoxification [81], altered signal pathway of JNK/p38 MAPK [82], Nrf2 Signaling [19], autophagy [83, 84] and epithelial–mesenchymal transition (EMT) [19], increased tolerance of DNA adduct [85], increased DNA repair [86] and increased apoptosis inhibitors [87]. In order to reduce drug resistance and toxicity, combination therapy is adopted in clinics. For example, cisplatin combined with pemetrexed shows excellent anticancer effects in the treatment of lung cancer [88]. Low-dose of cisplatin combined with low-dose of paclitaxel, which is also called dose-dense (DD) drug treatment methods, are normally employed to fight against cancer [89]. In addition, avoiding the repair of Pt/DNA conjugates by repair proteins has been mentioned to reduce cisplatin resistance theoretically, but not has been used in clinical trials.

DNA damage repair protein, high-speed surging protein and poly [adp-ribose] polymerase 1 (PARP1), have been shown to recognize Pt/DNA conjugates [69]. In response to these, high mobility group protein B1 (HMGB1) is mentioned, which may prevent the repair protein from identifying Pt/DNA conjugates, thus providing a guarantee for the success of cisplatin. More recently, with the quick development of pharmaceutics, nanoparticles with cisplatin have become a novel and more efficient way in curing disease with less side effects and drug resistance [19].

1.2.5 Conclusion and prospect of cisplatin

Cisplatin has undoubtedly played a huge role in the history of human anti-cancer therapeutics, but the problems caused by cisplatin are also obvious because most cisplatin could bind to many other targets, and less than 1% cisplatin targets DNA [90] (Figure 3). However, if cisplatin is over used, the damages to human body will increase, with more ototoxicity, nephrotoxicity, neurotoxicity (irreversible) and drug resistance. With the extension of the medication time, the effects of cisplatin will gradually weaken. In addition, oral administration of cisplatin is not biologically active and it requires intravenous injection, which also brings a certain degree of inconvenience to patients.

Since the introduction of cisplatin, second and third generation platinum drugs have appeared with similar mechanism to cisplatin, relatively less drug resistance, toxicity and side effects but more applicability by changing the platinum ligands (Table 1). However, the first three generations of platinum drugs also have their own shortcomings that are difficult to overcome. Therefore, innovative research and development beyond the limitations of traditional platinum drugs are novel prospects for platinum drugs, such as the development of tetravalent platinum and trans-platinum.

The various ligands involved in the coordination of the central atom of platinum drugs are the biggest difference among the first three generations of platinum drugs, because the different ligands will determine the different properties of the drugs, such

as molecular polarity and drug toxicity. So if the number of ligands increased, can the function of the drugs could be increased? Most of the divalent platinum is a tetracoordination compound, so scientists pay their attention on Pt(IV). When Pt(IV) forms a bond, d2sp3 hybridization occurs, which can form a more stable octahedral field structure instead of a plane formed by Pt(II). This is because Pt(IV) has six ligands, and it is easy to modify the structure and introduce groups with different functions to optimize the structure of drugs.

As the pioneer of platinum anti-cancer drugs, cisplatin has created a new window for future generations to study cancer treatment from the perspective of DNA complex. Compared with cisplatin, further generations of platinum based drugs present their superiorities in terms of more efficiency and less toxicity. But still, increasing the specificity and decreasing the side effects of platinum based drugs are a long march.

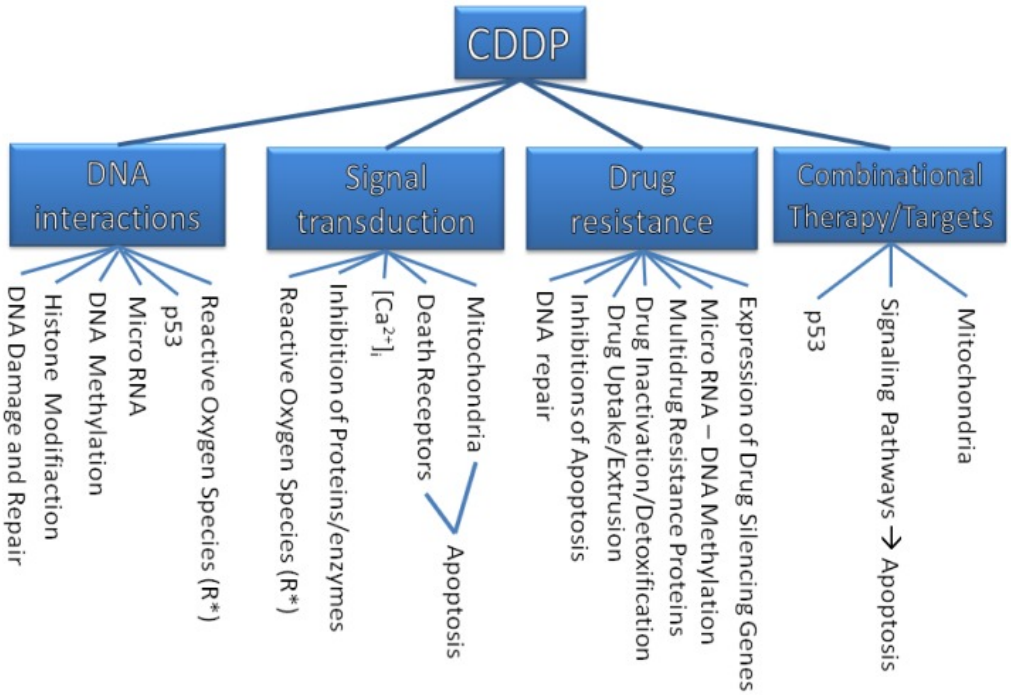

Figure 3: The targets and mechanisms of cisplatin [91].

1.3 Protein phosphorylation

Post-translational modifications (PTMs) of proteins, including phosphorylation, methylation, acetylation, etc., play important roles in the biological functions of

proteins. Phosphorylation, as an effective process to regulate protein functions, has great influence on signal transduction, metabolism and other intracellular processes. Any trouble in the process of phosphorylation may lead to inappropriate activation or inactivation of cells. Studies have shown that many diseases, including cancer, are related to abnormal phosphorylation of proteins [92-94].

1.3.1 Phosphorylation sites

One third of proteins in mammalian cells undergo phosphorylation. Among them, half of the proteins have more than one phosphorylation site, and different phosphorylation sites can cause different cellular responses. The most common phosphorylation sites in eukaryotic cells are serine, threonine and tyrosine [95]. Phosphorylation provides a mechanism for the rapid and reversible control of protein function by the addition of negative charge to amino acid side chains [96]. Negatively charged amino acids (glutamate and aspartate) can sometimes mimic the phosphorylated state of a protein [96]. Indeed, nature also employs this trick in reverse, evolving serine, threonine and tyrosine phosphorylation sites from glutamate and aspartate residues [96]. Structures of relative proteins where phosphosites evolved from acidic residues (DNA topoisomerase II, enolase, and C-Raf) show that the relevant acidic residues are presented in salt bridges with conserved basic residues, and that phosphorylation has the potential to conditionally restore the salt bridges [96]. The evolution of phosphorylation sites from glutamate and aspartate residues provides a rationale for why phosphorylation sometimes activate proteins, and helps explaining the origins of this important and complex process.

1.3.2 Phosphorylation regulation

Protein phosphorylation regulation in tissues could be activated/deactivated by means of kinases/phosphatases [97]. Briefly, the protein receives the γ phosphate group of adenosine triphosphate (ATP) after hydrolysis due to enzymatic activity of kinase, with the release of adenosine diphosphate (ADP); conversely, the

phosphorylated protein could lost a phosphate group under the control of phosphatase. Both of the two enzymes work together reversibly to keep the phosphorylation balanced. Once the phosphorylation level is out of balance, the function of protein from itself (epigenetic modifications, cytogenetic alterations, genetic mutations or the tumor micro-environment) to phosphoprotein (oncogenic pathway activation) will change, which might contribute to oncogenic process (Figure 4) [98].

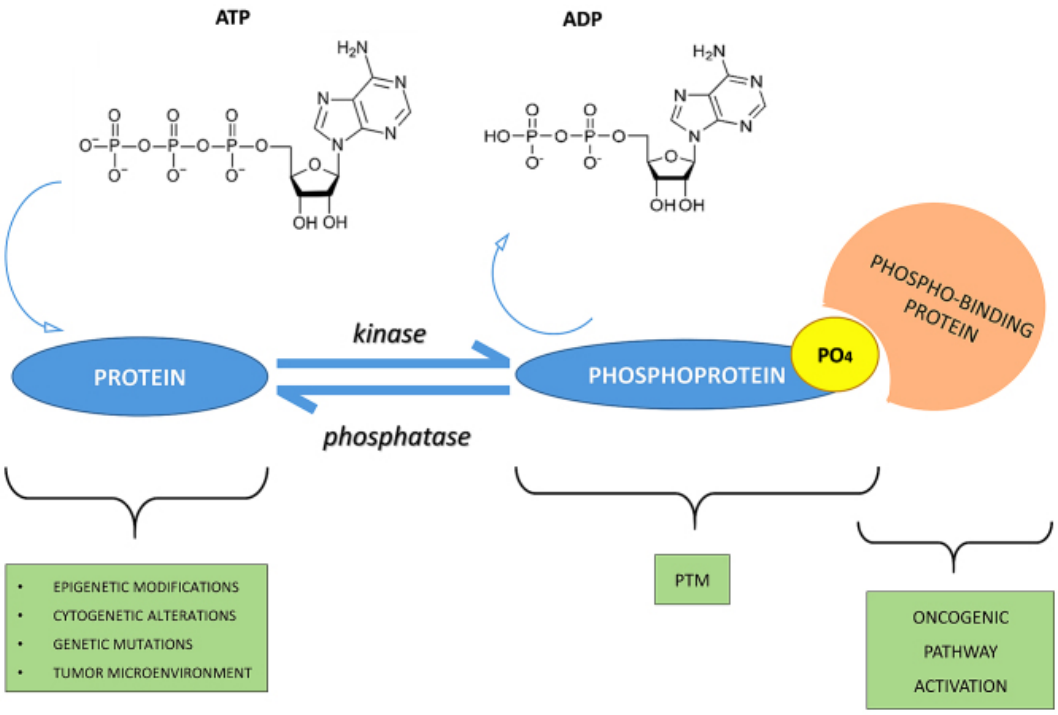

Figure 4: Phosphorylation regulation networks [97].

1.3.2.1 Protein kinases

Protein kinases are responsible for protein phosphorylation, contributing to enzyme activities, localization and overall functions, especially in signal transduction and the coordinated regulation of complex functions (such as cell cycle). So far, 518 human protein kinases have been discovered and can be divided into 3 groups based on the amino acid residues that they phosphorylate: mostly serine/threonine kinases (STKs), tyrosine kinases (TKs) and dual-specificity kinases (DSKs) [99]. At least 125 of the human protein kinases are STKs [100]. Besides, another classification of protein kinases is introduced, named AGC, CaMK, CK1, CMGC, STE, TK and TKL (Table

2). One interesting point is that most eukaryotic protein kinases share a common ancestral catalytic domain, which can be traced back to a common ancestor [101]. The catalytic domain of protein kinase has 2 subdomains, named N- and C-lobe [102]. Both are connected by a peptidic stand, allowing the formation of hinge domain, a front pocket and a back pocket, close to the gatekeeper residue. The catalytic domain is unavailable when it is active because of conformational movements within the N- and C-lobe. The activation of the catalytic domain occurs through phosphorylation of the activation loop or through an allosteric mechanism [102]. Moreover, the kinases also have non-catalytic domains, which could allow the attachment of substrates and the recruitment of other signaling proteins [103]. Activation or deactivation of kinases occur in different ways: through the kinases themselves with a cis-phosphorylation/autophosphorylation, by binding with activator or inhibitor proteins or checking their localization in the cell in relation to their substrates [97, 104].

Protein kinase family	Members	Reference
AGC	Kinase A/G/C	[105]
CaMK	Calmodulin-dependent protein kinase	[106]
CK1	Cell kinase 1	[107]
CMGC	CDK, MAPK, GSK3, CLK	[108-110]
STE	Sterile kinase	[111]
TK	Tyrosine kinase	[101]
TKL	Tyrosine kinase-like	[112]

Table 2: Subfamilies of protein kinases [97].

1.3.2.2 Protein phosphatases

Phosphatases have the opposite function of kinases, hence reverting the phosphoprotein to a non-phosphorylated state by hydrolyzing phosphoric acid monoesters into a phosphate group and a molecule with a free hydroxyl group [109, 113], with more rapid kinetics than kinases [97]. In contrast to kinases, the human protein phosphatases that dephosphorylate phosphoserine, phosphothreonine and phosphotyrosine may have distinct evolutionary origins [114], although some of the

core features of their catalytic domains may have converged during evolution [101]. However, it is common for these phosphatases to have catalytic activities towards non-protein substrates, or to share homology with non-protein phosphatases, or both. Currently, approximately 226 known protein phosphatases have been identified [115] which could be classified into 3 families: phosphoprotein phosphatases (PPPs), metallo-dependent protein phosphatases (PPMs) and protein-tyrosine phosphatases (PTPs) (Table 3) [101]. Current studies have confirmed that protein phosphatases are involved in many biological processes, including hematopoietic cell differentiation, myeloid cell and lymphocyte development and proliferation, cytokine receptor signaling, B cell receptor (BCR) and T cell receptor (TCR) and Fc receptor (FCR) signal activation [116, 117].

<table>
<tr><th colspan="3">Class</th><th>Subtype</th><th>Substrate</th></tr>
<tr><td colspan="3">PPPs</td><td>PP1/PP2A/PP2B/PP4/PP5/PP6/PP7</td><td>pSer/pThr</td></tr>
<tr><td colspan="3">PPMs</td><td>PP2C</td><td>pSer/pThr</td></tr>
<tr><td rowspan="5">PTPs</td><td rowspan="2">Cys-based class I</td><td>Classical tyrosine specific PTPs</td><td>PTP1B/TCPTP/SHP1/SHP2…</td><td>pTyr</td></tr>
<tr><td>Dual specific PTPs</td><td>MKPs/MTM1/PTENJSP1…</td><td>pTyr/pThr or pTyr/pSer</td></tr>
<tr><td colspan="2">Cys-based class II</td><td>LMWPTP</td><td>pTyr</td></tr>
<tr><td colspan="2">Cys-based class III</td><td>CDC25A/CDC25B/CDC25C</td><td>pTyr/pThr</td></tr>
<tr><td colspan="2">Cys-based class IV</td><td>EYA1/EYA2/EYA3/EYA4</td><td>pTyr/pSer</td></tr>
</table>

Table 3: Categories of protein phosphatases [101, 118].

1.4 Protein tyrosine phosphatases (PTPs)

PTPs, belonging to non-transmembrane proteins, are a family of enzymes that regulate the phosphorylation level of protein tyrosine residues during signal transduction. Presently, around 107 genes encoding PTPs have been identified in the human genome [118], which can be divided into 4 groups according to their amino acid sequence difference on catalytic site and functions (Figure 5) [118-121]. In tissues, PTPs and protein tyrosine kinases (PTKs) and their respective substrates work together to form a complex signal transduction network, which regulates cellular

processes such as cell growth, differentiation, metabolic process, cell cycle regulation, cell migration, gene transcription and immune response [2, 122]. Abnormal tyrosine phosphorylation is associated with many human diseases [2, 123, 124], including cancers, diabetes, rheumatoid arthritis, and hypertension. PTPs can exert both positive and negative effects on a signaling pathway and play crucial physiological roles in a variety of mammalian tissues and cells [125]. As aberrant tyrosine phosphorylation is a hallmark of different diseases [118], some PTPs have been considered to be the next generation drug targets [120, 123]. Therefore, those findings give us a hint that PTPs could be the next frontier in drug discovery.

Unlike PTKs, which share sequence identity with protein serine/threonine kinases, PTPs show no sequence similarity with protein serine/threonine phosphatases, but are characterized by the presence of the active site signature motif (H/V)C(X)5R(S/T) in the conserved catalytic domain [126]. Due to the shared mechanism among all the PTPs, with the participation of conserved cysteine residue in the catalytic domain, PTPs inhibitors present no specificity in targeting specific PTP. So far, only few PTPs inhibitors have been tested in clinical trials.

Apart from the fact that PTPs could dephosphorylate certain proteins, they are also well-known to dephosphorylate non-protein targets such as carbohydrates, mRNA and phosphoinositides as well [2, 127-129].

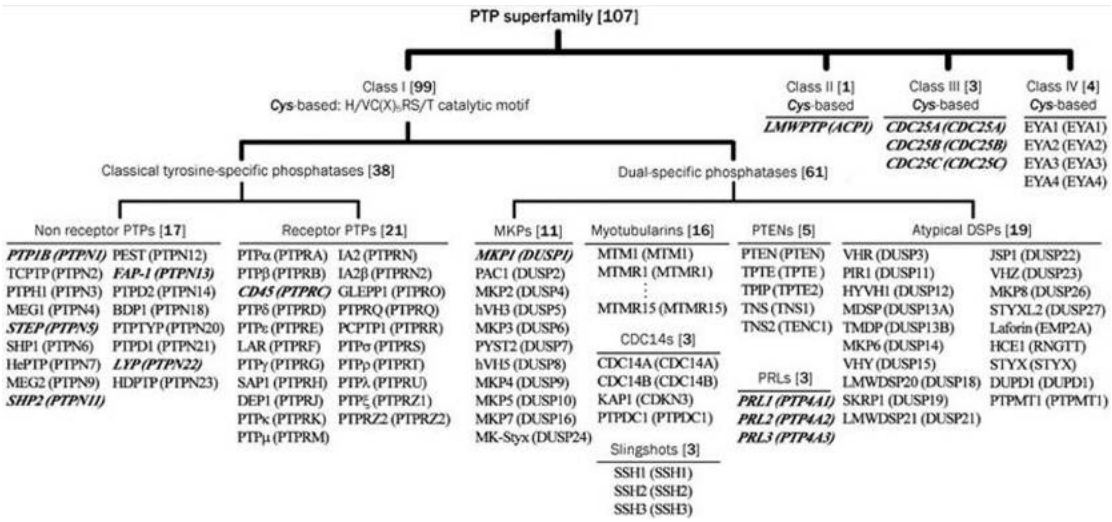

Figure 5: Classification of PTPs [118].

1.4.1 Receptor protein tyrosine phosphatases (RPTPs)

Structurally, RPTPs are made up of an extracellular domain, a transmembrane region and a cytoplasmic domain. The intracellular structure usually consists of two domains, the membrane-proximal (named D1) and the membrane-distal (named D2), where D1 is the active catalytic region and D2 is responsible for protein stability as well as protein–protein interactions that regulate RPTPs dimerization [2, 130, 131]. The extracellular domain of RPTPs typically contains immunoglobulin-like and fibronectin domains. RPTPs play vital roles in cellular migration, mitosis and proliferation [132]. Among all the 21 trans-membrane RPTPs, RPTPα plays the prominent way. It is well known as a signal transmembrane protein which is widely expressed in various tissues and cells, including the immune system, the nervous system and many cancer cells [133]. Specifically, RPTPα is highly expressed in the brain and its extracellular domain is associated with the neurite outgrowth, neuronal regeneration and migration [131].

1.4.2 Non receptor protein tyrosine phosphatases (NRPTPs)

NRPTPs own 17 family members and their structures differ greatly though they share the same catalytic motif and protein fold [134]. However, they have a highly conserved functional region, which is also called PTP catalytic domain (Table 4), with around 280 amino acids related to dephosphorylation activity [135]. Furthermore, following an alignment (Figure 6), all the PTP catalytic domain of NRPTPs show strongly identities (Table 5), which could help to explain their similar catalytic function. Meanwhile, the phylogenetic tree (Figure 7) also provides the evidence that NRPTPs may share the similar catalytic mechanism implicating the catalytic motif PXXVHCSAGXGRTG (Figure 6). Although all the NRPTPs dephosphorylate tyrosine in the same way, they can act on different substrates and have various expression in different tissues, organs and cells [136].

Gene name	Protein name	PTP catalytic domain		Number of residues
		From	To	
PTPN1	PTP1B	3	277	275
PTPN2	TCPTP	5	275	271
PTPN3	PTPH1	646	901	256
PTPN4	MEG1	655	911	257
PTPN5	STEP	300	555	256
PTPN6	SHP1	244	515	272
PTPN7	HePTP	97	350	254
PTPN9	MEG2	303	574	272
PTPN11	SHP2	247	517	271
PTPN12	PEST	28	293	266
PTPN13	FAP-1	2213	2467	255
PTPN14	PTPD2	909	1180	272
PTPN18	BDP1	26	291	266
PTPN20	PTPTYP	159	412	254
PTPN21	PTPD1	896	1167	272
PTPN22	LYP	24	289	266
PTPN23	HDPTP	1192	1452	261

Table 4: PTP catalytic domain of 17 NRPTPs.

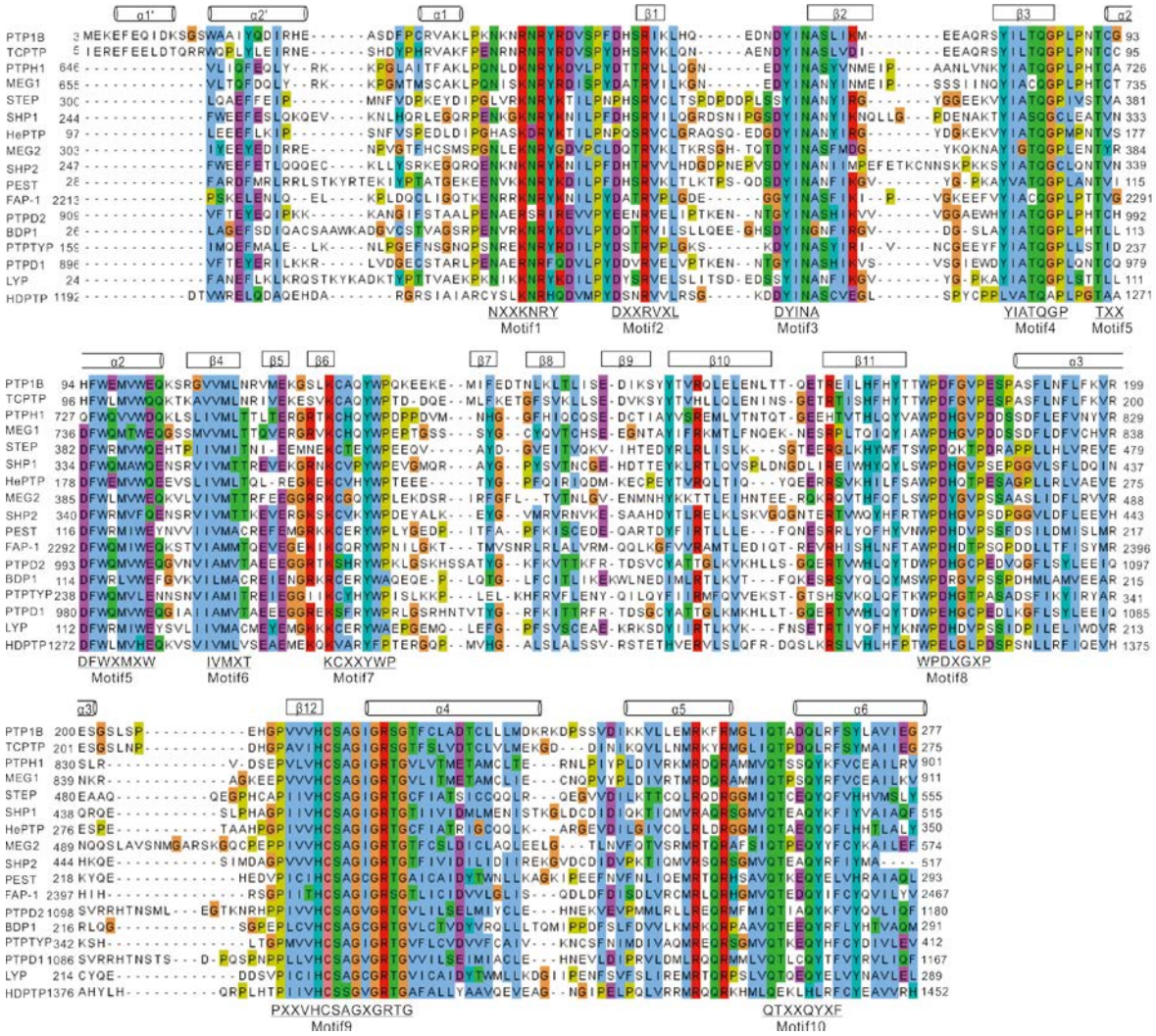

Figure 6: Alignment of PTP catalytic domain of 17 NRPTPs.

	PTP1B	TCPTP	PTPH1	MEG1	STEP	SHP1	HePTP	MEG2	SHP2	PEST	FAP-1	PTPD2	BDP1	PTPTYP	PTPD1	LYP	HDPTP
PTP1B	100	70	37	39	31	36	36	40	37	37	36	35	35	35	36	37	32
TCPTP	70	100	40	39	32	35	33	42	37	35	36	35	33	35	34	37	34
PTPH1	37	40	100	65	32	36	35	39	37	33	39	40	39	38	39	37	34
MEG1	39	39	65	100	33	39	36	41	39	35	39	40	38	38	37	37	32
STEP	31	32	32	33	100	40	57	34	40	34	34	32	35	34	33	34	30
SHP1	36	35	36	39	40	100	38	39	62	40	43	37	38	36	36	39	28
HePTP	36	33	35	36	57	38	100	36	39	36	36	34	38	37	33	37	30
MEG2	40	42	39	41	34	39	36	100	39	39	35	37	38	40	37	37	33
SHP2	37	37	37	39	40	62	39	39	100	40	43	35	38	39	36	39	32
PEST	37	35	33	35	34	40	36	39	40	100	38	31	48	37	33	67	29
FAP-1	36	36	39	39	34	43	36	35	43	38	100	36	37	46	35	37	34
PTPD2	35	35	40	40	32	37	34	37	35	31	36	100	36	37	73	34	31
BDP1	35	33	39	38	35	38	38	38	38	48	37	36	100	41	36	50	32
PTPTYP	35	35	38	38	34	36	37	40	39	37	46	37	41	100	36	37	30
PTPD1	36	34	39	37	33	36	33	37	36	33	35	73	36	36	100	34	30
LYP	37	37	37	37	34	39	37	37	39	67	37	34	50	37	34	100	29
HDPTP	32	34	34	32	30	28	30	33	32	29	34	31	32	30	30	29	100

Table 5: PTP catalytic domain identities of 17 NRPTPs.

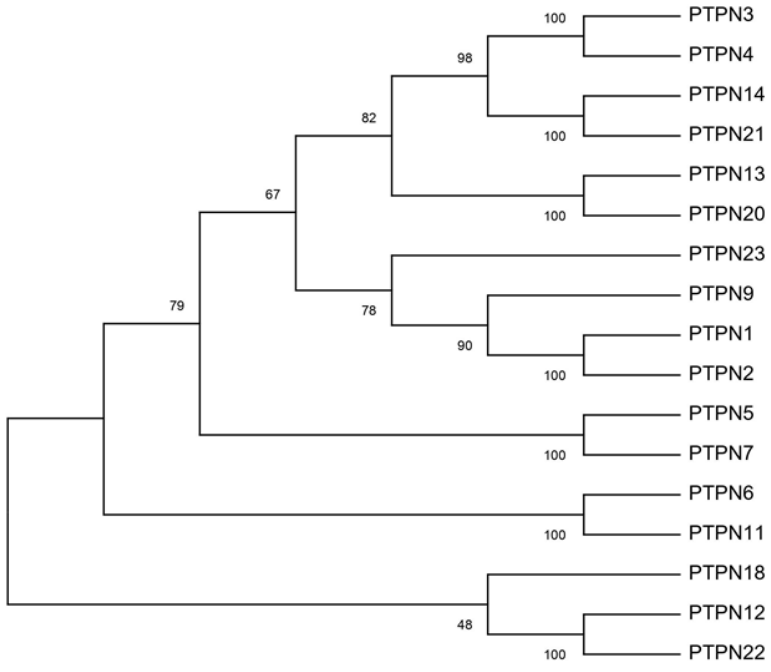

Figure 7: Phylogenetic tree of PTP catalytic domain of 17 NRPTPs.

1.5 Protein tyrosine phosphatase 1B (PTP1B)

PTP1B, encoded by *PTPN1*, is a typical NRPTP. It was first discovered in 1988 [2] and crystalized in M. Tonks laboratory in 1994 [137]. It is mainly a cytoplasmic enzyme that is also associated to endoplasmic reticulum membrane. As the most classical NRPTP, PTP1B has been well studied in many aspects, from structures to functions, as well as specific PTP1B inhibitors since it has been deemed as a promising target involved in different diseases [138-140].

1.5.1 PTP1B expression in different tissues

PTP1B is widely expressed in human tissues from the human protein atlas (THPA) (https://www.proteinatlas.org/) database. As shown in Figure 8, PTP1B protein is mainly expressed in brain, breast, colon, kidney, liver, as well as in bone marrow and lymphoid tissues. Gene expression of PTP1B is also consistent with the observation of its protein expression (Figure 9).

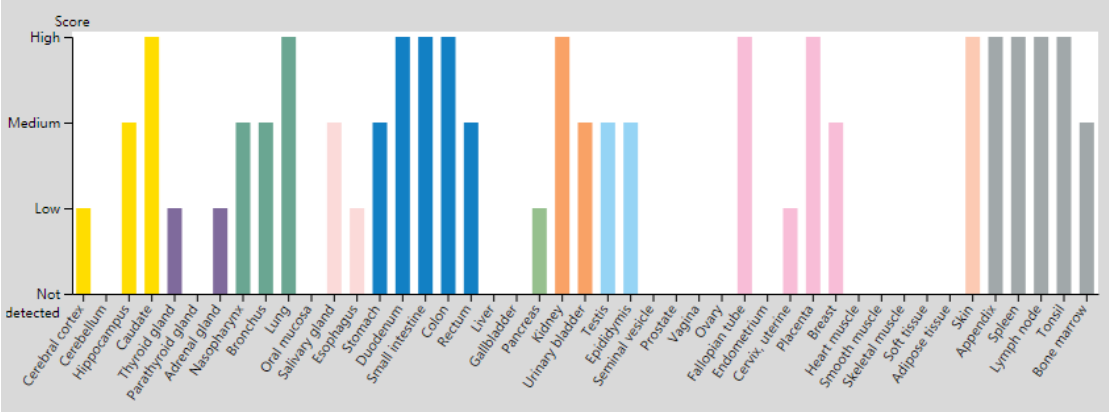

Figure 8: PTP1B protein expression in different tissues.

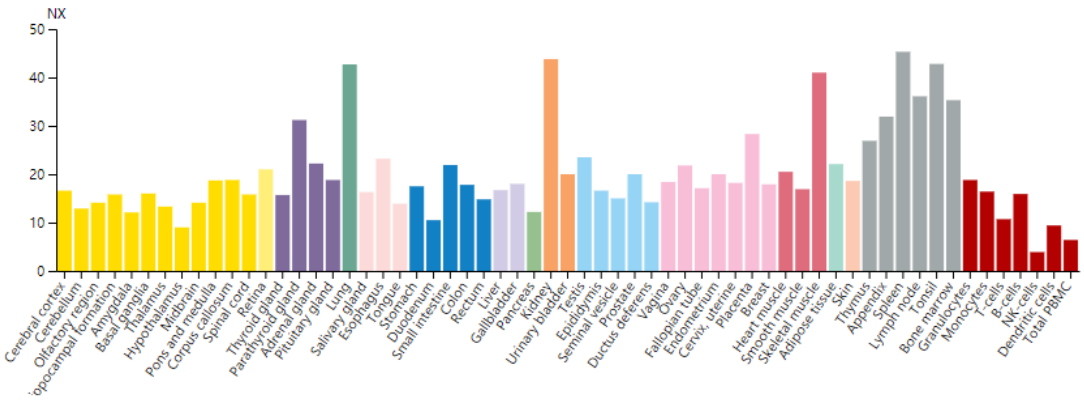

Figure 9: PTP1B mRNA expression in different tissues.

1.5.2 PTP1B involved gene ontology (GO)

PTP1B could be involved in cell growth, differentiation, metabolism process, cell cycle regulation, cell migration, gene transcription and immune response [2, 137]. PTP1B, in association with other proteins, is able to regulate several biological functions. As shown in Figure 10, PTP1B is tightly linked to EGFR, JAK2, SRC, IGF1R, IRS1, INSR, GRB2, BCAR1, CDH2 and RMDN3 by default options (https://string-db.org/). GO is shown here in order to better explain the functions of PTP1B. Three elements are included in GO: cellular component (CC), molecular function (MF) and biological process (BP). As shown in Table 6, the GO analysis indicate PTP1B is mainly involved in the function of “entry of bacterium into host cell”, “insulin-activated receptor activity” and “insulin receptor complex” regarding BP, MF and CC respectively.

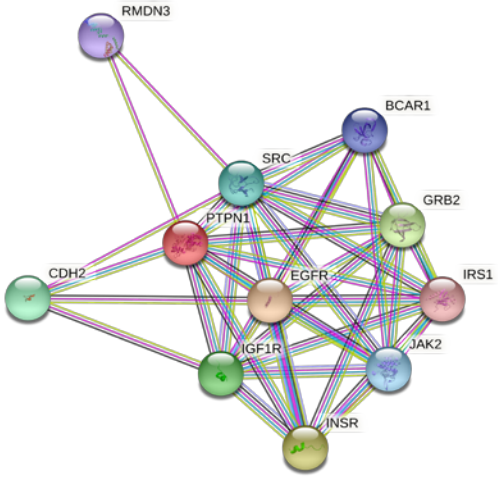

Figure 10: Gene/protein linked to PTP1B function from GO analysis.

GO	GO-term	Description	Count in network	Strength	False discovery rate
BP	GO:0035635	entry of bacterium into host cell	2 of 8	2.65	0.0019
	GO:0097062	dendritic spine maintenance	2 of 10	2.55	0.0026
	GO:2000194	regulation of female gonad development	2 of 13	2.44	0.0039
	GO:0048009	insulin-like growth factor receptor signaling pathway	2 of 13	2.44	0.0039
	GO:0048011	neurotrophin TRK receptor signaling pathway	3 of 20	2.43	7.26e-05
MF	GO:0005009	insulin-activated receptor activity	2 of 3	3.07	0.0012
	GO:0043560	insulin receptor substrate binding	4 of 10	2.85	2.81e-07
	GO:0043559	insulin binding	2 of 6	2.77	0.0025
	GO:0031994	insulin-like growth factor I binding	2 of 10	2.55	0.0044
	GO:0005158	insulin receptor binding	4 of 24	2.47	1.43e-06
CC	GO:0005899	insulin receptor complex	3 of 4	3.13	6.77e-06
	GO:0005901	caveola	4 of 78	1.96	3.78e-05
	GO:0044853	plasma membrane raft	5 of 109	1.91	6.77e-06
	GO:0045121	membrane raft	6 of 324	1.52	7.73e-06
	GO:0005925	focal adhesion	5 of 405	1.34	0.00050

Table 6: GO of PTP1B related genes.

1.5.3 PTP1B in cell signaling pathway

Given its wide and high expression in tissues, PTP1B may play an important regulator in many biological processes and diseases, ranging from non-tumor diseases (e.g. type 2 diabetes mellitus (T2DM), alzheimer's disease) to malignancies (e.g. hematopoietic system diseases, colorectal cancer, breast cancer). It has been well shown that PTP1B participates in many signaling pathways (Figure 11).

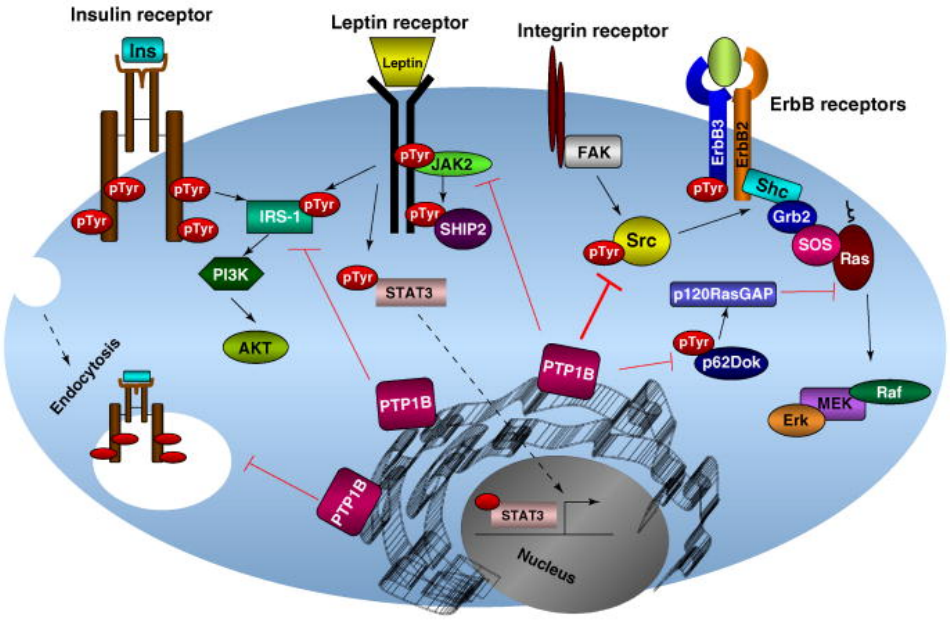

Figure 11: Signaling pathway involving PTP1B [141].

1.5.3.1 PTP1B in insulin pathway

Insufficient secretion or aberrant signaling of insulin is involved in diabetes, notably in T2DM. Insulin is secreted from pancreatic β cells and is the main hormone regulator that mediates glucose homeostasis. The function of insulin is to allow the storage of nutrients, regulated by insulin receptor (IR) [142]. Briefly, insulin can activate IR located on the plasma membrane of the cell, leading to the phosphorylation of substrates, such as PI3K [143]. The phosphorylated PI3K could further activate the downstream target AKT. Several studies have indicated PTP1B is associated with insulin signaling transduction [144, 145]. Results have shown that in PTP1B-deficient (PTP1B-/-) mice, insulin sensitivity and glucose tolerance are

improved, and the phosphorylation of IR in muscle and liver is also increased, indicating that PTP1B is a major tyrosine phosphatase enzyme acting on IR [146, 147]. Indeed, PTP1B can dephosphorylate the key tyrosine residues of IR and IRS, thereby inhibiting the insulin signaling pathway and inducing the occurrence of T2DM [148, 149].

1.5.3.2 PTP1B in leptin pathway

Obesity is a metabolic disorder with characteristics of increased tissue fat and high risk of hypertension [150]. In obesity, leptin resistance happens notably, with reduced sensitivity to leptin signaling. Leptin is a hormone derived from fat cells that controls energy homeostasis. Its function is to inhibit food intake and increase energy consumption [151, 152]. Generally, leptin signaling is activated by the interaction of leptin and leptin receptor, phosphorylation of janus kinase 2 (JAK-2), recruitment and phosphorylation of the downstream targets such as signal transducer and activator of transcription 3 (STAT3) [153, 154]. It has been reported that PTP1B is involved in leptin signaling through dephosphorylation of JAK2-STAT3 at tyrosine sites [42, 44], thereby inhibiting and reducing the activation of leptin signaling pathway. Animal studies have shown that in the PTP1B-deficient (PTP1B-/-) mouse model, both insulin signaling pathway and leptin signaling pathway are enhanced, with more energy consumption and reduced body weight [155]. Given the role of PTP1B in insulin and leptin transduction, PTP1B inhibitors have been studied for many years although none of them have been used in clinics.

1.5.3.3 PTP1B in integrin pathway

Integrins are heterodimeric receptors that depend on Ca^{2+} or Mg^{2+}. Currently 18 α subunits and 8 β subunits of integrins have been described. Integrins allow cells to adhere to the extracellular matrix (ECM) and adapt to environmental changes by triggering various signaling pathways. In addition to adhesion, they also induce cell survival, proliferation, differentiation, and motility. Integrins play a central role in cell signaling. Once bound to their specific ligand, they will change their conformation

and activate intracellular transduction pathways involving protein kinases. One of the main targets is focal adhesion kinase (FAK), a cytoplasmic tyrosine kinase. It binds to integrins and autophosphorylates when integrins form clusters (focal adhesion). FAK then phosphorylates other downstream target proteins such as the Src or paxillin [156]. Numerous studies have indicated that PTP1B is tightly associated with integrin signaling [157, 158]. As shown in Figure 11, PTP1B could dephosphorylate pSrc as well as focal-complex proteins such as $p130^{Cas}$ at tyrosine sites, reducing the activation of integrin signaling, further stopping genes expression.

1.5.3.4 PTP1B in ErbB pathway

ErbB receptor tyrosine kinase families include ErbB1/EGFR/HER1, ErbB2/HER2, ErbB3/HER3 and ErbB4/HER4. ErbB receptor is a typical cell membrane receptor tyrosine kinase, which is activated after the binding of its ligand, then triggering its dimerization and its intrinsic tyrosine kinase activity [159, 160]. Because of the ErbB family complex network in signal transduction, we will focus on the EGFR signaling to state. Generally, when ligand (EGF, TGF-alpha, etc.) interacts with EGFR, this results in the activation of EGFR signaling, phosphorylating proteins at tyrosine sites mainly in three different ways, including phosphorylation of PI3K-Akt-mTOR signaling, phosphorylation of STAT directly, and interaction with growth factor receptor-bound protein 2 (Grb2) and then phosphorylation of downstream Raf-MEK-ERK signaling. In addition to their functions as kinases, ErbB family proteins could also act as transcription regulators in cellular nucleus. For example, EGFR can be transported to the nucleus, where it phosphorylates and stabilizes proliferating cell nuclear antigen (PCNA) [161].

Many studies have pointed out that PTP1B, which play the opposite role of EGFR by dephosphorylation at tyrosine sites, is involved in the EGFR regulation [162, 163]. As stated, PTP1B could decrease EGFR signaling by dephosphorylating EGFR and downstream proteins (PI3K, Akt, STAT3, ERK…), resulting in the inhibition of genes expression (c-FOS [164], c-JUN [165], COX2 [166]…) induced by EGFR. While aberrant EGFR signaling is involved in many diseases, including various types of

cancers [167-169].

1.5.4 PTP1B in diseases

So far, a great number of studies have shown that PTP1B is aberrantly expressed in many types of malignancies, acting as a vital oncogene or suppressor in different cancer types [170, 171]. Besides, PTP1B is also related to diabetes mellitus, obesity, hypertension, etc., shown in Table 7.

Name	Z-score	Confidence
Diabetes mellitus	6.2	★★★★☆
Obesity	6.1	★★★★☆
Hyperglycemia	5.1	★★★☆☆
Cancer	4.9	★★★☆☆
Hyperinsulinism	4.5	★★★☆☆
Breast diseases	4.3	★★★☆☆
Neurodegenerative diseases	4.2	★★★☆☆
Hematopoietic system diseases	4.1	★★★☆☆
Lipid metabolism disorder	4.1	★★★☆☆
Hypertension	4.0	★★☆☆☆

Table 7: Involvement of PTP1B in diseases (https://diseases.jensenlab.org/ Search)

1.5.4.1 PTP1B in T2DM and obesity

T2DM and obesity are genetic diseases closely related to lifestyle, with increasing impact on the quality of human life. According to the statistics, nearly 50% of patients with T2DM have obesity problems. Similarly, around 50% of obesity patients have diabetes disorders. The pathogenesis of T2DM and obesity is mainly caused by insulin resistance, insufficient insulin secretion and abnormal leptin transduction. Several PTPs have been implicated in the regulation of insulin sensitivity and energy metabolism. However PTP1B is considered to be the main PTP, and inhibition of PTP1B could improve the activity of insulin and leptin signaling greatly [172, 173]. As stated above, PTP1B dephosphorylates tyrosine residues of IR and IRS, leading to inactivation of PI3K and downstream protein kinase B (PKB/Akt), and finally to the

modulation of insulin pathway [143, 148, 174, 175]. It has been shown that PTP1B overexpression in pancreatic cells could decrease insulin secretion [176], which indicates that PTP1B inhibition could improve glucose-stimulated insulin secretion [177]. In addition, PTP1B can act on leptin receptor (ObR), and also dephosphorylate and inactivate the leptin receptor-related JAK-2 and STAT3, finally modulate leptin signaling [143, 178]. All together, PTP1B appears a potential therapeutic target for T2DM and obesity. However, so far, there is still no specific PTP1B inhibitor in clinical trial in treating T2DM and obesity.

1.5.4.2 PTP1B in cancers

There is growing evidence that PTP1B is involved in cancers. It has both inhibitory and promoting effects on tumors growth, mainly depending on the tumor types and cell environment (Figure 12) [171]. The anti-tumorigenic effect of PTP1B could be mainly mediated by four ways [171]. First, PTP1B could directly interact with a specific oncoprotein and/or modulate downstream signaling pathways. The oncogene of src, crk, and ras combine with $p130^{Cas}$, which is a reported substrate and binding partner of PTP1B, mediating the tumors suppressing effects of PTP1B in different circumstances [179]. Second, PTP1B can also promote apoptosis by the down-regulation of pro-survival RTK signaling [180, 181] and the enhancement of ER stress signaling [182], or facilitating caspase 8/9 activities [183]. Third, PTP1B strengthens cell–cell interactions by dephosphorylating β-catenin and inducing the formation of the N-cadherin–β-catenin complex [184, 185], regulating tumor cell invasion and metastasis [186]. Fourth, genetic ablation of PTP1B was found to accelerate lymphomagenesis of p53-null mice through the regulation of B-cell development [41].

The controversial role of PTP1B in tumor development is also highlighted by the fact that it is described as a tumor promoter, depending on the different tumor types and circumstances. First, PTP1B has been reported to promote growth and invasion of cancer cells in a c-src-dependent manner in colon cancer [187] and breast cancer [188]. However, it is still unclear if this action on c-src is direct or indirect as several

laboratories seemingly reported opposite findings on the association of c-src with PTP1B substrate trapping mutants [171]. Second, it has been shown that PTP1B could negatively regulate the IL-4/JAK/STAT6 signaling pathway, which is known to mediate antitumor effects in carcinoma and lymphoma cell lines [189]. Third, specific overexpression of PTP1B in the mammary gland can induce spontaneous breast cancer development, supporting that PTP1B can act as an oncogene on its own [190]. Moreover, the strong correlation between PTP1B and ErbB-2 elevated expression in mammary carcinomas suggests that they may collaborate in tumorigenesis [191, 192].

To better explain the complex role of PTP1B in the pathology of various tumors, gene expression profiling interactive analysis (GEPIA) database has been used to compare the expression of PTP1B in tumor cells and normal cells [193]. Three kinds of solid carcinoma were chosen randomly (glioblastoma multiforme: GBM; lung adenocarcinoma: LUAD; pancreatic adenocarcinoma: PAAD), presenting PTP1B expression in normal and tumor cells, as well as survival plots in corresponding normal and tumor patients. As shown in Figure 13, the expression of PTP1B in different cancer types are not consistent, which indicates PTP1B could play the role of tumor suppressor or tumor promoter, depending on its localization environment. Meanwhile, no significance of survival plots were observed in GBM, LUAD and PAAD.

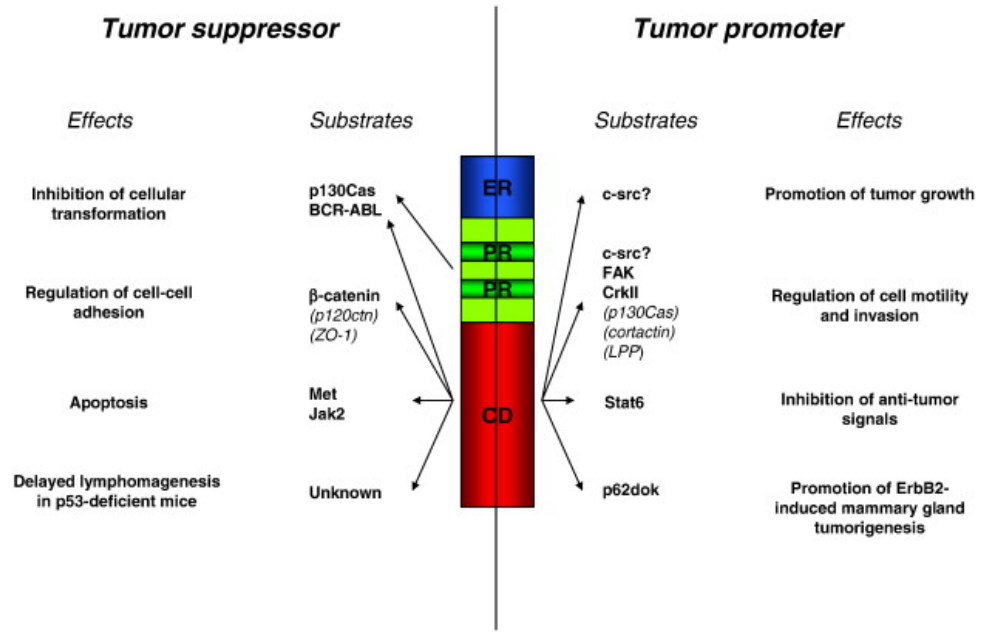

Figure 12: Schematic representation of the "two faces" of PTP1B in cancer, with its substrates and effects respectively [171]. ER: C-terminal hydrophobic tail anchored in the endoplasmic reticulum. PR: Proline-rich motif. CD: Catalytic domain.

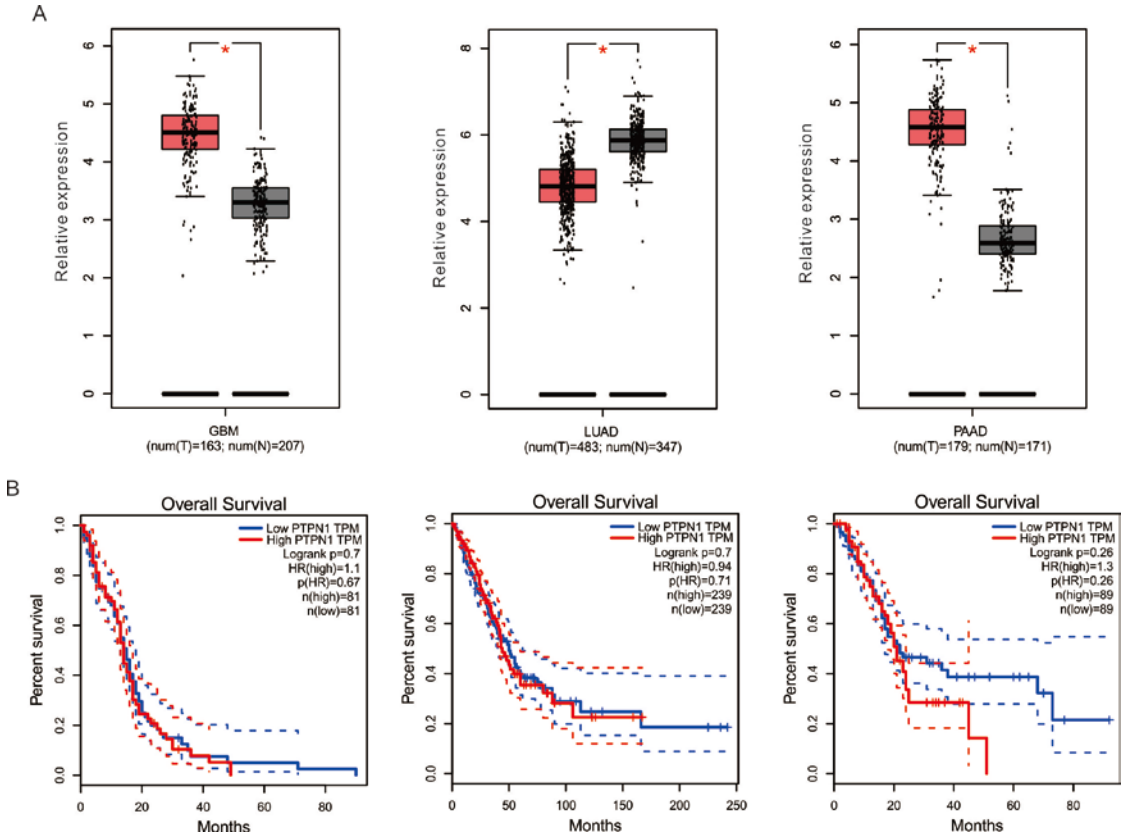

Figure 13: Relative expression of PTP1B (A) and corresponding survival plots (B) in GBM, LUAD and PAAD respectively

1.5.4.3 PTP1B in neurodegenerative disease

Neurodegenerative diseases, such as Alzheimer's disease (AD), Parkinson's disease (PD) and amyotrophic lateral sclerosis, are widespread over the world and their pathologic mechanisms remain unclear. Recently, studies have reported that PTP1B is a promising therapeutic target for neurodegenerative diseases by decreasing its expression [194, 195]. AD is an inflammatory neurodegenerative disease linked to amyloid beta and tau pathology. Inflammation activates PTP1B to block insulin signaling, which is required for neurons to form new synapses involved in memory process. Besides, evidence also suggest that ER stress plays a critical role in the pathogenesis of AD, while PTP1B is known to regulate the ER stress signaling pathway [196]. Therefore, it is believed that PTP1B is closely associated to AD. Alexandre F R Stewart *et al*. have mentioned the possible PTP1B signaling pathways involved in the regulation of AD (Figure 14) [195]. Concerning PTP1B in PD, less studies have been conducted. Similar to AD, neuroinflammation may play a critical role in PD progression, such as inflammatory cytokines [197] and ER stress [198, 199]. Chien-Wei Feng *et al*. developed a putative diagram to describe the inhibitory effect of PTP1B in PD, by showing the evidence of IFN-γ induced neuroinflammation, and suggesting IFN-γ could increase PTP1B expression and further modulate downstream cascade. Moreover, treatment with 6-hydroxydopamine (6-OHDA) could affect PTP1B and its downstream neuroprotection-related pathway (Figure 15) [200]. These results support that PTP1B could potentially contribute to AD/PD via various ways, most possibly by anti-neuroinflammation pathway.

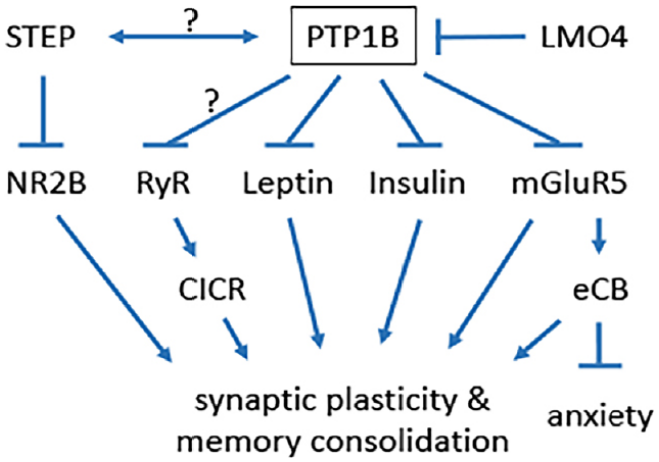

Figure 14: Pathways affected by neuronal PTP1B activation in Alzheimer's disease progression. (STEP, also called PTPN5; LMO4, LIM domain only 4; NR2B, also called GluN2B; CICR, calcium-induced calcium release; RyR, ryanodine receptor; eCB, endocannabinoid) [195].

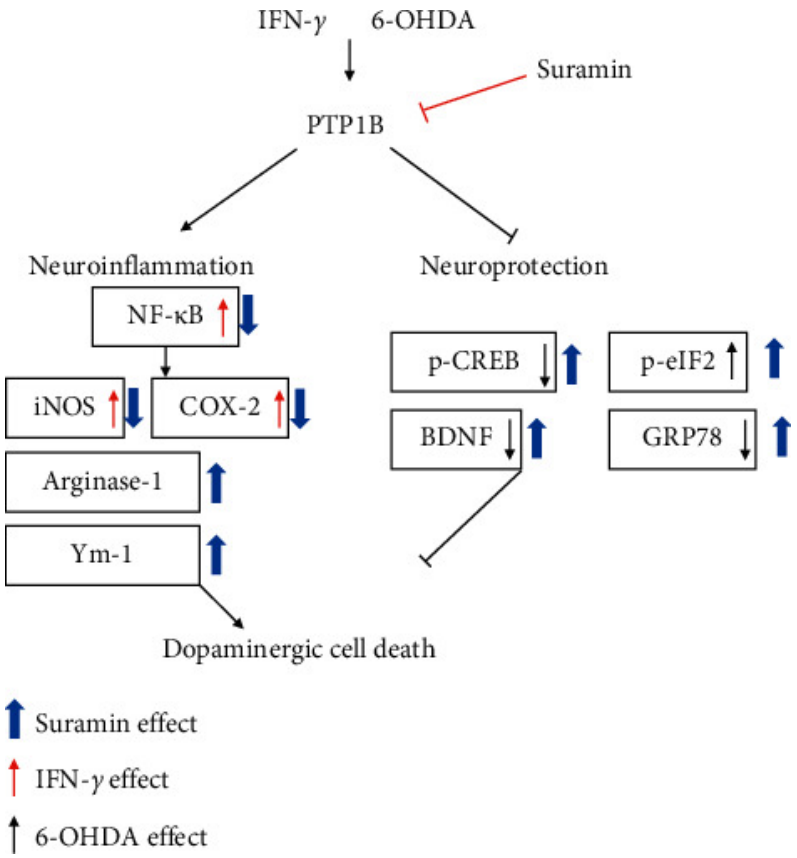

Figure 15: Schematic diagram of PTP1B in IFN-γ-induced neuroinflammation and 6-OHDA-induced neuronal death. (6-OHDA, 6-hydroxydopamine; p-CREB, phospho-cAMP response element-binding protein; p-eIF2, phospho-eukaryotic initiation factor 2; BDNF, brain-derived neurotrophic factor; GRP78, binding immunoglobulin protein) [200].

1.5.4.4 PTP1B in hematopoietic malignancies

Hematopoietic stem cells (HSCs) belongs to adult stem cell in the blood system. It is a heterogeneous group with long-term self-renewal ability and potential to proliferate and differentiate into various types of functional cells of the circulatory system [201, 202], including embryonic stem cells, somatic stem cells, totipotent stem cells (TSCs), pluripotent stem cells (PSCs) and unipotent stem cells (USCs), myeloid and lymphoid progenitors [203]. Therefore, any alteration of the differentiation of these functional cells by genetic disorders, microenvironment changes or external interference may cause hematological system disorders, such as leukemia, lymphoma and other malignancies [50].

Hematopoietic system diseases result from the imbalance between blood cells production and destruction, as well as possibility of heredity. Due to their aggressiveness pathology and treatment resistance, hematopoietic malignancies have become one of the most serious cancers that need to be deeply explored. Clinically, chemotherapy is administered for the treatment of hematopoietic malignancies. In the meantime, hematopoietic stem cell transplantation (HSCT) can be considered after the first complete remission (CR) following chemotherapy, when patients have an acceptable physical condition with a high cure rate, low recurrence rate, high tolerance and fewer complications. But for the treatment of hematopoietic malignancies, an autoimmune rejection action may occur when patients undergo HSCT.

Michelle H Townsend *et al*. have summarized some biomarker targets (CD5, BCMA, CD33, CD38, CD70, and IL13Rα2) for CAR therapy utilized to treat hematological malignancies in clinical trials (Figure 16) [204]. Interestingly, they are not cancer-specific and express in normal cells, but they have an elevated expression in cancer that is being used for targeting. Apart from the known targets, some other targets have been shown, like PTP1B, which is aberrantly expressed in hematopoietic malignancies [11, 41, 44]. For instance, the interleukin (IL)-4-JAK-STAT6 signaling pathway is of importance in the growth of lymphoma cell lines and PTP1B has been confirmed to be a negative regulator of this pathway, leading to overexpression of

PTP1B in B-cell lymphoma cells could silent the IL-4-JAK-STAT6 signaling so as to make the tumor cells out of control [189]; K562 is a chronic myeloid leukemia (CML) cell line with positive bcr-abl fusion protein, and PTP1B can promote the differentiation of K562 cells [205]. Drugs or siRNA known to reduce the expression of PTP1B can lead to the degradation of the bcr-abl fusion protein, thereby triggering the apoptosis of CML cells [206]. PTP1B could be deemed as a promising target in treating hematopoietic related malignancies. However, the role of PTP1B in cancer process remains complex. For example, both acute myeloid leukemia (LAML) and lymphoid neoplasm diffuse large B-cell lymphoma (DLBC) belong to hematopoietic malignancies, but the expression of PTP1B in LAML and DLBC is different (Figure 17). Importantly, patients with low PTP1B expression could survive longer than patients with high PTP1B expression in LAML, with statistical significance. All together, PTP1B could be used as a promising therapeutic target in certain hematopoietic malignancies.

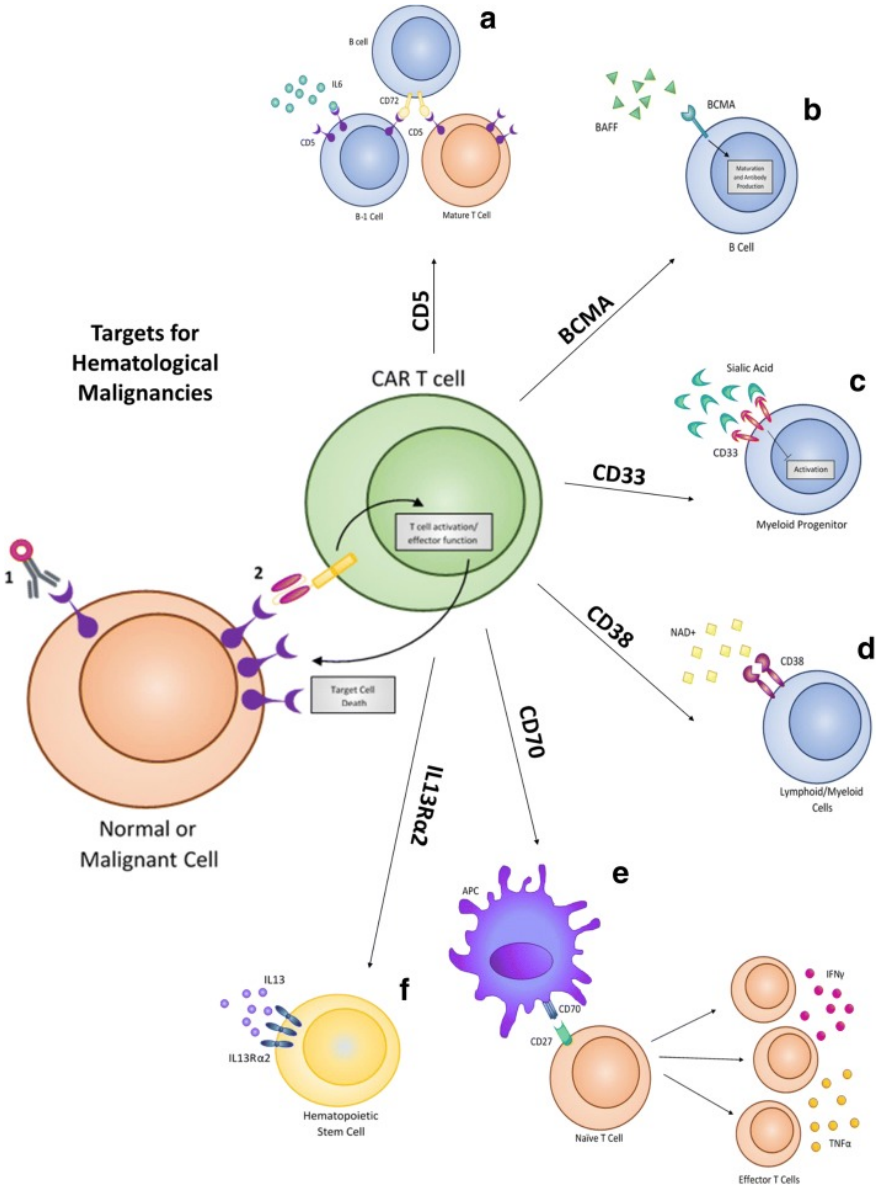

Figure 16: Biomarker targets for CAR therapy in hematological malignancies [204].

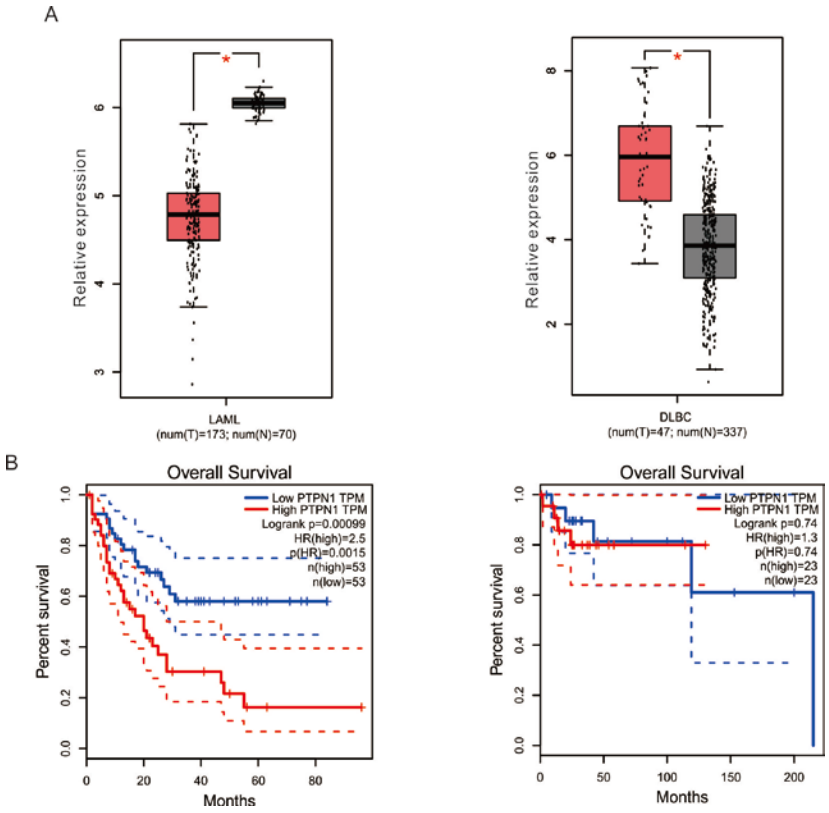

Figure 17: Relative expression of PTP1B (A) and corresponding survival plots (B) of patients in LAML and DLBC.

1.5.5 PTP1B structures

PTPN1 gene codes for PTP1B protein and is mapped to human chromosome 20 q13.1 ～ 13.2. At this site, gene augmentation or amplification have been found in numbers of cancers [207, 208]. Human *PTPN1* gene has 74×10^3 bp in length, with a total of 10 exons. Its cDNA encodes a protein of 435 amino acids and the relative molecular weight of the PTP1B protein is around 50 kDa [209].

So far, around 300 PTP1B related structures have been released in PDB database (https://www.rcsb.org/). Most of them are the short forms (residues from 1-298 or 1-321), corresponding to the catalytic domain. The first PTP1B structure (residues from 1-321, PDB code: 2HNP) was solved by Tonks and his collaborators [137]. It is composed of at least 8 alpha helices and 12 beta strands. Though the following PTP1B structures have been released with better resolution, no significant difference is observed compared with the first one.

1.5.5.1 PTP1B regulatory domains

Briefly, PTP1B contains 3 domains: N-terminal catalytic domain, proline-rich domain and C-terminal ER targeting domain. PTP1B can be regulated by four post-translational mechanisms, sometimes working in tandem, including phosphorylation of serine and tyrosine residues, oxidation at cys215, sumoylation as well as proteolysis (Figure 18) [141].

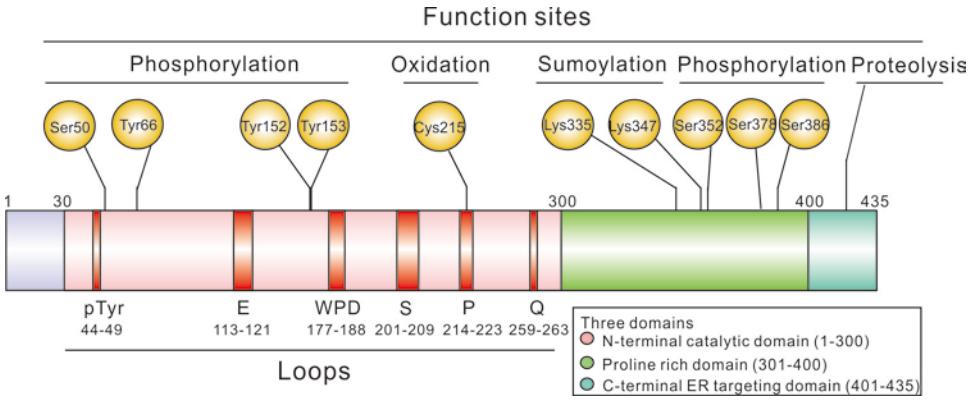

Figure 18: Schematic representation of the domain structures of PTP1B full length. It is composed of an N-terminal catalytic domain (1-300) and C-terminal ER targeting domain (401-435), flanking two proline-rich domains (301-400), with multiple functions at different sites of PTP1B [141, 210-213].

1.5.5.1.1 N-terminal catalytic domain of PTP1B

N-terminal catalytic domain is indispensable for catalytic activity of PTP1B. PTP1B activity could be regulated by two main post-translational mechanisms, including phosphorylation of serine and tyrosine residues at various sites, as well as oxidation at Cys215 in response to ROS. Phosphorylation of PTP1B at Ser50 by AKT, can decrease PTP1B activity and impairs its ability to dephosphorylate the IR *in vitro*. In addition to serine phosphorylation, tyrosine phosphorylation of PTP1B located at residues of 66, 152 and 153, can be induced by insulin signaling. PTP1B Tyr66 has been identified as one of the major insulin-stimulated tyrosine phosphorylation sites *in vivo* [214], negatively regulating insulin pathway. Besides, the sequence surrounding Tyr66, ^{66}YINA^{69}, conforms to the consensus binding site (YXNX) for the Src homology 2 (SH2) domain of Grb2 [215], which could interact with intracellular

receptor substrate 1 (IRS-1), thus activating Ras and MAPK pathway [216]. By replacement of Tyr152 and Tyr153 by Phe152 and Phe153 respectively, insulin-stimulated phosphorylation of PTP1B could be inhibited by association with the IR. PTP1B can react with the IR by either directly or within a complex involving additional proteins in normal cells [217]. As with Ser50, phosphorylation at these tyrosine sites has been reported to either increase or decrease PTP1B catalytic activity [141].

Oxidation of reactive cysteine residues is an important modification that can determine the extent and duration of phosphotyrosine-dependent signaling responses. Indeed, PTP1B activity could be abolished when Cys215 is oxidized. Usually, the chemical environment of Cys215 is acidic (pKa 4.5 - 5.5, compared to a pKa of a typical Cys being ~8.5) [141]. At physiological condition (pH 7 - 7.5), this residue is deprotonated, resulting in an enhanced nucleophilic activity in catalysis and increasing possibility to be oxidized by H_2O_2 to sulphenic acid (-SOH) which renders PTP1B inactive [12, 218]. The sulphenic group on cysteine will condense with its adjacent amine group of n+1 peptide residue to become a sulphenylamide, resulting in an isothiazolidine ring on the peptide backbone [219, 220]. At the sulphenylamide step, PTP1B enzyme activity can be restored by thiol reducing agents, such as glutathione (GSH) or dithiothreitol (DTT), to its active thiolate anion stage (Figure 19A). Thus, a mild oxidation on the catalytic cysteine of PTP1B is considered reversible, although the oxidation itself involves formation of covalent bonds. If the sulphenic group on PTP1B is further oxidized to sulphinic acid ($-SO_2H$) or sulphonic acid ($-SO_3H$), PTP1B enzyme activity is irreversibly lost (Figure 19A) [12, 219]. Rob L. M. van Montfort *et al*. have reported structures of the sulphonic, sulphinic, sulphenic acid derivatives and the reduced state of Cys215 (Figure 19B) [219]. In contrast to the sulphenylamide derivative, the structures of these oxidation states are very similar to the structure of reduced PTP1B.

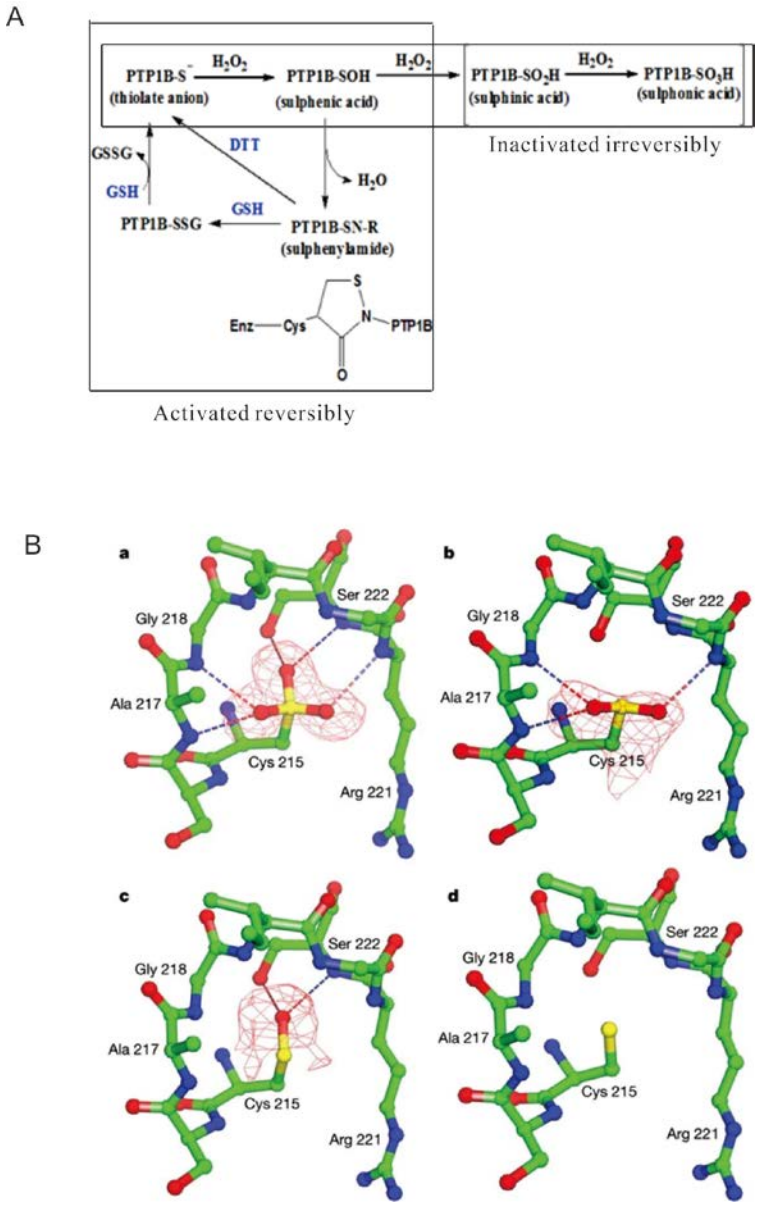

Figure 19: Oxidized status of PTP1B. A: reversible and irreversible oxidation of cysteine thiol on PTP1B; B: structures of the sulphonic (a), sulphinic (b), sulphenic (c) acid derivatives and the reduced state (d) of Cys215. The phosphate-binding cradle comprising residues 215–222 is shown in ball-and-stick representation. Hydrogen bonds are shown as dashed lines [219].

1.5.5.1.2 Proline rich domain of PTP1B

Proline-rich domain or C-terminal domain, contains two proline-rich motifs, spanning from Pro301 to Arg315, and from Ser386 to Lys397 [210]. It is identified as a binding site for Src homology 3 (SH3) domain-containing proteins like $p130^{Cas}$, Grb2, Crk, and Src [141, 179]. This domain is believed to endow substrate specificity

to PTP1B. Although substitution of some key proline residues in this domain does not facilitate PTP1B to dephosphorylate the IR, it abolishes the ability of PTP1B to bind to and activate Src [141, 179, 221, 222]. In addition, PTP1B can also be phosphorylated by protein kinase C (PKC) at Ser378, and at Ser352 and Ser386 by an unknown kinase in a cell cycle dependent manner, but without markedly change in PTP1B activity [223, 224]. Meantime, sumoylation was also reported at Lys335 and Lys347. Although the solved crystal structures of PTP1B do not include residues beyond 321, sumoylation at these sites may alter the conformation of PTP1B because of the steric hindrance, thus reducing interaction with the substrates and reduction in enzymatic activity [141, 225].

1.5.5.1.3 C-terminal ER targeting domain of PTP1B

In cells, PTP1B activity is strictly associated with the ER by post-translational C-terminal attachment of PTP1B to the ER membrane network. Removal of up to seven amino acids from the C-terminus and exchange of single amino acid in the putative transmembrane sequence have no obvious influence on subcellular localization of PTP1B [226, 227]. Additionally, it is reported that calpain-mediated cleavage of the C-terminal of PTP1B, is to proteolysis *in vivo*, activating platelets to produce an activated, soluble enzyme [228]. Meanwhile, disruption of calpain-1 could not only result in platelet aggregation and clot retraction, but also an overall reduction in protein tyrosine phosphorylation in mice [229, 230].

1.5.5.2 PTP1B functional loops

PTP1B architecture is formed by six conserved loop regions, which are responsible for substrate recognition, binding and catalysis (Figure 20) [231]. (1) The phosphotyrosine recognition loop, also called pTyr loop, contains a conserved motif, providing specificity for pTyr in classical PTPs; (2) the E loop, which contains multiple conserved residues, coordinates the dynamics of the WPD loop; (3) the WPD loop, which contains the catalytic amino acid tryptophan, proline and aspartate, presents two different conformations depending on ligand binding; (4) as for the S

loop, reduced mobility of the WPD loop is accompanied with reduced mobility in the S loop, further emphasizing the importance of the S loop for WPD loop movement as well as catalytic activity of PTP1B; (5) the hallmark that defines the PTPs is the conserved signature motif with catalytic cysteine and the invariant arginine, involved in P loop; (6) the Q loop, which contains a conserved glutamine, own the ability of hydrolysis when coordinating with water molecule. The position of those loops varies slightly based on different studies.

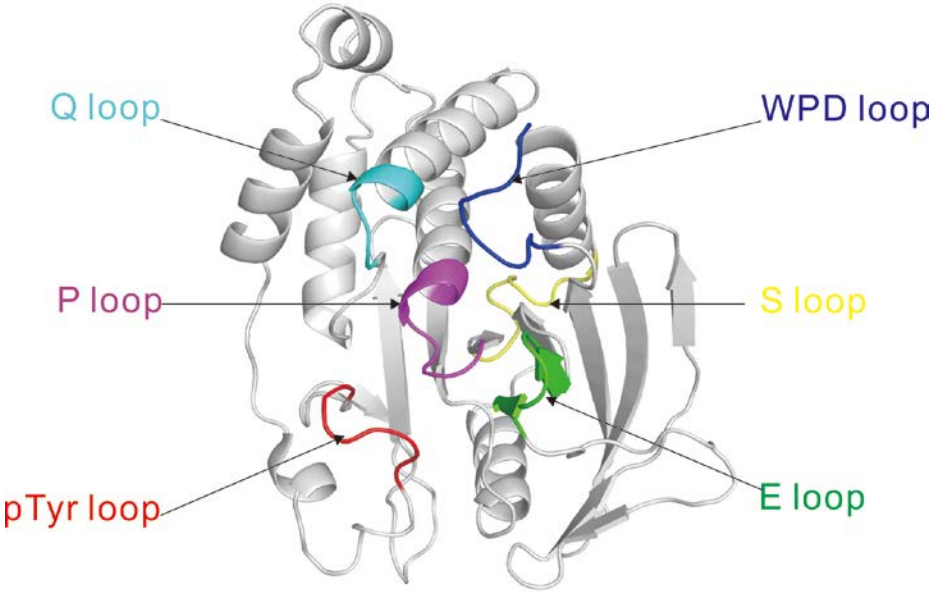

Figure 20: Overall structure and functional loops of PTP1B (PDB code: 2HNP, open form).

1.5.5.2.1 pTyr loop

The pTyr loop (Asn44-Val49) is a relatively conserved loop structure that is present in all classical tyrosine-specific phosphatases [232] (Figure 21). The pTyr loop delineates the boundaries of the active site binding pocket and define the depth of the active site crevice [233], thus contributing to substrate recognition and increased selectivity for pTyr over the shorter phosphoserine or phosphothreonine [233, 234]. Among all the residues in the loop, the conserved residues, Asn44-Arg45-Tyr46, are most likely to be involved in substrate recognition and loop stabilization. The conserved Tyr46 has not only a notable role in defining the active cleft depth, but also

forms aromatic π-π interactions with the substrate pTyr residue, facilitating access to the active site [235]. The guanidinium group of the highly conserved Arg45 is implicated in the loop stabilization, by interaction with nearby backbone oxygen atoms. Besides, the surface-exposed side chain of Arg45 may also act as a substrate binding site. The adjacent moderately conserved Asn44, can strengthen the interactions between the substrate pTyr and active site residues by forming a bipartite hydrogen bond with the nitrogen atoms of pTyr of the substrate and nearby residues [236].

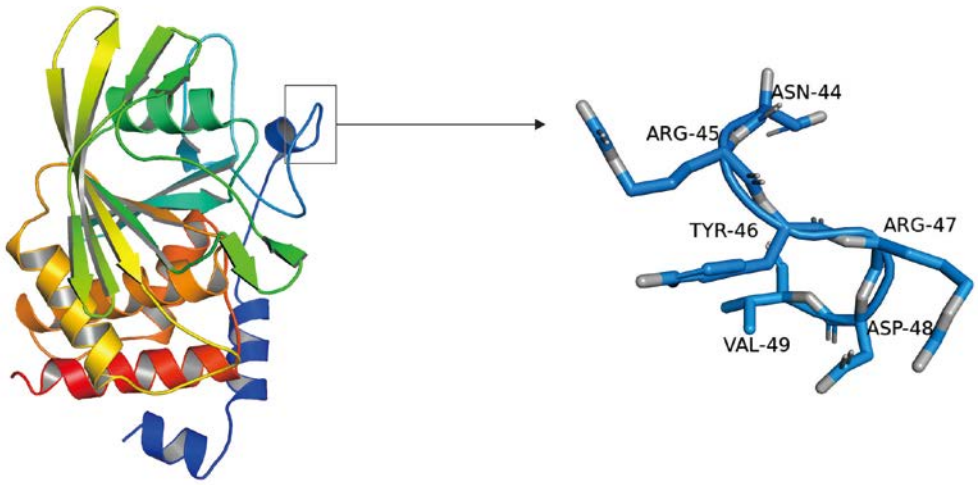

Figure 21: pTyr loop of PTP1B with corresponding residues (PDB code: 2HNP, open form).

1.5.5.2.2 E loop

The E loop (Val113-Cys121) is immediately contiguous to the P loop and WPD loop in crystal structure and is conserved in most human PTPs [47, 210] (Figure 22). The E loop contains a 100% conserved glutamate at residue 115 and an 89% conserved lysine at residue 120, which are only present in the pTyr-specific PTPs. In most PTP structures, the E loop forms a tight beta-hairpin, interacting with P loop and WPD loop. The conserved glutamate could form a bipartite hydrogen bond with the side chain of arginine at the residue 221 in P loop, which is found in nearly all of the reported classical PTP structures, stabilizing the guanidinium group in a position that

favors phosphate binding to the P loop [237, 238]. Besides, the less conserved lysine could form a hydrogen bond with a catalytic aspartate at the residue 181 in WPD loop at its closed conformation, maintaining the WPD loop in its closed and substrate-bound conformation [239]. Indeed, mutating this residue to alanine results in reduced catalytic efficiency in HePTP [239].

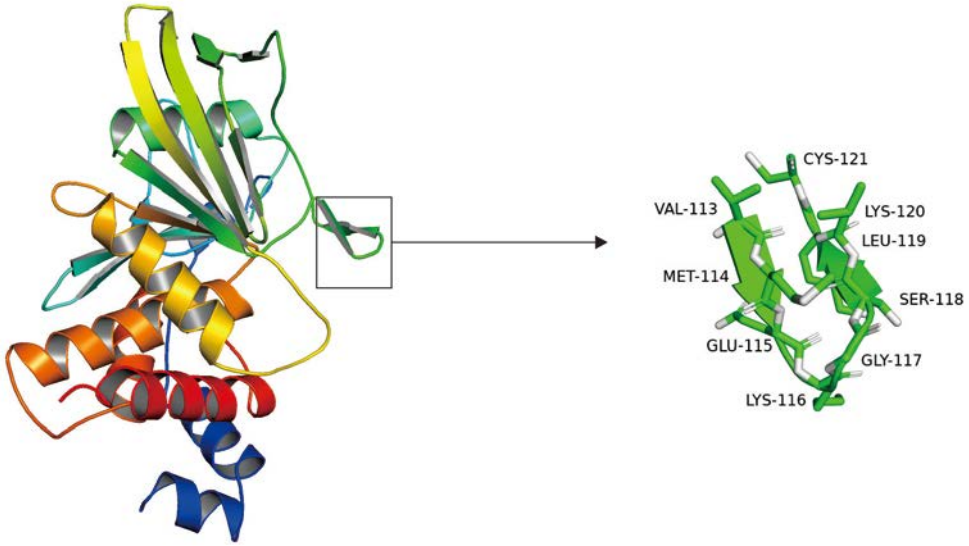

Figure 22: E loop of PTP1B with corresponding residues (PDB code: 2HNP, open form).

1.5.5.2.3 WPD loop

The WPD loop, spanning from Thr177 to Pro188, with a 100% conserved tryptophan (Trp179) and 97% conserved proline (Pro180) and less conserved aspartate (Asp181), exists in all pTyr-specific PTPs [49] (Figure 23A). It is a flexible loop in the PTP domain, acting as a regulatory switch with open and closed conformation [240]. When the WPD loop is in open form, which means there is no ligand/substrate binding, the WPD loop would likely fluctuate between open and closed conformation (Figure 23B) [241]. In the presence of ligand/substrate, the WPD loop moves close to the P loop so as to participate in catalysis. Among all the three essential residues, tryptophan and aspartate are much more important than proline. Tryptophan has been identified as a hinge residue for WPD loop flexibility [242, 243].

Mutation of tryptophan into other residues could result in substantially lower catalytic activity [242, 243] as well as loop flexibility [231]. On the other hand, aspartate acts as a general acid catalyst in catalysis. Upon substrate binding, closure of the WPD loop to P loop brings the aspartate close to the scissile oxygen of the tyrosyl substrate, allowing it to donate a proton to the phenolate leaving group, then regulating enzyme catalysis [126]. Not surprisingly, aspartate alterations could result in a lower catalytic activity [231]

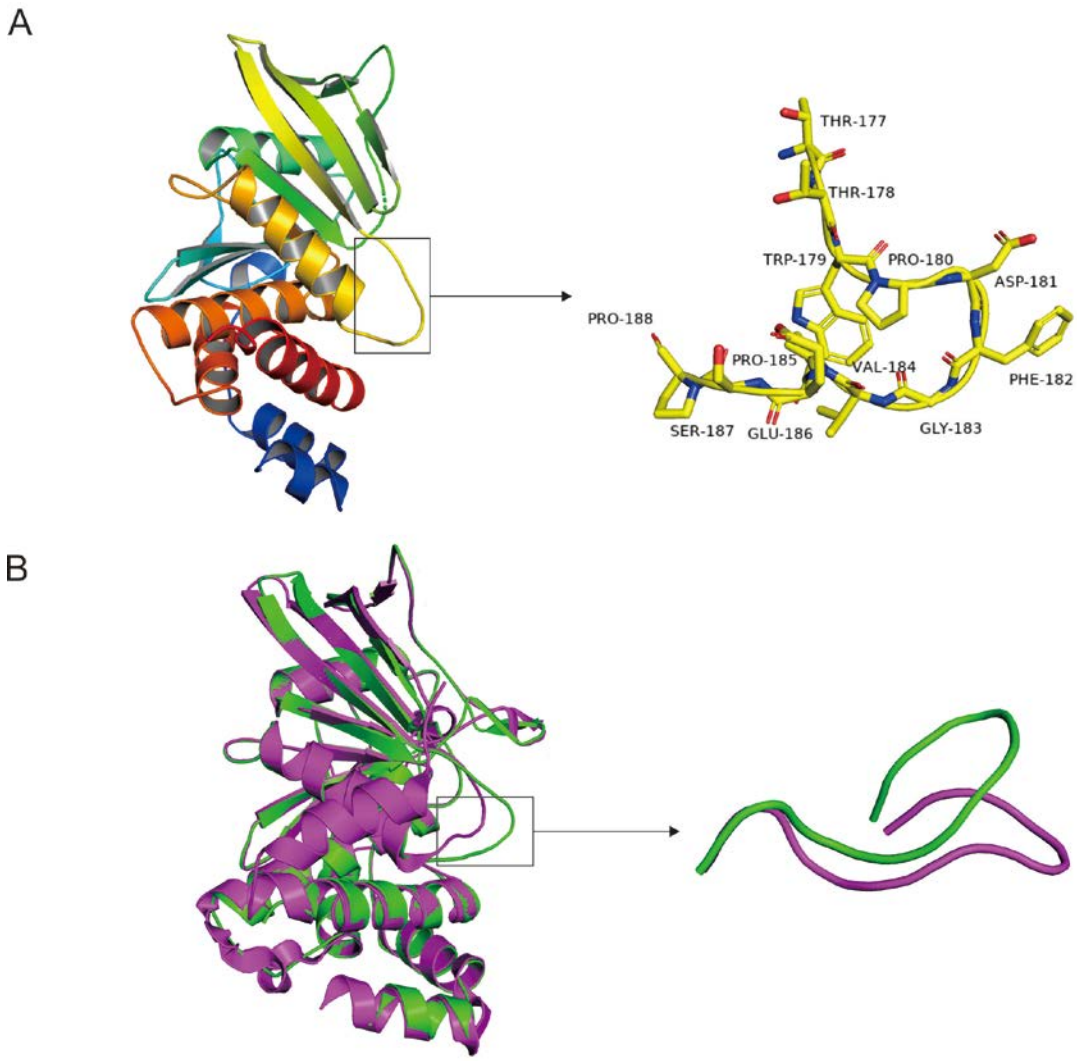

Figure 23: WPD loop of PTP1B with corresponding residues. A: WPD loop of PTP1B with corresponding residues (PDB code: 2HNP, open form); B: alignment and comparison of open form PTP1B (PDB code: 2HNP, green) and closed form PTP1B (PDB code: 1SUG, magenta).

1.5.5.2.4 S loop

The S loop of PTP1B (Ser201-Gly209) [135, 210] is less conserved and less well elaborated in the studies of PTP1B (Figure 24). But still it could move towards the active site and form a tight binding pocket for substrates when the WPD loop is in closed conformation, which is mainly contributed by Ser201, Leu204, Ser205 and Pro206 [135].

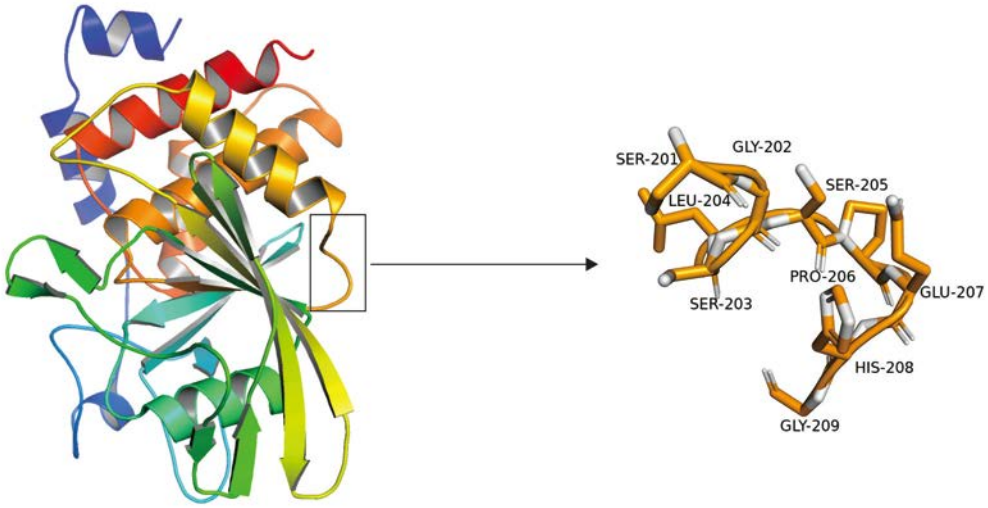

Figure 24: S loop of PTP1B with corresponding residues (PDB code: 2HNP, open form).

1.5.5.2.5 P loop

The base of the active site of most PTPs is formed by the P loop, a highly conserved loop structure ranging from His214 to Gly223 [49] (Figure 25). Among all the residues in the motif, cysteine (Cys215) and arginine (Arg221) are of great importance. Usually, the Cys215 has a pKa value of ~ 8.5, which would not allow for effective catalysis under physiological conditions because of the low nucleophilicity. While the Arg221 could create a positive charge in the active pocket, stabilizing the thiolate anion of cysteine (Cys-S^-) so as to decrease pKa value (from 4.5 to 5.5), permitting the enzyme reaction to be more efficient at physiological environment [244, 245]. Besides, the positively charged Arg221 could enhance exceptional affinity for tetrahedral oxyanions such as phosphate ions [47]. Apart from the low pKa value of

Cys215 with the effect of increased affinity and nucleophile activity, it is also more susceptible to oxidation [246], nitrosylation [247] and sulfhydration [248], resulting in the abrogation of enzyme phosphatase activity by reversible or irreversible modifications. Importantly, mutation of the catalytic Cys215 in this motif to serine or alanine abolishes all enzyme activity while maintaining affinity for substrates *in vivo* [249]. In conclusion, P loop is critical for PTP1B catalytic function.

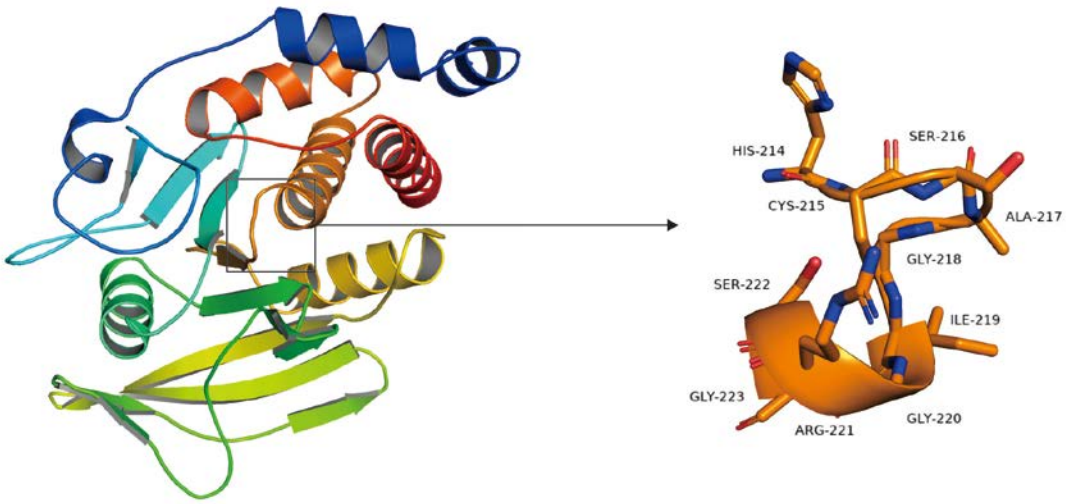

Figure 25: P loop of PTP1B with corresponding residues (PDB code: 2HNP, open form).

1.5.5.2.6 Q loop

The Q loop (Gly259-Thr263), which presents in all classical PTPs, contains a 97% conserved glutamine (Gln) at the residue 262 in PTP1B [49], moving towards the P loop and forming hydrogen bonds with an active site water as well as substrate oxygen anion (Figure 26) [212]. In addition, Gln262 contributes to the catalytic cysteine nucleophilic activity and thereby helping in cysteinyl phosphate hydrolysis. Meanwhile, Gln262 could combine with the Asp181 of the WPD loop and activate water molecules, facilitating in catalysis process of enzyme and maintaining the WPD loop in its active conformation as well [250, 251]. Mutations of the Gln262 to other residues that have no ability to form hydrogen bond with the nucleophilic water result in less restrictive enzymes and confer phosphotransferase activity [252].

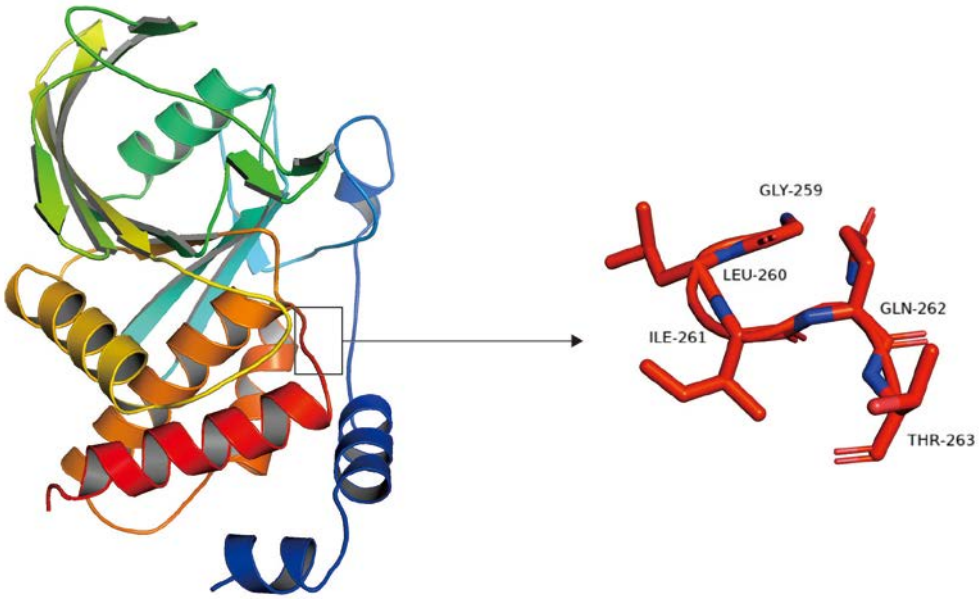

Figure 26: Q loop of PTP1B with corresponding residues (PDB code: 2HNP, open form).

1.5.6 Difference between PTP1B and TCPTP

TCPTP, encoded by *PTPN2*, is the second isolated and cloned PTPs member [253]. Like PTP1B, TCPTP belongs to classical non-receptor PTPs and exerts effects via similar tyrosine phosphatase activities. Two *PTPN2* mRNA have been found. One encodes a 48 kDa protein called TC48, which is located on the ER by the C-terminal hydrophobic domain; another encodes a 45 kDa protein called TC45, which is localized in the nucleus by a C-terminal atypical nuclear localization sequence (NLS) [254, 255]. Although TC45 is usually localized in the nucleus, TC45 gets out of the nucleus upon cell stimulation and dephosphorylates non-nucleoprotein substrates. PTP1B and TCPTP share 70% identities (Table 5) and similar substrates, like EGFR, JAK/STAT (Figure 27) [144, 256-260]. Besides, they also share the same mechanisms to some extent, but some differences do exist. For example, PTP1B knockout mice showed an increase in tyrosine phosphorylation at the site of insulin receptor of 972, 1162, 1163; while TCPTP knockout mice only displayed increased tyrosine phosphorylation at the site of insulin receptor 972, without affecting positions 1162,

1163 [144]. PTP1B has a very wide expression pattern while TCPTP is less widely expressed and is highly dysregulated in hematopoietic malignancies. Concerning their structure, though TCPTP own the unique functional loop (DDQ loop) (Figure 28A), no obvious difference has been identified in the tertiary structure between TCPTP and PTP1B (Figure 28B) [261, 262]. Although the crystal structure of the catalytic domain of TCPTP has been solved, no specific selective small molecule inhibitors of TCPTP have been found due to the high similarity between TCPTP and PTP1B. Based on the design of specific PTP1B small molecule inhibitors, the design of TCPTP selective inhibitors will be less challenging [263, 264].

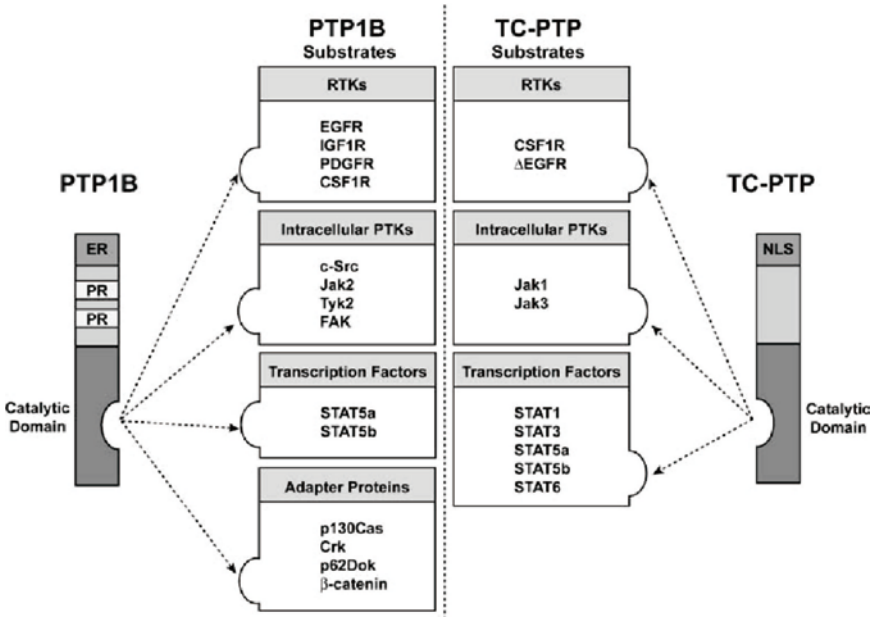

Figure 27: Schematic representation of the structures of PTP1B and TCPTP and their respective substrates linked to cancer.

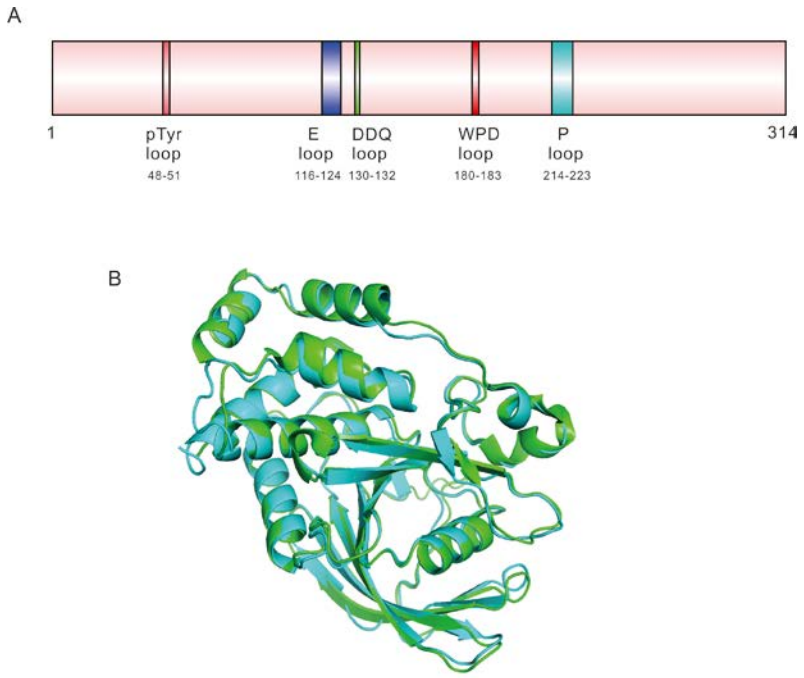

Figure 28: Schematic representation of the different key domains of TCPTP and 3D structural alignment of TCPTP and PTP1B. A: functional loops (pTyr loop, E loop, DDQ loop, WPD loop and catalytic P loop) of TCPTP TC45 form (1-314); B: alignment of PTP1B (PDB code: 2HNP, color in cyan) and TCPTP (PDB code: 1L8K, color in green).

1.5.7 PTP1B catalytic mechanism

The phosphatase activity of PTP1B occurs in P loop through 2 steps, according to the “ping-pong” mechanism shown in Figure 29 [265, 266]. In the process of catalysis, the flexible WPD loop significantly contributes to the peptide substrate recognition. When the substrate with dianionic phosphotyrosine (pTyr) residue binds, the WPD loop moves and adopts a closed conformation [249]. Cys215 in the P loop acts as a nucleophile to attack the pTyr to form a covalent thiol phosphate intermediate [267]. Meantime, Arg221 could form hydrogen bonds with pTyr to maintain the catalytically active structure of PTP1B [266]. Then conserved Asp181 in the WPD loop acts as a general acid to protonate the tyrosyl-leaving group [268, 269]. In this step, tyrosine without phosphate group is released. Then, an activated water molecule, coordinates with conserved Gln262 presented in the Q loop by hydrogen bonding interactions, attacks the phospho-cysteine intermediate (catalyzed by the same conserved Asp181

in the WPD loop as a general base) [249]. This leads the release of inorganic phosphate and regenerates the cysteine thiolate.

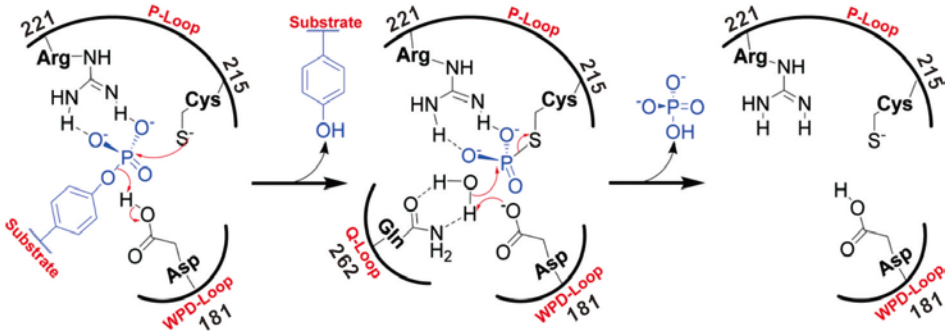

Figure 29: The two steps catalytic mechanism of PTP1B dephosphorylation [265].

1.5.8 PTP1B mutations

Gene mutation refers to a change in the base pair composition or sequence of the gene structure. Although genes are very stable and can accurately replicate themselves during cell division, this stability is relative. Genes can switch from the original sequence to another under certain conditions, resulting in the appearance of the new feature in the performance of the offspring. According to the type of mutation, it is mainly classified into substitutions, deletions and insertions.

It is widely accepted that some diseases have a genetic basis and mutations affecting the coding sequences of specific genes are hallmarks of diseases. Those genetic changes have close relationship with mechanisms of carcinogenesis, diagnosis and treatment. A great number of studies have shown that PTP1B is mutated in cancers and diabetes [9, 270, 271]. Those PTP1B mutants display a reduced activity or are completely inactive. In most cases, amino acids around pTyr loop, WPD loop, P loop and Q loop have the tendency to mutate because they are more significantly essential for substrate binding and catalytic function than other loops. Until now, more than 20 PTP1B mutants have been reported in the protein data bank (PDB), such as N193A, N185G, Y152A, Y153A, C215S, S295F, A122S, but most of them concern mutation done on purpose to study the catalytic mechanism of the enzyme [48, 272-274].

1.5.8.1 PTP1B mutations in pan-cancer

Pan-cancer projects, such as the Cancer Genome Atlas Project (CGAP), use the Next Generation Sequencing (NGS) to make a significant contribution to our understanding of DNA and RNA variations in multiple cancer types. Therefore, those mutation data from COSMIC database (https://cancer.sanger.ac.uk/cosmic) are collected. As shown in Figure 30, PTP1B is over expressed in ovary cancer (Figure 30A), with highest mutation rate in biliary tract cancer (Figure 30B). In addition, missense substitution accounts for more than half of *PTPN1* mutation types (Figure 30C), with the main substitution of base C replacement by base T (Figure 30D).

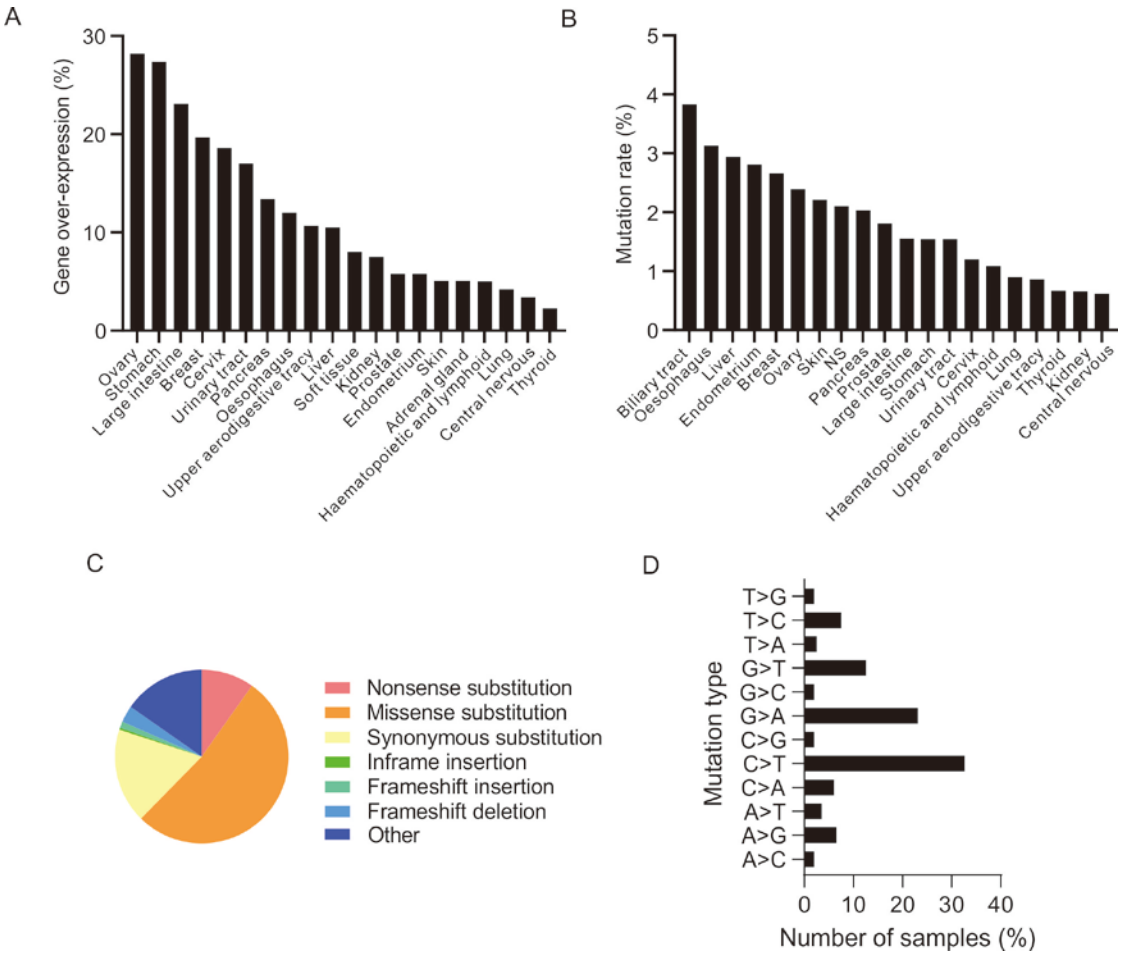

Figure 30: *PTPN1* gene mutation in pan-cancer from COSMIC database. Figure A, B, C, D represents *PTPN1* gene expression, *PTPN1* mutation rate, *PTPN1* mutation sorts as well as specific base substitution in pan-cancer respectively.

1.5.8.2 PTP1B mutations in hematopoietic malignancies

In hematopoietic malignancies, gene mutations have been deemed as a main cause. A great number of mutated genes have been discovered related to the occurrence or relapse of hematopoietic disease, like *DNMT3A*, *TET2*, *JAK2*, *TP53*, *IDH2*, *KRAS*, *NRAS*, *MYD88*, etc. [275]. Since PTP1B is expressed abnormally in certain hematopoietic diseases, it has been thought that PTP1B has the possibility to be mutated. Indeed, a variety of PTP1B mutants have been found in primary mediastinal B cell lymphoma (PMBCL) and Hodgkin lymphoma (HL), with missense substitution accounting for more than half of PTP1B mutation type (Figure 31) [9]. In addition, PTP1B mutants regarding missense substitution are listed (Table 8).

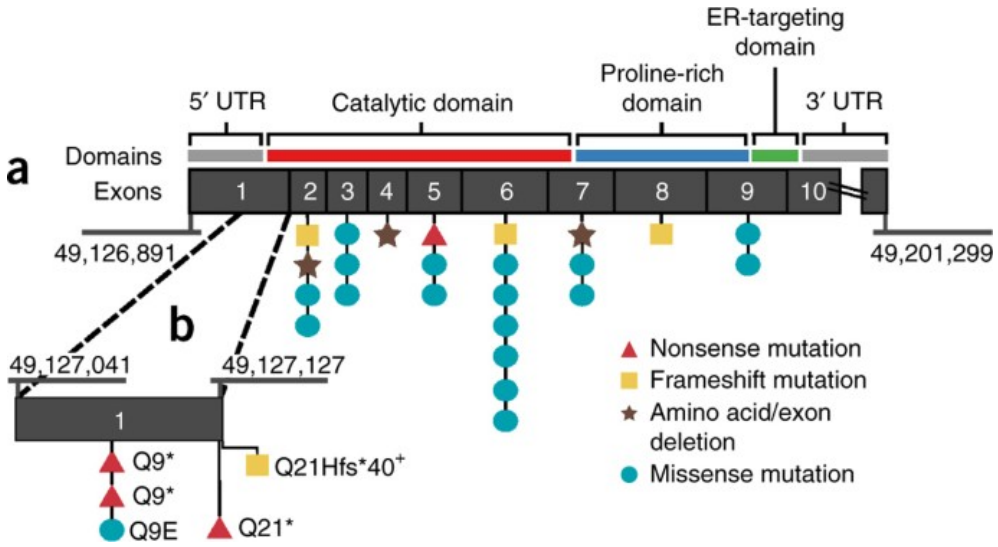

Figure 31: *PTPN1* mutations type in PMBCL and HL.

AA mutation	CDS mutation
Q9E	C>T
D22G	A>G
R45T	G>C
R56W	C>T
A69V	C>T
M74L	A>C
Q123P	A>C
T143P	A>C
H173Y	C>T
V184D	T>A
L192F	G>T
G209R	G>A
S219I	G>T
R221G	A>G
G259V	G>T
M282L	A>C
G381S	G>A
V415E	T>A

Table 8: Amino acid replacement and corresponding base change of *PTPN1* missense substitution in PMBCL and HL.

1.5.9 PTP1B inhibitors

Most NRPTPs have a consensus active catalytic signature (motif 9, $_{210}$PXXVHCSAGXGRTG$_{223,}$ Figure 6), where the Cys215 is conserved and essential for enzyme catalysis. Therefore, in past few decades, numerous PTP1B inhibitors have been discovered based on the interaction with this catalytic motif. However, the process of PTP1B inhibitor discovery is not as fluky as we expected, mainly due to two challenges. First, it is specificity and selectivity. PTP1B inhibitors mostly act on the catalytic Cys215. However the catalytic Cys215 of NRPTPs is highly conserved and become the biggest obstacle in PTP1B inhibitor development. Hence, it is difficult for inhibitors to distinguish among different subtypes of tyrosine phosphatases, resulting in potential side effects and difficulties in the study of pharmacological mechanisms. Second, it is cell permeability and bioavailability.

PTP1B is distributed inside the cell membrane and its catalytic Cys215 is positively charged. So inhibitors acting on the catalytic site are ideally negatively charged or highly polar. However, the negatively charged or strongly polar inhibitors cannot pass through the cell membrane effectively, leading to less efficiency.

With continuous efforts, three strategies have been put forward, including allosteric inhibitors which only interact with other sites instead of catalytic site of PTP1B, inhibitors binding both catalytic site and secondary aryl phosphorylation-binding sites which are distinct from other PTPs at corresponding residues [276], and antisense oligonucleotides (ASOs) inhibitors which selectively bind to a particular sequence of PTP1B mRNA and reduce its expression [277].

1.5.9.1 Allosteric PTP1B inhibitors

Allosteric sites, due to their lower sequence conservation pressure compared with conserved catalytic site, offer higher specificity for ligand binding, notably for inhibitors. Over the past decades, numerous PTP1B allosteric inhibitors have been discovered on ASD website (http://mdl.shsmu.edu.cn/ASD/), but none of them has been used in clinics. Here we summarized some representative allosteric PTP1B inhibitors as well as corresponding allosteric binding sites (Table 9).

Allosteric inhibitor	Allosteric binding site of PTP1B	Reference
Compound 1/2/3 (PDB code: 1T48, 1T49, 1T4J)	α3-α6-α7	[278]
Trodusquemine, DPM-1001	α3-α6-α7-α9	[279]
73U with electrophilic α-bromoacetamide	Cys121, Tyr124, His214	[280]
ZINC 57271411	Arg79, Phe196, Arg199, Glu200, Pro206, Lys237, Phe280 and Ile281	[281]
ZINC 77059302	Arg105, Ser146, Val155, Arg156, Gln157, Leu172, Lys197 and Glu200	
NSC 100729	Gln78, Arg79, Ser80, Ser203, Leu204, Ser205, Pro206, His208 and Val211	

Table 9: Allosteric inhibitors and corresponding allosteric binding sites of PTP1B.

1.5.9.2 Multiple aryl phosphorylation sites inhibitors of PTP1B

A large number of PTP1B inhibitors have been developed over last few decades. Most of these inhibitors target the A site (corresponding to the active site), which is the most reachable site where catalytic function of PTP1B occurs (Figure 32). Structurally, they mimic the phosphotyrosine (pTyr) moiety. However, the catalytic site of PTP1B is both conserved and charged. Thus, inhibitors only targeting the catalytic site are often not selective nor cell permeable. Targeting non-conserved residues may provide an opportunity to avoid selectivity issues. Three size limited aryl-phosphorylation-binding sites (B, C, and D sites) are close to the catalytic site of PTP1B structurally (Figure 32) [276], leading to the fact that most inhibitors could not only interact with the three sites alone, but also with most possibility to interact with the catalytic site as well. These three secondary aryl-phosphorylation sites are critical for the potency or selectivity of PTP1B inhibitors because of differing from other PTPs by some amino acids in the identical area, especially from TCPTP [282-285]. According to the extended binding mode based on the four sites, PTP1B inhibitors can be mainly divided into four types (Table 10) [276].

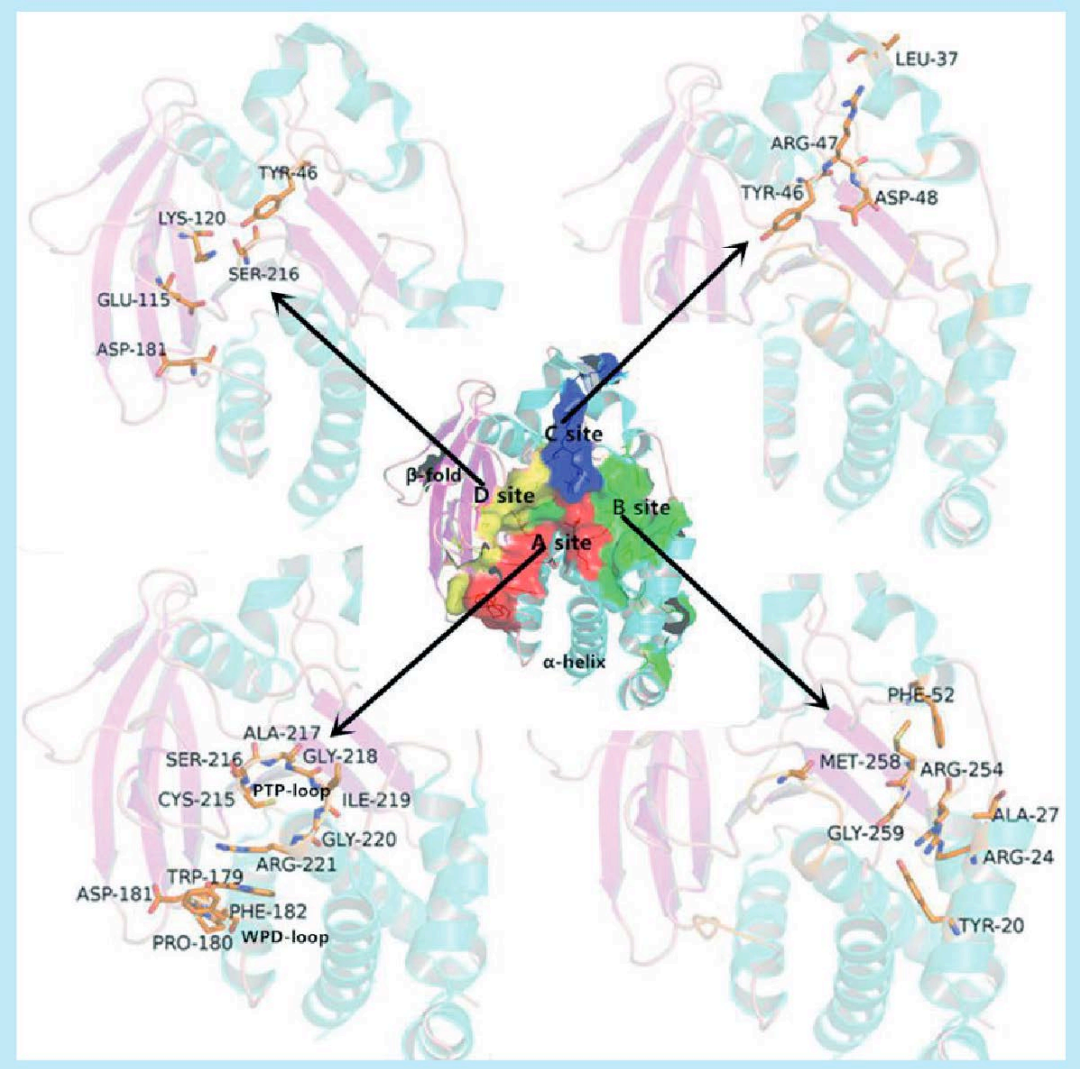

Figure 32: Multiple PTP1B binding sites in red, green, blue and yellow, representing A site, B site, C site and D site respectively [276].

AC type	2- (oxalyl-amino)-benzoic acid (2-OBA) derivatives
	2-carboxymethyl-benzoic acid-derived inhibitors
	difluoromethylphosphonic acid (DFMP)-based inhibitors
	isothiazolidinone (IZD)-contained inhibitors
	monocyclic thiophene-based inhibitors
AB type	monocyclic, bicyclic and tricyclic thiophene inhibitors
	sulfamic acid moiety-contained inhibitors
	other novel AB type inhibitors
ABC type	a series of OBA derivatives
	DFMP group-contained PTP1B inhibitors
	sulfamic acid moiety-contained PTP1B inhibitors
ADC type	N-(2,5-diethoxy-phenyl)-methanesulfonamide derivatives

Table 10: Categories of PTP1B inhibitors that bind to A, B, C and D sites [46].

1.5.9.3 PTP1B mRNA inhibitors

ASOs usually refer to a short-stranded nucleic acid (about 15-25 nucleotides) that has undergone certain chemical modifications. Its sequence is complementary to the specific target RNA sequence. After entering cells, it can form a double-stranded structure with the target RNA sequence according to the principle of Watson-Crick base complementary pairing, thus leading to degradation of the double-strand complex, hence blocking protein translation. The binding of ASOs to the target gene can affect its expression through various mechanisms [286].

So far, only two PTP1B ASOs inhibitors have been designed by Ionis Pharmaceuticals, Inc. (USA): IONIS 113715 and IONIS PTP1BR_X (Table 11). IONIS 113715 is a 20-base chimeric ASOs, which has been identified as the most potent antisense inhibitor of PTP1B mRNA [287], showing great binding affinity toward PTP1B mRNA sequences and great improvement in insulin sensitivity, reduction of lipogenic gene expression, triglyceride accumulation in rat liver and adipose tissue and confer nuclease resistance [287, 288]. IONIS 113715 is advanced into phase II clinical

trials, but it has been reportedly suspended due to unknown reasons, replaced by a new IONIS PTP1BR$_X$, currently in phase II trials. Compared with IONIS 113715, IONIS PTP1BRx is designed as a more potent inhibitor of PTP1B mRNA expression in humans [289]. IONIS PTP1BR$_X$ can help patients who do not have a significant response to existing oral medications for diabetes [290]. In its period of clinical trials, no severe hypoglycemia was observed, and no unexpected safety findings were reported [289]. But so far, no more data are provided.

Name	Targeted mRNA sequence
IONIS 113715	5’-GCTCCTTCCACTGATCCTGC-3’
IONIS PTP1BRx	5’-AATGGTTTATTCCATGGCCA-3’

Table 11: The two ASOs sequences of PTP1B mRNA inhibitors.

2 OBJECTIVES

Within the framework of this thesis, we carried out two main projects focusing on the human protein tyrosine phosphatase PTP1B.

The first project focused on the study of the effect of the anti-cancer drug cisplatin and in particular on the description of the molecular and enzymatic mechanisms that lead to the irreversible inhibition of PTP1B by this molecule. This work is part of the initial discovery that PTP1B could be a target of platinum salts and, more broadly, in the identification of protein targets of cisplatin.

The second project aimed to document the effect of oncogenic mutations in PTP1B in human B cell lymphoma. We were particularly interested in understanding the molecular and enzymatic effects of three point mutations affecting residues located in loops forming the enzyme's active site.

These research projects used molecular and cellular approaches and computational biology tools to describe and understand the effects and their underlying mechanisms of cisplatin and oncogenic mutations on PTP1B.

In addition, we also summarized some specific PTP1B inhibitors since PTP1B is considered as a promising target for treatment of certain diseases.

3 RESULTS

3.1 Result 1

Cisplatin causes covalent inhibition of protein-tyrosine phosphatase 1B (PTP1B): molecular, cellular and *in vivo* mice studies

Rongxing LIU[a], Wenchao ZHANG[a,b], Panhong GOU[b,c], Jérémy BERTHELET[a,d], Qing NIAN[a,e], Guillaume CHEVREUX[f], Véronique LEGROS[f], Gautier MOROY[a], Linh-Chi BUI[a], Li WANG[g], Jean-Marie DUPRET[a], Frédérique DESHAYES[a] and Fernando RODRIGUES LIMA[a,*]

[a] Université Paris Cité, CNRS, Unité de Biologie Fonctionnelle et Adaptative, F-75013 Paris, France

[b] Department of Lymphoma and Myeloma, The University of Texas MD Anderson Cancer Center, Houston, TX, USA; Department of Genomic Medicine, The University of Texas MD Anderson Cancer Center, Houston, TX, USA

[c] Université Paris Cité, INSERM, Institut de Recherche Saint Louis, UMRS 1131, F-75010, Paris, France

[d] Université Paris Cité, CNRS, Centre Epigénétique et Destin Cellulaire, F-75013, Paris, France

[e] Department of Blood Transfusion, Sichuan Provincial People's Hospital, University of Electronic Science and Technology of China and Chinese Academy of Sciences Sichuan Translational Medicine Research Hospital, Chengdu, China

[f] Université Paris Cité, CNRS, Institut Jacques Monod, F-75013, Paris, France

[g] Department of Hematology, The First Affiliated Hospital of Chongqing Medical University, Chongqing, China

* Corresponding author: Fernando RODRIGUES LIMA, Université Paris Cité, BFA, UMR 8251, CNRS, F-75013, Paris, France; email: fernando.rodrigues-lima@u-paris.fr

Abbreviations: PTP, protein tyrosine phosphatase; PTP1B, protein tyrosine phosphatase 1B; 5-IAF, 5-iodoacetamide fluorescein; DTT, dithiothreitol; *p*NPP, *p*-nitrophenyl phosphate; EGFR, epidermal growth factor receptor, RP-UFLC, reverse phase ultra fast liquid chromatography

ABSTRACT

Protein tyrosine phosphatase 1B (PTP1B) is a critical regulator of different signaling cascades such as the EGFR pathway. The biological importance of PTP1B is further evidenced by knockout mice studies and the identification of recurrent mutations/deletions in PTP1B linked to metabolic and oncogenic alterations. Cisplatin is among the most widely used anticancer drug. The biological effects of cisplatin are thought to arise primarily from DNA damaging events involving cisplatin-DNA adducts. However, increasing evidence indicate that the biological properties of cisplatin could also rely on the perturbation of other processes such as cell signaling through direct interaction with certain cysteine residues in proteins. Here, we provide molecular, cellular and *in vivo* evidence suggesting that PTP1B is a target of cisplatin. Mechanistic studies indicate that cisplatin inhibits PTP1B in an irreversible manner and binds covalently to the catalytic cysteine residue of the enzyme. Accordingly, experiments conducted in cells and mice exposed to cisplatin showed inhibition of endogenous PTP1B and concomitant increase in tyrosine phosphorylation of EGFR. These findings are consistent with previous studies showing tyrosine phosphorylation-dependent activation of the EGFR pathway by cisplatin and with recent studies suggesting that PTP1B inhibition by platinum complexes could represent a novel anticancer mechanism.

Overall, our work provides evidence that PTP1B is a protein target of cisplatin and a better understanding of the pathways undergoing modulation upon cisplatin administration beyond of the established genotoxic effect of cisplatin.

Keywords: Protein tyrosine phosphatase 1B, cisplatin, redox sensitive cysteine, cysteine adduct, EGFR signaling, drug target

1 INTRODUCTION

Phosphorylation of tyrosine residues by protein tyrosine kinases (PTKs) serves as a ubiquitous mechanism for cell signaling and plays an important role in numerous biological processes such as proliferation, differentiation, migration and apoptosis [1]. Protein tyrosine phosphorylation is negatively regulated by the opposing action of protein tyrosine phosphatases (PTPs) that dephosphorylate phosphotyrosine (pTyr) residues. PTPs are thus key players of cellular signaling and responses [2, 3]. Consequently, aberrant activity of PTPs is involved in different diseases such as diabetes, immune disorders and cancer [4-6]. The PTP1B is a ubiquitous and abundant intracellular prototypic non receptor tyrosine phosphatase that is recognized as a major negative regulator of numerous signaling cascades of metabolic and/or oncogenic relevance such as the insulin or epidermal growth factor (EGF) pathways [6-8]. The critical biological role of PTP1B is further highlighted by the identification of recurrent mutations/deletions of PTP1B in certain cancer and by knock-out mice models showing metabolic and oncogenic alterations [9-14]. PTP1B activity depends upon a conserved catalytic cysteine residue that renders the enzyme redox sensitive [15-17]. Reversible oxidation and inhibition of PTP1B by reactive oxygen species (ROS) is considered as a critical physiological mechanism in the activation and the redox control of tyrosine kinase signaling as observed in the EGFR pathway [18, 19]. In addition, chemical S-modification at the active site of PTP1B by environmental electrophiles (such as quinones or heavy metals) has been shown to inactivate the enzyme and drive aberrant EGFR tyrosine phosphorylation and signaling [20, 21].

Cisplatin is one of the most successful and widely used anticancer drug. The mechanism of action of cisplatin is thought to rely mainly on the formation of stable DNA adducts on guanine that lead to DNA damaging events and ultimately to cell death [22-24]. However, several studies indicate that cisplatin could also impact other biological processes such as DNA repair and cell signaling, most notably the EGFR pathway [23, 25-29]. In addition, cisplatin could exert, at least in part, these biological effects through binding to peptide or proteins with subsequent structural and/or functional alterations [24, 30, 31]. In particular, the functions of certain cellular

enzymes have been reported to be inhibited by cisplatin through binding to the thiol group of redox sensitive cysteines [26, 32-35].

In this paper, we provide molecular, cellular and *in vivo* evidence that the chemotherapeutic drug cisplatin inhibits the enzymatic functions of PTP1B. Mechanistic and kinetics experiments using recombinant purified human PTP1B show that the inhibition is irreversible and involves the formation of a covalent adduct of cisplatin with the redox-sensitive catalytic cysteine residue of the enzyme. Further studies carried out in cells and in mice indicate that treatment with cisplatin leads to the irreversible inhibition of endogenous PTP1B and concomitant activation of EGFR signaling. Altogether, our findings identify PTP1B as a target of cisplatin and suggest that inhibition of PTP1B by cisplatin could contribute, at least in part, to the pharmacological and/or toxicological effects of this widely used drug through aberrant activation of PTP1B-dependent signaling pathways. More broadly, our work provides a better understanding of the intricate network of pathways undergoing modulation upon cisplatin administration and that goes beyond the well-established genotoxic effect of cisplatin.

2 MATERIALS AND METHODS

2.1 Materials

Cisplatin, *p*-nitrophenyl phosphate (*p*NPP), 5-iodoacetamide fluorescein (5-IAF), N,N-dimethylformamide (DMF), hydrogen peroxide (H_2O_2), HClO4, dithiothreitol (DTT), sodium fluoride (NaF), sodium orthovanadate (Na3VO4), isopropyl β-D-thiogalactoside (IPTG), Triton X-100, lysozyme, His-select nickel resin, were obtained from Sigma-Aldrich (France). Protease inhibitors were purchased from Roche (France). PD-10 columns were from GE Healthcare (France). Trizol reagent and superscript II cDNA kit were from Invitrogen Carlsbad (USA). SYBR green was from Thermo Fischer Scientific (USA). EGFR antibody (SAB4300352), β-actin antibody (SC-81178) and Protein G plus-agarose beads (SC-2002) were obtained from Santa Cruz Biotechnology (France). PTP1B (FG6-1G) and phospho-EGFR antibody (Tyr 1069, 09-310) were obtained from Merck (France). Oxidized PTP

active site antibody (MAB2844) was obtained from R&D system (USA). Cisplatin was dissolved in DMF.

2.2 Cell culture

Human HaCaT cells were cultured in DMEM medium (Gibco, France) with 10% fetal bovine serum (Sigma, France) at 37°C with 5% CO2.

2.3 Expression and purification of recombinant human PTP1B

The complementary DNA (cDNA) coding for the shorter version of human PTP1B (1-321) was cloned into pET28a plasmid and was later transformed into Escherichia coli 21 (DE3). Bacteria were cultured at 37°C under agitation until reaching an OD of 0.6, then grown overnight at 16 °C in the presence of 0.5 mM IPTG. Cells were harvested by centrifugation and resuspended in lysis buffer (20 mM Tris HCl, 100 mM NaCl, 0.5% Triton X-100, 1 mg/ml lysozyme and protease inhibitor, pH 7.5). The lysate was sonicated (10 sec ON, 20 sec OFF, 10 min, 20 % power) on ice and pelleted (15,000 g, 30 min, 4°C). Supernatant was incubated with His-select nickel resin in the presence of 10 mM imidazole for 2 hours at 4°C under agitation. Beads were then poured into a column, washed with washing buffer (20 mM Tris-HCl, 100 mM NaCl, 20 mM imidazole, pH 7.5) and PTP1B was eluted with elution buffer (20 mM Tris-HCl, 100 mM NaCl, 300 mM imidazole, pH 7.5). Protein elution was controlled by Bradford assay and eluted samples were incubated with 10 mM DTT on ice for 20 min. Purified PTP1B was buffer exchanged to 20 mM Tris-HCl, 100 mM NaCl, pH 7.5 using PD-10 column. Protein concentration and purity were assessed by Bradford reagent and SDS-PAGE. Proteins were stored at –80°C until use.

2.4 Determination of PTP1B phosphatase activity using *p*NPP

The phosphatase activity of PTP1B was measured by *p*NPP assay as previously described [36, 37]. Briefly, samples containing PTP1B (200 nM) were incubated with different concentrations of cisplatin in 100 mM sodium acetate buffer, 1 mM DTT, pH 6 for 30 minutes at 37°C (total volume of 100 µl). 20 µl of each sample were taken and diluted 10 times with sodium acetate buffer containing 5 mM *p*NPP. The formation of the product (*p*-nitrophenol) was tracked by continuous measurement of the absorbance at 405 nm for 10 minutes at 37°C using thermostatic microplate reader

(BioTek, France) in a total volume of 200 µl. The final concentration of PTP1B after dilution was 20 nM.

2.5 Determination of recombinant PTP1B activity using FAM-conjugated tyrosine-phosphorylated STAT3 (pSTAT3) peptide by RP-UFLC

The tyrosine phosphatase activity of PTP1B was measured by RP-UFLC using FAM-conjugated peptide derived from the sequence of human STAT3 where tyrosine 704 is phosphorylated (701SAAPPYLKTK709, Proteogenix, France) as previously described [36, 38]. Briefly, samples containing PTP1B (200 nM) were incubated with different concentrations of cisplatin in 100 mM sodium acetate buffer, 1 mM DTT, pH 6 for 30 minutes at 37°C (total volume of 100 µl). 20 µl of each sample were taken, diluted 10 times and incubated in sodium acetate buffer for 30 minutes at 37°C in the presence of 50 µM FAM-conjugated pSTAT3 peptide (final concentration of PTP1B was 20 nM). The reaction was stopped with the addition of 50 µl HClO4 (15%, v/v) and samples were injected into a Shim-pack XR ODS column (100 mm, 2 mm, 2.2 µm) (Shimadzu) at 40 °C. The mobile phase used for the separation consisted of two eluents: solvent A was water with 0.12% trifluoacetic acid (TFA), and solvent B was acetonitrile with 0.12% TFA. Compounds were separated by an isocractic flow (80% A/20% B) rate of 0.6 ml/min. pSTAT3 peptide and its dephosphorylated form (product) were monitored by fluorescence emission ($\lambda = 530$ nm) after excitation at $\lambda = 485$ nm and quantified by integration of the peak absorbance area.

2.6 Effects of reducing agent and buffer exchange on cisplatin-inhibited PTP1B

PTP1B (200 nM) was first incubated with cisplatin (25 µM) in 100 mM sodium acetate buffer, pH 6 for 30 minutes at 37°C (total volume of 100 µl). Samples were either buffer exchanged (PD Spin Trap G-25; GE Healthcare) to sodium acetate buffer (100 mM, pH 6) or further incubated with 1 or 5 mM DTT (10 min at room temperature) before 10-fold dilution in sodium acetate buffer (100 mM, pH 6) and measurement of PTP1B residual activity using *p*NPP assay as described previously.

2.7 5-IAF labeling and H_2O_2 mediated oxidation of PTP1B catalytic cysteine

For IAF labeling, PTP1B (200 nM) was first incubated with cisplatin (25 µM) in sodium acetate buffer (100 mM, 1 mM DTT, pH 6) at 37°C for 30 minutes followed

by another incubation at 37 °C for 10 min in the dark in the presence of 20 µM 5-IAF. Samples were then split into two parts. One part was diluted 10-fold in sodium acetate buffer and used for measuring PTP1B residual activity using *p*NPP assay as described before; another part was separated by SDS-PAGE, transferred onto nitrocellulose membrane. 5-IAF fluorescence on PTP1B labelled cysteine residues was detected with a Fujifilm LAS 4000 detection system (λexc = 485 nm, λem = 530 nm). Membranes were later probed with anti-PTP1B antibody.

For the detection of PTP1B oxidized catalytic cysteine, PTP1B (200 nM) was incubated with cisplatin (25 µM) or H_2O_2 (250 µM) at 37°C for 30 minutes in sodium acetate buffer (100 mM, 1 mM DTT, pH 6) in a total volume of 100 µl. Samples were then split into two parts. One part was diluted 10-fold in sodium acetate buffer and used for measuring PTP1B residual activity using *p*NPP assay as described above; the other part was separated by SDS-PAGE, transferred onto nitrocellulose membrane and probed with an antibody specific to the oxidized catalytic cysteine of PTPs. Membranes were washed thoroughly with PBS and further probed with anti-PTP1B antibody.

2.8 Effects of cisplatin on PTP1B in the presence of the competitive PTP inhibitor Na3VO4

PTP1B (200 nM) was incubated with 200 µM Na3VO4 in the presence or absence of cisplatin (25 µM) in sodium acetate buffer (100 mM, 1 mM DTT, pH 6) at 37°C for 30 minutes (total volume of 100 µl). Samples were diluted 10-fold in sodium acetate buffer and PTP1B residual activity was quantified using *p*NPP assay as described before.

2.9 Mass spectrometry analysis of cisplatin binding to a PTP1B active site peptide containing the Cys215 residue.

The peptide approach previously used to characterize oxidative modifications of Cys215 in PTP1B was carried out [39]. Briefly, the PTP1B peptide derived from the sequence of the enzyme catalytic domain (214HCSAGIGRS222, Proteogenyx, France) (10 µg, 0.5 mM) was incubated with cisplatin (2.5 mM) in H2O at 37°C for 24 hours in a total volume of 20 µl. The peptide preparation (1µL) was injected into a

BioResolve RP (450Å, 2.7 µm, 0.3 mm X 150 mm) Polyphenyl Column (Waters, Milford, MA, USA) using an UltiMate 3000 RSLCnano chromatographic system fitted with a capillary flow meter from ThermoFisher Scientific (Waltham, MA, USA). Mobile phases A and B were respectively H2O/acetonitrile 98/2 and H2O/acetonitrile 20/80 acidified with 0.1% formic acid. The sample was eluted at a flow rate of 6 µl/min using the following slope change points: 0-5 min hold at 6.3% B, 5 min slope until 25% B, 40 min slope until 56% B, 5 min wash at 100% B and finally 10 min hold at 6.3% B. The eluent was sprayed using the conventional ESI ion source of a Q-Exactive Plus mass spectrometer from ThermoFisher Scientific operating in the positive ion mode. MS spectra were acquired at a resolution of 70,000 with a mass range of m/z 250-1700 and an AGC target value of 1.106 for a maximum ion accumulation time of 500 ms. MS/MS data were acquired at similar resolution, in data-dependent top2 acquisition mode with an AGC target value of 5.105 for a maximum ion accumulation time of 250 ms. Parent ions were selected for fragmentation by Higher-energy C-trap Dissociation (HCD) with a dynamic exclusion time of 30 seconds. Raw data were processed with Thermo Xcalibur v3.0.63 and especially the isotope simulation tool embedded in the software was used to simulate monoisotopic patterns obtained after reaction of cisplatin with the HCSAGIGRS peptide of interest.

2.10 Kinetics of PTP1B inactivation by cisplatin

PTP1B (200 nM) was incubated with different concentrations of cisplatin in sodium acetate buffer (100 mM, 1 mM DTT, pH 6) at 37°C. At different time points, aliquots were taken, diluted 10 times with sodium acetate buffer and then assayed for PTP1B residual activity using *p*NPP as described before. The inhibition rate of PTP1B by cisplatin can be represented as follows: ln [% residual activity] = $k_{obs} \times t$ (where t is time and k_{obs} is the apparent first-order inhibition rate constant). For each cisplatin concentration, the k_{obs} value can be calculated from the slope of the natural logarithm of the percentage of PTP1B residual activity as a function of time. The second-order rate constant (k_{inact}) was determined from the slope of k_{obs} plotted as a function of cisplatin concentration ($k_{obs} = k_{inact} \times$ [cisplatin]). The reaction order

between cisplatin and PTP1B could be determined by the slope of the linear plot of the natural logarithm of k_{obs} as a function of the natural logarithm of cisplatin concentration. The kinetic data were fitted and plotted using Prism 8.0.0 (GraphPad Software, La Jolla, CA).

2.11 Effects of cisplatin on EGFR tyrosine phosphorylation in cells

HaCaT cells were serum-starved overnight and then treated with different concentrations of cisplatin for 24 hours at 37°C, 5% CO2. Cells were then washed with PBS, harvested and lysed in lysis buffer (PBS, 1% Triton X-100, 1 mM Na3VO4, 1 mM NaF and protease inhibitor) on ice for 30 minutes under agitation. Cell lysates were centrifuged at 15,000g for 10 minutes at 4°C, and the supernatants (whole cell extracts) were kept. Samples were separated by SDS-PAGE and transferred onto a nitrocellulose membrane. EGFR activation was then assayed by western blot using anti-phospho-EGFR antibody. Membranes were stripped and re-probed sequentially with anti-EGFR, anti-PTP1B and anti-β-actin antibodies.

2.12 Immunoprecipitation of endogenous PTP1B

HaCaT cells were serum-starved overnight and treated with cisplatin (20 µM) for 24 hours at 37°C, 5% CO2. Whole cell extracts were obtained as stated above, but without the addition of Na3VO4 and NaF in lysis buffer. Endogenous PTP1B was immunoprecipitated by incubating 1 mg of whole cell extracts in the presence of 1 µg of PTP1B antibody overnight at 4°C under agitation. Samples were then rocked for 1 hour at 4°C in the presence of 30 µl of protein G–Agarose. The immunobeads were harvested by centrifugation, washed three times with lysis buffer (PBS, 1% Triton X-100), and split in two. Half of the beads was incubated with 50 µM FAM–phosphorylated STAT3 peptide in sodium acetate buffer (100 mM, 1 mM DTT, pH 6) at 37°C for 2 hours (total volume of 50 µl) to determine endogenous PTP1B residual activity by RP-UFLC as described previously. The second part of immunobeads were incubated with non-reducing Laemmli sample buffer and heated at 100°C for 10 minutes. Eluates were separated by SDS-PAGE, transferred onto nitrocellulose membrane and analyzed by western blot using an anti-PTP1B antibody.

2.13 RT-qPCR of EGFR-regulated genes

HaCaT cells were serum-starved overnight and then treated with cisplatin (20 μM) for 24 hours at 37°C, 5% CO2. Cells were harvested and washed three times with PBS. Total RNA was extracted in a classical method using trizol reagent. 500 ng of the extracted RNA was converted into cDNA using superscript II cDNA kit. Real-time quantitative PCR was performed to analyse relative gene expression levels for EGFR-regulated genes (COX2, JUN1 and FOS1) using SyberGreen Master Mix and 7500 Fast Real-time PCR System (Applied Bio-systems, Carlsbad, CA), according to manufacturer's protocol. Relative expression values were normalized with ubiquitin housekeeping gene. Primer sequences of the genes used in this study were as follow:

Ubiquitin_For: CACTTGGTCCTGCGCTTGA

Ubiquitin_Rev: TTTTTTGGGAATGCAACAACTTT

COX2_For: CCATTGACCAGAGCAGG CAGA

COX2_Rev: GGGCAGGATACAGCTCCACA

JUN1_For: TCGACAAGTAAGAGTGCGGGA

JUN1_Rev: GGGAAAGTTTCTCTAAGAGCGCA

FOS1_For: CTCTTACTACCACTCACCCGCA

FOS1_Rev: CCGTGGGAATGA AGTTGGCAC

2.14 Treatment of mice with cisplatin

C57BL/6 mice (12 weeks, female) were obtained from Janvier (Le Genest, France) and bred in pathogen-free conditions in the animal facility of the Institut de Recherche Saint-Louis (IRSL) (Hopital Saint-Louis, Universite de Paris). Mice (n=3) were treated by intraperitoneal injection of 7.5 mg/kg cisplatin in sodium chloride solution (0.9%). Control mice (n=3) were treated with vehicle only. After 5 hours, liver tissues were taken and washed 3 times with cold PBS, cutted into small pieces and washed again 3 times with cold PBS. Samples were lysed with lysis buffer (PBS, 1% Triton X-100, 1 mM Na3VO4, 1 mM NaF and protease inhibitor) for 30 minutes on ice under agitation. Lysates were centrifuged at 15,000g for 10 minutes at 4°C, supernatants were kept and analyzed for EGFR phosphorylation. Endogenous PTP1B was immunoprecipitated from lysates (without Na3VO4 and NaF) and assayed for

activity by RP-UFLC as described above. All the animal procedures performed were approved by the local Committee on the use and care of animal.

2.15 Statistical analysis

All data were reported as mean ± standard deviation (S.D.) of three independent experiments. Quantification of western blot signal was carried out using ImageJ software (National Institutes of Health, USA). Data were analyzed by either t-test or one-way analysis of variance (ANOVA) using GraphPad Prism version 8.0.0. A threshold of $p < 0.05$ was used to consider differences as statistically significant. (*P $\leqslant$ 0.05, **P $\leqslant$ 0.01).

3 RESULTS

3.1 Cisplatin impairs the tyrosine phosphatase activity of human PTP1B enzyme *in vitro*

As stated above, although cisplatin is mainly known as a DNA-interacting drug, a limited number of cellular enzymes have nonetheless been shown to be targeted and inhibited by cisplatin at clinically relevant levels, i.e. <100 μM [26, 32, 34, 35, 40-42]. We used purified recombinant human PTP1B to assess the effects of cisplatin on its activity. To this end, the enzyme was preincubated with different therapeutically-relevant concentrations of cisplatin (ranging from 0 to 25 μM) and residual PTP1B activity measured with the chromogenic prototypic phosphatase substrate para-nitrophenyl phosphate (*p*NPP) as previously described [36, 37]. As shown in Figure 1A, PTP1B was inhibited by cisplatin in a dose-dependent manner with almost full inhibition obtained at 25 μM final concentration. These results were further confirmed with a UFLC-based tyrosine phosphatase enzyme assay that uses a phospho-STAT3 peptide derived from the sequence of human STAT3 (701SAAPYLKTK709 where the Y705 is phosphorylated), a known substrate of PTP1B as described previously [36, 38]. As expected, we found that the tyrosine-phosphatase activity of PTP1B towards the substrate peptide was inhibited by cisplatin in a similar manner as to what was observed with the *p*NPP assay (Figure 1B).

3.2 PTP1B is irreversibly inhibited by cisplatin through the formation of a cisplatin adduct with its redox-sensitive active site cysteine residue

Cisplatin is known to be able to react with redox-sensitive cysteine within proteins to form irreversible covalent cisplatin adducts [24, 43, 44]. Moreover, it has been shown that the formation of these irreversible cysteine-cisplatin adducts could be responsible for the irreversible impairment of the catalytic activity of enzymes such as topoisomerase II, Na^+/K^+ ATPase or glutathione transferase P1-1 [35, 45, 46]. We further analysed the inhibition of human PTP1B by cisplatin by preincubating the enzyme with cisplatin prior to dialysis and measurement of residual activity. As shown in Figure 2A, dialysis did not permit recovery of enzymatic activity of PTP1B previously exposed to cisplatin. Moreover, experiments carried out with DTT also showed no recovery of the PTP1B activity by this reducing agent (Figure 2B). Altogether, these findings supported that inhibition of PTP1B by cisplatin proceeds through an irreversible mechanism, possibly through reaction with cysteine residues. We therefore investigated whether PTP1B cysteine residues were chemically modified by cisplatin. To this end, we used a method based on the labelling of free reduced cysteines by the sulfhydryl-reactive reagent iodoacetamide-fluorescein which has been used previously to detect the chemical modification of cysteine residues within proteins including PTP1B [47, 48]. As shown in Figure 2C, inhibition of PTP1B by cisplatin was concomitant with the modification of cysteine residues as indicated by the decrease in IAF-labelling of the enzyme. Interestingly, the activity of PTP1B is known to rely on a redox-sensitive cysteine residue in the active site of the enzyme (Cys215) that can be reversibly or irreversibly oxidized by reactive oxygen species to sulfenamide, sulfenic, sulfinic and sulfonic species that inactivates the enzyme [15, 16, 18]. In addition, it has been shown that this active site cysteine residue could be covalently modified by certain electrophilic compounds with subsequent PTP1B inactivation [20, 21]. We carried out western blots analyses using an antibody that specifically detects oxidized forms but not covalently adducted forms of the active cysteine residue of PTP1B or other PTPases [48, 49]. As shown in Figure 2D, we found that contrary to H_2O_2, inhibition of the enzyme by cisplatin was not due to

oxidation of its catalytic cysteine residue thus supporting that cisplatin could impair PTP1B through a covalent cisplatin-cysteine adduct as reported previously for other enzymes [26, 34, 35].

Consistent with the data reported above, we conducted further experiments to test whether cisplatin-dependent inhibition of PTP1B could be due to covalent binding of cisplatin to the active-site cysteine residue of the enzyme. To this end, we carried out active-site protection assays using orthovanadate, a reversible competitive inhibitor of PTP1B that interacts with the catalytic cysteine residue within the active site of the enzyme [50]. This approach has already been used to identify chemicals that react with the catalytic cysteine of PTP1B and that inhibit its activity [37, 48, 51]. We observed that the presence of orthovanadate markedly slowed the inhibition of PTP1B by cisplatin thereby supporting that the inhibition process was active site directed and involved the catalytic cysteine residue (Figure 3A). In line with these results, we found that preincubation of PTP1B with cisplatin strongly decreased the oxidation of the catalytic Cys215 residue by H_2O_2 as evidenced by western-blot using a specific antibody against oxidized forms of the catalytic cysteine residue of PTP1B thus supporting that cisplatin reacted with this cysteine (Figure 3B) [49, 52].

To confirm that cisplatin can indeed react with the Cys215 in the active site of human PTP1B, mass spectrometry (MS) approaches were carried out. Unfortunately, we experienced technical difficulties for the MS analysis of purified PTP1B treated with cisplatin. Notably, peptides containing Cys215 could not be detected and more broadly the mass spectra were very complex. This is likely due to the myriad of different types (and masses) of cisplatin adducts that can be formed on cysteine residues [43, 44, 53]. Similar technical difficulties were previously reported for the reaction of cisplatin with cysteine residues of topoisomerase IIα enzymes [45]. To circumvent this technical difficulties, MS experiments were conducted with a synthetic peptide (HCSAGIGRS) which is an active site sequence motif of PTP1B that contains the Cys215 residue. This peptide approach has been previously used to characterize oxidative modifications of Cys215 in PTP1B [39]. Consistent with the findings reported above, we found that cisplatin was able to covalently bind to the

catalytic cysteine residue of PTP1B. Indeed, as shown in Figure 3C (upper panel) covalent adducts of cisplatin on the peptide were clearly identified. Notably, the highest monoisotopic mass at m/z 1394.347 corresponded to the addition of two [Pt(NH3)2Cl] molecules on the free cysteine of the peptide. This type of cysteine-cisplatin adduct has already been identified in glutathione peptides treated with cisplatin [53]. The following peak at m/z 1375.396 likely corresponded to another stoichiometry in solution with the addition of both [Pt(NH3)2Cl] and [Pt(NH3)3] while the last peak at m/z 1358.371 could correspond to gas phase fragmentation with the loss of one HCl molecule. Simulations of the isotopic profiles of these species were generated using Excalibur (Thermo Scientific Fisher, Boston, USA). They fitted very well the identified molecular compositions of the cisplatin-peptide adducts. Isotopic patterns are indeed very informative in this case with both chlorine and platinum atoms that display very specific isotopes resulting in unambiguous attribution of molecular compositions.

Formation of covalent adducts of cisplatin with cysteine residues has been shown to produce a broad absorption band between 220 and 350 nm corresponding to the cysteine-cisplatin adduct [35, 54]. As shown in Supplementary Figure 1, incubation of the PTP1B active site peptide with cisplatin led to a time-dependent increase in absorbance between 220 and 350 nm thus supporting the formation of an adduct between the cysteine residue of the peptide and cisplatin. Finally, computational covalent docking approaches further supported that cisplatin can bind the catalytic cysteine residue within the active site of PTP1B (Supplementary Figure 2).

We carried out in depth kinetic analyses of PTP1B inhibition by cisplatin. Consistent with a process involving covalent modification of the active site cysteine of PTP1B, the enzyme was found to be inhibited in a time-dependent and dose-dependent manner (Figure 4A). The second-order rate inhibition constant (ki) was found to be close to 34 $M^{-1}.s^{-1}$ (Figure 4B). Stoichiometry of the PTP1B inhibition by cisplatin was close to 1 indicating that the inhibition relies on the reaction of one molecule of cisplatin with one molecule of enzyme (Figure 4C).

3.3 Cisplatin inhibits endogenous PTP1B and increases EGFR phosphorylation in human cultured cells and in mice.

As stated previously, PTP1B is known to be a major regulator of the EGFR signaling pathway through its tyrosine phosphatase activity [18, 19, 55]. In addition, covalent inhibition of PTP1B by electrophilic chemicals such as quinones is well known to increase EGFR tyrosine phosphorylation [20, 21, 56]. Interestingly, cisplatin has been shown to activate EGFR through increased tyrosine phosphorylation [25, 27, 57]. We thus exposed HaCaT human keratinocytes to cisplatin and monitored tyrosine phosphorylation of EGFR by western-blot as previously described [25, 56]. Hacat cells have been used in different studies aimed at analyzing PTP1B-dependent activation of EGFR phosphorylation and activation [56, 58]. Consistent with earlier reports, we observed that exposure of the cells to cisplatin led to increased EGFR tyrosine phosphorylation (Figure 5A) [25, 27, 57]. Activation of EGFR signaling by cisplatin was further confirmed by qPCR experiments which showed marked increase in the expression of COX2, JUN1 and FOS1, three genes known to be upregulated downstream of EGFR activation (Figure 5B) [59-61]. Importantly and in line with these results, we found that the activity of cellular PTP1B was markedly impaired in the cells exposed to cisplatin (Figure 5C). Finally, we carried out investigations in mice (C57BL/6j, n=3) treated or not with a clinically-relevant dose of cisplatin via intraperitoneal injection (7.5 mg/kg). As shown in Figure 6A, treatment with cisplatin led to increased EGFR tyrosine phosphorylation in liver extracts of the treated mice. Accordingly, we observed a marked decrease in intrinsic tyrosine phosphatase activity of endogenous PTP1B when mice were treated with cisplatin (Figure 6B). Taken together, these findings are consistent with the results reported above and support the notion that cisplatin is an inhibitor of PTP1B with subsequent impact on PTP1B-regulated signaling pathways such as EGFR [25, 27, 57].

4 DISCUSSION

Cisplatin is considered as one of the most potent anticancer drug in clinical use for the treatment of several cancers [23, 62]. The biological effects of this

chemotherapeutic drug is thought to arise primarily from the formation of covalent adducts with purine DNA bases [24]. Yet, other key biological processes in particular protein phosphorylation-mediated cell signaling have been shown to be impacted by cisplatin [23, 27, 29, 35]. We show here that the PTP1B, a key negative regulator of different protein tyrosine phosphorylation-dependent pathways, is impaired by cisplatin. In depth molecular and kinetic analyses using recombinant purified human PTP1B indicate that the inhibition of the tyrosine phosphatase activity of the enzyme is irreversible and occurs through the formation of covalent cisplatin-protein adducts with the active site cysteine residue of the enzyme (Cys 215). The activity of PTP1B is known to rely on the redox status of this reactive active site cysteine [16, 63]. Interestingly, covalent modification of this cysteine by environmental electrophilic compounds such as naphtoquinones or aldehydes have been shown to inhibit PTP1B irreversibly through covalent adduction [20, 21, 37]. Although cisplatin is mainly described as a DNA-interacting drug, it can covalently bind to certain reactive cysteine residues in proteins to form cisplatin adducts that can impact protein functions [24, 35, 43, 64]. Of note, the binding of cisplatin to proteins is increasingly recognized as a mechanism whereby cisplatin could exert, at least in part, its biological effects [24, 28, 30, 35]. In particular, certain cellular enzymes such as topoisomerase II, caspase 3 or Na^+/K^+-ATPase have been shown to be inhibited by cisplatin through covalent modification of important cysteine residues [26, 32, 34]. We found that the rate of inhibition of PTP1B by cisplatin (ki=34 $M^{-1}. s^{-1}$) was very similar to the rates determined for the inhibition of human arylamine N-acetyltransferase 1 (12 $M^{-1}. S^{-1}$) or GSTP1-1 (35 $M^{-1}. s^{-1}$), two enzymes that are inhibited through the formation of cisplatin-cysteine adducts [33, 35]. These rates are by far greater than rates of reaction of cisplatin with the cysteine residue of GSH, a known biological reducing agent that binds covalently to cisplatin (3.10^{-2} $M^{-1}.s^{-1}$) or the thiol group of sodium-2-mercaptoethnesulfonate (mesna), a drug used to mitigate the toxic adverse effects of cisplatin (7.10^{-2} $M^{-1}.s^{-1}$) [65, 66]. Interestingly, the rate of reaction of cisplatin with DNA has been reported to be close to 2 $M^{-1}.s^{-1}$ [67]. In addition, the rate of inhibition of PTP1B by cisplatin is comparable to that reported

previously for hydrogen peroxide (10 M^{-1}. s^{-1}) and acrolein (87 M^{-1}. s^{-1}), two known cellular inhibitors of PTP1B that modify the catalytic cysteine of the enzyme [37, 68]. As stated above, PTP1B activity is a key negative regulator of different cell signaling pathways such as the EGFR pathway and inhibition of PTP1B activity is known to trigger increased EGFR tyrosine phosphorylation and activation [17-19, 21]. In line with the results obtained with purified human PTP1B, we indeed observed that cisplatin was able to inhibit the activity of cellular PTP1B and, as expected, to increase tyrosine phosphorylation of EGFR and subsequent increased expression of EGFR-regulated genes (Figure 5B). In addition, these data are in agreement with studies conducted with different cell lines which showed that exposure to cisplatin leads to EGFR activation through increased tyrosine phosphorylation [25, 27, 57]. Experiments conducted in mice exposed to clinically-relevant concentrations of cisplatin further supported that cisplatin inhibits PTP1B and increases EGFR tyrosine phosphorylation. Interestingly, inhibition of PTP1B by chemical modification of its active site cysteine by certain electrophilic compound is known to trigger increased EGFR tyrosine phosphorylation and activation [19-21, 69].

It is increasingly recognized that in addition to DNA, cisplatin exerts its biological effects by targeting proteins with subsequent alteration of cellular processes such as signaling pathways [24, 28, 32, 35]. Interestingly, recent studies suggest that inhibition of PTP1B by platinum complexes could represent a novel anticancer mechanism [70]. In line with this, our work provides molecular, cellular and *in vivo* evidence that cisplatin can impair the enzymatic functions of PTP1B thus supporting that PTP1B could be a protein target of cisplatin.

AUTHOR CONTRIBUTIONS

RL, JB, JMD and FRL designed research; RL, WZ, PG, JB, QN, VL, GM, and LCB performed research; All authors analyzed the data; RL, JB and FRL wrote the paper. All the authors commented on the paper.

DECLARATION OF COMPETING INTEREST

The authors declare no competing financial interests.

ACKNOWLEDGMENTS

This work was supported by running grants from Université Paris Cité, CNRS. RL, WZ, PG and QN were supported by PhD fellowship from China Scholarship Council (CSC). We thank the technical platform “BioProfiler-UFLC” (BFA Unit, Université Paris Cité) for provision of UFLC facilities. We thank Florent Busi for his help on the design of q-PCR primers.

REFERENCES

1. Pawson, T., Specificity in signal transduction: from phosphotyrosine-SH2 domain interactions to complex cellular systems. Cell, 2004. 116(2): p. 191-203.
2. Tonks, N.K., Protein tyrosine phosphatases: from genes, to function, to disease. Nat Rev Mol Cell Biol, 2006. 7(11): p. 833-46.
3. Bohmer, F., et al., Protein tyrosine phosphatase structure-function relationships in regulation and pathogenesis. FEBS J, 2013. 280(2): p. 413-31.
4. Tiganis, T. and A.M. Bennett, Protein tyrosine phosphatase function: the substrate perspective. Biochem J, 2007. 402(1): p. 1-15.
5. Qi, X.M., et al., Targeting an oncogenic kinase/phosphatase signaling network for cancer therapy. Acta Pharm Sin B, 2018. 8(4): p. 511-517.
6. Villamar-Cruz, O., et al., Recent advances in PTP1B signaling in metabolism and cancer. Biosci Rep, 2021. 41(11).
7. Simoncic, P.D., C.J. McGlade, and M.L. Tremblay, PTP1B and TC-PTP: novel roles in immune-cell signaling. Can J Physiol Pharmacol, 2006. 84(7): p. 667-75.
8. Pike, K.A. and M.L. Tremblay, TC-PTP and PTP1B: Regulating JAK-STAT signaling, controlling lymphoid malignancies. Cytokine, 2016. 82: p. 52-7.
9. Elchebly, M., et al., Increased insulin sensitivity and obesity resistance in mice lacking the protein tyrosine phosphatase-1B gene. Science, 1999. 283(5407): p. 1544-8.
10. Julien, S.G., et al., Protein tyrosine phosphatase 1B deficiency or inhibition delays ErbB2-induced mammary tumorigenesis and protects from lung metastasis. Nat Genet, 2007. 39(3): p. 338-46.
11. Banno, R., et al., PTP1B and SHP2 in POMC neurons reciprocally regulate energy balance in mice. J Clin Invest, 2010. 120(3): p. 720-34.
12. Gunawardana, J., et al., Recurrent somatic mutations of PTPN1 in primary mediastinal B cell lymphoma and Hodgkin lymphoma. Nat Genet, 2014. 46(4): p. 329-35.
13. Jobe, F., et al., Deletion of Ptpn1 induces myeloproliferative neoplasm. Leukemia, 2017. 31(5): p. 1229-1234.
14. Le Sommer, S., et al., Deficiency in Protein Tyrosine Phosphatase PTP1B Shortens Lifespan and Leads to Development of Acute Leukemia. Cancer Res, 2018. 78(1): p. 75-87.
15. Salmeen, A., et al., Redox regulation of protein tyrosine phosphatase 1B involves a sulphenyl-amide intermediate. Nature, 2003. 423(6941): p. 769-73.
16. Lou, Y.W., et al., Redox regulation of the protein tyrosine phosphatase PTP1B in cancer cells. FEBS J, 2008. 275(1): p. 69-88.
17. Tonks, N.K., PTP1B: from the sidelines to the front lines! FEBS Lett, 2003. 546(1): p. 140-8.
18. Lee, S.R., et al., Reversible inactivation of protein-tyrosine phosphatase 1B in A431 cells stimulated with epidermal growth factor. J Biol Chem, 1998. 273(25): p. 15366-72.
19. Heppner, D.E. and A. van der Vliet, Redox-dependent regulation of epidermal growth factor receptor signaling. Redox Biol, 2016. 8: p. 24-7.
20. Iwamoto, N., et al., Chemical knockdown of protein-tyrosine phosphatase 1B by 1,2-naphthoquinone through covalent modification causes persistent transactivation of epidermal growth factor receptor. J Biol Chem, 2007. 282(46): p. 33396-33404.
21. Zheng, F., et al., Redox toxicology of environmental chemicals causing oxidative stress. Redox Biol, 2020. 34: p. 101475.

22. Cullen, K.J., et al., Mitochondria as a critical target of the chemotheraputic agent cisplatin in head and neck cancer. J Bioenerg Biomembr, 2007. 39(1): p. 43-50.
23. Dasari, S. and P.B. Tchounwou, Cisplatin in cancer therapy: molecular mechanisms of action. Eur J Pharmacol, 2014. 740: p. 364-78.
24. Pinato, O., C. Musetti, and C. Sissi, Pt-based drugs: the spotlight will be on proteins. Metallomics, 2014. 6(3): p. 380-95.
25. Benhar, M., D. Engelberg, and A. Levitzki, Cisplatin-induced activation of the EGF receptor. Oncogene, 2002. 21(57): p. 8723-31.
26. Hasinoff, B.B., X. Wu, and Y. Yang, Synthesis and characterization of the biological activity of the cisplatin analogs, cis-PtCl(2)(dexrazoxane) and cis-PtCl(2)(levrazoxane), of the topoisomerase II inhibitors dexrazoxane (ICRF-187) and levrazoxane (ICRF-186). J Inorg Biochem, 2004. 98(4): p. 616-24.
27. Yoshida, T., et al., The anti-EGFR monoclonal antibody blocks cisplatin-induced activation of EGFR signaling mediated by HB-EGF. FEBS Lett, 2008. 582(30): p. 4125-30.
28. Tundo, G.R., et al., Effect of cisplatin on proteasome activity. J Inorg Biochem, 2015. 153: p. 253-258.
29. Schmitt, N.C., S. Trivedi, and R.L. Ferris, STAT1 Activation Is Enhanced by Cisplatin and Variably Affected by EGFR Inhibition in HNSCC Cells. Mol Cancer Ther, 2015. 14(9): p. 2103-11.
30. Messori, L. and A. Merlino, Cisplatin binding to proteins: molecular structure of the ribonuclease a adduct. Inorg Chem, 2014. 53(8): p. 3929-31.
31. Miyazawa, M., A.R. Bogdan, and Y. Tsuji, Perturbation of Iron Metabolism by Cisplatin through Inhibition of Iron Regulatory Protein 2. Cell Chem Biol, 2019. 26(1): p. 85-97 e4.
32. Shin, J.N., et al., Cisplatin inactivation of caspases inhibits death ligand-induced cell death in vitro and fulminant liver damage in mice. J Biol Chem, 2005. 280(11): p. 10509-15.
33. Ragunathan, N., et al., Identification of the xenobiotic-metabolizing enzyme arylamine N-acetyltransferase 1 as a new target of cisplatin in breast cancer cells: molecular and cellular mechanisms of inhibition. Mol Pharmacol, 2008. 73(6): p. 1761-8.
34. Seflova, J., et al., Identification of cisplatin-binding sites on the large cytoplasmic loop of the Na(+)/K(+)-ATPase. J Enzyme Inhib Med Chem, 2018. 33(1): p. 701-706.
35. De Luca, A., et al., A structure-based mechanism of cisplatin resistance mediated by glutathione transferase P1-1. Proc Natl Acad Sci U S A, 2019. 116(28): p. 13943-13951.
36. Duval, R., et al., A RP-UFLC Assay for Protein Tyrosine Phosphatases: Focus on Protein Tyrosine Phosphatase Non-Receptor Type 2 (PTPN2). Sci Rep, 2015. 5: p. 10750.
37. Seiner, D.R., J.N. LaButti, and K.S. Gates, Kinetics and mechanism of protein tyrosine phosphatase 1B inactivation by acrolein. Chem Res Toxicol, 2007. 20(9): p. 1315-20.
38. Lund, I.K., et al., Mechanism of protein tyrosine phosphatase 1B-mediated inhibition of leptin signalling. J Mol Endocrinol, 2005. 34(2): p. 339-51.
39. Shetty, V. and T.A. Neubert, Characterization of novel oxidation products of cysteine in an active site motif peptide of PTP1B. J Am Soc Mass Spectrom, 2009. 20(8): p. 1540-8.
40. Townsend, D.M. and M.H. Hanigan, Inhibition of gamma-glutamyl transpeptidase or cysteine S-conjugate beta-lyase activity blocks the nephrotoxicity of cisplatin in mice. J Pharmacol Exp Ther, 2002. 300(1): p. 142-8.
41. Tegeder, I., et al., Cisplatin tumor concentrations after intra-arterial cisplatin infusion or

embolization in patients with oral cancer. Clin Pharmacol Ther, 2003. 73(5): p. 417-26.
42. Martens-de Kemp, S.R., et al., DNA-bound platinum is the major determinant of cisplatin sensitivity in head and neck squamous carcinoma cells. PLoS One, 2013. 8(4): p. e61555.
43. Zimmermann, T., M. Zeizinger, and J.V. Burda, Cisplatin interaction with cysteine and methionine, a theoretical DFT study. J Inorg Biochem, 2005. 99(11): p. 2184-96.
44. Minervini, T., et al., Fate of cisplatin and its main hydrolysed forms in the presence of thiolates: a comprehensive computational and experimental study. Metallomics, 2019. 11(4): p. 833-844.
45. Hasinoff, B.B., et al., Biochemical and proteomics approaches to characterize topoisomerase IIalpha cysteines and DNA as targets responsible for cisplatin-induced inhibition of topoisomerase IIalpha. Mol Pharmacol, 2005. 67(3): p. 937-47.
46. Huliciak, M., et al., Covalent binding of cisplatin impairs the function of Na(+)/K(+)-ATPase by binding to its cytoplasmic part. Biochem Pharmacol, 2012. 83(11): p. 1507-13.
47. Wu, T.T. and J.D. Castle, Tyrosine phosphorylation of selected secretory carrier membrane proteins, SCAMP1 and SCAMP3, and association with the EGF receptor. Mol Biol Cell, 1998. 9(7): p. 1661-74.
48. Duval, R., et al., Benzoquinone, a leukemogenic metabolite of benzene, catalytically inhibits the protein tyrosine phosphatase PTPN2 and alters STAT1 signaling. J Biol Chem, 2019. 294(33): p. 12483-12494.
49. Karisch, R. and B.G. Neel, Methods to monitor classical protein-tyrosine phosphatase oxidation. FEBS J, 2013. 280(2): p. 459-75.
50. Huyer, G., et al., Mechanism of inhibition of protein-tyrosine phosphatases by vanadate and pervanadate. J Biol Chem, 1997. 272(2): p. 843-51.
51. LaButti, J.N., et al., Redox regulation of protein tyrosine phosphatase 1B by peroxymonophosphate (=O3POOH). J Am Chem Soc, 2007. 129(17): p. 5320-1.
52. Held, J.M., et al., Targeted quantitation of site-specific cysteine oxidation in endogenous proteins using a differential alkylation and multiple reaction monitoring mass spectrometry approach. Mol Cell Proteomics, 2010. 9(7): p. 1400-10.
53. Esteban-Fernandez, D., et al., Speciation analysis of platinum antitumoral drugs in impacted tissues. Talanta, 2007. 72(2): p. 768-73.
54. Ishikawa, T. and F. Ali-Osman, Glutathione-associated cis-diamminedichloroplatinum(II) metabolism and ATP-dependent efflux from leukemia cells. Molecular characterization of glutathione-platinum complex and its biological significance. J Biol Chem, 1993. 268(27): p. 20116-25.
55. Truong, T.H. and K.S. Carroll, Redox regulation of epidermal growth factor receptor signaling through cysteine oxidation. Biochemistry, 2012. 51(50): p. 9954-65.
56. Klaus, V., et al., 1,4-Naphthoquinones as inducers of oxidative damage and stress signaling in HaCaT human keratinocytes. Arch Biochem Biophys, 2010. 496(2): p. 93-100.
57. Ahsan, A., et al., Role of epidermal growth factor receptor degradation in cisplatin-induced cytotoxicity in head and neck cancer. Cancer Res, 2010. 70(7): p. 2862-9.
58. Baier, P., et al., Effect of liver regeneration after partial hepatectomy and ischemia-reperfusion on expression of growth factor receptors. World J Gastroenterol, 2006. 12(24): p. 3835-40.
59. Xu, K. and H.K. Shu, Transcription factor interactions mediate EGF-dependent COX-2

expression. Mol Cancer Res, 2013. 11(8): p. 875-86.
60. Tang, X., T.P.W. McMullen, and D.N. Brindley, Increasing the low lipid phosphate phosphatase 1 activity in breast cancer cells decreases transcription by AP-1 and expressions of matrix metalloproteinases and cyclin D1/D3. Theranostics, 2019. 9(21): p. 6129-6142.
61. Sundqvist, A., et al., TGFbeta and EGF signaling orchestrates the AP-1- and p63 transcriptional regulation of breast cancer invasiveness. Oncogene, 2020. 39(22): p. 4436-4449.
62. Wang, D. and S.J. Lippard, Cellular processing of platinum anticancer drugs. Nat Rev Drug Discov, 2005. 4(4): p. 307-20.
63. Schwertassek, U., et al., Reactivation of oxidized PTP1B and PTEN by thioredoxin 1. FEBS J, 2014. 281(16): p. 3545-58.
64. Zimmermann, T., Z. Chval, and J.V. Burda, Cisplatin interaction with cysteine and methionine in aqueous solution: computational DFT/PCM study. J Phys Chem B, 2009. 113(10): p. 3139-50.
65. Hagrman, D., J. Goodisman, and A.K. Souid, Kinetic study on the reactions of platinum drugs with glutathione. J Pharmacol Exp Ther, 2004. 308(2): p. 658-66.
66. Dabrowiak, J.C., J. Goodisman, and A.K. Souid, Kinetic study of the reaction of cisplatin with thiols. Drug Metab Dispos, 2002. 30(12): p. 1378-84.
67. Jestin, J., Lambert, B. & Chottard, JC., Kinetic study of DNA binding of cisplatin and of a bicycloalkyl-substituted (ethylenediamine)dichloroplatinum(II) complex. J Biol Inorg Chem, 1998. 3: p. 5.
68. Denu, J.M. and K.G. Tanner, Specific and reversible inactivation of protein tyrosine phosphatases by hydrogen peroxide: evidence for a sulfenic acid intermediate and implications for redox regulation. Biochemistry, 1998. 37(16): p. 5633-42.
69. Abiko, Y., et al., Activation of PTP1B/EGFR signaling and cytotoxicity during combined exposure to ambient electrophiles in A431 cells. J Toxicol Sci, 2021. 46(4): p. 177-185.
70. Yuan, C., et al., Potent and selective PTP1B inhibition by a platinum(ii) complex: possible implications for a new antitumor strategy. Chem Commun (Camb), 2019. 56(1): p. 102-105.

LEGEND FIGURES

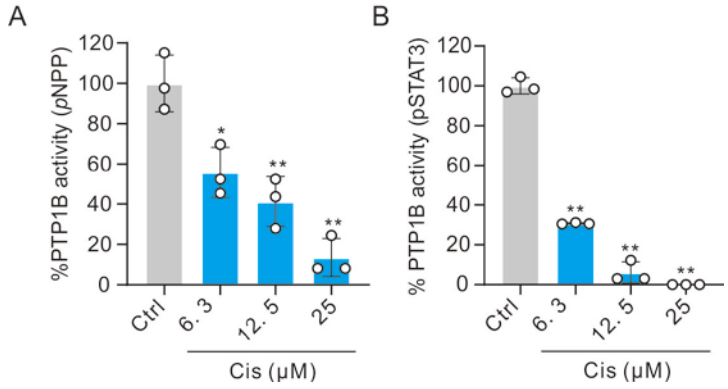

Figure 1: Impairment of PTP1B phosphatase activity by cisplatin

PTP1B (200 nM) was incubated with increasing cisplatin concentrations (0 µM (Ctrl), 6.3 µM, 12.5 µM, 25 µM)) at 37°C for 30 minutes and residual PTP1B activity was assayed. (A) PTP1B residual phosphatase activity determined with *p*NPP assay by following the absorbance of the solution at 405 nm. Data are represented as the mean of three independent experiments +/- SD. * p-value < 0.05, ** p-value < 0.01. (B) PTP1B residual tyrosine phosphatase activity was measured using pSTAT3 peptide by RP-UFLC. Data are represented as the mean of three independent experiments +/- SD. ** p-value < 0.01.

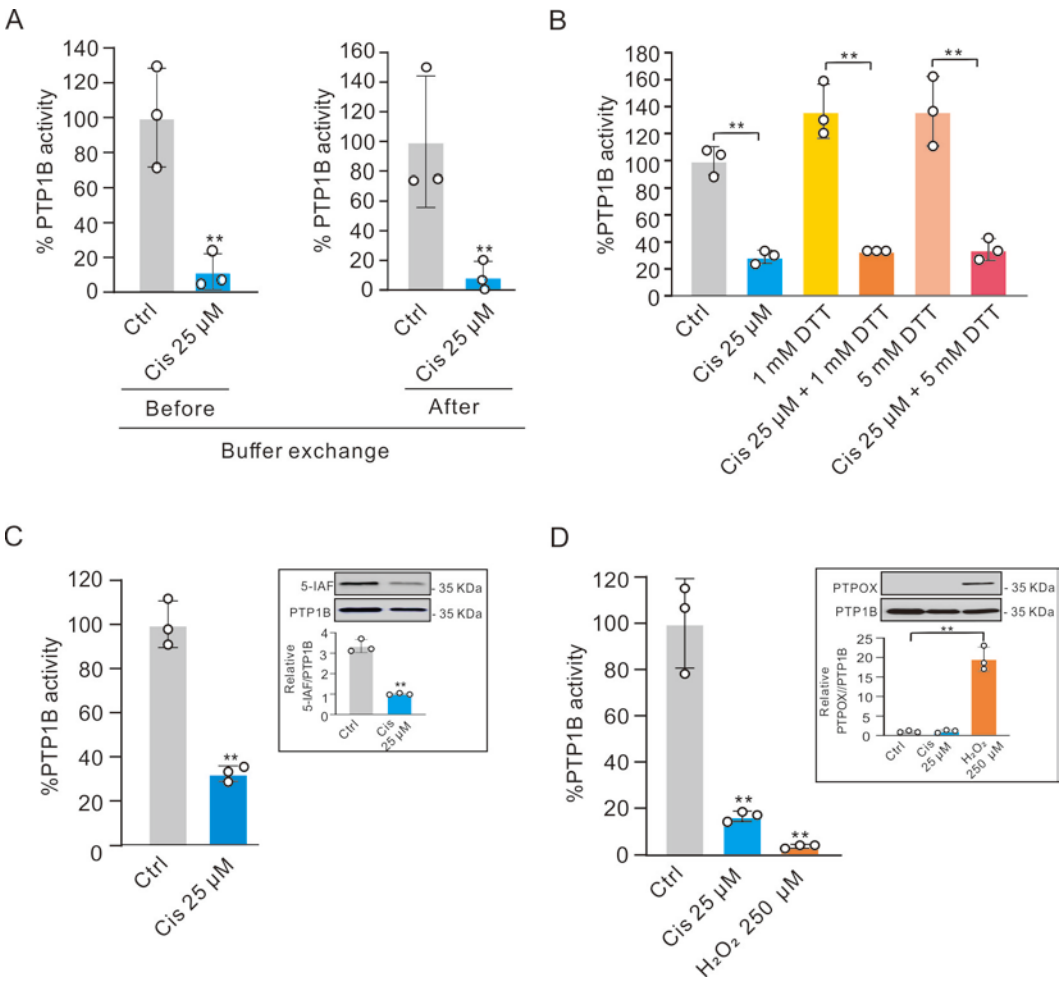

Figure 2: Irreversibility of PTP1B inhibition by cisplatin and modification of cysteine residues

(A) PTP1B (200 nM) was incubated with cisplatin (25 µM) at 37°C for 30 minutes and then subjected to buffer exchange. A control (Ctrl) was done in absence of cisplatin. PTP1B residual activity was measured by *p*NPP before and after buffer exchange. Data are represented as the mean of three independent experiments +/- SD. ** p-value < 0.01. (B) PTP1B (200 nM) was incubated with cisplatin (25 µM) at 37°C for 30 minutes, followed by the addition of DTT (1 or 5 mM) and incubation at room temperature for 10 more minutes. A control (Ctrl) was done with PTP1B only. Other controls were done with PTP1B in presence of DTT. PTP1B residual activity in samples was measured by *p*NPP. Data are represented as the mean of three independent experiments +/- SD. ** p-value < 0.01. (C) PTP1B (200 nM) was incubated with or without (Ctrl) cisplatin (25 µM) at 37°C for 30 minutes, followed by the addition of 5-IAF (20 µM) and further incubation at 37°C for 10 more minutes.

PTP1B residual activity was measured by *p*NPP assay and modification of PTP1B cysteine residues by 5-IAF was evidenced by fluorescence as described in Materials and methods section. Data are represented as the mean of three independent experiments +/- SD. ** p-value < 0.01. Membrane is representative of three independent experiments. (D) PTP1B (200 nM) was incubated with cisplatin (25 µM), H_2O_2 (250 µM) or buffer (Ctrl) for 30 minutes at 37°C. PTP1B residual activity and oxidation of PTP1B catalytic cysteine residue were detected by *p*NPP assay and western blot using an anti-oxidized PTP active site cysteine antibody, respectively. Data are represented as the mean of three independent experiments +/- SD. ** p-value < 0.01. Membrane is representative of three independent experiments.

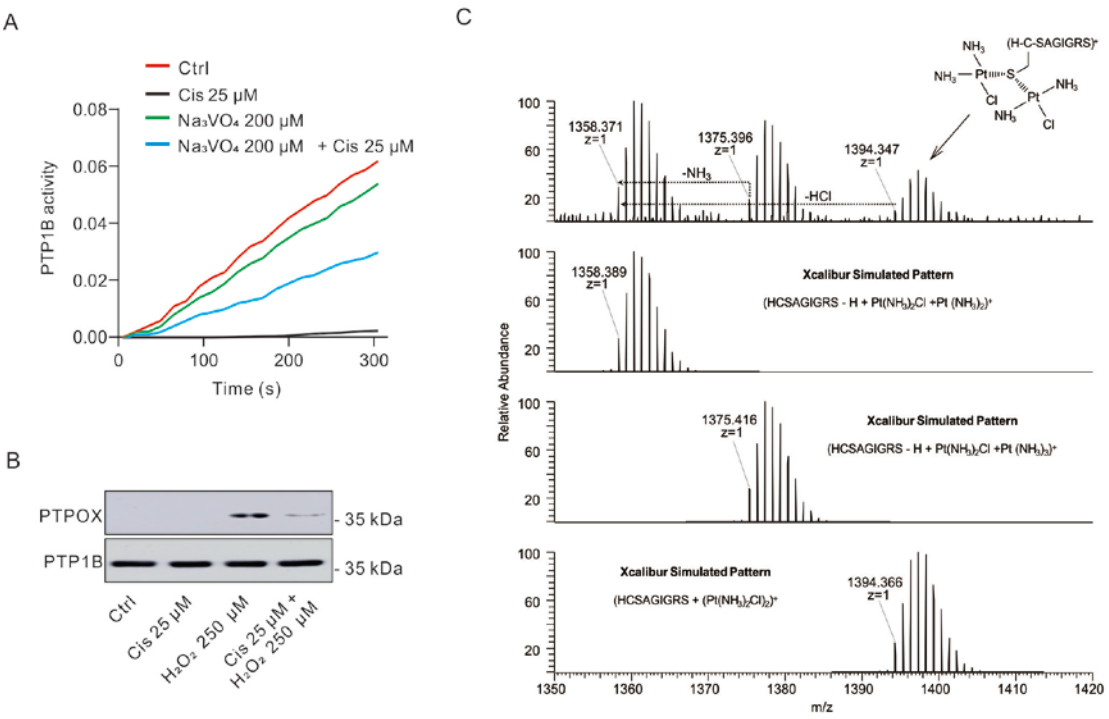

Figure 3: Analysis of PTP1B-cisplatin adduct on PTP1B active site cysteine

(A) PTP1B (200 nM) was incubated with Na3VO4 (200 µM) at 37°C for 30 minutes in the presence or absence of cisplatin (25 µM). Incubations of the enzyme in presence of cisplatin only were carried out. Incubation with PTP1B only was also done (Ctrl). PTP1B residual activity was measured by *p*NPP. (B) PTP1B (200 nM) was pre-incubated with cisplatin (25 µM) at 37°C for 30 minutes prior to incubation with H_2O_2 (250 µM) for 10 minutes. Control samples with PTP1B incubated with cisplatin or H_2O_2 were also carried out. Oxidation of PTP1B catalytic cysteine residue was evidenced by western blot using an anti-oxidized PTP active site cysteine antibody. Membrane is representative of three independent experiments. (C) 10 µg of PTP1B peptide derived from the sequence of the enzyme catalytic domain (214HCSAGIGRS222) was incubated with cisplatin (2.5 mM) at 37°C for 24 hours prior to LC-MS/MS analysis. The combined non-deconvoluted signal of the modified peptide at charge state 1+ are shown (top panel). Thermo Xcalibur v3.0.63 and especially the isotope simulation tool embedded in the software was used to simulate isotopic patterns obtained after reaction of cisplatin with the HCSAGIGRS peptide (lower panels).

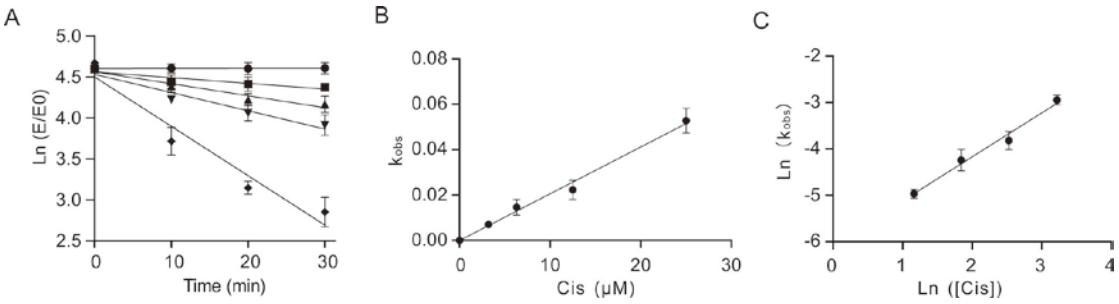

Figure 4: Kinetics of PTP1B inhibition by cisplatin

(A) PTP1B (200 nM) was incubated with different concentrations of cisplatin (circle represents 0 µM, square represents 3.1 µM, triangle represents 6.3 µM, inverted triangle represents 12.5 µM, diamond represents 25 µM) at 37°C. At different time points, an aliquot of the mix was taken and PTP1B residual activity was determined with *p*NPP assay. k_{obs} were calculated from the slope of the natural logarithm of PTP1B residual activity as a function of time for each cisplatin concentration. Data are represented as the mean of three independent experiments +/- SD. (B) k_{obs} were plotted as a function of cisplatin concentration and the second order inhibition rate constant (ki) was determined from the slope of the linear regression (slope: 2063 ± 106 $M^{-1}{\cdot}min^{-1}$, R^2 = 0.97). Data are represented as the mean of three independent experiments +/- SD. (C) Reaction order value was determined by a least-square procedure from the slope of the linear plot of the natural logarithm of k_{obs} as a function of the natural logarithm of cisplatin concentration (slope: 0.95 ± 0.068, R^2 = 0.95). Data are represented as the mean of three independent experiments +/- SD.

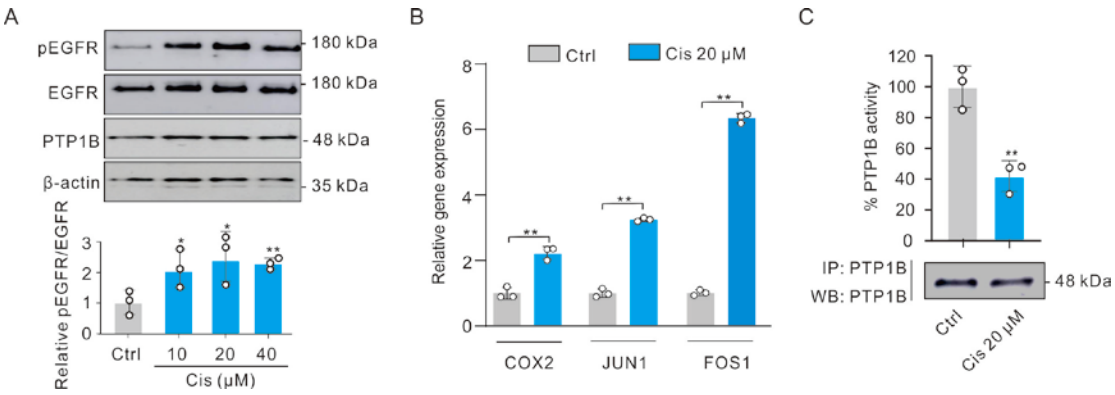

Figure 5: Effects of cisplatin on EGFR tyrosine phosphorylation and on endogenous PTP1B activity in cells

(A) HaCaT cells were treated with different concentrations of cisplatin (0 µM, 10 µM, 20 µM, 40 µM) for 24 hours as described previously [25]. Total cell extracts were obtained and EGFR tyrosine phosphorylation and total EGFR protein expression were determined by western blot and quantified. PTP1B and β-actin amounts in cell extracts were also determined by western blot. Data are represented as the mean of three independent experiments +/- SD. * p-value < 0.05, ** p-value < 0.01. Membrane is representative of three independent experiments. (B) HaCaT cells were treated with cisplatin (20 µM) for 24 hours at 37°C. Relative gene expression of COX2, JUN1 and FOS1 were analyzed by RT-qPCR. Data were normalized using ubiquitin gene. Data are represented as the mean of three independent experiments +/- SD. ** p-value < 0.01. (C) HaCaT cells were treated with cisplatin (20 µM) for 24 hours at 37°C and endogenous PTP1B protein was immunoprecipitated from whole cell extracts. Residual PTP1B activity and PTP1B protein content were determined by RP-UFLC and western blot, respectively. Data are represented as the mean of three independent experiments +/- SD. ** p-value < 0.01. Membrane is representative of three independent experiments.

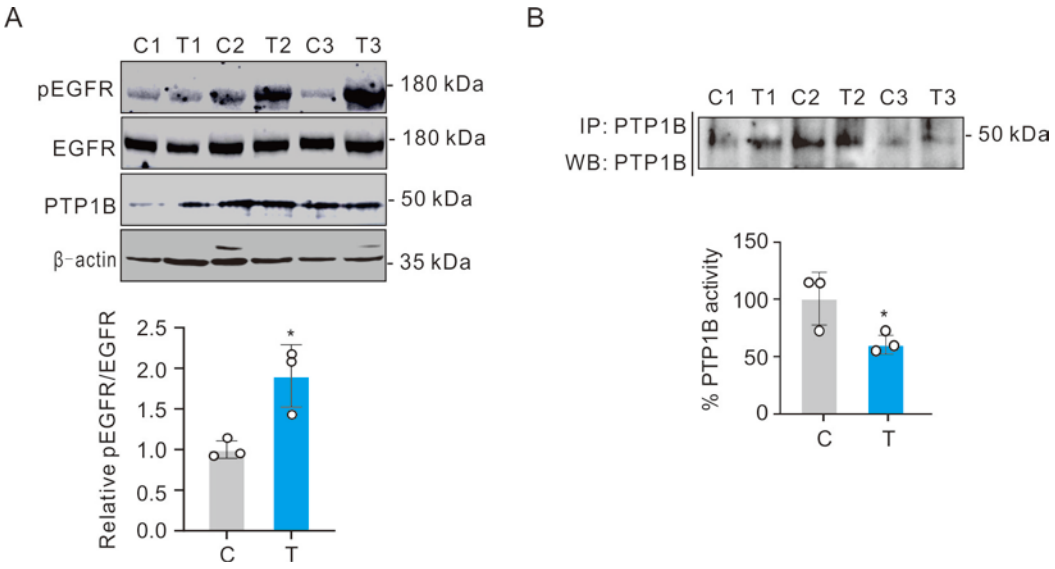

Figure 6: Exposure of mice to cisplatin and subsequent effects on EGFR tyrosine phosphorylation and PTP1B activity in liver

(A) Mice were treated or not with cisplatin (7.5 mg/kg) for 5 hours (C: control group; T: cisplatin treated group). Livers were taken, lysed and EGFR phosphorylation levels were determined by western blot. Data are represented as the mean of three independent experiments +/- SD. * p-value < 0.05. Membrane is representative of three independent experiments. (B) Endogenous PTP1B protein was immunoprecipitated from liver whole cell extracts. Residual PTP1B activity and PTP1B protein content were determined by RP-UFLC and western blot, respectively. Data are represented as the mean of three independent experiments +/- SD. * p-value < 0.05. Membrane is representative of three independent experiments.

SUPPLEMENTARY MATERIALS AND METHODS

Spectroscopic analysis of cisplatin binding to PTP1B active site peptide

PTP1B peptide (100 μM) was incubated with cisplatin (400 μM) at room temperature for 24 h. At different time points, absorbance of the solution was measured from 220 nm to 400 nm using UV-VIS spectrophotometer.

Docking study

The crystal structure of the human Protein Tyrosine Phosphatase 1B (PDB ID: 2CM2 (Ala *et al*. 2006) was obtained from the Protein Data Bank (Berman *et al*. 2000). This crystal structure was chosen based on its high resolution of 1.5 Å and on the structure of the catalytic site, which is in open form. In this conformation, the Cys^{215} is exposed toward the solvent and is not buried by any loop surrounding the active site, such as Ala^{217}-Gly^{218}-Ile^{219}-Gly^{220} loop or Pro^{180}-Asp^{181}-Phe^{182}-Gly^{183}-Val^{184}, as observed in several other structures. The atoms that did not belong to PTP1B were removed. All hydrogen atoms were added to the PTP1B structure using PROPKA program (Sondergaard *et al*. 2011; Olsson *et al*. 2011). The thiol group of the Cys^{215} was deprotonated. The structure of cisplatin (Deposition Number: 924182 (Lewis *et al*. 2013)) was downloaded from the Cambridge Structural Database (Groom *et al*. 2016). The docking studies were performed using AutoDock 4.2 program (Morris *et al*. 2009). For the docking computations, the grid box was centered on the Cys^{215} with a size of 126×126×126 points separated by a spacing of 0.258 Å. The Lamarckian genetic algorithm (LGA) was employed. Four independent runs of docking computations were performed with, for each, the parameters as following: 250 LGA operations, a population size of 150 individuals, a maximum of 2,500,000 energy evaluations and a maximum of 27,000 generations. The default parameters for the LGA operation and Sollis and Wet local search were used. All dihedral angles of the cisplatin were allowed to rotate during the docking procedure. For the PTP1B, the sidechain of Tyr^{46}, LYS^{116}, Lys^{120}, Cys^{215}, Ser^{216}, Ala^{217}, Gln^{262} and Gln^{266} were flexible.

REFERENCES

Ala, P.J., Gonneville, L., Hillman, M.C., Becker-Pasha, M., Wei, M., Reid, B.G., Klabe, R., Yue, E.W., Wayland, B., Douty, B., Polam, P., Wasserman, Z., Bower, M., Combs, A.P., Burn, T.C., Hollis, G.F., Wynn, R. Structural Basis for Inhibition of Protein-Tyrosine Phosphatase 1B by Isothiazolidinone Heterocyclic Phosphonate Mimetics. J Biol Chem. 281: 32784 (2006).

H.M. Berman, J. Westbrook, Z. Feng, G. Gilliland, T.N. Bhat, H. Weissig, I.N. Shindyalov, P.E. Bourne. The Protein Data Bank. Nucleic Acids Research. 28: 235-242 (2000).

C. R. Groom, I. J. Bruno, M. P. Lightfoot and S. C. Ward. The Cambridge Structural Database. Acta Cryst. B72: 171-179 (2016)

J. E. M. Lewis, C. J. McAdam, M. G. Gardiner and J. D. Crowley. A facile “click” approach to functionalised metallosupramolecular architectures. Chem. Commun. 49: 3398-3400 (2013).

G.M. Morris, R. Huey, W. Lindstrom, M.F. Sanner, R.K. Belew, D.S. Goodsell, A.J. Olson. Autodock4 and AutoDockTools4: automated docking with selective receptor flexibility. J. Comput. Chem. 16: 2785–2791 (2009).

C.R. Sondergaard, M.H.M. Olsson, M. Rostkowski, J.H. Jensen. Improved treatment of ligands and coupling effects in empirical calculation and rationalization of pKa values. J. Chem. Theory Comput. 7: 2284–2295 (2011).

M.H.M. Olsson, C.R. Sondergaard, M. Rostkowski, J.H. Jensen. PROPKA3: consistent treatment of internal and surface residues in empirical pKa predictions. J. Chem. Theory Comput. 7: 525–537 (2011).

SUPPLEMENTARY LEGEND FIGURES

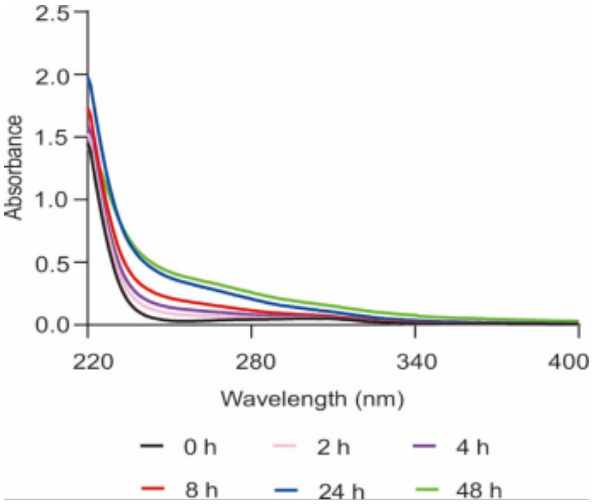

Figure S1: Spectroscopic analysis of the binding of cisplatin to a PTP1B peptide derived from the sequence of the active site of the enzyme and containing the catalytic Cys215 residue. 100 μM of PTP1B peptide derived from the sequence of the enzyme catalytic domain ($_{214}$HCSAGIGRS$_{222}$) were incubated with cisplatin (400 μM) in H_2O at room temperature. At different time points (0, 2, 4, 8, 24, 48 h), the absorbance of the solution (between 220 and 400 nm) was determined using UV-VIS spectrophotometer (SHIMADZU, Japan).

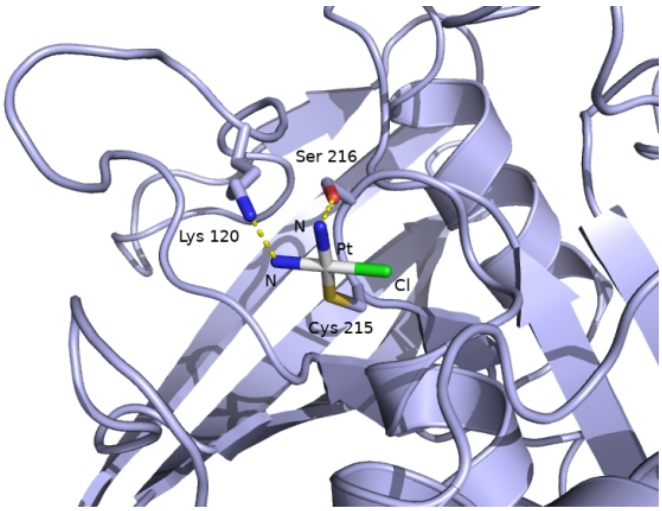

Figure S2: Covalent docking of cisplatin on the Cys215 within the active site of human PTP1B. PTP1B is in cartoon representation, the important residues and cisplatin are in sticks. Hydrogen bonds are displayed as yellow broken lines. The figure was created using PyMOL program (https://www.pymol.org/).

3.2 Result 2

Biochemical, enzymatic and computational characterization of recurrent somatic mutations of the human protein tyrosine phosphatase PTP1B in primary mediastinal B cell lymphoma

Rongxing LIU[1], Yujie SUN[2], Jérémy BERTHELET[3], Linh-Chi BUI[1], Ximing XU[2], Jean-Marie DUPRET[1], Mireille VIGUIER[1], Frédérique DESHAYES[1] and Fernando RODRIGUES LIMA[1,*]

1 Université Paris Cité, BFA, UMR 8251, CNRS, F-75013, Paris, France

2 School of Medicine and Pharmacy, Ocean University of China, Qingdao, 266071, Shandong, China

3 Université Paris Cité, CEDC, UMR 7216, CNRS, F-75013, Paris, France

* Correspondence: Fernando.rodrigues-lima@u-paris.fr (F Rodrigues Lima)

Running title: Effects of lymphoma associated mutations on PTP1B

ABSTRACT

Human protein tyrosine phosphatase 1B (PTP1B) is a ubiquitous non-receptor tyrosine phosphatase that serves as a major negative regulator of tyrosine phosphorylation cascades of metabolic and oncogenic importance such as the insulin, EGFR and JAK/STAT pathways. Increasing evidence point to a key role of PTP1B-dependent signaling in cancer. Interestingly, genetic defects in PTP1B have been found in different human malignancies. Notably, recurrent somatic mutations and splice variants of PTP1B were identified in human B cell and Hodgkin lymphoma. In this work, we analyzed the molecular and functional levels of three PTP1B mutations identified in PMBCL patients and located in WPD-loop (V184D), P-loop (R221G) and Q-loop (G259V). Using biochemical, enzymatic and molecular dynamics approaches, we show that these mutations lead to PTP1B mutants with extremely low intrinsic tyrosine phosphatase activity and displaying alterations in overall protein stability and in the flexibility of the active site loops of the enzyme. This is in agreement with the key role of the active site loop regions which are preorganized to interact with substrate and to enable catalysis. All together our study provide molecular and enzymatic evidence for the loss of protein tyrosine phosphatase activity of PTP1B active-site loop mutants identified in human lymphoma.

Keywords: lymphoma, protein tyrosine phosphatase, PTP1B, oncogenic mutations, enzyme activity

Abbreviations: PTP, protein tyrosine phosphatase; PTP1B, protein tyrosine phosphatase 1B; PMBCL, primary mediastinal B cell lymphoma; RP-UFLC, reverse-phase ultra fast liquid chromatography; TSA, thermal shift assay; MD, molecular dynamics.

1. INTRODUCTION

Primary mediastinal B cell lymphoma (PMBCL) is a rare subtype of aggressive B cell lymphoma that is putatively derived from thymic B cells [1]. Although PMBCL is considered distinct from other B cell non-Hodgkin lymphoma subtypes, it has features that overlap with Hodgkin lymphoma [1]. The malignant cells express B cell markers (CD19, CD20, CD22) and B cell transcription factors such as PAX5, OCT2, BCL6 [2]. The pathobiology of PMBCL is known to rely on the alteration of different molecular pathways. In particular, different cell signaling cascades such as JAK/STAT and nuclear factor-κB (NF-κB) pathways have been shown to be dysregulated in PMBCL, leading to increased protein tyrosine phosphorylation [3-5]. Recently, recurrent mutations in the PTPN1 gene encoding the human protein tyrosine phosphatase 1B (PTP1B) were reported in PMBCL and Hodgkin lymphoma thus supporting previous evidence of the involvement of PTP1B enzyme in lymphomagenesis [6, 7]. In addition, an inactive splice variant of PTP1B has been identified in classical Hodgkin lymphoma cells and shown to increase tyrosine phosphorylation signaling [8]. Further studies in mice models have also reported that lack of PTP1B induces myeloproliferative neoplasm and can lead to development of acute leukemia [9, 10].

PTP1B is a ubiquitous non-receptor tyrosine phosphatase that serves as a major negative regulator of tyrosine phosphorylation cascades of metabolic importance such as insulin or leptin signaling [11, 12]. In addition to its metabolic impact, mounting evidence points out for a critical role of PTP1B in cancer serving both as a tumor suppressor or promoter depending on the context [13]. In particular, PTP1B plays a pivotal role in the modulation of relevant oncogenic signaling pathways such as the EGFR and the JAK/STAT cascades through tyrosine dephosphorylation of several protein effectors [13-17]. Interestingly, genetic defects impacting these pathways and/or aberrant signaling are known in lymphoma [18-20].

All PTPs catalyze the cleavage and hydrolysis of phosphotyrosine in their protein targets. PTP1B shares a common catalytic mechanism based on a nucleophilic cysteine and other important invariant residues that are located in a number of highly conserved adjacent loops that form the active site (such as pTyr-loop, WPD-loop,

P-loop and Q-loop) [21]. Structure, flexibility and dynamics of these active site loops (notably the WPD-loop, residues 177-188) but also of adjacent residues are key for catalysis and modulation of PTP1B activity [22-24]. In addition, it is now known that there is also a regulatory network (allosteric network) of different residues throughout the enzyme structure (such as Arg56, Ala69, Tyr153 or Asn193) that contribute to PTP1B activity notably through impacting the motion of the WPD-loop [22, 23, 25]. In this manuscript, we further analyzed the molecular and enzymatic levels of three PTP1B mutations identified in PMBCL patients and located in the WPD-loop (V184D), the P-loop (R221G) and the Q-loop (G259V) of the enzyme [7, 21]. We found that recombinantly expressed and purified PTP1B mutants displayed extremely low phosphatase activity. In line with this, expression of the three PTP1B mutants in cells also led to enzymes with very low intrinsic tyrosine phosphatase activity and, as expected, concomitant increase of the tyrosine phosphorylation of EGFR, a known PTP1B substrate. Further biochemical and molecular dynamics approaches indicated that these PTP1B mutations impact overall protein stability, protein dynamics and the flexibility of the active site PTP1B loops, notably WPD-loop, P-loop and Q-loop. Our study thus provides molecular and enzymatic evidence that the PTP1B active-site loop mutants identified in human lymphoma are strongly impaired in their tyrosine phosphatase activity thus contributing to aberrant cell signaling.

2. MATERIALS AND METHODS

2.1. Materials

p-nitrophenyl phosphate (*p*NPP), HClO4, dithiothreitol (DTT), sodium fluoride (NaF), sodium orthovanadate (Na3VO4), isopropyl β-D-thiogalactoside (IPTG), Triton X-100, lysozyme, His-select nickel resin, SYPRO, were obtained from Sigma-Aldrich (France). Protease inhibitors were purchased from Roche (France). PD-10 columns were from Cytiva (France). α-EGFR antibody (SAB4300352) and Protein G plus-agarose beads (SC-2002) were obtained from Santa Cruz Biotechnology (France). α-PTP1B antibody (FG6-1G) was purchased from Merck (France) and α-pan-phospho-tyrosine antibody (9411) was obtained from Cell

Signaling (France).

2.2. Cell culture

HEK 293T and COS7 cells were cultured in DMEM medium (Gibco, France) supplemented with 10% fetal bovine serum (Sigma, France) at 37°C under 5% CO2.

2.3. Generation of PTP1B mutants

Mutations V184D, R221G and G259V of PTP1B were generated in pET28-PTP1B (residues 1-321) and pCMV flag-PTP1B (full length) plasmids using the Agilent QuikChange XL site-directed mutagenesis kit with the following mutagenesis primers. Presence of the mutations was then verified by DNA sequencing (Eurofins).

V184D-For: GGCCTGACTTTGGAGACCCTGAATCACACCAG

V184D-Rev: CTGGTGTGATTCAGGGTCTCCAAAGTCAGGCC

R221G-For: GTGCAGGCATCGGCGGGTCTGGAACCTTC

R221G-Rev: GAAGGTTCCAGACCCGCCGATGCCTGCAC

G259V-For: GGAAGTTTCGGATGGTGCTGATCCAGACAGC

G259V-Rev: GCTGTCTGGATCAGCACCATCCGAAACTTCC

2.4. Expression and purification of recombinant PTP1B enzymes

pET28 WT and mutants PTP1B plasmids were transformed into BL21 HI-Control™ (DE3) E.Coli. Bacteria were cultured at 37°C under agitation until reaching an OD of 0.6, then grown overnight at 16 °C in the presence of 0.5 mM IPTG. Cells were harvested by centrifugation and resuspended in lysis buffer (20 mM Tris HCl, 100 mM NaCl, 0.5% Triton X-100, 1 mg/ml lysozyme and protease inhibitor, pH 7.5). The lysate was sonicated (10 sec ON, 20 sec OFF, 10 min, 20 % power) on ice and pelleted (15,000 g, 30 min, 4°C). Supernatant was incubated with His-select nickel resin in the presence of 10 mM imidazole for 2 hours at 4°C under agitation. Beads were then poured into a column, washed with washing buffer (20 mM Tris-HCl, 100 mM NaCl, 20 mM imidazole, pH 7.5) and enzyme was eluted with elution buffer (20 mM Tris-HCl, 100 mM NaCl, 300 mM imidazole, pH 7.5). Protein elution was controlled by Bradford assay and eluted samples were incubated with 10 mM DTT on ice for 20 min. Purified enzyme was buffer exchanged to 20 mM Tris-HCl, 100 mM NaCl, pH 7.5 using a PD-10 column. Protein concentration and

purity were assessed by Bradford reagent and SDS-PAGE. Proteins were stored at –80°C until use.

2.5. Determination of recombinant PTP1B activity using FAM-conjugated tyrosine-phosphorylated STAT1 (pSTAT1) peptide by RP-UFLC

The tyrosine phosphatase activity of enzymes were measured by RP-UFLC using FAM-conjugated peptide derived from the sequence of human STAT1 where tyrosine 701 is phosphorylated (KGTGY701IKTE, Proteogenix, France) as previously described [29]. Briefly, samples containing PTP1B enzymes were incubated with FAM-conjugated pSTAT1 peptide in 100 mM sodium acetate buffer, 1 mM DTT, pH 6 for 30 minutes at 37°C (total volume of 50 µl). The reaction was stopped with the addition of 50 µl HClO4 (15%, v/v) and samples were injected into a Shim-pack XR ODS column (100 mm, 2 mm, 2.2 µm) (Shimadzu) at 40 °C. The mobile phase used for the separation consisted of two eluents: solvent A was water with 0.12% trifluoacetic acid (TFA), and solvent B was acetonitrile with 0.12% TFA. Compounds were separated by an isocractic flow (80% A/20% B) rate of 0.6 ml/min. pSTAT1 peptide and its dephosphorylated form (product) were monitored by fluorescence emission ($\lambda = 530$ nm) after excitation at $\lambda = 485$ nm and quantified by integration of the peak absorbance area.

2.6. PTP1B transfection, immunoprecipitation and tyrosine phosphorylation immunodetection in HEK 293T and COS7 cells.

HEK 293T and COS7 cells were seeded at 100 000 cells/cm² in a 100 cm² Petri dish and directly transfected using a solution containing 3 µg of WT or mutants pCMV flag-PTP1B and 6 µl metafectene (Biontex) according to manufacturer's instructions. Cells were then put back in the incubator at 37°C, 5 % CO2 for 48 hours.

For PTP1B immunoprecipitation, transfected HEK 293T cells were later washed with PBS, harvested and lysed in lysis buffer (PBS 1X, 1% Triton X-100 and protease inhibitor) at 4 °C for 30 minutes under agitation. Cell lysates were centrifuged at 15,000g for 10 minutes at 4°C, and the supernatants (whole cell extracts) were kept. Transfected PTP1B was immunoprecipitated by incubating 1 mg of whole cell extracts in the presence of 1 µg of PTP1B antibody overnight at 4°C under agitation.

Samples were then rocked for 1 hour at 4°C in the presence of 30 µl protein G–Agarose beads. Immunobeads were harvested by centrifugation, washed three times with lysis buffer (PBS, 1% Triton X-100), and split in two. Half of the beads was incubated with 50 µM FAM–phosphorylated STAT1 peptide in sodium acetate buffer (100 mM, 1 mM DTT, pH 6) at 37°C for 2 hours (total volume of 50 µl) to determine PTP1B residual activity by RP-UFLC as described previously [28]. The second part of immunobeads were incubated with non-reducing Laemmli sample buffer and heated at 100°C for 10 minutes. Samples were separated by SDS-PAGE, transferred onto nitrocellulose membrane and analyzed by western blot using α-PTP1B antibody.

COS7 cells transfected with WT and the different PTP1B mutants were used to evaluate the tyrosine phosphorylation of EGFR as previously described by Flint et al. [30]. Briefly, transfected COS7 cells were washed with PBS, harvested and lysed in lysis buffer (PBS 1X, 1% Triton X-100, 1 mM Na3VO4, 1 mM NaF and protease inhibitors) at 4 °C for 30 minutes under agitation. Cell lysates were centrifuged at 15,000g for 10 minutes at 4°C, and the supernatants (whole cell extracts) were kept. Samples were separated by SDS-PAGE and transferred onto a nitrocellulose membrane. EGFR tyrosine phosphorylation was then assessed by western blot using an anti-phospho-tyrosine antibody as described by Flint et al. [30]. Membranes were later stripped and re-probed sequentially with α-EGFR and α-PTP1B antibodies.

2.7. Determination of PTP1B intrinsic stability by thermal shift assay (TSA)

TSA was performed to monitor the thermal intrinsic stability of PTP1B proteins. Briefly, WT and mutants PTP1B proteins (5 µM) were incubated in the presence of 10X SYPRO orange dye in a total volume of 10 µl buffer (25 mM Tris, 100 mM NaCl, pH 7.5) in 384-well opaque PCR plates (Roche). Plates were then centrifuged (1300 rpm, 4°C) and real-time analysis of the thermal stability of the proteins were performed by fluorescence reading (excitation: 465 nm, emission: 580 nm) on a Light Cycler 480 (Rock). The program was the following: 1) 15 sec incubation at 20°C; 2) temperature rise from 20°C to 95°C with an increment of 0.05°C/sec and 12 readings/degree; 3) return to 20°C for 15 sec. The obtained fluorescence data were analyzed and quantified using LightCycling 480 SW 1.5. Tm values were measured

by determining the minimum of the first derivative of fluorescence emission as a function of temperature (dFluo/dT).

2.8. Evaluation of protein stability/aggregation by western blot

WT and mutants PTP1B proteins (10 µg) were incubated at 37°C in a total volume of 50 µl (25 mM Tris, 100 mM NaCl, pH 7.5). At different time point (0, 1, 2, 4 hours), 10 µl of the reaction mix were taken and samples were separated by SDS-PAGE and transferred onto a nitrocellulose membrane. Ponceau staining was conducted on the membrane prior to incubation with α-PTP1B antibody.

2.9. Molecular dynamics of WT PTP1B and mutant PTP1B

The PTP1B WT (PDB code: 2HNP) and its three mutants generated by PyMol (version 2.5, academic license) with the least constraints were simulated using the Amber20 software and the charmm36m force field. The biomolecules were solvated with water molecules and a rectangular system with an edge distance of 10 Å was selected. Na+ ions were also added to neutralize the system using the Monte Carlo method. Periodic boundary conditions were then applied according to the shape and size of the system. The Particle Mesh Ewald (PME) FFT mesh information was determined and then minimization was performed to eliminate steric clashes. The temperature was increased from 0 K to 303.15 K for 5 ns at constant volume and temperature. After equilibrium was reached, molecular dynamics was performed for 100 ns at a constant pressure and temperature of 1 atm and 303.15 K. Trajectories every 0.1ns and an output file were recorded. Visual Molecular Dynamics (VMD) software was used to load the visualized trajectory file to analyse the root mean square deviation (RMSD) of the protein backbone atoms as well as the root mean square fluctuation (RMSF) of residues.

2.10. Statistical analysis

All data were reported as mean ± standard deviation (S.D.) of three independent experiments. Quantification of western blot signal was carried out using ImageJ software (National Institutes of Health, USA). Data were analyzed by one-way analysis of variance (ANOVA) using GraphPad Prism version 8.0.0. A threshold of $p < 0.05$ was used to consider differences as statistically significant. (*$P \leq 0.05$, **$P \leq$

0.01).

3. RESULTS AND DISCUSSION

Recurrent somatic mutations of human PTP1B in PMBCL have been recently reported. While these mutations occurred throughout the PTP1B sequence, the majority were nonetheless found in the catalytic domain of the enzyme (spanning residues 1-321) [7]. Analysis of the tyrosine phosphatase activity in cell lysates of these mutants indicated that certain mutations can lead to PTP1B variants with significantly decreased activity whereas other mutations have little impact [7]. As stated previously, the activity of PTP1B and its catalytic regulation rely on the architecture and flexibility of a number of conserved active site loops, and in particular in the optimal arrangement of amino acids within these loops[21, 24]. Interestingly, three point mutations were found within the WPD-loop (V184D), P-loop (R221G) and Q-loop (G259V) in PMBCL patients. Although the V184D mutation has been shown to reduce the overall tyrosine phosphatase activity of cell lysates overexpressing the PTP1B V184D mutant, the molecular and enzymatic impact of these three loop mutations on human PTP1B were not addressed [7].

The catalytic domain (residues 1-321) of human WT PTP1B and the V184D, R221G and G259V PTP1B mutants were expressed in E.coli and purified by IMAC chromatography. This domain was used as it is more amenable to heterologous expression in bacteria and to purification. In addition, the PTP1B catalytic domain has been used in most studies devoted at understanding the catalytic mechanism, the structure and/or the regulation of PTP1B activity, notably through the use of purified PTP1B mutants [22-27]. As shown in Figure 1, the WT and mutant forms of human PTP1B were readily expressed and purified, indicating that the mutations had no gross effects on the expression of the proteins. To assess the intrinsic protein tyrosine phosphatase activity of WT PTP1B and the three mutants, we carried out reverse-phase ultra fast liquid chromatography (RP-UFLC) using a known tyrosine-phosphorylated peptide substrate of PTP1B (sequence: KGTGYphosphoIKTE) derived from human STAT1 as previously described [28, 29].

Compared to WT PTP1B, the intrinsic protein tyrosine phosphatase activity of the three mutants was found to be extremely low, V184D mutant displaying around 5% residual activity and the R221G and G259V mutants being almost inactive (Figure 2A). Similar results were obtained when a classical non-peptidic phosphatase substrate (*p*NPP) known to be dephosphorylated by PTP1B was used (Supplementary Figure 1). These data show that the three PMBCL-associated mutations (V184D, R221G, G259V) that occurred in active site loops lead to PTP1B variants that are strongly impaired in their intrinsic tyrosine phosphatase activity. Our results on the V184D PTP1B mutation concur with activity assays conducted in extracts of transfected cells and showing that this mutant albeit strongly impaired retained some residual tyrosine phosphatase activity (~30% activity compared to WT) [7]. Nonetheless, as these activities were measured in cells extracts, it is thus possible that other PTP enzymes present in the extracts have contributed to the overall tyrosine phosphatase activity. The two other PTP1B mutants, R221G and G259V identified in PBMCL, were not analyzed in the Gunawardana et al. study [7]. To further characterize the V184D, R221G and G259V PTP1B mutants, transfection studies were carried out in HEK293T cells followed by immunoprecipitation and measurement of their intrinsic tyrosine phosphatase activity by RP-UFLC as previously described [29]. In agreement with the results reported above with the recombinant purified proteins, we found that the R221G and G259V mutants displayed no intrinsic protein tyrosine phosphatase activity while the V184D mutant displayed around 5% of the WT activity (Figure 2B). Transfection studies in COS7 cells expressing the EGFR receptor (which is a well-known endogenous substrate of PTP1B) were carried out to analyze the tyrosine phosphatase activity of the mutants as described previously [30]. As shown in Figure 2C, compared to WT PTP1B, the three mutants were much less effective at dephosphorylating EGFR in transfected cells thus further supporting that the V184D, R221G and G259V PTP1B mutants have impaired intrinsic tyrosine phosphatase activity in cells. Interestingly, similar results were obtained for the V184D PTP1B mutation in transfection studies where this mutant was shown to dephosphorylate poorly pSTAT6 [7]. As in our hands the V184D

mutant was active enough for accurate quantitative measurement of its phosphatase activity, we further characterized it. We found that the mutation impacts substrate binding (K_m constant) and more importantly the catalytic constant (k_{cat}) gives rise to a mutant with a strongly decreased (8 to 10 times lower compared to WT) catalytic efficiency (k_{cat}/K_m) (Supplementary Figure 2). This is in agreement with the key role of the WPD-loop in the catalysis and substrate interaction [21, 22]. Interestingly, similar results were obtained with a V184G mutant which was found to be poorly active with a catalytic efficiency 10 times lower compared to the WT [22].

To test whether the mutations affect the overall protein stability of V184D, R221G and G259V, PTP1B proteins thermal shift assay (TSA) were carried out as previously described [31]. As shown in Figure 3A, the V184D and G259V mutants showed significant decreased thermal stabilities when compared to WT enzyme (temperature of melting, Tm, around 42°C for the two mutants compared to 52°C for WT). Consistent with these results, the two mutants were also found to be more prone to temperature-dependent protein aggregation as shown in Figure 3B. In addition, determination of the first-order heat inactivation constant (k_{inact}) for V184D ($k_{inactV184D}=67.10^{-3}$ min^{-1}) and for WT PTP1B ($k_{inactWT}=21.10^{-3}$ min^{-1}) confirmed that the V184D mutant has a lower intrinsic stability (Supplementary Figure 3). Molecular dynamics (MD) simulations were carried out to further analyze the intrinsic stability of the PTP1B mutants. Interestingly this approach has been used previously for the study of a point mutation of PTP1B Asp181, and in particular their impact on protein flexibility/stability [32]. While the root mean square deviation (RMSD) values for WT PTP1B backbone Cα atoms fluctuated around 1.3 Å and the amplitude remained within 1.5 Å, and for the PTP1B mutants the values were higher with fluctuations above 1.5 Å and amplitudes close to 2 Å, in particular for the V184D and G259V PTP1B mutants (Figure 3C). These data further support that, in addition to their strong impact on intrinsic tyrosine phosphatase activity, the V184D, R221G and G259V mutations also impact intrinsic protein stability. Interestingly, it has been shown that oncogenic point mutations affecting the catalytic domain of human PTPRT lead to impaired intrinsic enzyme activity and also to decreased intrinsic protein

stability of the mutants compared to WT [33].

As stated above, the V184D, R221G and G259V PTP1B mutations identified in PMBCL occur in three highly conserved adjacent loops (WPD-loop, P-loop and Q-loop) that contribute to the active site of the enzyme [21] (Figure 4). Val184 is a highly conserved WPD-loop residue in PTP enzymes. The WPD-loop is a mobile loop that also contains the key catalytic acid/base Asp181 residue. Upon substrate binding, the WPD-loop closes about the active site so that the catalytic Asp181 is correctly positioned to participate to catalysis [21, 22, 34]. As shown in Figure 4, replacement of a Val residue into a Asp leads to a steric clash with the residue Gln266, a residue that flanks the catalytically-important Q-loop [21]. This clash may impact the flexibility and motion of the WPD-loop thus altering the activity of the enzyme. MD analysis shows a significant increase of the root mean square fluctuations (RMSF) of the Cα of the WPD-loop residues (residues 177-188) in the V184D mutant compared to WT (with ΔRMSF close to 1 Å). The RMSF values reflects the mobility of a given residue around its mean position and thus gives important information about the flexibility and stability of the system [32]. Thus, these data clearly indicate that the V184D impacts strongly the flexibility and the dynamics of the WPD-loop. Interestingly, it is now well-known that conformational dynamics of the WPD-loop is key for enzyme activity notably through the positioning of catalytically important WPD-loop residues, in particular Asp181 [22, 24]. In addition, MD analysis indicates that the V184D mutation by impacting the structure/motion of the WPD-loop also modifies the flexibility of other active site loops, notably the Q-loop (residues 259-263) and the P-loop (residues 214-223) (Figure 5). This is in agreement with the fact that these loops are adjacent and form the catalytic site [21]. In addition, as stated above, V184D mutation induces a steric clash with the Gln266 residue which flanks the Q-loop. The latter contains the very important Gln262 residue which flexibility and correct positioning in the active site is key for catalysis in conjunction with the Asp181 residue of the WPD-loop [21, 22, 35]. It is not surprising that a mutation impacting the structure/flexibility of one active-site loop such as the WPD-loop also modifies the structure/flexibility of neighboring loop [24]. Interestingly, it is now well

know that the WPD-loop and other active site loops (P-loop and Q-loop notably) are part of network which also includes dispersed residues that contribute to enzyme activity through modulation of loop motions (in particular the motion of WPD-loop) [22-24]. In agreement with this, MD dynamics of the V184D mutant shows significant RMSF differences with WT PTP1B for the Q-loop, the P-loop but also for residues 52-56 and residues 191-193 (Figure 5). Interestingly these residues are known to be "allosterically" connected to the WPD-loop motion and enzyme activity [22, 25].

The Arg221 residue is also a highly conserved residue that belongs to the P-loop motif (Figure 5). This residue plays a key structural and catalytic role notably through interaction with the phosphate group of the substrate during catalysis and also through ionic bonds with the Glu115 residue of the E-loop (residues 113-121) [21]. In addition, interactions of Arg221 with the WPD-loop Trp179 and Pro180 residues are important in particular for closure of the WPD-loop during catalysis [22]. The R221G mutation introduces a small non-charged glycine residue that, contrary to the Arg residue, cannot form ionic nor H-bonds and cannot interact with the WPD-loop Trp179 and Pro180 residues (Figure 4). This radical changes explain well why the R221G PTP1B mutant is devoid of tyrosine phosphatase activity. As stated above, MD dynamics analyses of the R221G mutant confirmed that the mutation impacts the flexibility of the P-loop, which could be due, at least in part, to the lack of side-chain of the Gly residue at position 221, thereby providing more conformational flexibility to adjacent P-loop residues (Figure 5). More importantly and in agreement with the points discussed above, mutation of the Arg221 residue of the P-loop not only impacts the flexibility of this loop but also give rise to significant changes in the flexibility of the WPD-loop (with ΔRMSF around 1 Å) and more modestly of the Q-loop (ΔRMSF around 0.5 Å) (Figure 5). This is consistent with the fact that Arg221 interacts directly with WPD-loop residues (Trp179 and Pro180) [22].

The Gly259 residue is part of the Q-loop (residues 259-263) (Figure 5). Due to the absence of side chain, the Gly259 residue has been shown to allow easy access to the substrate in the active site. Interestingly, mutation of Gly259 into a Gln residue has

been shown to impair PTP1B activity by causing steric hindrance but also impacting the flexibility and correct positioning of the Q-loop Gln262 residue in the active site during catalysis [35]. As shown in Figure 4, the G259V PTP1B mutation identified in PMBCL patients leads to a significant steric clash with the key catalytic residue Gln262, which may prevent the Gln262 residue from adopting a correct position during catalysis [21, 23, 35]. MD analyses confirmed that the mutation impacted the flexibility of the Q-loop (with ΔRMSF around 0.5 Å) but also of the WPD-loop and certain residues of the PTP1B allosteric network (residues 52-56 and residues 191-193) (Figure 5). These data are in agreement with previous results showing that mutating the Gly259 residue into a bulkier Gln residue leads to altered flexibility of the key catalytic Gln262 residue, and subsequently to a poorly active PTP1B mutant enzyme [35].

Taken together our results provide molecular, structural and enzymatic evidence that the three P1PT1B mutants (V184D, R221G and G259V) identified in human primary mediastinal B cell lymphoma are strongly impaired in their protein tyrosine phosphatase activity, thereby contributing to aberrant cell signaling as previously shown by Gunawardna et al. [7]. Our data further underline the pathogenic role of oncogenic mutations that affect active-site loops in PTP enzymes [36].

ACKNOWLEDGMENTS

This work was supported by running grants from Université Paris Cité and CNRS. RL was supported by a PhD fellowship from the China Scholarship Council (CSC).

We thank the technical platform “BioProfiler-UFLC” (BFA Unit, Université Paris Cité) for provision of UFLC facilities.

AUTHORS CONTRIBUTIONS

RL, JB, and FRL designed research; RL, YS, JB, L-CB, and XX performed research; All authors analyzed the data; RL, JB and FRL wrote the paper. All the authors commented on the paper.

CONFLICT OF INTERESTS

The authors declare no conflict of interests.

REFERENCES

1. Chen, H., Pan, T., He, Y., Zeng, R., Li, Y., Yi, L., Zang, H., Chen, S., Duan, Q., Xiao, L., et al. (2021). Primary Mediastinal B-Cell Lymphoma: Novel Precision Therapies and Future Directions. Front Oncol 11, 654854.
2. Giulino-Roth, L. (2018). How I treat primary mediastinal B-cell lymphoma. Blood 132, 782-790.
3. Savage, K.J., Monti, S., Kutok, J.L., Cattoretti, G., Neuberg, D., De Leval, L., Kurtin, P., Dal Cin, P., Ladd, C., Feuerhake, F., et al. (2003). The molecular signature of mediastinal large B-cell lymphoma differs from that of other diffuse large B-cell lymphomas and shares features with classical Hodgkin lymphoma. Blood 102, 3871-3879.
4. Irish, J.M., Myklebust, J.H., Alizadeh, A.A., Houot, R., Sharman, J.P., Czerwinski, D.K., Nolan, G.P., and Levy, R. (2010). B-cell signaling networks reveal a negative prognostic human lymphoma cell subset that emerges during tumor progression. Proc Natl Acad Sci U S A 107, 12747-12754.
5. Steidl, C., and Gascoyne, R.D. (2011). The molecular pathogenesis of primary mediastinal large B-cell lymphoma. Blood 118, 2659-2669.
6. Dube, N., Bourdeau, A., Heinonen, K.M., Cheng, A., Loy, A.L., and Tremblay, M.L. (2005). Genetic ablation of protein tyrosine phosphatase 1B accelerates lymphomagenesis of p53-null mice through the regulation of B-cell development. Cancer Res 65, 10088-10095.
7. Gunawardana, J., Chan, F.C., Telenius, A., Woolcock, B., Kridel, R., Tan, K.L., Ben-Neriah, S., Mottok, A., Lim, R.S., Boyle, M., et al. (2014). Recurrent somatic mutations of PTPN1 in primary mediastinal B cell lymphoma and Hodgkin lymphoma. Nat Genet 46, 329-335.
8. Zahn, M., Marienfeld, R., Melzner, I., Heinrich, J., Renner, B., Wegener, S., Miessner, A., Barth, T.F., Dorsch, K., Bruderlein, S., et al. (2017). A novel PTPN1 splice variant upregulates JAK/STAT activity in classical Hodgkin lymphoma cells. Blood 129, 1480-1490.
9. Jobe, F., Patel, B., Kuzmanovic, T., Makishima, H., Yang, Y., Przychodzen, B., Hutchison, R.E., Bence, K.K., Maciejewski, J.P., and Mohi, G. (2017). Deletion of Ptpn1 induces myeloproliferative neoplasm. Leukemia 31, 1229-1234.
10. Le Sommer, S., Morrice, N., Pesaresi, M., Thompson, D., Vickers, M.A., Murray, G.I., Mody, N., Neel, B.G., Bence, K.K., Wilson, H.M., et al. (2018). Deficiency in Protein Tyrosine Phosphatase PTP1B Shortens Lifespan and Leads to Development of Acute Leukemia. Cancer Res 78, 75-87.
11. Elchebly, M., Payette, P., Michaliszyn, E., Cromlish, W., Collins, S., Loy, A.L., Normandin, D., Cheng, A., Himms-Hagen, J., Chan, C.C., et al. (1999). Increased insulin sensitivity and obesity resistance in mice lacking the protein tyrosine phosphatase-1B gene. Science 283, 1544-1548.
12. Yip, S.C., Saha, S., and Chernoff, J. (2010). PTP1B: a double agent in metabolism and oncogenesis. Trends Biochem Sci 35, 442-449.
13. Villamar-Cruz, O., Loza-Mejia, M.A., Arias-Romero, L.E., and Camacho-Arroyo, I. (2021). Recent advances in PTP1B signaling in metabolism and cancer. Biosci Rep 41.
14. Tiganis, T. (2002). Protein tyrosine phosphatases: dephosphorylating the epidermal growth factor receptor. IUBMB Life 53, 3-14.
15. Haj, F.G., Markova, B., Klaman, L.D., Bohmer, F.D., and Neel, B.G. (2003). Regulation of receptor tyrosine kinase signaling by protein tyrosine phosphatase-1B. J Biol Chem 278, 739-744.

16. Dube, N., and Tremblay, M.L. (2004). Beyond the metabolic function of PTP1B. Cell Cycle 3, 550-553.
17. Pike, K.A., and Tremblay, M.L. (2016). TC-PTP and PTP1B: Regulating JAK-STAT signaling, controlling lymphoid malignancies. Cytokine 82, 52-57.
18. Ritz, O., Guiter, C., Castellano, F., Dorsch, K., Melzner, J., Jais, J.P., Dubois, G., Gaulard, P., Moller, P., and Leroy, K. (2009). Recurrent mutations of the STAT6 DNA binding domain in primary mediastinal B-cell lymphoma. Blood 114, 1236-1242.
19. Vainchenker, W., and Constantinescu, S.N. (2013). JAK/STAT signaling in hematological malignancies. Oncogene 32, 2601-2613.
20. Bachegowda, L.S., and Barta, S.K. (2014). Genetic and molecular targets in lymphoma: implications for prognosis and treatment. Future Oncol 10, 2509-2528.
21. Tautz, L., Critton, D.A., and Grotegut, S. (2013). Protein tyrosine phosphatases: structure, function, and implication in human disease. Methods Mol Biol 1053, 179-221.
22. Choy, M.S., Li, Y., Machado, L., Kunze, M.B.A., Connors, C.R., Wei, X., Lindorff-Larsen, K., Page, R., and Peti, W. (2017). Conformational Rigidity and Protein Dynamics at Distinct Timescales Regulate PTP1B Activity and Allostery. Mol Cell 65, 644-658 e645.
23. Cui, D.S., Lipchock, J.M., Brookner, D., and Loria, J.P. (2019). Uncovering the Molecular Interactions in the Catalytic Loop That Modulate the Conformational Dynamics in Protein Tyrosine Phosphatase 1B. J Am Chem Soc 141, 12634-12647.
24. Crean, R.M., Biler, M., van der Kamp, M.W., Hengge, A.C., and Kamerlin, S.C.L. (2021). Loop Dynamics and Enzyme Catalysis in Protein Tyrosine Phosphatases. J Am Chem Soc 143, 3830-3845.
25. Hjortness, M.K., Riccardi, L., Hongdusit, A., Zwart, P.H., Sankaran, B., De Vivo, M., and Fox, J.M. (2018). Evolutionarily Conserved Allosteric Communication in Protein Tyrosine Phosphatases. Biochemistry 57, 6443-6451.
26. Barford, D., Flint, A.J., and Tonks, N.K. (1994). Crystal structure of human protein tyrosine phosphatase 1B. Science 263, 1397-1404.
27. Peters, G.H., Iversen, L.F., Branner, S., Andersen, H.S., Mortensen, S.B., Olsen, O.H., Moller, K.B., and Moller, N.P. (2000). Residue 259 is a key determinant of substrate specificity of protein-tyrosine phosphatases 1B and alpha. J Biol Chem 275, 18201-18209.
28. Duval, R., Bui, L.C., Berthelet, J., Dairou, J., Mathieu, C., Guidez, F., Dupret, J.M., Cools, J., Chomienne, C., and Rodrigues-Lima, F. (2015). A RP-UFLC Assay for Protein Tyrosine Phosphatases: Focus on Protein Tyrosine Phosphatase Non-Receptor Type 2 (PTPN2). Sci Rep 5, 10750.
29. Nian, Q., Berthelet, J., Parlato, M., Mechaly, A.E., Liu, R., Dupret, J.M., Cerf-Bensussan, N., Haouz, A., and Rodrigues Lima, F. (2022). Structural characterization of a pathogenic mutant of human protein tyrosine phosphatase PTPN2 (Cys216Gly) that causes very early onset autoimmune enteropathy. Protein Sci 31, 538-544.
30. Flint, A.J., Tiganis, T., Barford, D., and Tonks, N.K. (1997). Development of "substrate-trapping" mutants to identify physiological substrates of protein tyrosine phosphatases. Proc Natl Acad Sci U S A 94, 1680-1685.
31. Kroeger, T., Frieg, B., Zhang, T., Hansen, F.K., Marmann, A., Proksch, P., Nagel-Steger, L., Groth, G., Smits, S.H.J., and Gohlke, H. (2017). EDTA aggregates induce SYPRO orange-based fluorescence in thermal shift assay. PLoS One 12, e0177024.

32. Liu, M., Wang, L., Sun, X., and Zhao, X. (2014). Investigating the impact of Asp181 point mutations on interactions between PTP1B and phosphotyrosine substrate. Sci Rep 4, 5095.
33. Pasquo, A., Consalvi, V., Knapp, S., Alfano, I., Ardini, M., Stefanini, S., and Chiaraluce, R. (2012). Structural stability of human protein tyrosine phosphatase rho catalytic domain: effect of point mutations. PLoS One 7, e32555.
34. Tonks, N.K. (2003). PTP1B: from the sidelines to the front lines! FEBS Lett 546, 140-148.
35. Peters, G.H., Iversen, L.F., Andersen, H.S., Moller, N.P., and Olsen, O.H. (2004). Residue 259 in protein-tyrosine phosphatase PTP1B and PTPalpha determines the flexibility of glutamine 262. Biochemistry 43, 8418-8428.
36. Zhao, S., Sedwick, D., and Wang, Z. (2015). Genetic alterations of protein tyrosine phosphatases in human cancers. Oncogene 34, 3885-3894.

LEGEND FIGURES

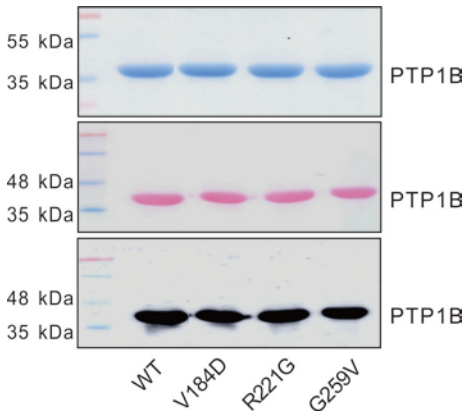

Figure 1: Purification of WT and mutants PTP1B proteins

WT and mutants PTP1B proteins were separated by SDS-PAGE post-purification and stained using Coomassie dye, or further transferred onto nitrocellulose membrane for PTP1B immunodetection following Ponceau staining.

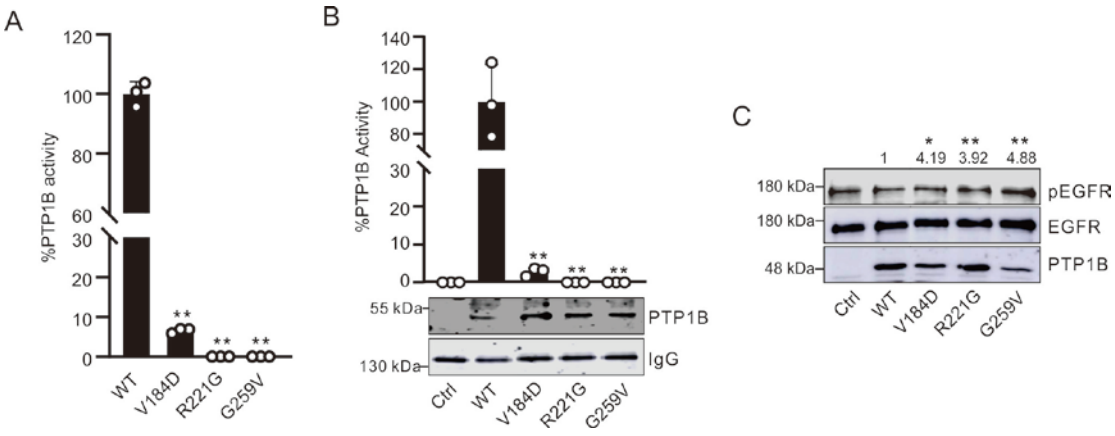

Figure 2: *In vitro* and *in cellulo* determination of WT and mutants PTP1B activity

(A) WT or mutants PTP1B enzyme (5 nM) activity was assessed by RP-UFLC using a pSTAT1 fluorescent peptide. Data are represented as the mean of three independent experiments +/- SD. ** p-value < 0.01 (compared to WT PTP1B).

(B) HEK 293T cells transfected with WT or mutants flag-PTP1B plasmids were lysed, PTP1B exogenous proteins were immunoprecipitated and splited into 2 parts: one part was used to assess immunoprecipitated PTP1B residual activity by RP-UFLC using a pSTAT1 fluorescent peptide as described before [28], and the second part was separated by SDS-PAGE and further proceeded for PTP1B immunodetection. Data are represented as the mean of three independent experiments +/- SD. * p-value < 0.05, ** p-value < 0.01 (compared to WT PTP1B). Membrane is representative of three independent experiments.

(C) COS7 cells transfected with WT or mutants flag-PTP1B plasmids were lysed and samples were separated by SDS-PAGE for tyrosine phosphorylation immunodetection as described by Flint et al. [30]. Membranes were later stripped and reprobed sequentially with α-EGFR and α-PTP1B antibodies. Data are represented as the mean of three independent experiments +/- SD. * p-value < 0.05, ** p-value < 0.01 (compared to WT PTP1B). Membrane is representative of three independent experiments.

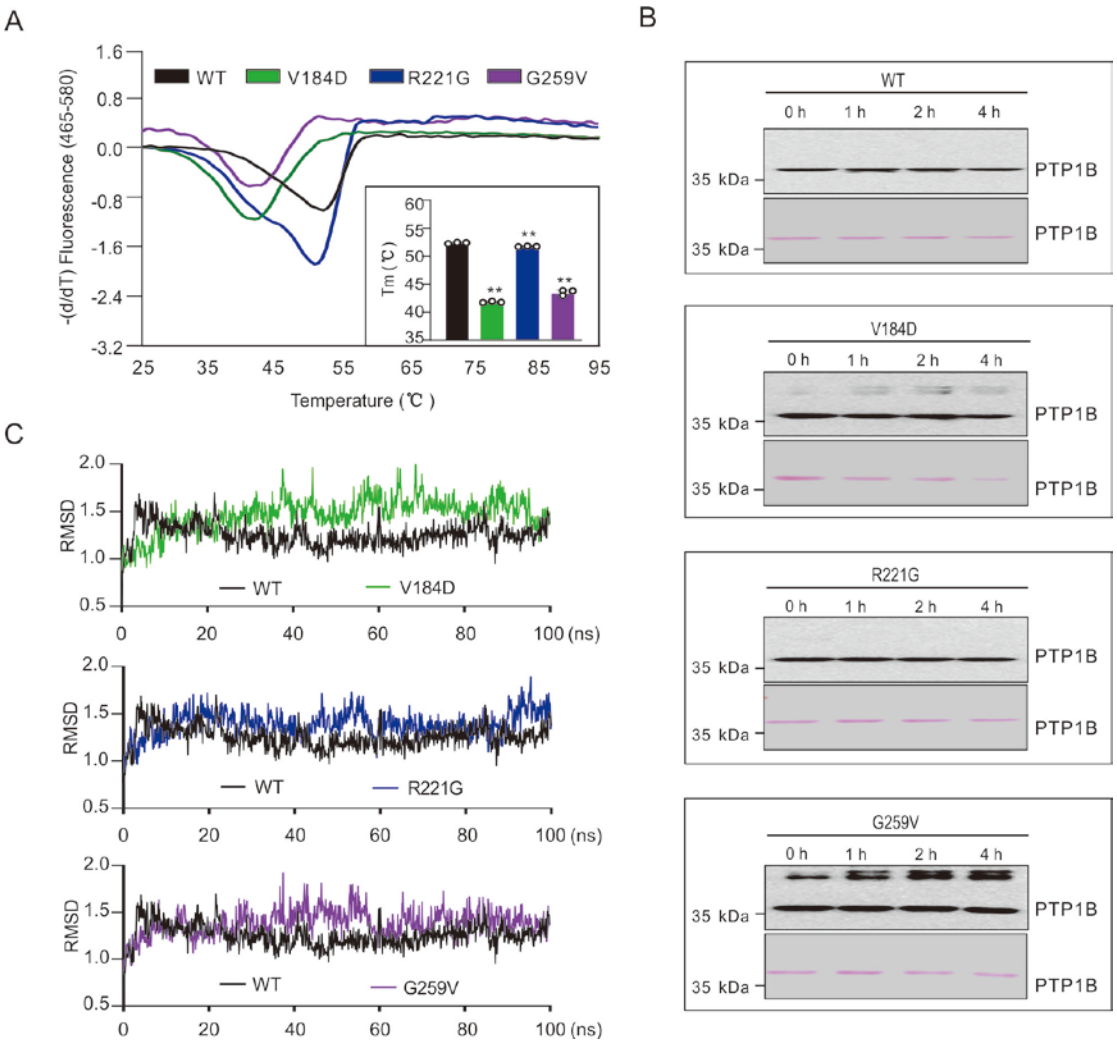

Figure 3: Evaluation of WT and mutant PTP1B proteins stability

(A) Thermal shift assay of WT and mutant PTP1B proteins (5 µM) in the presence of 10 X SYPRO. Tm values were determined from the first order derivative of the fluorescence as a function of temperature. Data are represented as the mean of three independent experiments +/- SD. ** p-value < 0.01 (compared to WT PTP1B).

(B) WT and mutant PTP1B proteins (10 µg) were incubated at 37°C and aliquot of the solution were taken at different time points (0, 1, 2, 4 hours), separated by SDS-PAGE and further proceeded for PTP1B immunodetection following Ponceau staining. Membrane is representative of three independent experiments.

(C) Molecular dynamics simulation of WT and mutant PTP1B proteins were conducted for 100 ns using Amber20 software (PTP1B PDB code: 2HNP). Data were extracted with VMD and presented in the form of RMSD.

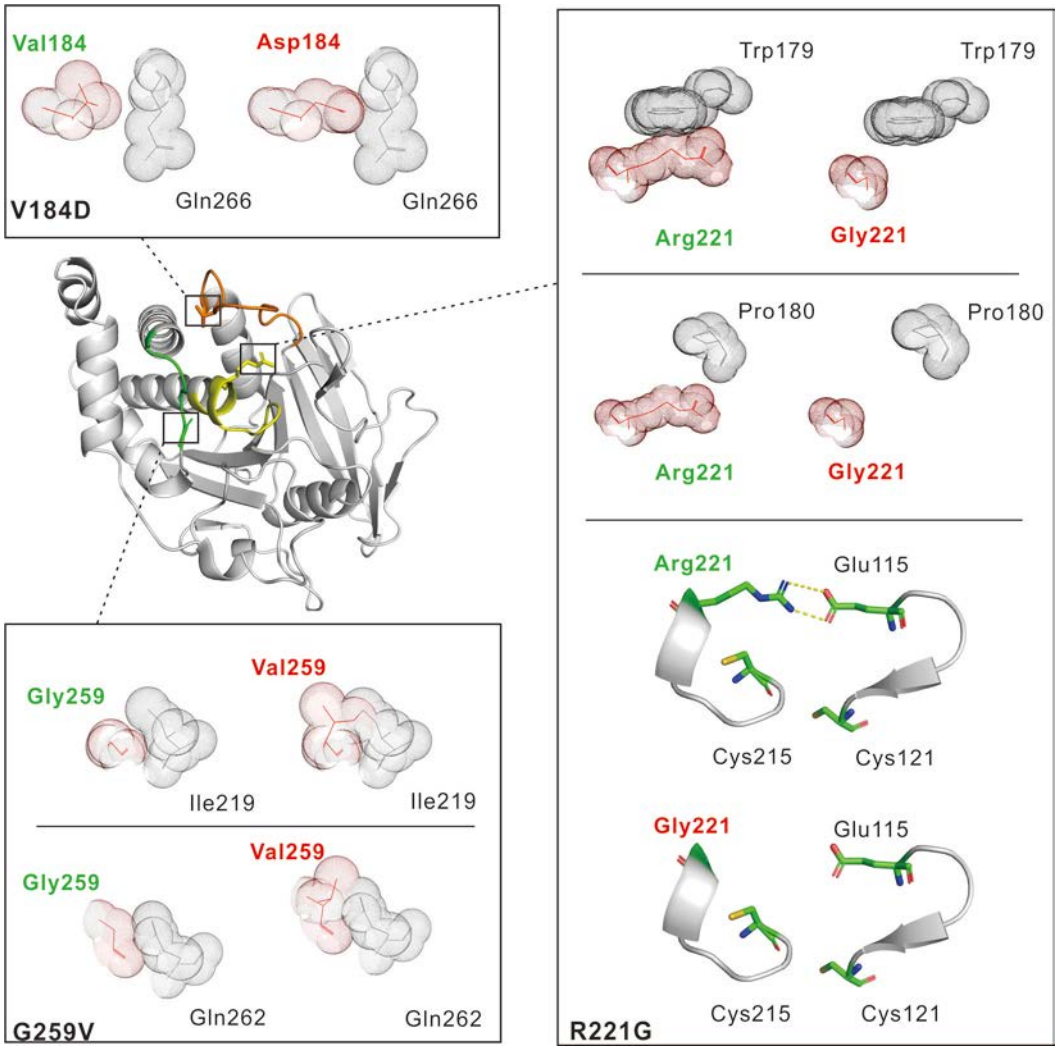

Figure 4: Impact of the mutations on PTP1B loops

PTP1B mutants were generated *in silico* using PyMol software (PTP1B PDB code: 2HNP). Positions of the mutations are shown in PTP1B global structure. WPD-Loop (residues 177-188), catalytic P-loop (residues 214-223) and Q-loop (residues 259-263) are shown in orange, yellow and green respectively. Close-up views of V184D, R221G and G259V mutations are displayed. Van der Waals radii are represented for each atom and mutated residues are displayed in red. Salt bridges are depicted with yellow dashed lines.

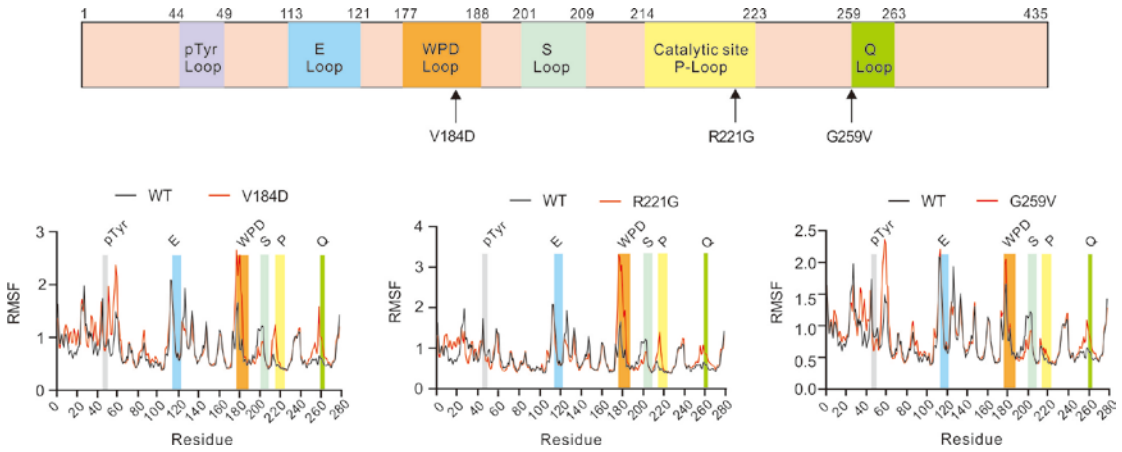

Figure 5: Molecular dynamic simulations of WT and mutants PTP1B

Upper panel: schematic representation of the different key loops of PTP1B (residues 1-435, pTyr-loop is shown in purple, E-loop in blue, WPD-loop in orange, S-loop in light green, catalytic P-loop in yellow and Q-loop in green).

Lower panel: molecular dynamics simulation of WT and mutants PTP1B proteins generated by PyMol for 100 ns using Amber20 software. Data were extracted with VMD and presented as RMSF. Differences between WT and mutants PTP1B were highlighted according to the loop color scheme defined in the upper panel.

SUPPLEMENTARY MATERIALS AND METHODS

1. Determination of PTP1B activity using *p*NPP assay

The tyrosine phosphatase activity of WT and mutants PTP1B proteins were measured by *p*NPP assay as previously described (Nian *et al*., 2019). Briefly, samples containing PTP1B (20 nM) were incubated with *p*NPP in 100 mM sodium acetate buffer, 1 mM DTT, pH 6 (total volume of 200 µl). The formation of the product (*p*-nitrophenol) was followed by continuous measurement of the absorbance at 405 nm for 10 minutes at 37°C using thermostatic microplate reader (BioTek, France).

2. Determination of WT and V184D PTP1B kinetic parameters

Kinetic parameters of WT and V184D PTP1B were assessed using *p*NPP and RP-UFLC assays. For *p*NPP assay, WT and V184D PTP1B proteins (20 nM) were mixed with increasing concentrations of *p*NPP (ranging from 1.25 to 20 mM) and PTP1B activity was determined as described before (Nian *et al*., 2019). For RP-UFLC assay, WT and V184D PTP1B proteins (5 nM) were incubated with increasing concentrations of pSTAT1 peptide (ranging from 25 to 400 µM) for 30 minutes at 37°C and PTP1B activity was determined as described before (Duval *et al*., 2015). The apparent kinetic parameters V_{max}, K_m and k_{cat} were obtained by non-linear curve fitting against the Michaelis–Menten equation using Prism 8.0.0 software.

3. Determination of first-order heat inactivation constants for WT and V184D PTP1B

WT and V184D PTP1B (20 nM) were incubated at 37°C. At different time points (0, 3, 6, 9, 12 minutes), an aliquot of the solution was taken and mixed with *p*NPP (5 mM) in a total volume of 200 µl sodium acetate buffer (100 mM, 1 mM DTT, pH 6). Natural logarithm of PTP1B residual activity tested by *p*NPP assay was then plotted as a function of time using Prism 8.0.0 software.

SUPPLEMENTARY LEGEND FIGURES

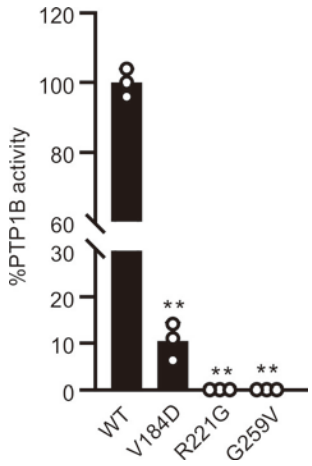

Figure S1: Determination of WT and mutants PTP1B activity using *p*NPP assay

WT or mutants PTP1B enzyme (20 nM) activity was determinated using *p*NPP assay. Data are represented as the mean of three independent experiments +/- SD. ** p-value < 0.01 (compared to WT PTP1B).

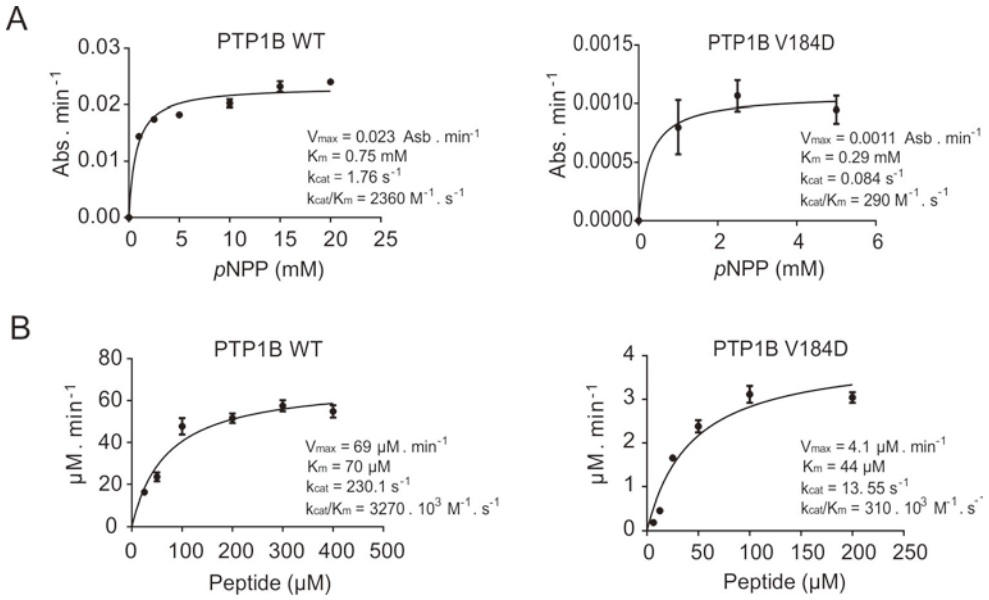

Figure S2: Determination of WT and V184D PTP1B kinetic parameters

(A/B) WT or mutants PTP1B enzyme (20 nM) activity was assessed using different *p*NPP concentrations (ranging from 1.25 mM to 20 mM). The apparent kinetic parameters V_{max}, K_m and k_{cat} were obtained by non-linear curve fitting against the Michaelis–Menten equation. Data are represented as the mean of three independent experiments +/- SD.

(C/D) WT or mutants PTP1B enzyme (5 nM) were incubated in the presence of different concentrations of pSTAT1 peptide (ranging from 25 to 400 µM) for 30 minutes at 37°C. PTP1B activity was then assessed by RP-UFLC. The apparent kinetic parameters V_{max}, K_m and k_{cat} were obtained by non-linear curve fitting against the Michaelis–Menten equation. Data are represented as the mean of three independent experiments +/- SD.

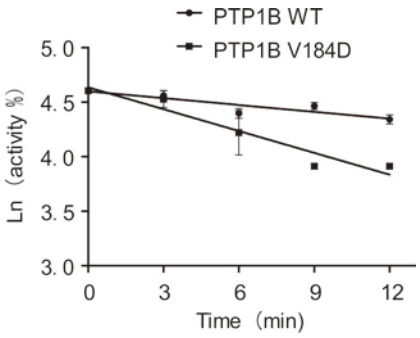

Figure S3: Determination of first-order heat inactivation constant of WT and V184D PTP1B

WT and V184D PTP1B (20 nM) were incubated at 37°C. At different time points (0, 3, 6, 9, 12 minutes), an aliquot of the solution was taken and PTP1B residual activity was assessed using *p*NPP assay. Natural logarithm of PTP1B residual activity was then plotted as a function of time.

REFERENCES

Nian Q, Berthelet J, Zhang W, Bui LC, Liu R, Xu X, Duval R, Ganesan S, Leger T, Chomienne C, Busi F, Guidez F, Dupret JM, Rodrigues Lima F. T-Cell Protein Tyrosine Phosphatase Is Irreversibly Inhibited by Etoposide-Quinone, a Reactive Metabolite of the Chemotherapy Drug Etoposide. Mol Pharmacol. 2019 Aug;96(2):297-306. doi: 10.1124/mol.119.116319. Epub 2019 Jun 20. PMID: 31221825.

Duval R, Bui LC, Berthelet J, Dairou J, Mathieu C, Guidez F, Dupret JM, Cools J, Chomienne C, Rodrigues-Lima F. A RP-UFLC Assay for Protein Tyrosine Phosphatases: Focus on Protein Tyrosine Phosphatase Non-Receptor Type 2 (PTPN2). Sci Rep. 2015 Jun 4;5:10750. doi: 10.1038/srep10750. PMID: 26040922; PMCID: PMC4455150.

3.3 Result 3

Human protein tyrosine phosphatase 1B (PTP1B), from structure to clinical inhibitor perspectives

Rongxing LIU[a], Cécile MATHIEU[b], Jérémy BERTHELET[a,c], Wenchao ZHANG[a,d], Jean-Marie DUPRET[a] and Fernando RODRIGUES LIMA[a]*

a Université Paris Cité, CNRS, Unité de Biologie Fonctionnelle et Adaptative, F-75013 Paris, France

b Faze Medicines, Cambridge, MA, USA

c Université Paris Cité, CNRS, Centre Epigénétique et Destin Cellulaire, F-75013, Paris, France

d Department of Lymphoma and Myeloma, The University of Texas MD Anderson Cancer Center, Houston, TX, USA; Department of Genomic Medicine, The University of Texas MD Anderson Cancer Center, Houston, TX, USA

* Corresponding author: Fernando RODRIGUES LIMA, Université Paris Cité, BFA, UMR 8251, CNRS, F-75013, Paris, France; email: fernando.rodrigues-lima@u-paris.fr

Abbreviations: PPs, protein phosphatases; PTP1B, protein tyrosine phosphatase 1B; PTMs, post-translational modifications; TCPTP, T-cell protein tyrosine phosphatase

ABSTRACT

Phosphorylation is an essential process in biological events and is considered critical for biological functions. In tissues, protein phosphorylation mainly occurs on tyrosine (Tyr), serine (Ser) and threonine (Thr) residues. The balance between phosphorylation and dephosphorylation is under the control of two super enzyme families, protein kinases (PKs) and protein phosphatases (PPs), respectively. Although there are many selective and effective drugs targeting phosphokinases, developing drugs targeting phosphatases has been challenging. PTP1B, one of the most central protein tyrosine phosphatases (PTPs), is a key player in several human diseases and disorders, such as diabetes, obesity, and hematopoietic malignancies, through modulation of different signaling pathways. However, due to high conservation among PTPs, most PTP1B inhibitors lack specificity, raising the need to develop new strategies targeting this enzyme. In this mini-review, we summarize 3 classes of PTP1B inhibitors with different mechanisms: 1) targeting multiple aryl-phosphorylation sites including the catalytic site of PTP1B; 2) targeting allosteric sites of PTP1B; 3) targeting specific mRNA sequence of PTP1B. All the 3 types of PTP1B inhibitors present good specificity over other PTPs and offer promises for the development of efficient small molecules targeting this enzyme.

Key words: PTP1B, crystal structure, inhibitors, specificity, challenge

1 Introduction

PTP1B is a ubiquitous and abundant intracellular prototypic non receptor tyrosine phosphatase that is recognized as a major negative regulator of numerous signaling cascades of metabolic and/or oncogenic relevance such as the insulin or epidermal growth factor (EGF) pathways [1-3]. In the case of insulin signaling, PTP1B dephosphorylates the insulin receptor (IR) as well as its substrates (Insulin Receptor Substrates (IRS) proteins) [4]. Confirmation of PTP1B importance in glucose metabolism came from PTP1B knock out (KO) mice which showed increased tyrosine phosphorylation of the IR in the liver and displayed lower blood glucose and insulin levels compared to wild type (WT) [5]. In addition to insulin signaling, PTP1B also plays an important role in leptin signaling through dephosphorylation of JAK2, a downstream effector of leptin receptor. This results in the inhibition of the synthesis of the appetite-stimulating hormone, neuropeptide Y [1]. In addition to its metabolic impact, several reports have pointed out the role of PTP1B in cancer serving both as a tumor suppressor or oncogene, depending on the cellular context [1, 6]. In particular, mutations that affect PTP1B activity and subsequently different signaling pathway of oncogenic relevance such as the EGFR and JAK/STAT cascades have been reported [1]. The fact that PTP1B can play both negative and positive roles in different signaling pathways make PTP1B an interesting therapeutic target and has thus attracted attention for the discovery and use of PTP1B modulators in diabetes, obesity and possibly in cancer [4].

As stated above, given its key functions in several signaling cascades, PTP1B activity is regulated by several mechanisms that may work in tandem to modulate enzyme’s functions. Especially, reversible and irreversible post-translational modifications (PTMs) such as phosphorylation, oxidation, sumoylation, and proteolysis, have been put forward as essential for regulating PTP1B activity [4, 7-10].

1.1 Structure of PTP1B

PTP1B is one of the major non-receptor protein tyrosine phosphatases (PTPs)

whose first crystal structure was solved in 1994 [11]. At the structural level, PTP1B is composed of 3 domains: an N-terminal catalytic domain (1-300), a regulatory domain (301-400), and a C-terminal domain (401-435) responsible for targeting the enzyme to the endoplasmic reticulum (ER) membrane [1, 2]. To date, the structure of the full-length protein (1-435) has not been solved. However, truncations of human PTP1B (1-298 or 1-321) were successfully crystallized [2]. These various crystal structures all contain the first 298 amino acids corresponding to the catalytic site. This domain contains 8 α-helices and 12 β-strands and shares high similarity with other non-receptor PTPs, as shown in Figure 1 where sequences from the catalytic domain of 17 non-receptor PTPs were aligned. Nevertheless, it is important to note that even though only the N-terminal catalytic domain of PTP1B has been crystallized, all 3 domains play a critical role in the regulation of PTP1B. For more information on the structure of PTPs and notably PTP1B, we suggest the review by Tautz L. *et al*. [12].

1.1.1 N-terminal catalytic domain

The N-terminal catalytic domain of PTP1B is regulated through the PTMs of key residues found within this domain: (i) phosphorylation of crucial serine (Ser) and tyrosine (Tyr) residues and (ii) oxidation of the catalytic cysteine (Cys) 215 in response to reactive oxygen species (ROS).

Phosphorylation within the catalytic domain of PTP1B is one of the main mechanisms resulting in the modulation of PTP1B activity. For example, phosphorylation of PTP1B at Ser50 by Akt, a Ser/Thr effector kinase involved in insulin signaling, decreases the activity of PTP1B and impairs its ability to dephosphorylate the insulin receptor *in vitro* [13]. In addition to Ser phosphorylation, Tyr phosphorylation of PTP1B catalytic domain also occurs on residues 66, 152 and 153. In particular, Tyr66 has been identified as one of the major sites being phosphorylated in response to insulin stimulation *in vivo*, leading to negative regulation of insulin pathway [14]. Interestingly, the sequence surrounding Tyr66, 66YINA69, is consistent with the consensus binding site (YXNX) for the Src homology 2 (SH2) domain of Grb2 (growth factor receptor-related protein 2) [15], which could interact with intracellular insulin receptor substrate 1 (IRS-1), thereby

activating Ras and the mitogen-activated protein kinase (MAPK) pathway and regulating cell proliferation and signal transduction [16]. Moreover, mutating Tyr66 or Tyr152 and Tyr153 to phenylalanine (Phe) residues may alter the conformation of PTP1B and inhibit PTP1B binding to the insulin receptor, thereby preventing its phosphorylation by the activated IR tyrosine kinase [14].

On the other hand, oxidation of the catalytic cysteine residue of PTP1B is a key modification that was found to regulate the extent and duration of phosphotyrosine-dependent signaling response. Indeed, Cys215 oxidation abolishes PTP1B activity. Typically, due to the unique environment surrounding the active site, this catalytic Cys215 residue displays an unusually low pKa (between 4.5 and 5.5, compared to the pKa of a typical Cys, being ~8.5) [12]. Under physiological conditions (pH 7 - 7.5), this residue is deprotonated, resulting in increased reactivity and susceptibility to oxidation by ROS. Experiments indicated that ROS could rapidly convert the sulfenic acid (S-OH) form of PTP1B Cys215 to a cyclic sulfenamide (S-N-R), inhibiting the catalytic activity of PTP1B, but remaining a reversible modification that can be reverted by reducing agents such as reduced glutathione (GSH). However, oxidation of Cys215 to sulfinic (S-O2H) or sulfonic (S-O3H) acid inhibits PTP1B activity irreversibly [7, 17].

1.1.2 Regulatory domain

The regulatory domain of PTP1B, also known as the proline-rich domain or C-terminal domain, is thought to confer substrate specificity to PTP1B. It contains two proline-rich motifs, spanning from Pro301 to Arg315, and from Ser386 to Lys397 [18], which are well known interaction sites for Src homology 3 (SH3) domain-containing proteins [4, 19], suggesting that SH3 domain-containing proteins may be a physiological target of PTP1B. Consistent with this hypothesis, the substitution of some key proline residues in the regulatory domain of PTP1B abolishes the capability of PTP1B to bind to and activate Src, although it does not impact dephosphorylation of IR [4, 19-21].

The regulatory domain of PTP1B harbors various PTMs, including phosphorylation. Many sites have been identified, including Ser378, targeted by protein kinase C

(PKC), and Ser352 and Ser386, that are modified by an unknown kinase in a cell cycle-dependent manner [22, 23]. Several studies suggested that these sites may be modified in response to osmotic stress, and do not impair PTP1B activity [22, 23]. Similarly, sumoylation has been reported at Lys73, Lys335, Lys347 and Lys389 [10]. Although crystal structures of PTP1B do not include residues beyond 321, these sumoylation sites are located close to PTP1B catalytic site, suggesting that these PTMs may alter the conformation of PTP1B through steric hindrances, thereby reducing interactions with PTP1B substrates and resulting in reduced enzymatic activity [4, 24].

1.1.3 C-terminal membrane localization domain

In cells, PTP1B activity is associated with the ER due to binding of the C-terminus of PTP1B to the ER membrane. It has been reported that, in human platelets, cleavage of PTP1B C-terminus by calpain *in vivo* leads to the generation of a soluble and active enzyme, and to the concomitant changes in the pattern of protein tyrosyl phosphorylation [25]. Interestingly, disruption of calpain-1 could not only lead to an overall reduction in protein tyrosine phosphorylation in mice but also to platelet aggregation and clot retraction, emphasizing the potential of PTP1B pharmacological modulation as a therapeutic approach [4, 26, 27].

1.2 Failed PTP1B inhibitors in pre-clinical or clinical trials

As stated previously, PTP1B serves as a master regulator of different signaling cascades of physiopathological importance, notably in obesity and type 2 diabetes [1]. PTP1B has thus attracted particular attention over the last decades as a therapeutic target and several molecules acting as inhibitors of PTP1B have been studied.

To date, only a few PTP1B inhibitors have been tested in clinical trials (Figure 2, Table 1), and include ertiprotafib (a noncompetitive multiple-action inhibitor [28]), trodusquemine (a natural allosteric inhibitor [29, 30]) and JTT-551 (a mixed-type inhibitor [31, 32]). Unfortunately, these inhibitors have all been discontinued due to their insufficient efficiency, lack of specificity and notable side effects [33].

1.2.1 Ertiprotafib

Ertiprotafib is a phosphotyrosine (pTyr) monocarboxylic acid mimetic developed by Wyeth and the first PTP1B inhibitor to be tested in clinical trials for the treatment of diabetes [34]. This inhibitor was particularly interesting due to its atypical mechanism of action. Indeed, unlike most drugs that can tightly bind to their targets and increase their melting temperature (Tm) (i.e., binding of the small molecule stabilizes the target protein), ertiprotafib lowers PTP1B Tm and destabilizes it [35, 36]. To better understand the molecular basis underlying this phenomenon and develop new PTP1B inhibitors, Kumar G. S. and colleagues investigated the impact of ertiprotafib on PTP1B structure. They found that ertiprotafib can inhibit PTP1B activity by inducing protein aggregation in a dose-response manner, providing insights on the mechanism of action of this drug. However, as we will describe later, ertiprotafib being an active site inhibitor of PTP1B, the selectivity of this compound for PTP1B (IC50: 1.6 to 29 µM depending on assay conditions) [28] was not as high as expected. Indeed, evidence of interaction with other proteins such as dual peroxisome proliferator-activated receptor (PPAR) alpha and gamma (EC50: 1.4 ± 0.5 µM and 1.1 ± 0.4 µM) [28] and IkappaB beta (IKK-beta) kinase (IC50: 400 ± 40 nM) was found [37], raising the need to develop new and more specific inhibitors.

1.2.2 Trodusquemine

Trodusquemine (also known as MSI-1436), is a small molecule inhibitor that primary binds to the PTP1B C-terminal domain in a reversible and selective manner [38]. It was first identified by Krishnan N. *et al*. and showed excellent specificity for PTP1B (IC50: 1 µM), with very little impact on T-cell protein tyrosine phosphatase (TCPTP) (IC50: 224 µM), the major protein tyrosine phosphatase commonly used to assess PTP1B inhibitors specificity [38]. At the structural level, trodusquemine acts as a non-competitive inhibitor of PTP1B. Two molecules of the inhibitor can bind to PTP1B in a cooperative manner and induce significant conformational changes in the protein, a mechanism that was validated by least-energy molecular dynamics simulations [32]. Indeed, trodusquemine first binds in a cavity mainly formed by Arg371, Arg373 and Val375 in α9, and then by Val287, Lys292 and Leu294 in α7 as well as residues Leu299, His310, Ile311 of PTP1B [38]. This first binding event

results in a structural rearrangement of PTP1B, bringing helix α7 near the two helices α3 and α6, forming a secondary binding site [32] (Figure 3A). Therefore, this inhibitor revealed a novel allosteric binding site located within the C-terminus of PTP1B. In addition, biochemical studies showed that this small molecule largely had an increased specificity compared to previous inhibitors, reducing adverse effects. Unfortunately, due to the low activity and poor bioavailability, this inhibitor was discontinued.

1.2.3 JTT-551

JTT-551, developed by the Japan Tobacco Company, is a recently developed PTP1B inhibitor. Chronic administration of JTT-551 to mice with diet-induced obesity showed anti-obesity effect, improved resistance to leptin and lipid disorders, and may also mediate glucose metabolism abnormalities [32]. Comparatively to trodusquemine, JTT-551 was reported to have good selectivity towards PTP1B over TCPTP [31, 39, 40]. Therefore, Fukuda S. *et al*. set up a series of studies to measure the enzyme inhibition constant (Ki) of JTT-551. They found a Ki of 0.22 ± 0.04 μM for PTP1B, whereas values of 9.3 ± 0.4 μM were measured for TCPTP, and more than 30 μM was obtained for CD45 and LAR [31]. In addition, JTT-551 could reduce blood glucose levels and exhibit antidiabetic effects without changes in body weight in diabetic mice. All these data indicate that JTT-551 had good potential for the treatment of type 2 diabetes mellitus (T2DM) and obesity. Unfortunately, it was discontinued due to insufficient efficacy in patients and adverse effects [33].

2 NEWLY DEVELOPED SPECIFIC PTP1B INHIBITORS

As we previously mentioned, it is essential to develop new selective and effective inhibitors of PTP1B to treat PTP1B-related diseases, such as T2DM, obesity, lymphoma, and breast cancer [33, 41-47]. However, PTPs are highly conserved, making the development of such inhibitor challenging. For example, the catalytic domain of TCPTP, a protein tyrosine phosphatase essential to various cellular processes and survival *in vivo* [48], shares 72% sequence identity and 86% similarity with the catalytic domain with PTP1B, and thus represents a major constraint to the

development of specific and effective PTP1B inhibitors [49].

In this study, we propose three strategies to specifically target PTP1B: 1) developing two-way inhibitors, binding to the catalytic site and another secondary site that is specific for PTP1B [50, 51]; 2) taking advantage of allosteric inhibitors of PTP1B; 3) using antisense oligonucleotides (ASOs) inhibitors that can selectively bind to a particular sequence of PTP1B mRNA and reduce its expression [52, 53].

2.1 Specific PTP1B inhibitors targeting PTP1B A, B, C and D sites

The catalytic site of PTP1B, also called A site, is the most accessible site within the protein. However, three additional secondary arylphosphorylation binding sites were subsequently identified, and were named B, C, and D sites, respectively. Together, these four sites constitute attractive structural cavities for the creation of specific inhibitors, especially due to the presence of specific residues that are not conserved among PTPs.

2.1.1 A site

The A site is the most polar of the four sites. It is 9 Å deep (from residues Phe182 to Cys215) and 10 Å wide (from residues Tyr46 to Gln262) [50], and harbors the key highly conserved catalytic motif (motif 9: PXXVHCSAGXGRTG, Figure 1), which include the catalytic Cys215 [54, 55]. Catalysis mainly relies on both the catalytic Cys215 and the flexible WPD loop (motif 8: WPDXGXP, Figure 1). This loop contributes significantly to the recognition of the peptide substrate and mediates substrate specificity [54]. Upon binding of a dianionic pTyr residue, the WPD loop interacts with the substrates and switches to a closed conformation, accompanying the movement of the substrate near the A site, then inducing catalysis of PTP1B. The catalytic mechanism of PTP1B has been largely studied at the atomic level and includes two main steps [56-58].

First, Cys215, which exists as a thiolate ion, acts as a nucleophile and attacks pTyr, forming a covalent thiol phosphate intermediate [33]. The highly conserved Asp181, located in the WPD loop, acts as an acid, and protonates the dephosphorylated tyrosyl group that is then released [59, 60]. During this step, Arg221 forms hydrogen bonds

with pTyr which maintains PTP1B in a catalytically active conformation [56]. In a second time, an activated water molecule, which establishes hydrogen bonds with the highly conserved Gln262 present in the Q-loop (motif 10: QTXXQYXF, Figure 1), reacts with the phospho-cysteine intermediate [54, 61] leading to the release of inorganic phosphate and regeneration of the thiolate group of the catalytic cysteine [62].

This site, due its primary role in PTP1B function, raised a lot of interest for the development of inhibitors. However, inhibitors that bind only to the A site result in poor selectivity especially due to the universality of the conserved A site among PTPs. Moreover, the high polarity of the A site results in many chemical constraints for the development of small molecules that often results in poor membrane permeability.

2.1.2 B site

The B site, discovered by Puius Y. A. *et al*., is a specific lipophilic, low-affinity, non-catalytic aryl-phosphate binding site [63]. It is adjacent to A site with 13 × 20 Å deep and almost 4 Å width, and involves mainly residues Tyr20, Arg24, Ala27, Phe52 Arg254 and Met258 - Gly259, and contributes to substrate binding and substrate specificity [50, 63, 64]. Indeed, among the main contacts between pTyr residue and the B site, we can note the direct interactions of the phosphate group with the guanidinium group of residues Arg24 and Arg254. These interactions allow some inhibitors to approach Phe52 and Ala27 residues, two residues specific from PTP1B, contributing greatly to their selectivity for PTP1B [51, 63]. Thus, development of small molecules establishing contacts with residues specific from the B site is a good strategy to find selective inhibitors of PTP1B [51]. Consistent with this idea, inhibitors that can interact with both the A and B site have previously shown good specificity [65]. For example, Puius Y. A. *et al*. identified bis-(para-phosphophenyl) methane (BPPM), a synthetic non-peptide tight binding substrate with low molecular weight and high affinity (K_m = 16 μM on PTP1B), which can bind to both the A and B site (PDB code: 1AAX) [63]. In the A site, BPPM establishes electrostatic interactions with Arg221, hydrogen bonds with nitrogens from the backbone chain of residues Ser216 and Arg221, van der Waals contacts with side chains of several aliphatic

residues, and pi-pi stacking with residues Tyr46 and Phe182. In the B site, a second BPPM molecule interacts with residues Arg24 and Arg254, establishes weakly polar interactions with residues Met258 and Gln262, and van der Waals contacts with residues Ile219, Asp48 and Val49 [63].

2.1.3 C site

The C site is a charged region and is mainly formed by residues Tyr46, Ary47 and Asp48 [64]. It is wide and flat, and completely exposed to the surface of the protein, and thus to the solvent. This site is quite close to the A site and was found to be targeted by inhibitors binding to the A site. Importantly, the C site is particularly prevalent for the selectivity of inhibitors for PTP1B.

Indeed, these inhibitors take advantage of interactions such as the salt bridge and hydrogen bonds with the PTP1B-specific residue Asp48, as well as with residues Try46 and Ary47 [64, 66]. For example, compound 3 (Ki = 0.29 μM for PTP1B at pH 5.5) exhibits a 40-fold increase in potency and significant selectivity for PTP1B compared to other PTPs. This is particularly due to a novel pi-pi interaction between the thiophene ring of compound 3 and Phe182, but also the basic nitrogen of the tetrahydropyridine ring that establishes a new salt bridge with the carboxyl group of Asp48 of PTP1B. These additional interactions significantly increase selectivity (PDB code: 1C88) [67]. Similarly compound 5, another PTP1B inhibitor which associate with site A and C (Ki = 39 ± 14 μM to PTP1B), displays good selectivity for PTP1B over other PTPs except TCPTP, due to hydrogen interactions between the urea group of the compound and the carboxylic acid side chain of Asp48 (PDB code: 1NL9) [51, 68]. Interestingly, to date, there are no inhibitors of PTP1B interacting only with the C site.

2.1.4 D site

The D site is a small and narrow pocket, very close to the A site and C site, and partially shielded from the solvent. It is mainly composed of polar and charged residues such as Tyr46, Glu115, Lys120, Asp181 and Ser216 [50, 51]. Unexpectedly, interaction with the D site shows great superiority in the potency and selectivity of PTP1B inhibitors over other PTPs, especially over TCPTP [51]. Indeed,

among all D site residues, Lys120 is identified as a determinant of selectivity between PTP1B and TCPTP [69]. Due to the significant difference between the spatial position and the corresponding residue (Lys122) of TCPTP, Lys120 of PTP1B is an attractive residue for the design of selective inhibitors. For example, a previous report found that adding a hydroxyl or carboxylic acid groups on PTP1B inhibitors can induce more than 20-fold selectivity via interaction with this lysine [69]. In addition, Lys120 presents numerous attractive features for the design of new drugs. Indeed, its long side chain is highly flexible and is located close to the A site. Moreover, a simple hydrogen bond donor or a carboxylic acid can form a hydrogen bond or a salt bridge with this alkaline lysine [69]. Nevertheless, the D site is narrow, small, and polar, requiring developing inhibitors with low molecular weights and reduced cell permeability [69].

2.1.5 Multiple sites inhibitors of PTP1B

As we reviewed so far, many PTP1B inhibitors have been developed over the past decades. Most of these inhibitors target the A site and are mimics of the pTyr portion of the enzyme substrate. However, the A site of PTP1B is both highly conserved, and charged. Thus, inhibitors targeting only the A site are often neither selective nor cell permeable. Targeting residues that are not conserved in PTPs may avoid the selectivity problems of inhibitors. Three arylphosphorylation binding sites with limited size (B, C, and D sites) are structurally close to the A site of PTP1B, meaning that most inhibitors can interact not only with the three sites alone, but also with the A site. As seen previously, these three secondary sites are critical for the potency or selectivity of known PTP1B inhibitors because they differ from other PTPs by a few amino acids [70-75]. According to the extended four-site based binding mode, PTP1B inhibitors can be mainly divided into four types (Table 2), including AC type (binding to A and C sites), AB type (binding to A and B sites), ABC type (binding to A, B, and C sites), and ADC type (binding to A, D, and C sites) [51].

Among all the residues involved in the B, C and D sites, some play critical roles in the selectivity and potency of PTP1B inhibitors. Residues Arg24 and Arg254 in the B site of PTP1B, corresponding to residues Arg26 and Tyr252 of TCPTP, are key

anchors. Many moieties, such as the carboxylate moiety of salicylate, exhibit good hydrogen interaction strength with Arg24 and Arg254 residues of PTP1B, resulting in a 20-fold higher selectivity compared to TCPTP [39, 69]. Similarly, in the B site, interaction with Cys32, Phe52, and Met258 residues of PTP1B, corresponding to His34, Tyr54, and Met256 in TCPTP, could largely improve the selectivity of PTP1B inhibitors [69, 76]. Suitable hydrophobic moieties, such as 1,2-dithiolane, 1,3-dithian, pyrrolidine, diphenyl ether and pyridinyl group, can also form hydrogen interactions with residues Cys32, Phe52, and Met258 of PTP1B, resulting in more than 20-fold selectivity over TCPTP [69, 76]. Compared to hydrogen bonding, hydrophobic interactions with the cyclic group are easier to achieve in the B site [69]. In addition to the B site, Lys120 in the D site of PTP1B, which corresponds to Lys122 in TCPTP, is also a key determinant for selectivity [69, 77, 78]. Lys120 is located near the A site, and only a hydrogen bond donor or acceptor group may be required to form an interaction with this lysine. Inhibitors binding to the A site could very easily interact with Lys120, also increasing the selectivity of inhibitors for PTP1B over TCPTP. Additionally, it has been shown that a hydroxyl or carboxylic acid group interacting with Lys120 could help the design of more selective inhibitors [69]. Compared to the interactions with the B and D sites, the interaction network in the C site is more complex, relying mainly on a salt bridge between the inhibitor and residues of PTP1B. This is mainly because the C site is large and flat, and entirely exposed to the solvent, without decisive factor when interacting with inhibitors. However, all these studies about specific PTP1B inhibitors relying on these four sites need to be validated by structural studies.

2.2 Allosteric inhibitors

Allosteric inhibition is considered a very promising approach in the drug discovery field, especially due to a lower sequence conservation pressure than the conserved catalytic site, higher specificity, reduced adverse effects and limited toxicity [79, 80]. These aspects make allosteric inhibitors very appealing when targeting proteins that share high sequence similarity and identity with others. Over the past few decades,

numerous allosteric modulators of PTP1B have been reported on ASD website (http://mdl.shsmu.edu.cn/ASD/). Among them, three allosteric inhibitors have been co-crystallized with human PTP1B (PDB code: 1T49, 1T48, 1T4J), providing clear insights on their mechanism of action [81]. Other allosteric inhibitors of PTP1B have their mechanism of action well illustrated, but only theoretically as they have not been confirmed by structural studies.

2.2.1 Allosteric inhibitors binding to PTP1B α3-α6-α7 helices

The main allosteric site of PTP1B is formed by three helices: α3-α6-α7. This site is located ~20 Å away from the catalytic site and mainly involves residues Leu192, Asn193, Phe196, Glu200 on helix α3, Glu276, Phe280 on helix α6, and Trp291 on helix α7 (Figure 3B, left panel) [81].

Three noncompetitive compounds, developed by Wiesmann C. *et al*., target the α3-α6-α7 allosteric site of PTP1B, and were co-crystallized with the protein (PDB code: 1T48, 1T49, and 1T4J, respectively) [81]. Biochemical studies showed that compound 1 is a weak PTP1B inhibitor (IC50 = 350 μM), whereas compound 2 (IC50 = 22 μM) and compound 3 (IC50 = 8 μM) show strong dose-dependent inhibition of this enzyme [81].

At the structural level, compound 1 only interacts with helix 3, establishing a hydrogen bond with Asn193, and interacting with Glu200 via a water molecule. Compound 2, on the other hand, interacts with both helix 3 and 6 and more particularly with Asn193, Glu276, and Phe196 (via a water molecule). Interestingly, compound 3 only establishes a hydrogen bond with Asn193 and Glu276, and no water-mediated interaction is observed (Figure 3B, right panel).

All three compounds share a benzofuran core, which could perfectly fit into the hydrophobic site formed by the three helices and block the α3-α6-α7 interactions, thus preventing the closure of the catalytic WPD loop, maintaining PTP1B in the inactive state [81]. In their molecular dynamic experiments, Li S. *et al*. found that compound 3 induces a conformational rearrangement of α7, disrupting the triangular interaction between α7, α3, and loop11 (residues 151-152) [82]. This leads to the displacement of α3, promotion of an interaction between Ser190-Tyr176, abrogation of hydrophobic

interactions between Trp179-Tyr176, and the impairment of WPD loop [82]. These rearrangement ultimately modulate hydrogen bond formation to constrain the WPD loop in its open conformation [82-87], a mechanism that was confirmed in both truncated and full-length PTP1B [81].

Interestingly, some key residues involved in the allosteric binding site are not conserved in most PTPs [88], explaining for instance the important selectivity of compound 2 towards PTP1B (IC50 for LAR, PTP1B-ARC, and TCPTP are respectively 500 µM, 151 µM, 129 µM) [81].

2.2.2 Allosteric inhibitors binding to PTP1B α3-α6-α7-α9 helices

As we mentioned above, trodusquemine is a natural spermine-cholesterol adduct that can take advantage of a novel allosteric binding site located within the C-terminus of PTP1B (Figure 3A). Although DepYmed discontinued its clinical trials in 2017, insights obtained from the study of trodusquemine lead to the development of new potential PTP1B inhibitor: DPM-1001 (Figure 2).

DPM-1001 shares similar inhibitory mechanisms with trodusquemine. However, several studies showed that this drug provides better results than its predecessor. Indeed, DPM-1001 is a potent inhibitor of PTP1B (IC50 = 100 nM) [89]. In addition, DPM-1001 is not charged, increasing its ability to cross the cell membrane and to be used as a potential drug [89]. Finally, DPM-1001 binding to PTP1B slightly differ from trodusquemine. The later interacts with the α9 of PTP1B C-terminus and then binds with α3, α6 and α 7 helices, whereas DPM-1001, which is also an effective copper chelator, interacts with the C-terminus of PTP1B in an ion-dependent manner [89-91]. Consequently, many studies already emphasized the important efficiency of DPM-1001 as a drug *in vivo* and in cells. Indeed, not only it inhibits diet-induced obesity in mice by improving insulin and leptin signaling, but also slows the growth rate of breast tumors and reduce the possibility of cancer metastasis in lungs [89]. Nevertheless, DPM-1001 binds weakly to the catalytic domain of PTP1B, presumably by binding around the α7 helix [92].

To date, DPM-1001 is the most promising allosteric PTP1B inhibitor in terms of selectivity, efficacy, and bioavailability, and is still in preclinical trials.

2.2.3 Allosteric inhibitors binding to PTP1B Cys121, Tyr124 and His214 residues

Cys121 is a conserved residue, found in most PTPs and is part of the hydrophobic motif 7 (KCXXYWP, Figure 1). This site is structurally adjacent to the catalytic site, the distance between Cys121 and Cys215 being of about ~8.1 Å (distance between Cα atoms) [93]. The sulfur atom of Cys121 packs against the side chain of Tyr 124, which in turn forms a hydrogen bond with His 214, thus forming a potential allosteric binding site for PTP1B inhibitors (Figure 3C) [93-95]. At the structural level, these three residues are critical for WPD loop mobility. Indeed, covalent modification of Cys121 was found to impair the mobility of the WPD loop, thereby preventing the formation of the active conformation of PTP1B and ultimately inhibiting the enzyme activity.

To date, most allosteric inhibitors targeting Cys121 contain a negative charge located either on α-bromoacetamide or α-fluoroacetamide group, and thus form a covalent bond with Cys121, consistent with a covalent inactivation mechanism [93-95]. Indeed, Khan S. *et al*. highlighted a highly selective inhibitor, 73U, harboring an electrophilic α-bromoacetamide group that can interact with Cys121 in molecular simulations. This results in increased inhibitor-Cys121 complex stability, interruption of the overall network among Cys121, Tyr124 and His214, and protection of the highly reactive nucleophile Cys215 from covalent inhibition [95]. Similarly, Hansen S. K. *et al*. demonstrated that the inhibitor ABDF selectively reacts with Cys121 of PTP1B, decreasing the activity of the enzyme *in vitro* and *in vivo*, and activating the insulin signaling pathway [93]. Interestingly, Punthasee P. *et al*. proposed a different model, in which a noncovalent binding of an inhibitor–electrophile conjugate to the active site of PTP1B protects the highly reactive catalytic residue Cys215 from covalent modification, thus allowing inactivation of the enzyme via alkylation of the distal allosteric residue Cys121 [94].

2.2.4 Allosteric inhibitors binding to three different sites on PTP1B

Kumar A. P. *et al*. identified three novel allosteric binding sites and a set of small molecules that bind to these sites using fragment-based binding site mapping methods [96] (Figure 3D). The first site is surrounded by the Pro188 - Glu200 helix, the

Ser201 - Pro210 loop, the Gly220 - Arg238 helix, and the β-strand Gln78 - Thr84. The second site is surrounded by the Pro188 - Glu200 helix, β-strands Gln78 - Thr84, Leu140 - Ile149, and Tyr153 - Asn162. The third site, on the other hand, is surrounded by the β-strand Gln78 - Thr84 and Ser201 - Pro210 loop. Common to all three sites are residues Arg79, Glu200, and Pro206, which interact with most tested ligands. In addition, the flexible Pro188 - Glu200 helix, which surrounds site 1 and site 2, are essential for the allosteric regulation of PTP1B (especially residues Leu192 and Asn193), offering new opportunities for targeting PTP1B through allosteric inhibitors [57], although the structural characteristics of the three allosteric binding sites and the small molecule inhibitors binding to them have not been clearly established. In addition, it is likely that inhibitors covering multiple allosteric sites at the same time instead of single one will have better affinity and increased specificity for PTP1B.

2.3 PTP1B ASOs inhibitors

ASOs generally refer to a short-stranded nucleic acid (about 15 - 25 nucleotides) that has undergone some chemical modifications. Its base sequence is complementary to the specific sequence of the target mRNA. After entering the cells, it can form a double-stranded structure with the target mRNA sequence, blocking protein synthesis, and finally stopping the translation machinery (Figure 4). Until now, studies on ASOs inhibitors have some limitations, such as the chemical modifications and delivery vehicles of ASOs.

To date, only two ASOs inhibitors targeting PTP1B have been designed by Ionis Pharmaceuticals, Inc. (USA): IONIS 113715 and IONIS PTP1BRx (Figure 2). IONIS 113715 is a 20-base chimeric ASOs that has been identified as the most potent antisense inhibitor of PTP1B [97]. IONIS 113715 shows high binding affinity towards PTP1B mRNA sequences and induces a great improvement in insulin sensitivity, reduced expression of lipogenic genes, triglyceride accumulation in rat liver and adipose tissue, and confers nuclease resistance [97, 98]. Also, Swarbrick M. M. *et al*. demonstrated that treatment with IONIS 113715 could reduce PTP1B expression in insulin-sensitive tissues in monkeys, resulting in significant improvements in insulin

sensitivity, reduction in fasting insulin concentrations, and prevention of insulin resistance and T2DM associated with obesity [99]. IONIS 113715 was advanced into phase II clinical trials but was then suspended for unknown reasons and replaced by a new ASOs (IONIS PTP1BRx) currently in phase II trials. IONIS PTP1BRx presents many advantages over IONIS 113715 and may help patients who do not have a significant response to existing oral diabetes medications [100]. Indeed, IONIS PTP1BRx is a more potent inhibitor of PTP1B expression than IONIS 113715 in humans [101]. The positive effect of IONIS PTP1BRx occurs mainly through two mechanisms: 1) improvement of HbA1c levels that could improve medium-term glycemic parameters and reduce leptin signaling; 2) increase of adiponectin levels as well as significant weight reduction compared to placebo. In clinical trials, no severe hypoglycemia was observed, and no unexpected safety findings were reported [101]. However, to date, no further data have been published on this inhibitor.

3 FURTHER CHALLENGES AND PERSPECTIVES OF PTP1B INHIBITORS

Specificity is always a hurdle in drug discovery, especially for phosphatase inhibitors. The process of discovering PTP1B inhibitors has been a long journey for researchers over the past decades due to two challenges. The first challenge is selectivity. The discovered PTP1B inhibitors act primarily on the catalytic site of the enzyme. However, the catalytic site of non-receptor PTPs is highly conserved, in particular with TCPTP which shares 72% sequence identity and 86% similarity in the catalytic domain with PTP1B [49], and thus becomes the main obstacle to the development of PTP1B inhibitors. This makes it difficult for inhibitors to target a particular phosphatase subtype, leading to potential side effects and difficulties in studying pharmacological mechanisms. The second challenge is cellular permeability and bioavailability. The catalytic site of PTP1B is positively charged, so inhibitors acting on the catalytic site are ideally negatively charged or highly polar. However, negatively charged or highly polar inhibitors cannot effectively cross the cell membrane, and thus reach the phosphatase.

Phosphorylation (by protein kinases) and dephosphorylation (by protein

phosphatases) play an essential role in cellular regulation and signal transduction. Although there are many specific and effective drugs on the market targeting kinases, the development of drugs targeting phosphatases has proven to be challenging. As stated above, some inhibitors have shown excellent inhibitory effect on PTP1B, but their study has been discontinued because of their low specificity and side effects. In this mini-review, 3 categories of PTP1B inhibitors were reviewed with the aim of informing the inhibition mechanisms of specific PTP1B inhibitors. The cellular permeability and bioavailability of these inhibitors are still poorly understood. Therefore, other related tests, such as pharmacokinetic properties, should be further investigated.

ACKNOWLEDGMENTS

Work in FRL laboratory is supported by running grants from Université Paris Cité and CNRS. RL was supported by a PhD fellowship from China Scholarship Council (CSC).

AUTHOR CONTRIBUTIONS

RL, CM and FRL wrote the paper. All the authors commented on the paper.

DATA AVAILABILITY STATEMENT

NA

CONFLICT OF INTERESTS

The authors declare no conflict of interests.

REFERENCE

1. Villamar-Cruz, O., et al., Recent advances in PTP1B signaling in metabolism and cancer. Biosci Rep, 2021. 41(11).
2. Simoncic, P.D., C.J. McGlade, and M.L. Tremblay, PTP1B and TC-PTP: novel roles in immune-cell signaling. Can J Physiol Pharmacol, 2006. 84(7): p. 667-75.
3. Pike, K.A. and M.L. Tremblay, TC-PTP and PTP1B: Regulating JAK-STAT signaling, controlling lymphoid malignancies. Cytokine, 2016. 82: p. 52-7.
4. Yip, S.C., S. Saha, and J. Chernoff, PTP1B: a double agent in metabolism and oncogenesis. Trends Biochem Sci, 2010. 35(8): p. 442-9.
5. Haj, F.G., et al., Liver-specific protein-tyrosine phosphatase 1B (PTP1B) re-expression alters glucose homeostasis of PTP1B-/-mice. J Biol Chem, 2005. 280(15): p. 15038-46.
6. Lessard, L., M. Stuible, and M.L. Tremblay, The two faces of PTP1B in cancer. Biochim Biophys Acta, 2010. 1804(3): p. 613-9.
7. van Montfort, R.L., et al., Oxidation state of the active-site cysteine in protein tyrosine phosphatase 1B. Nature, 2003. 423(6941): p. 773-7.
8. Meng, T.C., et al., Regulation of insulin signaling through reversible oxidation of the protein-tyrosine phosphatases TC45 and PTP1B. J Biol Chem, 2004. 279(36): p. 37716-25.
9. Dadke, S., A. Kusari, and J. Kusari, Phosphorylation and activation of protein tyrosine phosphatase (PTP) 1B by insulin receptor. Mol Cell Biochem, 2001. 221(1-2): p. 147-54.
10. Saha, S. and J. Chernoff, Analysis of PTP1B sumoylation. Methods, 2014. 65(2): p. 201-6.
11. Barford, D., A.J. Flint, and N.K. Tonks, Crystal structure of human protein tyrosine phosphatase 1B. Science, 1994. 263(5152): p. 1397-404.
12. Tautz, L., D.A. Critton, and S. Grotegut, Protein tyrosine phosphatases: structure, function, and implication in human disease. Methods Mol Biol, 2013. 1053: p. 179-221.
13. Ravichandran, L.V., et al., Phosphorylation of PTP1B at Ser(50) by Akt impairs its ability to dephosphorylate the insulin receptor. Mol Endocrinol, 2001. 15(10): p. 1768-80.
14. Bandyopadhyay, D., et al., Protein-tyrosine phosphatase 1B complexes with the insulin receptor in vivo and is tyrosine-phosphorylated in the presence of insulin. J Biol Chem, 1997. 272(3): p. 1639-45.
15. Songyang, Z., et al., Specific motifs recognized by the SH2 domains of Csk, 3BP2, fps/fes, GRB-2, HCP, SHC, Syk, and Vav. Mol Cell Biol, 1994. 14(4): p. 2777-85.
16. Cheatham, B. and C.R. Kahn, Insulin action and the insulin signaling network. Endocr Rev, 1995. 16(2): p. 117-42.
17. Salmeen, A., et al., Redox regulation of protein tyrosine phosphatase 1B involves a sulphenyl-amide intermediate. Nature, 2003. 423(6941): p. 769-73.
18. Shinde, R.N., et al., Screening and identification of potential PTP1B allosteric inhibitors using in silico and in vitro approaches. PLoS One, 2018. 13(6): p. e0199020.
19. Liu, F., D.E. Hill, and J. Chernoff, Direct binding of the proline-rich region of protein tyrosine phosphatase 1B to the Src homology 3 domain of p130(Cas). J Biol Chem, 1996. 271(49): p. 31290-5.
20. Dadke, S. and J. Chernoff, Protein-tyrosine phosphatase 1B mediates the effects of insulin on the actin cytoskeleton in immortalized fibroblasts. J Biol Chem, 2003. 278(42): p. 40607-11.
21. Liu, F. and J. Chernoff, Protein tyrosine phosphatase 1B interacts with and is tyrosine phosphorylated by the epidermal growth factor receptor. Biochem J, 1997. 327 (Pt 1): p. 139-45.

22. Flint, A.J., et al., Multi-site phosphorylation of the protein tyrosine phosphatase, PTP1B: identification of cell cycle regulated and phorbol ester stimulated sites of phosphorylation. EMBO J, 1993. 12(5): p. 1937-46.
23. Shifrin, V.I., R.J. Davis, and B.G. Neel, Phosphorylation of protein-tyrosine phosphatase PTP-1B on identical sites suggests activation of a common signaling pathway during mitosis and stress response in mammalian cells. J Biol Chem, 1997. 272(5): p. 2957-62.
24. Dadke, S., et al., Regulation of protein tyrosine phosphatase 1B by sumoylation. Nat Cell Biol, 2007. 9(1): p. 80-5.
25. Frangioni, J.V., et al., Calpain-catalyzed cleavage and subcellular relocation of protein phosphotyrosine phosphatase 1B (PTP-1B) in human platelets. EMBO J, 1993. 12(12): p. 4843-56.
26. Azam, M., et al., Disruption of the mouse mu-calpain gene reveals an essential role in platelet function. Mol Cell Biol, 2001. 21(6): p. 2213-20.
27. Kuchay, S.M., et al., Double knockouts reveal that protein tyrosine phosphatase 1B is a physiological target of calpain-1 in platelets. Mol Cell Biol, 2007. 27(17): p. 6038-52.
28. Erbe, D.V., et al., Ertiprotafib improves glycemic control and lowers lipids via multiple mechanisms. Mol Pharmacol, 2005. 67(1): p. 69-77.
29. Zasloff, M., et al., A spermine-coupled cholesterol metabolite from the shark with potent appetite suppressant and antidiabetic properties. Int J Obes Relat Metab Disord, 2001. 25(5): p. 689-97.
30. Lantz, K.A., et al., Inhibition of PTP1B by trodusquemine (MSI-1436) causes fat-specific weight loss in diet-induced obese mice. Obesity (Silver Spring), 2010. 18(8): p. 1516-23.
31. Fukuda, S., et al., Pharmacological profiles of a novel protein tyrosine phosphatase 1B inhibitor, JTT-551. Diabetes Obes Metab, 2010. 12(4): p. 299-306.
32. Ito, M., et al., Pharmacological effects of JTT-551, a novel protein tyrosine phosphatase 1B inhibitor, in diet-induced obesity mice. J Diabetes Res, 2014. 2014: p. 680348.
33. Qian, S., et al., Recent advances in the development of protein tyrosine phosphatase 1B inhibitors for Type 2 diabetes. Future Med Chem, 2016. 8(11): p. 1239-58.
34. Zhang, Z.Y. and S.Y. Lee, PTP1B inhibitors as potential therapeutics in the treatment of type 2 diabetes and obesity. Expert Opin Investig Drugs, 2003. 12(2): p. 223-33.
35. Matulis, D., et al., Thermodynamic stability of carbonic anhydrase: measurements of binding affinity and stoichiometry using ThermoFluor. Biochemistry, 2005. 44(13): p. 5258-66.
36. Weber, P.C. and F.R. Salemme, Applications of calorimetric methods to drug discovery and the study of protein interactions. Curr Opin Struct Biol, 2003. 13(1): p. 115-21.
37. Shrestha, S., et al., PTP1B inhibitor Ertiprotafib is also a potent inhibitor of IkappaB kinase beta (IKK-beta). Bioorg Med Chem Lett, 2007. 17(10): p. 2728-30.
38. Krishnan, N., et al., Targeting the disordered C terminus of PTP1B with an allosteric inhibitor. Nat Chem Biol, 2014. 10(7): p. 558-66.
39. Liu, G., et al., Selective protein tyrosine phosphatase 1B inhibitors: targeting the second phosphotyrosine binding site with non-carboxylic acid-containing ligands. J Med Chem, 2003. 46(16): p. 3437-40.
40. Bourdeau, A., N. Dube, and M.L. Tremblay, Cytoplasmic protein tyrosine phosphatases, regulation and function: the roles of PTP1B and TC-PTP. Curr Opin Cell Biol, 2005. 17(2): p. 203-9.

41. Tamrakar, A.K., C.K. Maurya, and A.K. Rai, PTP1B inhibitors for type 2 diabetes treatment: a patent review (2011 - 2014). Expert Opin Ther Pat, 2014. 24(10): p. 1101-15.
42. Cho, H., Protein tyrosine phosphatase 1B (PTP1B) and obesity. Vitam Horm, 2013. 91: p. 405-24.
43. Tsou, R.C. and K.K. Bence, The Genetics of PTPN1 and Obesity: Insights from Mouse Models of Tissue-Specific PTP1B Deficiency. J Obes, 2012. 2012: p. 926857.
44. Dube, N., et al., Genetic ablation of protein tyrosine phosphatase 1B accelerates lymphomagenesis of p53-null mice through the regulation of B-cell development. Cancer Res, 2005. 65(21): p. 10088-95.
45. Le Sommer, S., et al., Deficiency in Protein Tyrosine Phosphatase PTP1B Shortens Lifespan and Leads to Development of Acute Leukemia. Cancer Res, 2018. 78(1): p. 75-87.
46. Yu, M., et al., PTP1B markedly promotes breast cancer progression and is regulated by miR-193a-3p. FEBS J, 2019. 286(6): p. 1136-1153.
47. Rivera Franco, M.M., et al., Association of PTP1B with Outcomes of Breast Cancer Patients Who Underwent Neoadjuvant Chemotherapy. Breast Cancer (Auckl), 2016. 10: p. 177-184.
48. You-Ten, K.E., et al., Impaired bone marrow microenvironment and immune function in T cell protein tyrosine phosphatase-deficient mice. J Exp Med, 1997. 186(5): p. 683-93.
49. Galic, S., et al., Regulation of insulin receptor signaling by the protein tyrosine phosphatase TCPTP. Mol Cell Biol, 2003. 23(6): p. 2096-108.
50. Ala, P.J., et al., Structural insights into the design of nonpeptidic isothiazolidinone-containing inhibitors of protein-tyrosine phosphatase 1B. J Biol Chem, 2006. 281(49): p. 38013-21.
51. Zhang, Y. and Y. Du, The development of protein tyrosine phosphatase1B inhibitors defined by binding sites in crystalline complexes. Future Med Chem, 2018. 10(19): p. 2345-2367.
52. Koller, E., W.A. Gaarde, and B.P. Monia, Elucidating cell signaling mechanisms using antisense technology. Trends Pharmacol Sci, 2000. 21(4): p. 142-8.
53. Liu, G., Protein tyrosine phosphatase 1B inhibition: opportunities and challenges. Curr Med Chem, 2003. 10(15): p. 1407-21.
54. Andersen, J.N., et al., Structural and evolutionary relationships among protein tyrosine phosphatase domains. Mol Cell Biol, 2001. 21(21): p. 7117-36.
55. Jia, Z., et al., Structural basis for phosphotyrosine peptide recognition by protein tyrosine phosphatase 1B. Science, 1995. 268(5218): p. 1754-8.
56. Brandao, T.A., A.C. Hengge, and S.J. Johnson, Insights into the reaction of protein-tyrosine phosphatase 1B: crystal structures for transition state analogs of both catalytic steps. J Biol Chem, 2010. 285(21): p. 15874-83.
57. Choy, M.S., et al., Conformational Rigidity and Protein Dynamics at Distinct Timescales Regulate PTP1B Activity and Allostery. Mol Cell, 2017. 65(4): p. 644-658 e5.
58. Ruddraraju, K.V. and Z.Y. Zhang, Covalent inhibition of protein tyrosine phosphatases. Mol Biosyst, 2017. 13(7): p. 1257-1279.
59. Pannifer, A.D., et al., Visualization of the cysteinyl-phosphate intermediate of a protein-tyrosine phosphatase by x-ray crystallography. J Biol Chem, 1998. 273(17): p. 10454-62.
60. Zhang, Z.Y., Y. Wang, and J.E. Dixon, Dissecting the catalytic mechanism of protein-tyrosine phosphatases. Proc Natl Acad Sci U S A, 1994. 91(5): p. 1624-7.
61. Zhao, Y., et al., Altering the nucleophile specificity of a protein-tyrosine phosphatase-catalyzed reaction. Probing the function of the invariant glutamine residues. J Biol

Chem, 1998. 273(10): p. 5484-92.
62. Tonks, N.K., PTP1B: from the sidelines to the front lines! FEBS Lett, 2003. 546(1): p. 140-8.
63. Puius, Y.A., et al., Identification of a second aryl phosphate-binding site in protein-tyrosine phosphatase 1B: a paradigm for inhibitor design. Proc Natl Acad Sci U S A, 1997. 94(25): p. 13420-5.
64. Salmeen, A., et al., Molecular basis for the dephosphorylation of the activation segment of the insulin receptor by protein tyrosine phosphatase 1B. Mol Cell, 2000. 6(6): p. 1401-12.
65. Low, J.L., C.L. Chai, and S.Q. Yao, Bidentate inhibitors of protein tyrosine phosphatases. Antioxid Redox Signal, 2014. 20(14): p. 2225-50.
66. Asante-Appiah, E., et al., The YRD motif is a major determinant of substrate and inhibitor specificity in T-cell protein-tyrosine phosphatase. J Biol Chem, 2001. 276(28): p. 26036-43.
67. Iversen, L.F., et al., Structure-based design of a low molecular weight, nonphosphorus, nonpeptide, and highly selective inhibitor of protein-tyrosine phosphatase 1B. J Biol Chem, 2000. 275(14): p. 10300-7.
68. Szczepankiewicz, B.G., et al., Discovery of a potent, selective protein tyrosine phosphatase 1B inhibitor using a linked-fragment strategy. J Am Chem Soc, 2003. 125(14): p. 4087-96.
69. Li, X., L. Wang, and D. Shi, The design strategy of selective PTP1B inhibitors over TCPTP. Bioorg Med Chem, 2016. 24(16): p. 3343-52.
70. Asante-Appiah, E., et al., The structure of PTP-1B in complex with a peptide inhibitor reveals an alternative binding mode for bisphosphonates. Biochemistry, 2002. 41(29): p. 9043-51.
71. Zhang, Z.Y., et al., Protein tyrosine phosphatase substrate specificity: size and phosphotyrosine positioning requirements in peptide substrates. Biochemistry, 1994. 33(8): p. 2285-90.
72. Zhang, Z.Y., et al., Substrate specificity of the protein tyrosine phosphatases. Proc Natl Acad Sci U S A, 1993. 90(10): p. 4446-50.
73. Bilwes, A.M., et al., Structural basis for inhibition of receptor protein-tyrosine phosphatase-alpha by dimerization. Nature, 1996. 382(6591): p. 555-9.
74. Peters, G.H., et al., Residue 259 is a key determinant of substrate specificity of protein-tyrosine phosphatases 1B and alpha. J Biol Chem, 2000. 275(24): p. 18201-9.
75. Buist, A., et al., Restoration of potent protein-tyrosine phosphatase activity into the membrane-distal domain of receptor protein-tyrosine phosphatase alpha. Biochemistry, 1999. 38(3): p. 914-22.
76. Adams, D.R., et al., 2-Aryl-3,3,3-trifluoro-2-hydroxypropionic acids: a new class of protein tyrosine phosphatase 1B inhibitors. Bioorg Med Chem Lett, 2007. 17(23): p. 6579-83.
77. Xin, Z., et al., Potent, selective inhibitors of protein tyrosine phosphatase 1B. Bioorg Med Chem Lett, 2003. 13(11): p. 1887-90.
78. Lund, I.K., et al., Mechanism of protein tyrosine phosphatase 1B-mediated inhibition of leptin signalling. J Mol Endocrinol, 2005. 34(2): p. 339-51.
79. Huang, Z., et al., ASD: a comprehensive database of allosteric proteins and modulators. Nucleic Acids Res, 2011. 39(Database issue): p. D663-9.
80. Huang, Z., et al., ASD v2.0: updated content and novel features focusing on allosteric regulation. Nucleic Acids Res, 2014. 42(Database issue): p. D510-6.
81. Wiesmann, C., et al., Allosteric inhibition of protein tyrosine phosphatase 1B. Nat Struct Mol Biol, 2004. 11(8): p. 730-7.

82. Li, S., et al., The mechanism of allosteric inhibition of protein tyrosine phosphatase 1B. PLoS One, 2014. 9(5): p. e97668.
83. Kamerlin, S.C., R. Rucker, and S. Boresch, A molecular dynamics study of WPD-loop flexibility in PTP1B. Biochem Biophys Res Commun, 2007. 356(4): p. 1011-6.
84. Kamerlin, S.C., R. Rucker, and S. Boresch, A targeted molecular dynamics study of WPD loop movement in PTP1B. Biochem Biophys Res Commun, 2006. 345(3): p. 1161-6.
85. Kumar, R., et al., Probing interaction requirements in PTP1B inhibitors: a comparative molecular dynamics study. J Chem Inf Model, 2010. 50(6): p. 1147-58.
86. Olmez, E.O. and B. Alakent, Alpha7 helix plays an important role in the conformational stability of PTP1B. J Biomol Struct Dyn, 2011. 28(5): p. 675-93.
87. Cui, W., et al., Unraveling the allosteric inhibition mechanism of PTP1B by free energy calculation based on umbrella sampling. J Chem Inf Model, 2013. 53(5): p. 1157-67.
88. Hassan, M.I., A. Aijaz, and F. Ahmad, Structural and functional analysis of human prostatic acid phosphatase. Expert Rev Anticancer Ther, 2010. 10(7): p. 1055-68.
89. Krishnan, N., et al., A potent, selective, and orally bioavailable inhibitor of the protein-tyrosine phosphatase PTP1B improves insulin and leptin signaling in animal models. J Biol Chem, 2018. 293(5): p. 1517-1525.
90. Krishnan, N., et al., DPM-1001 decreased copper levels and ameliorated deficits in a mouse model of Wilson's disease. Genes Dev, 2018. 32(13-14): p. 944-952.
91. Wang, Q., et al., Potent inhibition of protein tyrosine phosphatase 1B by copper complexes: implications for copper toxicity in biological systems. Chem Commun (Camb), 2010. 46(20): p. 3547-9.
92. Hongdusit, A., et al., Minimally disruptive optical control of protein tyrosine phosphatase 1B. Nat Commun, 2020. 11(1): p. 788.
93. Hansen, S.K., et al., Allosteric inhibition of PTP1B activity by selective modification of a non-active site cysteine residue. Biochemistry, 2005. 44(21): p. 7704-12.
94. Punthasee, P., et al., Covalent Allosteric Inactivation of Protein Tyrosine Phosphatase 1B (PTP1B) by an Inhibitor-Electrophile Conjugate. Biochemistry, 2017. 56(14): p. 2051-2060.
95. Khan, S., I. Bjij, and M.E.S. Soliman, Selective Covalent Inhibition of "Allosteric Cys121" Distort the Binding of PTP1B Enzyme: A Novel Therapeutic Approach for Cancer Treatment. Cell Biochem Biophys, 2019. 77(3): p. 203-211.
96. Kumar, A.P., et al., Structural analysis of protein tyrosine phosphatase 1B reveals potentially druggable allosteric binding sites. Proteins, 2018. 86(3): p. 301-321.
97. Zinker, B.A., et al., PTP1B antisense oligonucleotide lowers PTP1B protein, normalizes blood glucose, and improves insulin sensitivity in diabetic mice. Proc Natl Acad Sci U S A, 2002. 99(17): p. 11357-62.
98. Monia, B.P., et al., Evaluation of 2'-modified oligonucleotides containing 2'-deoxy gaps as antisense inhibitors of gene expression. J Biol Chem, 1993. 268(19): p. 14514-22.
99. Swarbrick, M.M., et al., Inhibition of protein tyrosine phosphatase-1B with antisense oligonucleotides improves insulin sensitivity and increases adiponectin concentrations in monkeys. Endocrinology, 2009. 150(4): p. 1670-9.
100. Koizumi, M., et al., In vivo antisense activity of ENA oligonucleotides targeting PTP1B mRNA in comparison of that of 2'-MOE-modified oligonucleotides. Nucleic Acids Symp Ser (Oxf), 2007(51): p. 111-2.

101. Digenio, A., et al., Antisense Inhibition of Protein Tyrosine Phosphatase 1B With IONIS-PTP-1BRx Improves Insulin Sensitivity and Reduces Weight in Overweight Patients With Type 2 Diabetes. Diabetes Care, 2018. 41(4): p. 807-814.

LEGEND TABLES AND FIGURES

Compound	Company	IC_{50} or K_i (μM)		Clinical phase	Continued or not
		PTP1B	TCPTP		
Ertiprotafib	Pfizer	> 20	Unknown	Phase II	×
JTT-551	Tobacco	0.22	9.30	Pre-clinical	×
Trodusquemine	DepYmed	1.0	224	Phase I	×
DPM-1001	DepYmed	0.10	Unknown	Pre-clinical	√
IONIS 113715	IONIS Pharmaceuticals	< 0.01	Unknown	Phase II	×
IONIS PTP1BRx	IONIS Pharmaceuticals	Unknown	Unknown	Phase II	√

Table 1: Summary of PTP1B inhibitors (was/undergo in clinical trials).

AC type	2- (oxalyl-amino)-benzoic acid (2-OBA) derivatives
	2-carboxymethyl-benzoic acid-derived inhibitors
	difluoromethylphosphonic acid (DFMP)-based inhibitors
	isothiazolidinone (IZD)-contained inhibitors
	monocyclic thiophene-based inhibitors
AB type	monocyclic, bicyclic and tricyclic thiophene inhibitors
	sulfamic acid moiety-contained inhibitors
	other novel AB type inhibitors
ABC type	a series of OBA derivatives
	DFMP group-contained PTP1B inhibitors
	sulfamic acid moiety-contained PTP1B inhibitors
ADC type	N-(2,5-diethoxy-phenyl)-methanesul-fonamide derivatives

Table 2: Categories of PTP1B inhibitors on A/B/C/D sites [51].

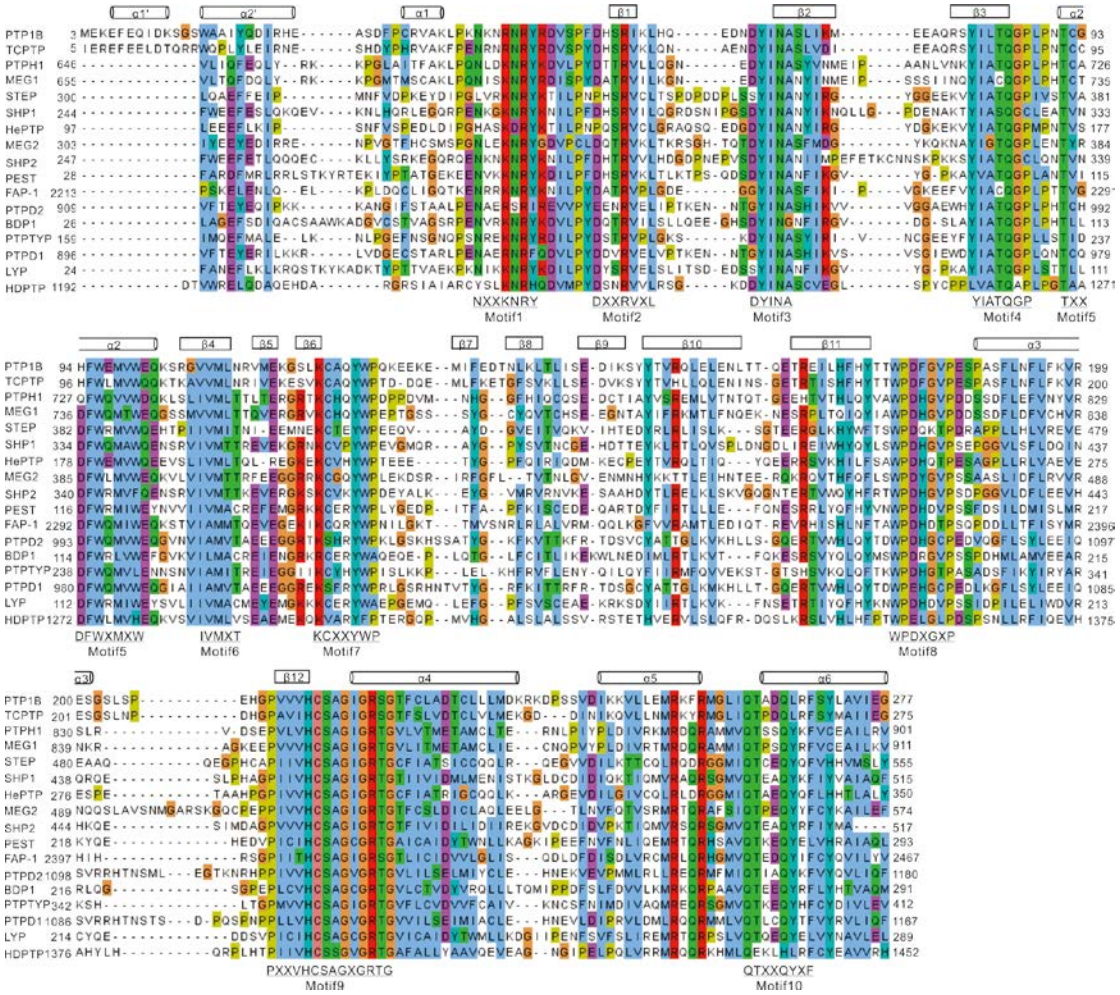

Figure 1: Sequence alignment of 17 human non-receptor PTPs catalytic domains. Sequences were obtained from Uniprot (https://www.uniprot.org/) database and aligned using EMBL-Clustal Omega (https://www.ebi.ac.uk/Tools/msa/clustalo) database using default options. The alignment was further processed by Jalview (version 2.11.1.3), and colored with Clustal default option.

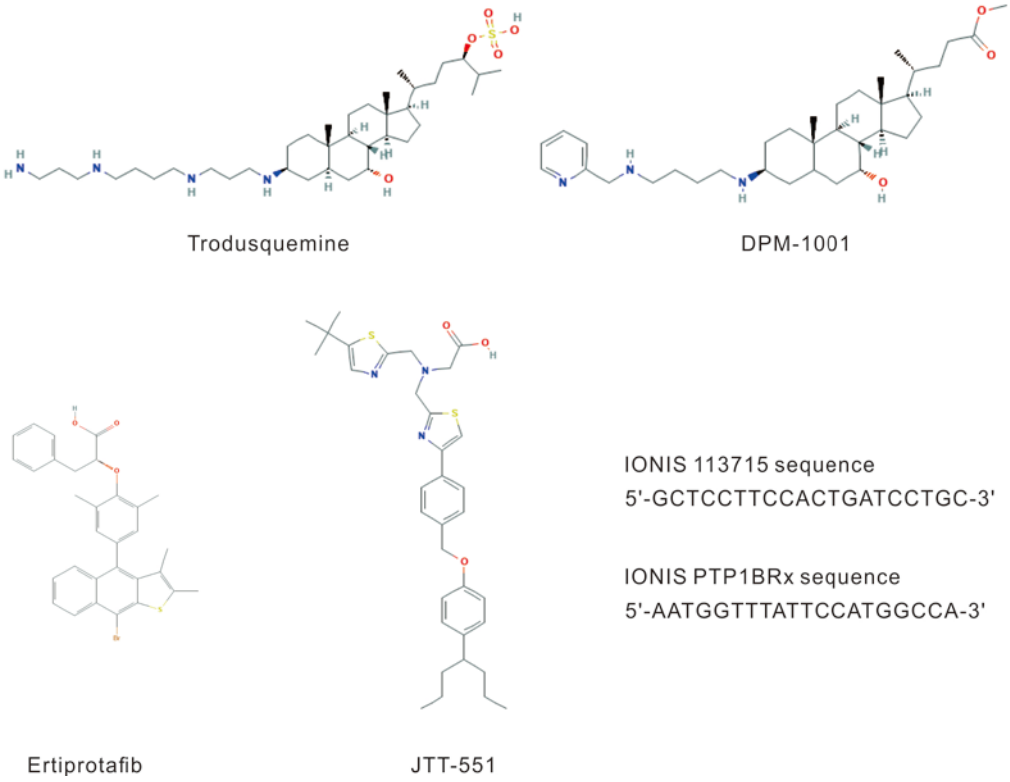

Figure 2: PTP1B inhibitors investigated in clinical trials.

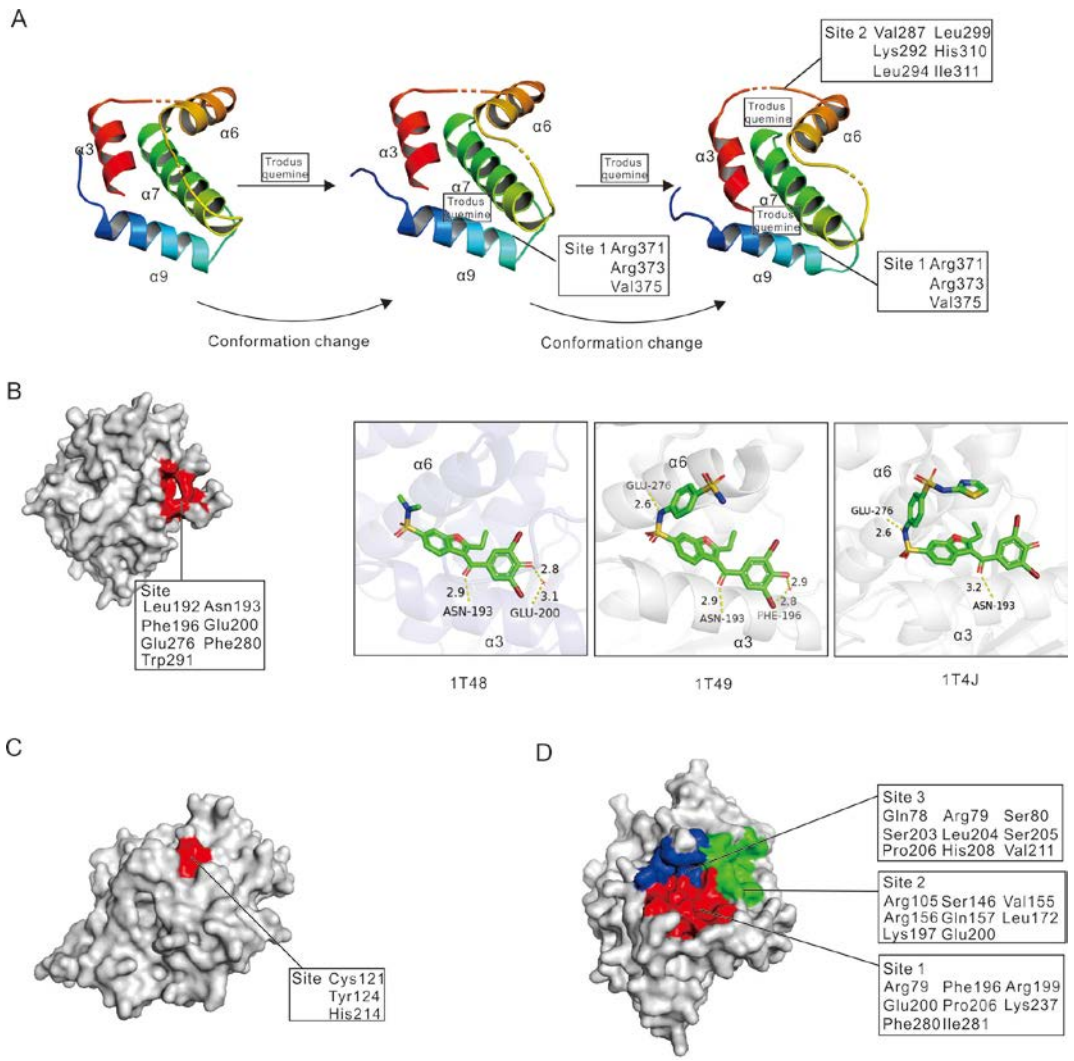

Figure 3: The allosteric binding sites of PTP1B inhibitors.

(A) The step-by-step mechanism of PTP1B inhibition by trodusquemine. (B) (left panel) PTP1B was represented as surface structure and its allosteric binding site was highlighted in red; (right panel) structural representation of three inhibitors bound to the allosteric site of PTP1B (inhibitors are colored by elements; hydrogen bounds are depicted with distance in yellow dash). (C)/(D): PTP1B was represented as surface structure and its allosteric binding site was highlighted in color respectively.

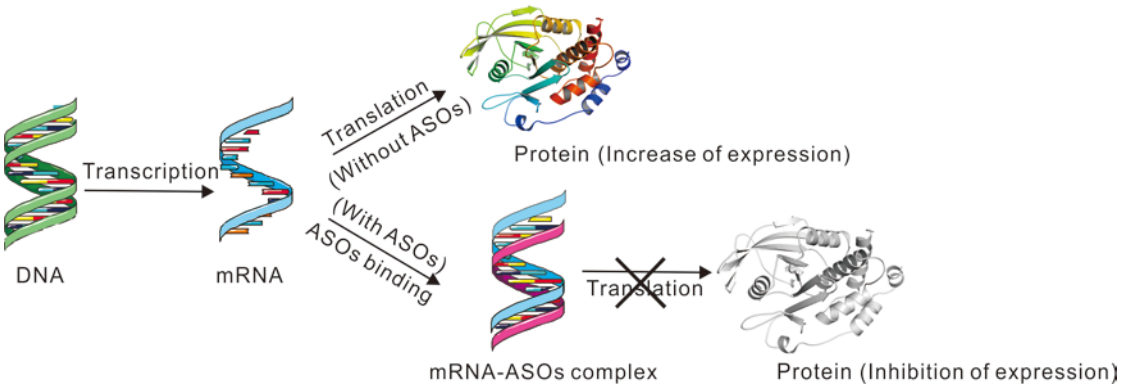

Figure 4: PTP1B protein expression in the presence or absence of ASOs.

4 CONCLUSION

In this thesis, we aimed at describing and understanding the impact of the widely used chemotherapeutic drug cisplatin on human PTP1B tyrosine phosphatase activity. Indeed, while cisplatin is mainly known to act as a drug targeting DNA, it is now well-known that it may also impact other cellular processes, notably cell signaling, through reaction with proteins [31, 32]. Interestingly, it has been shown that the functions of human PTP1B could be altered by cisplatin-derivatives thus suggesting that cisplatin could act on PTP1B and thereby on signaling pathways regulated by PTP1B. Of note, while PTP1B is known to be a major regulator of the EGFR cascade, it has also been shown that cisplatin altered the EGFR pathway through increased tyrosine phosphorylation [6, 32]. We clearly show in this thesis, that indeed, cisplatin can impair PTP1B activity through direct covalent reaction with its catalytic cysteine residue within the active site. Consistent with these mechanistic results, we show that, as expected, inhibition of PTP1B leads to increased tyrosine phosphorylation of the EGFR receptor, a well-known substrate of the enzyme. These results thus further support previous studies indicating that cisplatin was able to impact cell signaling and in particular the EGFR cascade by inducing its activation through increased tyrosine phosphorylation [33]. Our work also points to the potential effect of cisplatin and other platinum salts on other protein tyrosine phosphatases such as PTPN2 (encoding protein TCPTP) or PTPN11 (encoding protein SHP2) and subsequently on the numerous signaling cascades that are regulated by these enzymes. Indeed, similarly to PTP1B, the functions of PTPs rely on a catalytic cysteine that could also be targeted by cisplatin [47]. It is nonetheless possible that the reactivity of this catalytic cysteine may vary (in particular due to different amino acids environment of the catalytic cysteine) making certain PTPs more prone to chemical modification and inhibition by cisplatin. More broadly, this work also further underline recent hypothesis that the biological effects of cisplatin not only rely on its genotoxic effect on DNA, but also depend on the dysregulation of other cellular processes [31].

Cisplatin is a widely used and efficient chemotherapeutic drug, nonetheless its administration is also known to induce secondary treatment-dependent hematological

malignancies. Interestingly, recent studies have shown that PTP1B deficiency can contribute the development of malignant hematopoietic disorders such as lymphoma and acute leukemia [10, 11, 41], supporting a tumor suppressor role of the enzyme. However, evidence also suggest that PTP1B loss of function could produce cancer-promoting effects [141]. Therefore depending on the biological context, PTP1B activity appears thus as a double agent in oncogenesis. The role of PTP1B in lymphomagenesis was further underlined by studies that identified genetic defects, in particular, point mutations, in PTP1B in human B cell lymphomas [9, 42]. Although the effects of these mutations were not all characterized in depth, evidence indicated that at least certain would lead to loss of PTP1B function [9]. However, it has been reported that certain oncogenic mutations in certain PTPs, such as SHP2 can either lead loss or gain of function [291]. We thus carried out the molecular and enzymatic analysis of three PTP1B mutants (V184D, R221G and G259V) identified in patients with primary mediastinal B cell lymphoma. These single point mutations are the only one affecting residues that are in active site loops of the enzyme (WPD-loop, P-loop and Q-loop, respectively) and known to be key for enzyme chemistry [47]. Using recombinant purified enzymes and cell transfections studies, we clearly show that these mutations lead to PTP1B mutant forms strongly impacted in their intrinsic tyrosine phosphatase activity. Assays were conducted with a generic non-peptidic phosphatase substrate (*p*NPP) and a specific tyrosine phosphorylated peptide-derived from a known PTP1B substrate (STAT1) and both gave similar results thus supporting that loss of activity of the mutants are unlikely to depend on substrate specificity. Transfection studies confirmed that the PTP1B mutants displayed impaired intrinsic tyrosine phosphatase activity. Moreover, the PTP1B V184D and G259V showed altered thermostability, indicating that these mutations are likely to alter intrinsic protein stability. Molecular dynamics studies further supported that these two mutations displayed altered dynamics compared to WT. More importantly, molecular dynamics studies indicated that the three mutations lead to altered protein flexibility of the active site loops (notably WPD-loop, P-loop and Q-loop), thus likely contributing to loss of enzyme activity by preventing important catalytic residues

within this loops (such as Asp181 or Gln262) to adopt a proper conformation/position for catalysis [47]. Interestingly, we found that each mutation in addition to impact flexibility/structure of the loop where it occurs, it also modifies the flexibility/structure of neighboring active site loops. This is in agreement with previous studies showing "coordinated" movements of active site loops during catalysis [47, 48]. In addition, it is now well documented that an "allosteric network" involving amino acids in different regions of the PTP1B structure (such as Ala69, Tyr153, Asn193) could contribute to enzyme activity through impacting active site loops dynamics (notably WPD-loop) [48, 274]. This suggests that cancer-associated mutations affecting these residues are likely to impact PTP1B activity. Altogether, our study on lymphoma-associated PTP1B mutations that affect active site loops residues provides first clear molecular and functional evidence that these mutations lead to loss of function PTP1B mutants. These data also support that alteration of PTP1B tyrosine phosphatase contributes to lymphomagenesis.

5. REFERENCES

1. Pawson, T. (2004). Specificity in signal transduction: from phosphotyrosine-SH2 domain interactions to complex cellular systems. Cell *116*, 191-203.
2. Tonks, N.K. (2006). Protein tyrosine phosphatases: from genes, to function, to disease. Nat Rev Mol Cell Biol *7*, 833-846.
3. Bohmer, F., Szedlacsek, S., Tabernero, L., Ostman, A., and den Hertog, J. (2013). Protein tyrosine phosphatase structure-function relationships in regulation and pathogenesis. FEBS J *280*, 413-431.
4. Tiganis, T., and Bennett, A.M. (2007). Protein tyrosine phosphatase function: the substrate perspective. Biochem J *402*, 1-15.
5. Qi, X.M., Wang, F., Mortensen, M., Wertz, R., and Chen, G. (2018). Targeting an oncogenic kinase/phosphatase signaling network for cancer therapy. Acta Pharm Sin B *8*, 511-517.
6. Villamar-Cruz, O., Loza-Mejia, M.A., Arias-Romero, L.E., and Camacho-Arroyo, I. (2021). Recent advances in PTP1B signaling in metabolism and cancer. Biosci Rep *41*.
7. Simoncic, P.D., McGlade, C.J., and Tremblay, M.L. (2006). PTP1B and TC-PTP: novel roles in immune-cell signaling. Can J Physiol Pharmacol *84*, 667-675.
8. Elchebly, M., Payette, P., Michaliszyn, E., Cromlish, W., Collins, S., Loy, A.L., Normandin, D., Cheng, A., Himms-Hagen, J., Chan, C.C., et al. (1999). Increased insulin sensitivity and obesity resistance in mice lacking the protein tyrosine phosphatase-1B gene. Science *283*, 1544-1548.
9. Gunawardana, J., Chan, F.C., Telenius, A., Woolcock, B., Kridel, R., Tan, K.L., Ben-Neriah, S., Mottok, A., Lim, R.S., Boyle, M., et al. (2014). Recurrent somatic mutations of PTPN1 in primary mediastinal B cell lymphoma and Hodgkin lymphoma. Nat Genet *46*, 329-335.
10. Jobe, F., Patel, B., Kuzmanovic, T., Makishima, H., Yang, Y., Przychodzen, B., Hutchison, R.E., Bence, K.K., Maciejewski, J.P., and Mohi, G. (2017). Deletion of Ptpn1 induces myeloproliferative neoplasm. Leukemia *31*, 1229-1234.
11. Le Sommer, S., Morrice, N., Pesaresi, M., Thompson, D., Vickers, M.A., Murray, G.I., Mody, N., Neel, B.G., Bence, K.K., Wilson, H.M., et al. (2018). Deficiency in Protein Tyrosine Phosphatase PTP1B Shortens Lifespan and Leads to Development of Acute Leukemia. Cancer Res *78*, 75-87.
12. Salmeen, A., Andersen, J.N., Myers, M.P., Meng, T.C., Hinks, J.A., Tonks, N.K., and Barford, D. (2003). Redox regulation of protein tyrosine phosphatase 1B involves a sulphenyl-amide intermediate. Nature *423*, 769-773.
13. Lou, Y.W., Chen, Y.Y., Hsu, S.F., Chen, R.K., Lee, C.L., Khoo, K.H., Tonks, N.K., and Meng, T.C. (2008). Redox regulation of the protein tyrosine phosphatase PTP1B in cancer cells. FEBS J *275*, 69-88.
14. Heppner, D.E., and van der Vliet, A. (2016). Redox-dependent regulation of epidermal growth factor receptor signaling. Redox Biol *8*, 24-27.
15. Iwamoto, N., Sumi, D., Ishii, T., Uchida, K., Cho, A.K., Froines, J.R., and Kumagai, Y. (2007). Chemical knockdown of protein-tyrosine phosphatase 1B by 1,2-naphthoquinone through covalent modification causes persistent transactivation of epidermal growth factor receptor. J Biol Chem *282*, 33396-33404.
16. Zheng, F., Goncalves, F.M., Abiko, Y., Li, H., Kumagai, Y., and Aschner, M. (2020). Redox toxicology of environmental chemicals causing oxidative stress. Redox Biol *34*, 101475.

17. Rosenberg, B., Vancamp, L., and Krigas, T. (1965). Inhibition of Cell Division in Escherichia Coli by Electrolysis Products from a Platinum Electrode. Nature *205*, 698-699.
18. Rosenberg, B., VanCamp, L., Trosko, J.E., and Mansour, V.H. (1969). Platinum compounds: a new class of potent antitumour agents. Nature *222*, 385-386.
19. Tchounwou, P.B., Dasari, S., Noubissi, F.K., Ray, P., and Kumar, S. (2021). Advances in Our Understanding of the Molecular Mechanisms of Action of Cisplatin in Cancer Therapy. J Exp Pharmacol *13*, 303-328.
20. Siddik, Z.H. (2003). Cisplatin: mode of cytotoxic action and molecular basis of resistance. Oncogene *22*, 7265-7279.
21. Sosa, V., Moline, T., Somoza, R., Paciucci, R., Kondoh, H., and ME, L.L. (2013). Oxidative stress and cancer: an overview. Ageing Res Rev *12*, 376-390.
22. Ueda, N., Kaushal, G.P., and Shah, S.V. (2000). Apoptotic mechanisms in acute renal failure. Am J Med *108*, 403-415.
23. Kumar, S., and Tchounwou, P.B. (2015). Molecular mechanisms of cisplatin cytotoxicity in acute promyelocytic leukemia cells. Oncotarget *6*, 40734-40746.
24. Brozovic, A., Ambriovic-Ristov, A., and Osmak, M. (2010). The relationship between cisplatin-induced reactive oxygen species, glutathione, and BCL-2 and resistance to cisplatin. Crit Rev Toxicol *40*, 347-359.
25. Shen, L., Wen, N., Xia, M., Zhang, Y.U., Liu, W., Xu, Y.E., and Sun, L. (2016). Calcium efflux from the endoplasmic reticulum regulates cisplatin-induced apoptosis in human cervical cancer HeLa cells. Oncol Lett *11*, 2411-2419.
26. Johnson, G.L., and Lapadat, R. (2002). Mitogen-activated protein kinase pathways mediated by ERK, JNK, and p38 protein kinases. Science *298*, 1911-1912.
27. Potapova, O., Basu, S., Mercola, D., and Holbrook, N.J. (2001). Protective role for c-Jun in the cellular response to DNA damage. J Biol Chem *276*, 28546-28553.
28. Persons, D.L., Yazlovitskaya, E.M., and Pelling, J.C. (2000). Effect of extracellular signal-regulated kinase on p53 accumulation in response to cisplatin. J Biol Chem *275*, 35778-35785.
29. Peng, D.J., Wang, J., Zhou, J.Y., and Wu, G.S. (2010). Role of the Akt/mTOR survival pathway in cisplatin resistance in ovarian cancer cells. Biochem Biophys Res Commun *394*, 600-605.
30. Cullen, K.J., Yang, Z., Schumaker, L., and Guo, Z. (2007). Mitochondria as a critical target of the chemotheraputic agent cisplatin in head and neck cancer. J Bioenerg Biomembr *39*, 43-50.
31. Dasari, S., and Tchounwou, P.B. (2014). Cisplatin in cancer therapy: molecular mechanisms of action. Eur J Pharmacol *740*, 364-378.
32. Benhar, M., Engelberg, D., and Levitzki, A. (2002). Cisplatin-induced activation of the EGF receptor. Oncogene *21*, 8723-8731.
33. Yoshida, T., Okamoto, I., Iwasa, T., Fukuoka, M., and Nakagawa, K. (2008). The anti-EGFR monoclonal antibody blocks cisplatin-induced activation of EGFR signaling mediated by HB-EGF. FEBS Lett *582*, 4125-4130.
34. Messori, L., and Merlino, A. (2014). Cisplatin binding to proteins: molecular structure of the ribonuclease a adduct. Inorg Chem *53*, 3929-3931.
35. Ragunathan, N., Dairou, J., Pluvinage, B., Martins, M., Petit, E., Janel, N., Dupret, J.M., and Rodrigues-Lima, F. (2008). Identification of the xenobiotic-metabolizing enzyme arylamine

N-acetyltransferase 1 as a new target of cisplatin in breast cancer cells: molecular and cellular mechanisms of inhibition. Mol Pharmacol *73*, 1761-1768.

36. De Luca, A., Parker, L.J., Ang, W.H., Rodolfo, C., Gabbarini, V., Hancock, N.C., Palone, F., Mazzetti, A.P., Menin, L., Morton, C.J., et al. (2019). A structure-based mechanism of cisplatin resistance mediated by glutathione transferase P1-1. Proceedings of the National Academy of Sciences of the United States of America *116*, 13943-13951.
37. Chen, H., Pan, T., He, Y., Zeng, R., Li, Y., Yi, L., Zang, H., Chen, S., Duan, Q., Xiao, L., et al. (2021). Primary Mediastinal B-Cell Lymphoma: Novel Precision Therapies and Future Directions. Front Oncol *11*, 654854.
38. Giulino-Roth, L. (2018). How I treat primary mediastinal B-cell lymphoma. Blood *132*, 782-790.
39. Savage, K.J., Monti, S., Kutok, J.L., Cattoretti, G., Neuberg, D., De Leval, L., Kurtin, P., Dal Cin, P., Ladd, C., Feuerhake, F., et al. (2003). The molecular signature of mediastinal large B-cell lymphoma differs from that of other diffuse large B-cell lymphomas and shares features with classical Hodgkin lymphoma. Blood *102*, 3871-3879.
40. Irish, J.M., Myklebust, J.H., Alizadeh, A.A., Houot, R., Sharman, J.P., Czerwinski, D.K., Nolan, G.P., and Levy, R. (2010). B-cell signaling networks reveal a negative prognostic human lymphoma cell subset that emerges during tumor progression. Proceedings of the National Academy of Sciences of the United States of America *107*, 12747-12754.
41. Dube, N., Bourdeau, A., Heinonen, K.M., Cheng, A., Loy, A.L., and Tremblay, M.L. (2005). Genetic ablation of protein tyrosine phosphatase 1B accelerates lymphomagenesis of p53-null mice through the regulation of B-cell development. Cancer Res *65*, 10088-10095.
42. Zahn, M., Marienfeld, R., Melzner, I., Heinrich, J., Renner, B., Wegener, S., Miessner, A., Barth, T.F., Dorsch, K., Bruderlein, S., et al. (2017). A novel PTPN1 splice variant upregulates JAK/STAT activity in classical Hodgkin lymphoma cells. Blood *129*, 1480-1490.
43. Haj, F.G., Markova, B., Klaman, L.D., Bohmer, F.D., and Neel, B.G. (2003). Regulation of receptor tyrosine kinase signaling by protein tyrosine phosphatase-1B. J Biol Chem *278*, 739-744.
44. Pike, K.A., and Tremblay, M.L. (2016). TC-PTP and PTP1B: Regulating JAK-STAT signaling, controlling lymphoid malignancies. Cytokine *82*, 52-57.
45. Ritz, O., Guiter, C., Castellano, F., Dorsch, K., Melzner, J., Jais, J.P., Dubois, G., Gaulard, P., Moller, P., and Leroy, K. (2009). Recurrent mutations of the STAT6 DNA binding domain in primary mediastinal B-cell lymphoma. Blood *114*, 1236-1242.
46. Vainchenker, W., and Constantinescu, S.N. (2013). JAK/STAT signaling in hematological malignancies. Oncogene *32*, 2601-2613.
47. Tautz, L., Critton, D.A., and Grotegut, S. (2013). Protein tyrosine phosphatases: structure, function, and implication in human disease. Methods Mol Biol *1053*, 179-221.
48. Choy, M.S., Li, Y., Machado, L., Kunze, M.B.A., Connors, C.R., Wei, X., Lindorff-Larsen, K., Page, R., and Peti, W. (2017). Conformational Rigidity and Protein Dynamics at Distinct Timescales Regulate PTP1B Activity and Allostery. Mol Cell *65*, 644-658 e645.
49. Cui, D.S., Lipchock, J.M., Brookner, D., and Loria, J.P. (2019). Uncovering the Molecular Interactions in the Catalytic Loop That Modulate the Conformational Dynamics in Protein Tyrosine Phosphatase 1B. J Am Chem Soc *141*, 12634-12647.

50. Civini, S., Jin, P., Ren, J., Sabatino, M., Castiello, L., Jin, J., Wang, H., Zhao, Y., Marincola, F., and Stroncek, D. (2013). Leukemia cells induce changes in human bone marrow stromal cells. J Transl Med *11*, 298.
51. Martellucci, S., Clementi, L., Sabetta, S., Mattei, V., Botta, L., and Angelucci, A. (2020). Src Family Kinases as Therapeutic Targets in Advanced Solid Tumors: What We Have Learned so Far. Cancers (Basel) *12*.
52. Binks, S.P., and Dobrota, M. (1990). Kinetics and mechanism of uptake of platinum-based pharmaceuticals by the rat small intestine. Biochem Pharmacol *40*, 1329-1336.
53. Lin, X., Okuda, T., Holzer, A., and Howell, S.B. (2002). The copper transporter CTR1 regulates cisplatin uptake in Saccharomyces cerevisiae. Mol Pharmacol *62*, 1154-1159.
54. Rocha, C.R.R., Silva, M.M., Quinet, A., Cabral-Neto, J.B., and Menck, C.F.M. (2018). DNA repair pathways and cisplatin resistance: an intimate relationship. Clinics *73*, e478s.
55. Lieberthal, W., Triaca, V., and Levine, J. (1996). Mechanisms of death induced by cisplatin in proximal tubular epithelial cells: apoptosis vs. necrosis. Am J Physiol *270*, F700-708.
56. Dasari, S.R., Velma, V., Yedjou, C.G., and Tchounwou, P.B. (2015). Preclinical Assessment of Low Doses of Cisplatin in the Management of Acute Promyelocytic Leukemia. Int J Cancer Res Mol Mech *1*.
57. Potapova, O., Haghighi, A., Bost, F., Liu, C., Birrer, M.J., Gjerset, R., and Mercola, D. (1997). The Jun kinase/stress-activated protein kinase pathway functions to regulate DNA repair and inhibition of the pathway sensitizes tumor cells to cisplatin. J Biol Chem *272*, 14041-14044.
58. Hayakawa, J., Ohmichi, M., Kurachi, H., Ikegami, H., Kimura, A., Matsuoka, T., Jikihara, H., Mercola, D., and Murata, Y. (1999). Inhibition of extracellular signal-regulated protein kinase or c-Jun N-terminal protein kinase cascade, differentially activated by cisplatin, sensitizes human ovarian cancer cell line. J Biol Chem *274*, 31648-31654.
59. Grossi, V., Peserico, A., Tezil, T., and Simone, C. (2014). p38alpha MAPK pathway: a key factor in colorectal cancer therapy and chemoresistance. World J Gastroenterol *20*, 9744-9758.
60. Einhorn, L.H. (1990). Treatment of testicular cancer: a new and improved model. Journal of clinical oncology : official journal of the American Society of Clinical Oncology *8*, 1777-1781.
61. Kuhlmann, M.K., Burkhardt, G., and Kohler, H. (1997). Insights into potential cellular mechanisms of cisplatin nephrotoxicity and their clinical application. Nephrol Dial Transplant *12*, 2478-2480.
62. Tanaka, H., Ishikawa, E., Teshima, S., and Shimizu, E. (1986). Histopathological study of human cisplatin nephropathy. Toxicol Pathol *14*, 247-257.
63. Cornelison, T.L., and Reed, E. (1993). Nephrotoxicity and hydration management for cisplatin, carboplatin, and ormaplatin. Gynecol Oncol *50*, 147-158.
64. Pabla, N., Murphy, R.F., Liu, K., and Dong, Z. (2009). The copper transporter Ctr1 contributes to cisplatin uptake by renal tubular cells during cisplatin nephrotoxicity. Am J Physiol Renal Physiol *296*, F505-511.
65. Miller, R.P., Tadagavadi, R.K., Ramesh, G., and Reeves, W.B. (2010). Mechanisms of Cisplatin nephrotoxicity. Toxins (Basel) *2*, 2490-2518.
66. Rybak, L.P., Whitworth, C.A., Mukherjea, D., and Ramkumar, V. (2007). Mechanisms of cisplatin-induced ototoxicity and prevention. Hear Res *226*, 157-167.

67. Marklund, L., Andersson, B., Behnam-Motlagh, P., Sandstrom, P.E., Henriksson, R., and Grankvist, K. (2004). Cellular potassium ion deprivation enhances apoptosis induced by cisplatin. Basic Clin Pharmacol Toxicol *94*, 245-251.
68. Gutteridge, J.M., and Halliwell, B. (2010). Antioxidants: Molecules, medicines, and myths. Biochem Biophys Res Commun *393*, 561-564.
69. Waissbluth, S., and Daniel, S.J. (2013). Cisplatin-induced ototoxicity: transporters playing a role in cisplatin toxicity. Hear Res *299*, 37-45.
70. Choi, M.J., Kang, H., Lee, Y.Y., Choo, O.S., Jang, J.H., Park, S.H., Moon, J.S., Choi, S.J., and Choung, Y.H. (2019). Cisplatin-Induced Ototoxicity in Rats Is Driven by RIP3-Dependent Necroptosis. Cells *8*.
71. Cepeda, V., Fuertes, M.A., Castilla, J., Alonso, C., Quevedo, C., and Perez, J.M. (2007). Biochemical mechanisms of cisplatin cytotoxicity. Anticancer Agents Med Chem *7*, 3-18.
72. Noach, E.J., Ausema, A., van Os, R., Akkerman, I., Koopal, S., Weersing, E., Dontje, B., Vellenga, E., and de Haan, G. (2003). Chemotherapy prior to autologous bone marrow transplantation impairs long-term engraftment in mice. Exp Hematol *31*, 528-534.
73. Park, M.H., Jung, I.K., Min, W.K., Choi, J.H., Kim, G.M., Jin, H.K., and Bae, J.S. (2017). Neuropeptide Y improves cisplatin-induced bone marrow dysfunction without blocking chemotherapeutic efficacy in a cancer mouse model. BMB Rep *50*, 417-422.
74. Lucas, D., Scheiermann, C., Chow, A., Kunisaki, Y., Bruns, I., Barrick, C., Tessarollo, L., and Frenette, P.S. (2013). Chemotherapy-induced bone marrow nerve injury impairs hematopoietic regeneration. Nat Med *19*, 695-703.
75. Wong, T.N., Ramsingh, G., Young, A.L., Miller, C.A., Touma, W., Welch, J.S., Lamprecht, T.L., Shen, D., Hundal, J., Fulton, R.S., et al. (2015). Role of TP53 mutations in the origin and evolution of therapy-related acute myeloid leukaemia. Nature *518*, 552-555.
76. Barroso-Vicens, E., Ramirez, G., and Rabb, H. (1996). Multiple primary malignancies in a renal transplant patient. Transplantation *61*, 1655-1656.
77. Chen, X., Othus, M., Wood, B.L., Walter, R.B., Becker, P.S., Percival, M.E., Abkowitz, J.L., Appelbaum, F.R., and Estey, E.H. (2021). Comparison of myeloid blast counts and variant allele frequencies of gene mutations in myelodysplastic syndrome with excess blasts and secondary acute myeloid leukemia. Leuk Lymphoma *62*, 1226-1233.
78. Ishida, S., Lee, J., Thiele, D.J., and Herskowitz, I. (2002). Uptake of the anticancer drug cisplatin mediated by the copper transporter Ctr1 in yeast and mammals. Proceedings of the National Academy of Sciences of the United States of America *99*, 14298-14302.
79. Komatsu, M., Sumizawa, T., Mutoh, M., Chen, Z.S., Terada, K., Furukawa, T., Yang, X.L., Gao, H., Miura, N., Sugiyama, T., et al. (2000). Copper-transporting P-type adenosine triphosphatase (ATP7B) is associated with cisplatin resistance. Cancer Res *60*, 1312-1316.
80. Liedert, B., Materna, V., Schadendorf, D., Thomale, J., and Lage, H. (2003). Overexpression of cMOAT (MRP2/ABCC2) is associated with decreased formation of platinum-DNA adducts and decreased G2-arrest in melanoma cells resistant to cisplatin. The Journal of investigative dermatology *121*, 172-176.
81. Holzer, A.K., Samimi, G., Katano, K., Naerdemann, W., Lin, X., Safaei, R., and Howell, S.B. (2004). The copper influx transporter human copper transport protein 1 regulates the uptake of cisplatin in human ovarian carcinoma cells. Mol Pharmacol *66*, 817-823.

82. Mansouri, A., Ridgway, L.D., Korapati, A.L., Zhang, Q., Tian, L., Wang, Y., Siddik, Z.H., Mills, G.B., and Claret, F.X. (2003). Sustained activation of JNK/p38 MAPK pathways in response to cisplatin leads to Fas ligand induction and cell death in ovarian carcinoma cells. J Biol Chem *278*, 19245-19256.
83. Sirichanchuen, B., Pengsuparp, T., and Chanvorachote, P. (2012). Long-term cisplatin exposure impairs autophagy and causes cisplatin resistance in human lung cancer cells. Mol Cell Biochem *364*, 11-18.
84. Wu, H.M., Jiang, Z.F., Ding, P.S., Shao, L.J., and Liu, R.Y. (2015). Hypoxia-induced autophagy mediates cisplatin resistance in lung cancer cells. Sci Rep *5*, 12291.
85. Furuta, T., Ueda, T., Aune, G., Sarasin, A., Kraemer, K.H., and Pommier, Y. (2002). Transcription-coupled nucleotide excision repair as a determinant of cisplatin sensitivity of human cells. Cancer Res *62*, 4899-4902.
86. Wu, F., Lin, X., Okuda, T., and Howell, S.B. (2004). DNA polymerase zeta regulates cisplatin cytotoxicity, mutagenicity, and the rate of development of cisplatin resistance. Cancer Res *64*, 8029-8035.
87. Brozovic, A., Fritz, G., Christmann, M., Zisowsky, J., Jaehde, U., Osmak, M., and Kaina, B. (2004). Long-term activation of SAPK/JNK, p38 kinase and fas-L expression by cisplatin is attenuated in human carcinoma cells that acquired drug resistance. Int J Cancer *112*, 974-985.
88. Scagliotti, G.V., Parikh, P., von Pawel, J., Biesma, B., Vansteenkiste, J., Manegold, C., Serwatowski, P., Gatzemeier, U., Digumarti, R., Zukin, M., et al. (2008). Phase III study comparing cisplatin plus gemcitabine with cisplatin plus pemetrexed in chemotherapy-naive patients with advanced-stage non-small-cell lung cancer. Journal of clinical oncology : official journal of the American Society of Clinical Oncology *26*, 3543-3551.
89. Chang, C.L., Hsu, Y.T., Wu, C.C., Lai, Y.Z., Wang, C., Yang, Y.C., Wu, T.C., and Hung, C.F. (2013). Dose-dense chemotherapy improves mechanisms of antitumor immune response. Cancer Res *73*, 119-127.
90. Gonzalez, V.M., Fuertes, M.A., Alonso, C., and Perez, J.M. (2001). Is cisplatin-induced cell death always produced by apoptosis? Mol Pharmacol *59*, 657-663.
91. Florea, A.M., and Busselberg, D. (2011). Cisplatin as an anti-tumor drug: cellular mechanisms of activity, drug resistance and induced side effects. Cancers (Basel) *3*, 1351-1371.
92. Lopez Villar, E., Madero, L., J, A.L.-P., and W, C.C. (2015). Study of phosphorylation events for cancer diagnoses and treatment. Clin Transl Med *4*, 59.
93. Cohen, P. (2001). The role of protein phosphorylation in human health and disease. The Sir Hans Krebs Medal Lecture. Eur J Biochem *268*, 5001-5010.
94. Abramczyk, H., Imiela, A., Brozek-Pluska, B., Kopec, M., Surmacki, J., and Sliwinska, A. (2019). Aberrant Protein Phosphorylation in Cancer by Using Raman Biomarkers. Cancers (Basel) *11*.
95. Manning, G., Plowman, G.D., Hunter, T., and Sudarsanam, S. (2002). Evolution of protein kinase signaling from yeast to man. Trends Biochem Sci *27*, 514-520.
96. Pearlman, S.M., Serber, Z., and Ferrell, J.E., Jr. (2011). A mechanism for the evolution of phosphorylation sites. Cell *147*, 934-946.
97. Ardito, F., Giuliani, M., Perrone, D., Troiano, G., and Lo Muzio, L. (2017). The crucial role of protein phosphorylation in cell signaling and its use as targeted therapy (Review). Int J Mol Med *40*, 271-280.

98. Hanahan, D., and Weinberg, R.A. (2011). Hallmarks of cancer: the next generation. Cell *144*, 646-674.
99. Miller, M.L., Jensen, L.J., Diella, F., Jorgensen, C., Tinti, M., Li, L., Hsiung, M., Parker, S.A., Bordeaux, J., Sicheritz-Ponten, T., et al. (2008). Linear motif atlas for phosphorylation-dependent signaling. Sci Signal *1*, ra2.
100. Capra, M., Nuciforo, P.G., Confalonieri, S., Quarto, M., Bianchi, M., Nebuloni, M., Boldorini, R., Pallotti, F., Viale, G., Gishizky, M.L., et al. (2006). Frequent alterations in the expression of serine/threonine kinases in human cancers. Cancer Res *66*, 8147-8154.
101. Jin, J., and Pawson, T. (2012). Modular evolution of phosphorylation-based signalling systems. Philos Trans R Soc Lond B Biol Sci *367*, 2540-2555.
102. Schwartz, P.A., and Murray, B.W. (2011). Protein kinase biochemistry and drug discovery. Bioorg Chem *39*, 192-210.
103. Nishi, H., Shaytan, A., and Panchenko, A.R. (2014). Physicochemical mechanisms of protein regulation by phosphorylation. Front Genet *5*, 270.
104. Roskoski, R., Jr. (2012). ERK1/2 MAP kinases: structure, function, and regulation. Pharmacol Res *66*, 105-143.
105. Pearce, L.R., Komander, D., and Alessi, D.R. (2010). The nuts and bolts of AGC protein kinases. Nat Rev Mol Cell Biol *11*, 9-22.
106. Wayman, G.A., Tokumitsu, H., Davare, M.A., and Soderling, T.R. (2011). Analysis of CaM-kinase signaling in cells. Cell Calcium *50*, 1-8.
107. Eide, E.J., and Virshup, D.M. (2001). Casein kinase I: another cog in the circadian clockworks. Chronobiol Int *18*, 389-398.
108. Sundaram, M.V. (2006). RTK/Ras/MAPK signaling. WormBook, 1-19.
109. Barford, D. (1996). Molecular mechanisms of the protein serine/threonine phosphatases. Trends Biochem Sci *21*, 407-412.
110. Moeslein, F.M., Myers, M.P., and Landreth, G.E. (1999). The CLK family kinases, CLK1 and CLK2, phosphorylate and activate the tyrosine phosphatase, PTP-1B. J Biol Chem *274*, 26697-26704.
111. Muller-Taubenberger, A., Ishikawa-Ankerhold, H.C., Kastner, P.M., Burghardt, E., and Gerisch, G. (2009). The STE group kinase SepA controls cleavage furrow formation in Dictyostelium. Cell Motil Cytoskeleton *66*, 929-939.
112. Abdi, A.I., Carvalho, T.G., Wilkes, J.M., and Doerig, C. (2013). A secreted Plasmodium falciparum kinase reveals a signature motif for classification of tyrosine kinase-like kinases. Microbiology (Reading) *159*, 2533-2547.
113. Zhang, Z.Y. (2002). Protein tyrosine phosphatases: structure and function, substrate specificity, and inhibitor development. Annu Rev Pharmacol Toxicol *42*, 209-234.
114. Stern, D.F. (2005). Phosphoproteomics for oncology discovery and treatment. Expert Opin Ther Targets *9*, 851-860.
115. Liu, Y., and Chance, M.R. (2014). Integrating phosphoproteomics in systems biology. Comput Struct Biotechnol J *10*, 90-97.
116. Humphrey, S.J., James, D.E., and Mann, M. (2015). Protein Phosphorylation: A Major Switch Mechanism for Metabolic Regulation. Trends Endocrinol Metab *26*, 676-687.

117. Doody, K.M., Bourdeau, A., and Tremblay, M.L. (2009). T-cell protein tyrosine phosphatase is a key regulator in immune cell signaling: lessons from the knockout mouse model and implications in human disease. Immunol Rev *228*, 325-341.
118. He, R.J., Yu, Z.H., Zhang, R.Y., and Zhang, Z.Y. (2014). Protein tyrosine phosphatases as potential therapeutic targets. Acta Pharmacol Sin *35*, 1227-1246.
119. Julien, S.G., Dube, N., Hardy, S., and Tremblay, M.L. (2011). Inside the human cancer tyrosine phosphatome. Nat Rev Cancer *11*, 35-49.
120. Bialy, L., and Waldmann, H. (2005). Inhibitors of protein tyrosine phosphatases: next-generation drugs? Angew Chem Int Ed Engl *44*, 3814-3839.
121. Alonso, A., Sasin, J., Bottini, N., Friedberg, I., Friedberg, I., Osterman, A., Godzik, A., Hunter, T., Dixon, J., and Mustelin, T. (2004). Protein tyrosine phosphatases in the human genome. Cell *117*, 699-711.
122. Sun, H., and Tonks, N.K. (1994). The coordinated action of protein tyrosine phosphatases and kinases in cell signaling. Trends Biochem Sci *19*, 480-485.
123. Tonks, N.K., and Neel, B.G. (2001). Combinatorial control of the specificity of protein tyrosine phosphatases. Curr Opin Cell Biol *13*, 182-195.
124. Walton, K.M., and Dixon, J.E. (1993). Protein tyrosine phosphatases. Annu Rev Biochem *62*, 101-120.
125. Van Vactor, D., O'Reilly, A.M., and Neel, B.G. (1998). Genetic analysis of protein tyrosine phosphatases. Curr Opin Genet Dev *8*, 112-126.
126. Zhang, Z.Y. (1998). Protein-tyrosine phosphatases: biological function, structural characteristics, and mechanism of catalysis. Crit Rev Biochem Mol Biol *33*, 1-52.
127. Gentry, M.S., Dixon, J.E., and Worby, C.A. (2009). Lafora disease: insights into neurodegeneration from plant metabolism. Trends Biochem Sci *34*, 628-639.
128. Gentry, M.S., Dowen, R.H., 3rd, Worby, C.A., Mattoo, S., Ecker, J.R., and Dixon, J.E. (2007). The phosphatase laforin crosses evolutionary boundaries and links carbohydrate metabolism to neuronal disease. J Cell Biol *178*, 477-488.
129. Niittyla, T., Comparot-Moss, S., Lue, W.L., Messerli, G., Trevisan, M., Seymour, M.D., Gatehouse, J.A., Villadsen, D., Smith, S.M., Chen, J., et al. (2006). Similar protein phosphatases control starch metabolism in plants and glycogen metabolism in mammals. J Biol Chem *281*, 11815-11818.
130. Blanchetot, C., Tertoolen, L.G., Overvoorde, J., and den Hertog, J. (2002). Intra- and intermolecular interactions between intracellular domains of receptor protein-tyrosine phosphatases. J Biol Chem *277*, 47263-47269.
131. Jiang, G., den Hertog, J., and Hunter, T. (2000). Receptor-like protein tyrosine phosphatase alpha homodimerizes on the cell surface. Mol Cell Biol *20*, 5917-5929.
132. Pike, K.A., and Tremblay, M.L. (2018). Protein Tyrosine Phosphatases: Regulators of CD4 T Cells in Inflammatory Bowel Disease. Front Immunol *9*, 2504.
133. Blanchetot, C., and den Hertog, J. (2000). Multiple interactions between receptor protein-tyrosine phosphatase (RPTP) alpha and membrane-distal protein-tyrosine phosphatase domains of various RPTPs. J Biol Chem *275*, 12446-12452.
134. Lee, H.H., Lee, H.C., Chou, C.C., Hur, S.S., Osterday, K., del Alamo, J.C., Lasheras, J.C., and Chien, S. (2013). Shp2 plays a crucial role in cell structural orientation and force polarity in

response to matrix rigidity. Proceedings of the National Academy of Sciences of the United States of America *110*, 2840-2845.

135. Wang, J.F., Gong, K., Wei, D.Q., and Li, Y.X. (2009). Structural flexibility and interactions of PTP1B's S-loop. Interdiscip Sci *1*, 214-219.

136. Ostman, A., Hellberg, C., and Bohmer, F.D. (2006). Protein-tyrosine phosphatases and cancer. Nat Rev Cancer *6*, 307-320.

137. Barford, D., Flint, A.J., and Tonks, N.K. (1994). Crystal structure of human protein tyrosine phosphatase 1B. Science *263*, 1397-1404.

138. Byeon, H.J., Kim, J.Y., Ko, J., Lee, E.J., Don, K., and Yoon, J.S. (2020). Protein tyrosine phosphatase 1B as a therapeutic target for Graves' orbitopathy in an in vitro model. PLoS One *15*, e0237015.

139. Vieira, M.N., Lyra, E.S.N.M., Ferreira, S.T., and De Felice, F.G. (2017). Protein Tyrosine Phosphatase 1B (PTP1B): A Potential Target for Alzheimer's Therapy? Front Aging Neurosci *9*, 7.

140. Kumar, A., Rana, D., Rana, R., and Bhatia, R. (2020). Protein Tyrosine Phosphatase (PTP1B): A promising Drug Target Against Life-threatening Ailments. Curr Mol Pharmacol *13*, 17-30.

141. Yip, S.C., Saha, S., and Chernoff, J. (2010). PTP1B: a double agent in metabolism and oncogenesis. Trends Biochem Sci *35*, 442-449.

142. Taniguchi, C.M., Emanuelli, B., and Kahn, C.R. (2006). Critical nodes in signalling pathways: insights into insulin action. Nat Rev Mol Cell Biol *7*, 85-96.

143. Egawa, K., Maegawa, H., Shimizu, S., Morino, K., Nishio, Y., Bryer-Ash, M., Cheung, A.T., Kolls, J.K., Kikkawa, R., and Kashiwagi, A. (2001). Protein-tyrosine phosphatase-1B negatively regulates insulin signaling in l6 myocytes and Fao hepatoma cells. J Biol Chem *276*, 10207-10211.

144. Galic, S., Hauser, C., Kahn, B.B., Haj, F.G., Neel, B.G., Tonks, N.K., and Tiganis, T. (2005). Coordinated regulation of insulin signaling by the protein tyrosine phosphatases PTP1B and TCPTP. Mol Cell Biol *25*, 819-829.

145. Shi, K., Egawa, K., Maegawa, H., Nakamura, T., Ugi, S., Nishio, Y., and Kashiwagi, A. (2004). Protein-tyrosine phosphatase 1B associates with insulin receptor and negatively regulates insulin signaling without receptor internalization. J Biochem *136*, 89-96.

146. Klaman, L.D., Boss, O., Peroni, O.D., Kim, J.K., Martino, J.L., Zabolotny, J.M., Moghal, N., Lubkin, M., Kim, Y.B., Sharpe, A.H., et al. (2000). Increased energy expenditure, decreased adiposity, and tissue-specific insulin sensitivity in protein-tyrosine phosphatase 1B-deficient mice. Mol Cell Biol *20*, 5479-5489.

147. Rondinone, C.M., Trevillyan, J.M., Clampit, J., Gum, R.J., Berg, C., Kroeger, P., Frost, L., Zinker, B.A., Reilly, R., Ulrich, R., et al. (2002). Protein tyrosine phosphatase 1B reduction regulates adiposity and expression of genes involved in lipogenesis. Diabetes *51*, 2405-2411.

148. Goldstein, B.J., Bittner-Kowalczyk, A., White, M.F., and Harbeck, M. (2000). Tyrosine dephosphorylation and deactivation of insulin receptor substrate-1 by protein-tyrosine phosphatase 1B. Possible facilitation by the formation of a ternary complex with the Grb2 adaptor protein. J Biol Chem *275*, 4283-4289.

149. Fernandez-Ruiz, R., Vieira, E., Garcia-Roves, P.M., and Gomis, R. (2014). Protein tyrosine phosphatase-1B modulates pancreatic beta-cell mass. PLoS One *9*, e90344.

150. Witkamp, R.F. (2011). Current and future drug targets in weight management. Pharm Res *28*, 1792-1818.
151. Haynes, W.G., Morgan, D.A., Walsh, S.A., Mark, A.L., and Sivitz, W.I. (1997). Receptor-mediated regional sympathetic nerve activation by leptin. J Clin Invest *100*, 270-278.
152. Friedman, J.M., and Halaas, J.L. (1998). Leptin and the regulation of body weight in mammals. Nature *395*, 763-770.
153. Bence, K.K., Delibegovic, M., Xue, B., Gorgun, C.Z., Hotamisligil, G.S., Neel, B.G., and Kahn, B.B. (2006). Neuronal PTP1B regulates body weight, adiposity and leptin action. Nat Med *12*, 917-924.
154. Tsou, R.C., Rak, K.S., Zimmer, D.J., and Bence, K.K. (2014). Improved metabolic phenotype of hypothalamic PTP1B-deficiency is dependent upon the leptin receptor. Mol Metab *3*, 301-312.
155. Ali, M.I., Ketsawatsomkron, P., Belin de Chantemele, E.J., Mintz, J.D., Muta, K., Salet, C., Black, S.M., Tremblay, M.L., Fulton, D.J., Marrero, M.B., et al. (2009). Deletion of protein tyrosine phosphatase 1b improves peripheral insulin resistance and vascular function in obese, leptin-resistant mice via reduced oxidant tone. Circ Res *105*, 1013-1022.
156. Ginsberg, M.H. (2014). Integrin activation. BMB Rep *47*, 655-659.
157. Liang, F., Lee, S.Y., Liang, J., Lawrence, D.S., and Zhang, Z.Y. (2005). The role of protein-tyrosine phosphatase 1B in integrin signaling. J Biol Chem *280*, 24857-24863.
158. Liu, F., Sells, M.A., and Chernoff, J. (1998). Protein tyrosine phosphatase 1B negatively regulates integrin signaling. Curr Biol *8*, 173-176.
159. Olayioye, M.A., Neve, R.M., Lane, H.A., and Hynes, N.E. (2000). The ErbB signaling network: receptor heterodimerization in development and cancer. EMBO J *19*, 3159-3167.
160. Hynes, N.E., and MacDonald, G. (2009). ErbB receptors and signaling pathways in cancer. Curr Opin Cell Biol *21*, 177-184.
161. Wang, S.C., Nakajima, Y., Yu, Y.L., Xia, W., Chen, C.T., Yang, C.C., McIntush, E.W., Li, L.Y., Hawke, D.H., Kobayashi, R., et al. (2006). Tyrosine phosphorylation controls PCNA function through protein stability. Nat Cell Biol *8*, 1359-1368.
162. Hughes, S.K., Oudin, M.J., Tadros, J., Neil, J., Del Rosario, A., Joughin, B.A., Ritsma, L., Wyckoff, J., Vasile, E., Eddy, R., et al. (2015). PTP1B-dependent regulation of receptor tyrosine kinase signaling by the actin-binding protein Mena. Mol Biol Cell *26*, 3867-3878.
163. Abiko, Y., Kurosawa, K., Yamakawa, H., and Kumagai, Y. (2021). Activation of PTP1B/EGFR signaling and cytotoxicity during combined exposure to ambient electrophiles in A431 cells. J Toxicol Sci *46*, 177-185.
164. Jimeno, A., Kulesza, P., Kincaid, E., Bouaroud, N., Chan, A., Forastiere, A., Brahmer, J., Clark, D.P., and Hidalgo, M. (2006). C-fos assessment as a marker of anti-epidermal growth factor receptor effect. Cancer Res *66*, 2385-2390.
165. Kani, K., Garri, C., Tiemann, K., Malihi, P.D., Punj, V., Nguyen, A.L., Lee, J., Hughes, L.D., Alvarez, R.M., Wood, D.M., et al. (2017). JUN-Mediated Downregulation of EGFR Signaling Is Associated with Resistance to Gefitinib in EGFR-mutant NSCLC Cell Lines. Mol Cancer Ther *16*, 1645-1657.

166. Lo, H.W., Cao, X., Zhu, H., and Ali-Osman, F. (2010). Cyclooxygenase-2 is a novel transcriptional target of the nuclear EGFR-STAT3 and EGFRvIII-STAT3 signaling axes. Mol Cancer Res *8*, 232-245.

167. Pan, B.Q., Xie, Z.H., Hao, J.J., Zhang, Y., Xu, X., Cai, Y., and Wang, M.R. (2020). PTP1B up-regulates EGFR expression by dephosphorylating MYH9 at Y1408 to promote cell migration and invasion in esophageal squamous cell carcinoma. Biochem Biophys Res Commun *522*, 53-60.

168. Martinelli, E., Ciardiello, D., Martini, G., Troiani, T., Cardone, C., Vitiello, P.P., Normanno, N., Rachiglio, A.M., Maiello, E., Latiano, T., et al. (2020). Implementing anti-epidermal growth factor receptor (EGFR) therapy in metastatic colorectal cancer: challenges and future perspectives. Ann Oncol *31*, 30-40.

169. da Cunha Santos, G., Shepherd, F.A., and Tsao, M.S. (2011). EGFR mutations and lung cancer. Annu Rev Pathol *6*, 49-69.

170. Bollu, L.R., Mazumdar, A., Savage, M.I., and Brown, P.H. (2017). Molecular Pathways: Targeting Protein Tyrosine Phosphatases in Cancer. Clin Cancer Res *23*, 2136-2142.

171. Lessard, L., Stuible, M., and Tremblay, M.L. (2010). The two faces of PTP1B in cancer. Biochim Biophys Acta *1804*, 613-619.

172. Koren, S., and Fantus, I.G. (2007). Inhibition of the protein tyrosine phosphatase PTP1B: potential therapy for obesity, insulin resistance and type-2 diabetes mellitus. Best Pract Res Clin Endocrinol Metab *21*, 621-640.

173. Goldstein, B.J. (2001). Protein-tyrosine phosphatase 1B (PTP1B): a novel therapeutic target for type 2 diabetes mellitus, obesity and related states of insulin resistance. Curr Drug Targets Immune Endocr Metabol Disord *1*, 265-275.

174. Gonzalez-Rodriguez, A., Mas Gutierrez, J.A., Sanz-Gonzalez, S., Ros, M., Burks, D.J., and Valverde, A.M. (2010). Inhibition of PTP1B restores IRS1-mediated hepatic insulin signaling in IRS2-deficient mice. Diabetes *59*, 588-599.

175. Ji, W., Chen, X., Lv, J., Wang, M., Ren, S., Yuan, B., Wang, B., and Chen, L. (2014). Liraglutide Exerts Antidiabetic Effect via PTP1B and PI3K/Akt2 Signaling Pathway in Skeletal Muscle of KKAy Mice. Int J Endocrinol *2014*, 312452.

176. Lu, B., Gu, P., Xu, Y., Ye, X., Wang, Y., Du, H., and Shao, J. (2016). Overexpression of protein tyrosine phosphatase 1B impairs glucose-stimulated insulin secretion in INS-1 cells. Minerva Endocrinol *41*, 1-9.

177. Lu, B., Wu, H., Gu, P., Du, H., Shao, J., Wang, J., and Zou, D. (2012). Improved glucose-stimulated insulin secretion by intra-islet inhibition of protein-tyrosine phosphatase 1B expression in rats fed a high-fat diet. J Endocrinol Invest *35*, 63-70.

178. Lund, I.K., Hansen, J.A., Andersen, H.S., Moller, N.P., and Billestrup, N. (2005). Mechanism of protein tyrosine phosphatase 1B-mediated inhibition of leptin signalling. J Mol Endocrinol *34*, 339-351.

179. Liu, F., Hill, D.E., and Chernoff, J. (1996). Direct binding of the proline-rich region of protein tyrosine phosphatase 1B to the Src homology 3 domain of p130(Cas). J Biol Chem *271*, 31290-31295.

180. Sangwan, V., Paliouras, G.N., Cheng, A., Dube, N., Tremblay, M.L., and Park, M. (2006). Protein-tyrosine phosphatase 1B deficiency protects against Fas-induced hepatic failure. J Biol Chem *281*, 221-228.

181. Gonzalez-Rodriguez, A., Escribano, O., Alba, J., Rondinone, C.M., Benito, M., and Valverde, A.M. (2007). Levels of protein tyrosine phosphatase 1B determine susceptibility to apoptosis in serum-deprived hepatocytes. J Cell Physiol *212*, 76-88.

182. Gu, F., Nguyen, D.T., Stuible, M., Dube, N., Tremblay, M.L., and Chevet, E. (2004). Protein-tyrosine phosphatase 1B potentiates IRE1 signaling during endoplasmic reticulum stress. J Biol Chem *279*, 49689-49693.

183. Akasaki, Y., Liu, G., Matundan, H.H., Ng, H., Yuan, X., Zeng, Z., Black, K.L., and Yu, J.S. (2006). A peroxisome proliferator-activated receptor-gamma agonist, troglitazone, facilitates caspase-8 and -9 activities by increasing the enzymatic activity of protein-tyrosine phosphatase-1B on human glioma cells. J Biol Chem *281*, 6165-6174.

184. Balsamo, J., Arregui, C., Leung, T., and Lilien, J. (1998). The nonreceptor protein tyrosine phosphatase PTP1B binds to the cytoplasmic domain of N-cadherin and regulates the cadherin-actin linkage. J Cell Biol *143*, 523-532.

185. Balsamo, J., Leung, T., Ernst, H., Zanin, M.K., Hoffman, S., and Lilien, J. (1996). Regulated binding of PTP1B-like phosphatase to N-cadherin: control of cadherin-mediated adhesion by dephosphorylation of beta-catenin. J Cell Biol *134*, 801-813.

186. Hazan, R.B., Qiao, R., Keren, R., Badano, I., and Suyama, K. (2004). Cadherin switch in tumor progression. Ann N Y Acad Sci *1014*, 155-163.

187. Zhu, S., Bjorge, J.D., and Fujita, D.J. (2007). PTP1B contributes to the oncogenic properties of colon cancer cells through Src activation. Cancer Res *67*, 10129-10137.

188. Cortesio, C.L., Chan, K.T., Perrin, B.J., Burton, N.O., Zhang, S., Zhang, Z.Y., and Huttenlocher, A. (2008). Calpain 2 and PTP1B function in a novel pathway with Src to regulate invadopodia dynamics and breast cancer cell invasion. J Cell Biol *180*, 957-971.

189. Lu, X., Malumbres, R., Shields, B., Jiang, X., Sarosiek, K.A., Natkunam, Y., Tiganis, T., and Lossos, I.S. (2008). PTP1B is a negative regulator of interleukin 4-induced STAT6 signaling. Blood *112*, 4098-4108.

190. Julien, S.G., Dube, N., Read, M., Penney, J., Paquet, M., Han, Y., Kennedy, B.P., Muller, W.J., and Tremblay, M.L. (2007). Protein tyrosine phosphatase 1B deficiency or inhibition delays ErbB2-induced mammary tumorigenesis and protects from lung metastasis. Nat Genet *39*, 338-346.

191. Wiener, J.R., Kerns, B.J., Harvey, E.L., Conaway, M.R., Iglehart, J.D., Berchuck, A., and Bast, R.C., Jr. (1994). Overexpression of the protein tyrosine phosphatase PTP1B in human breast cancer: association with p185c-erbB-2 protein expression. J Natl Cancer Inst *86*, 372-378.

192. Wiener, J.R., Hurteau, J.A., Kerns, B.J., Whitaker, R.S., Conaway, M.R., Berchuck, A., and Bast, R.C., Jr. (1994). Overexpression of the tyrosine phosphatase PTP1B is associated with human ovarian carcinomas. Am J Obstet Gynecol *170*, 1177-1183.

193. Tang, Z., Li, C., Kang, B., Gao, G., Li, C., and Zhang, Z. (2017). GEPIA: a web server for cancer and normal gene expression profiling and interactive analyses. Nucleic Acids Res *45*, W98-W102.

194. Ricke, K.M., Cruz, S.A., Qin, Z., Farrokhi, K., Sharmin, F., Zhang, L., Zasloff, M.A., Stewart, A.F.R., and Chen, H.H. (2020). Neuronal Protein Tyrosine Phosphatase 1B Hastens Amyloid beta-Associated Alzheimer's Disease in Mice. J Neurosci *40*, 1581-1593.

195. Stewart, A.F.R., and Chen, H.H. (2020). Activation of tyrosine phosphatases in the progression of Alzheimer's disease. Neural Regen Res *15*, 2245-2246.

196. Monteleone, M.C., Gonzalez Wusener, A.E., Burdisso, J.E., Conde, C., Caceres, A., and Arregui, C.O. (2012). ER-bound protein tyrosine phosphatase PTP1B interacts with Src at the plasma membrane/substrate interface. PLoS One *7*, e38948.
197. Hald, A., and Lotharius, J. (2005). Oxidative stress and inflammation in Parkinson's disease: is there a causal link? Exp Neurol *193*, 279-290.
198. Kim, I., Xu, W., and Reed, J.C. (2008). Cell death and endoplasmic reticulum stress: disease relevance and therapeutic opportunities. Nat Rev Drug Discov *7*, 1013-1030.
199. Ryu, E.J., Harding, H.P., Angelastro, J.M., Vitolo, O.V., Ron, D., and Greene, L.A. (2002). Endoplasmic reticulum stress and the unfolded protein response in cellular models of Parkinson's disease. J Neurosci *22*, 10690-10698.
200. Feng, C.W., Chen, N.F., Chan, T.F., and Chen, W.F. (2020). Therapeutic Role of Protein Tyrosine Phosphatase 1B in Parkinson's Disease via Antineuroinflammation and Neuroprotection In Vitro and In Vivo. Parkinsons Dis *2020*, 8814236.
201. de Bruin, A.M., Demirel, O., Hooibrink, B., Brandts, C.H., and Nolte, M.A. (2013). Interferon-gamma impairs proliferation of hematopoietic stem cells in mice. Blood *121*, 3578-3585.
202. Seita, J., and Weissman, I.L. (2010). Hematopoietic stem cell: self-renewal versus differentiation. Wiley Interdiscip Rev Syst Biol Med *2*, 640-653.
203. Hawley, R.G., Ramezani, A., and Hawley, T.S. (2006). Hematopoietic stem cells. Methods Enzymol *419*, 149-179.
204. Townsend, M.H., Shrestha, G., Robison, R.A., and O'Neill, K.L. (2018). The expansion of targetable biomarkers for CAR T cell therapy. J Exp Clin Cancer Res *37*, 163.
205. LaMontagne, K.R., Jr., Hannon, G., and Tonks, N.K. (1998). Protein tyrosine phosphatase PTP1B suppresses p210 bcr-abl-induced transformation of rat-1 fibroblasts and promotes differentiation of K562 cells. Proceedings of the National Academy of Sciences of the United States of America *95*, 14094-14099.
206. Alvira, D., Naughton, R., Bhatt, L., Tedesco, S., Landry, W.D., and Cotter, T.G. (2011). Inhibition of protein-tyrosine phosphatase 1B (PTP1B) mediates ubiquitination and degradation of Bcr-Abl protein. J Biol Chem *286*, 32313-32323.
207. Furukawa, T., Sunamura, M., and Horii, A. (2006). Molecular mechanisms of pancreatic carcinogenesis. Cancer Sci *97*, 1-7.
208. Nishimura, T. (2008). Total number of genome alterations in sporadic gastrointestinal cancer inferred from pooled analyses in the literature. Tumour Biol *29*, 343-350.
209. Klupa, T., Malecki, M.T., Pezzolesi, M., Ji, L., Curtis, S., Langefeld, C.D., Rich, S.S., Warram, J.H., and Krolewski, A.S. (2000). Further evidence for a susceptibility locus for type 2 diabetes on chromosome 20q13.1-q13.2. Diabetes *49*, 2212-2216.
210. Shinde, R.N., Kumar, G.S., Eqbal, S., and Sobhia, M.E. (2018). Screening and identification of potential PTP1B allosteric inhibitors using in silico and in vitro approaches. PLoS One *13*, e0199020.
211. Ha, M.T., Shrestha, S., Tran, T.H., Kim, J.A., Woo, M.H., Choi, J.S., and Min, B.S. (2020). Inhibition of PTP1B by farnesylated 2-arylbenzofurans isolated from Morus alba root bark: unraveling the mechanism of inhibition based on in vitro and in silico studies. Arch Pharm Res *43*, 961-975.

212. Reddy, R.H., Kim, H., Cha, S., Lee, B., and Kim, Y.J. (2017). Structure-Based Virtual Screening of Protein Tyrosine Phosphatase Inhibitors: Significance, Challenges, and Solutions. J Microbiol Biotechnol *27*, 878-895.
213. Kamerlin, S.C., Rucker, R., and Boresch, S. (2006). A targeted molecular dynamics study of WPD loop movement in PTP1B. Biochem Biophys Res Commun *345*, 1161-1166.
214. Ravichandran, L.V., Chen, H., Li, Y., and Quon, M.J. (2001). Phosphorylation of PTP1B at Ser(50) by Akt impairs its ability to dephosphorylate the insulin receptor. Mol Endocrinol *15*, 1768-1780.
215. Songyang, Z., Shoelson, S.E., McGlade, J., Olivier, P., Pawson, T., Bustelo, X.R., Barbacid, M., Sabe, H., Hanafusa, H., Yi, T., et al. (1994). Specific motifs recognized by the SH2 domains of Csk, 3BP2, fps/fes, GRB-2, HCP, SHC, Syk, and Vav. Mol Cell Biol *14*, 2777-2785.
216. Cheatham, B., and Kahn, C.R. (1995). Insulin action and the insulin signaling network. Endocr Rev *16*, 117-142.
217. Bandyopadhyay, D., Kusari, A., Kenner, K.A., Liu, F., Chernoff, J., Gustafson, T.A., and Kusari, J. (1997). Protein-tyrosine phosphatase 1B complexes with the insulin receptor in vivo and is tyrosine-phosphorylated in the presence of insulin. J Biol Chem *272*, 1639-1645.
218. Dagnell, M., Pace, P.E., Cheng, Q., Frijhoff, J., Ostman, A., Arner, E.S.J., Hampton, M.B., and Winterbourn, C.C. (2017). Thioredoxin reductase 1 and NADPH directly protect protein tyrosine phosphatase 1B from inactivation during H2O2 exposure. J Biol Chem *292*, 14371-14380.
219. van Montfort, R.L., Congreve, M., Tisi, D., Carr, R., and Jhoti, H. (2003). Oxidation state of the active-site cysteine in protein tyrosine phosphatase 1B. Nature *423*, 773-777.
220. Tsai, H., and Chen, C.J.A.O.W.M.C. (2017). A New Perspective on Appetite Control: Protein Tyrosine Phosphatase 1b (Ptp1b) Inactivation by Oxidative Phytochemicals. *7*, 00197.
221. Dadke, S., and Chernoff, J. (2003). Protein-tyrosine phosphatase 1B mediates the effects of insulin on the actin cytoskeleton in immortalized fibroblasts. J Biol Chem *278*, 40607-40611.
222. Liu, F., and Chernoff, J. (1997). Protein tyrosine phosphatase 1B interacts with and is tyrosine phosphorylated by the epidermal growth factor receptor. Biochem J *327 (Pt 1)*, 139-145.
223. Flint, A.J., Gebbink, M.F., Franza, B.R., Jr., Hill, D.E., and Tonks, N.K. (1993). Multi-site phosphorylation of the protein tyrosine phosphatase, PTP1B: identification of cell cycle regulated and phorbol ester stimulated sites of phosphorylation. EMBO J *12*, 1937-1946.
224. Shifrin, V.I., Davis, R.J., and Neel, B.G. (1997). Phosphorylation of protein-tyrosine phosphatase PTP-1B on identical sites suggests activation of a common signaling pathway during mitosis and stress response in mammalian cells. J Biol Chem *272*, 2957-2962.
225. Dadke, S., Cotteret, S., Yip, S.C., Jaffer, Z.M., Haj, F., Ivanov, A., Rauscher, F., 3rd, Shuai, K., Ng, T., Neel, B.G., et al. (2007). Regulation of protein tyrosine phosphatase 1B by sumoylation. Nat Cell Biol *9*, 80-85.
226. Anderie, I., Schulz, I., and Schmid, A. (2007). Characterization of the C-terminal ER membrane anchor of PTP1B. Exp Cell Res *313*, 3189-3197.
227. Frangioni, J.V., Beahm, P.H., Shifrin, V., Jost, C.A., and Neel, B.G. (1992). The nontransmembrane tyrosine phosphatase PTP-1B localizes to the endoplasmic reticulum via its 35 amino acid C-terminal sequence. Cell *68*, 545-560.

228. Frangioni, J.V., Oda, A., Smith, M., Salzman, E.W., and Neel, B.G. (1993). Calpain-catalyzed cleavage and subcellular relocation of protein phosphotyrosine phosphatase 1B (PTP-1B) in human platelets. EMBO J *12*, 4843-4856.

229. Azam, M., Andrabi, S.S., Sahr, K.E., Kamath, L., Kuliopulos, A., and Chishti, A.H. (2001). Disruption of the mouse mu-calpain gene reveals an essential role in platelet function. Mol Cell Biol *21*, 2213-2220.

230. Kuchay, S.M., Kim, N., Grunz, E.A., Fay, W.P., and Chishti, A.H. (2007). Double knockouts reveal that protein tyrosine phosphatase 1B is a physiological target of calpain-1 in platelets. Mol Cell Biol *27*, 6038-6052.

231. Yang, J., Niu, T., Zhang, A., Mishra, A.K., Zhao, Z.J., and Zhou, G.W. (2001). Relation between the flexibility of the WPD loop and the activity of the catalytic domain of protein tyrosine phosphatase SHP-1. J Cell Biochem *84*, 47-55.

232. Reddy, M.V., Ghadiyaram, C., Panigrahi, S.K., Hosahalli, S., and Mangamoori, L.N. (2013). Diphenylether derivative as selective inhibitor of protein tyrosine phosphatase 1B (PTP1B) over t-cell protein tyrosine phosphatase (TCPTP) identified through virtual screening. Mini Rev Med Chem *13*, 1602-1606.

233. Jia, Z., Barford, D., Flint, A.J., and Tonks, N.K. (1995). Structural basis for phosphotyrosine peptide recognition by protein tyrosine phosphatase 1B. Science *268*, 1754-1758.

234. Yang, J., Cheng, Z., Niu, T., Liang, X., Zhao, Z.J., and Zhou, G.W. (2000). Structural basis for substrate specificity of protein-tyrosine phosphatase SHP-1. J Biol Chem *275*, 4066-4071.

235. Ren, L., Chen, X., Luechapanichkul, R., Selner, N.G., Meyer, T.M., Wavreille, A.S., Chan, R., Iorio, C., Zhou, X., Neel, B.G., et al. (2011). Substrate specificity of protein tyrosine phosphatases 1B, RPTPalpha, SHP-1, and SHP-2. Biochemistry *50*, 2339-2356.

236. Peti, W., and Page, R. (2015). Strategies to make protein serine/threonine (PP1, calcineurin) and tyrosine phosphatases (PTP1B) druggable: achieving specificity by targeting substrate and regulatory protein interaction sites. Bioorg Med Chem *23*, 2781-2785.

237. Sharma, B., Kaushik, N., Upadhyay, A., Tripathi, S., Singh, K., and Pandey, V.N. (2003). A positively charged side chain at position 154 on the beta8-alphaE loop of HIV-1 RT is required for stable ternary complex formation. Nucleic Acids Res *31*, 5167-5174.

238. Feng, Y., Hadjikyriacou, A., and Clarke, S.G. (2014). Substrate specificity of human protein arginine methyltransferase 7 (PRMT7): the importance of acidic residues in the double E loop. J Biol Chem *289*, 32604-32616.

239. Critton, D.A., Tautz, L., and Page, R. (2011). Visualizing active-site dynamics in single crystals of HePTP: opening of the WPD loop involves coordinated movement of the E loop. J Mol Biol *405*, 619-629.

240. Barr, A.J., Ugochukwu, E., Lee, W.H., King, O.N., Filippakopoulos, P., Alfano, I., Savitsky, P., Burgess-Brown, N.A., Muller, S., and Knapp, S. (2009). Large-scale structural analysis of the classical human protein tyrosine phosphatome. Cell *136*, 352-363.

241. Kurkcuoglu, Z., Bakan, A., Kocaman, D., Bahar, I., and Doruker, P. (2012). Coupling between catalytic loop motions and enzyme global dynamics. PLoS Comput Biol *8*, e1002705.

242. Keng, Y.F., Wu, L., and Zhang, Z.Y. (1999). Probing the function of the conserved tryptophan in the flexible loop of the Yersinia protein-tyrosine phosphatase. Eur J Biochem *259*, 809-814.

243. Hoff, R.H., Hengge, A.C., Wu, L., Keng, Y.F., and Zhang, Z.Y. (2000). Effects on general acid catalysis from mutations of the invariant tryptophan and arginine residues in the protein tyrosine phosphatase from Yersinia. Biochemistry *39*, 46-54.

244. Gruninger, R.J., Selinger, L.B., and Mosimann, S.C. (2008). Effect of ionic strength and oxidation on the P-loop conformation of the protein tyrosine phosphatase-like phytase, PhyAsr. FEBS J *275*, 3783-3792.

245. Zhang, Z.Y., and Dixon, J.E. (1993). Active site labeling of the Yersinia protein tyrosine phosphatase: the determination of the pKa of the active site cysteine and the function of the conserved histidine 402. Biochemistry *32*, 9340-9345.

246. Tonks, N.K. (2005). Redox redux: revisiting PTPs and the control of cell signaling. Cell *121*, 667-670.

247. Chen, Y.Y., Chu, H.M., Pan, K.T., Teng, C.H., Wang, D.L., Wang, A.H., Khoo, K.H., and Meng, T.C. (2008). Cysteine S-nitrosylation protects protein-tyrosine phosphatase 1B against oxidation-induced permanent inactivation. J Biol Chem *283*, 35265-35272.

248. Krishnan, N., Fu, C., Pappin, D.J., and Tonks, N.K. (2011). H2S-Induced sulfhydration of the phosphatase PTP1B and its role in the endoplasmic reticulum stress response. Sci Signal *4*, ra86.

249. Andersen, J.N., Mortensen, O.H., Peters, G.H., Drake, P.G., Iversen, L.F., Olsen, O.H., Jansen, P.G., Andersen, H.S., Tonks, N.K., and Moller, N.P. (2001). Structural and evolutionary relationships among protein tyrosine phosphatase domains. Mol Cell Biol *21*, 7117-7136.

250. Ananthaswamy, N., Rutledge, R., Sauna, Z.E., Ambudkar, S.V., Dine, E., Nelson, E., Xia, D., and Golin, J. (2010). The signaling interface of the yeast multidrug transporter Pdr5 adopts a cis conformation, and there are functional overlap and equivalence of the deviant and canonical Q-loop residues. Biochemistry *49*, 4440-4449.

251. Wei, R.R., and Richardson, J.P. (2001). Mutational changes of conserved residues in the Q-loop region of transcription factor Rho greatly reduce secondary site RNA-binding. J Mol Biol *314*, 1007-1015.

252. Zhao, Y., Wu, L., Noh, S.J., Guan, K.L., and Zhang, Z.Y. (1998). Altering the nucleophile specificity of a protein-tyrosine phosphatase-catalyzed reaction. Probing the function of the invariant glutamine residues. J Biol Chem *273*, 5484-5492.

253. Cool, D.E., Tonks, N.K., Charbonneau, H., Walsh, K.A., Fischer, E.H., and Krebs, E.G. (1989). cDNA isolated from a human T-cell library encodes a member of the protein-tyrosine-phosphatase family. Proceedings of the National Academy of Sciences of the United States of America *86*, 5257-5261.

254. Lorenzen, J.A., Dadabay, C.Y., and Fischer, E.H. (1995). COOH-terminal sequence motifs target the T cell protein tyrosine phosphatase to the ER and nucleus. J Cell Biol *131*, 631-643.

255. Tiganis, T. (2013). PTP1B and TCPTP--nonredundant phosphatases in insulin signaling and glucose homeostasis. FEBS J *280*, 445-458.

256. Tiganis, T., Bennett, A.M., Ravichandran, K.S., and Tonks, N.K. (1998). Epidermal growth factor receptor and the adaptor protein p52Shc are specific substrates of T-cell protein tyrosine phosphatase. Mol Cell Biol *18*, 1622-1634.

257. Walchli, S., Curchod, M.L., Gobert, R.P., Arkinstall, S., and Hooft van Huijsduijnen, R. (2000). Identification of tyrosine phosphatases that dephosphorylate the insulin receptor. A brute force approach based on "substrate-trapping" mutants. J Biol Chem *275*, 9792-9796.

258. Simoncic, P.D., Lee-Loy, A., Barber, D.L., Tremblay, M.L., and McGlade, C.J. (2002). The T cell protein tyrosine phosphatase is a negative regulator of janus family kinases 1 and 3. Curr Biol *12*, 446-453.
259. Galic, S., Klingler-Hoffmann, M., Fodero-Tavoletti, M.T., Puryer, M.A., Meng, T.C., Tonks, N.K., and Tiganis, T. (2003). Regulation of insulin receptor signaling by the protein tyrosine phosphatase TCPTP. Mol Cell Biol *23*, 2096-2108.
260. Stuible, M., Doody, K.M., and Tremblay, M.L. (2008). PTP1B and TC-PTP: regulators of transformation and tumorigenesis. Cancer Metastasis Rev *27*, 215-230.
261. Iversen, L.F., Moller, K.B., Pedersen, A.K., Peters, G.H., Petersen, A.S., Andersen, H.S., Branner, S., Mortensen, S.B., and Moller, N.P. (2002). Structure determination of T cell protein-tyrosine phosphatase. J Biol Chem *277*, 19982-19990.
262. Nian, Q., Berthelet, J., Parlato, M., Mechaly, A.E., Liu, R., Dupret, J.M., Cerf-Bensussan, N., Haouz, A., and Rodrigues Lima, F. (2021). Structural characterization of a pathogenic mutant of human protein tyrosine phosphatase PTPN2 (Cys216Gly) that causes very early onset autoimmune enteropathy. Protein Sci.
263. Yu, X., Sun, J.P., He, Y., Guo, X., Liu, S., Zhou, B., Hudmon, A., and Zhang, Z.Y. (2007). Structure, inhibitor, and regulatory mechanism of Lyp, a lymphoid-specific tyrosine phosphatase implicated in autoimmune diseases. Proceedings of the National Academy of Sciences of the United States of America *104*, 19767-19772.
264. Sun, J.P., Fedorov, A.A., Lee, S.Y., Guo, X.L., Shen, K., Lawrence, D.S., Almo, S.C., and Zhang, Z.Y. (2003). Crystal structure of PTP1B complexed with a potent and selective bidentate inhibitor. J Biol Chem *278*, 12406-12414.
265. Ruddraraju, K.V., and Zhang, Z.Y. (2017). Covalent inhibition of protein tyrosine phosphatases. Mol Biosyst *13*, 1257-1279.
266. Brandao, T.A., Hengge, A.C., and Johnson, S.J. (2010). Insights into the reaction of protein-tyrosine phosphatase 1B: crystal structures for transition state analogs of both catalytic steps. J Biol Chem *285*, 15874-15883.
267. Qian, S., Zhang, M., He, Y., Wang, W., and Liu, S. (2016). Recent advances in the development of protein tyrosine phosphatase 1B inhibitors for Type 2 diabetes. Future Med Chem *8*, 1239-1258.
268. Pannifer, A.D., Flint, A.J., Tonks, N.K., and Barford, D. (1998). Visualization of the cysteinyl-phosphate intermediate of a protein-tyrosine phosphatase by x-ray crystallography. J Biol Chem *273*, 10454-10462.
269. Zhang, Z.Y., Wang, Y., and Dixon, J.E. (1994). Dissecting the catalytic mechanism of protein-tyrosine phosphatases. Proceedings of the National Academy of Sciences of the United States of America *91*, 1624-1627.
270. Mei, W., Wang, K., Huang, J., and Zheng, X. (2016). Cell Transformation by PTP1B Truncated Mutants Found in Human Colon and Thyroid Tumors. PLoS One *11*, e0166538.
271. Liu, M., Wang, L., Sun, X., and Zhao, X. (2014). Investigating the impact of Asp181 point mutations on interactions between PTP1B and phosphotyrosine substrate. Sci Rep *4*, 5095.
272. Scapin, G., Patel, S., Patel, V., Kennedy, B., and Asante-Appiah, E. (2001). The structure of apo protein-tyrosine phosphatase 1B C215S mutant: more than just an S --> O change. Protein Sci *10*, 1596-1605.

273. Montalibet, J., Skorey, K., McKay, D., Scapin, G., Asante-Appiah, E., and Kennedy, B.P. (2006). Residues distant from the active site influence protein-tyrosine phosphatase 1B inhibitor binding. J Biol Chem *281*, 5258-5266.

274. Hjortness, M.K., Riccardi, L., Hongdusit, A., Zwart, P.H., Sankaran, B., De Vivo, M., and Fox, J.M. (2018). Evolutionarily Conserved Allosteric Communication in Protein Tyrosine Phosphatases. Biochemistry *57*, 6443-6451.

275. Fuster, J.J., and Walsh, K. (2018). Somatic Mutations and Clonal Hematopoiesis: Unexpected Potential New Drivers of Age-Related Cardiovascular Disease. Circ Res *122*, 523-532.

276. Zhang, Y., and Du, Y. (2018). The development of protein tyrosine phosphatase1B inhibitors defined by binding sites in crystalline complexes. Future Med Chem *10*, 2345-2367.

277. Liu, G. (2003). Protein tyrosine phosphatase 1B inhibition: opportunities and challenges. Curr Med Chem *10*, 1407-1421.

278. Wiesmann, C., Barr, K.J., Kung, J., Zhu, J., Erlanson, D.A., Shen, W., Fahr, B.J., Zhong, M., Taylor, L., Randal, M., et al. (2004). Allosteric inhibition of protein tyrosine phosphatase 1B. Nat Struct Mol Biol *11*, 730-737.

279. Krishnan, N., Konidaris, K.F., Gasser, G., and Tonks, N.K. (2018). A potent, selective, and orally bioavailable inhibitor of the protein-tyrosine phosphatase PTP1B improves insulin and leptin signaling in animal models. J Biol Chem *293*, 1517-1525.

280. Khan, S., Bjij, I., and Soliman, M.E.S. (2019). Selective Covalent Inhibition of "Allosteric Cys121" Distort the Binding of PTP1B Enzyme: A Novel Therapeutic Approach for Cancer Treatment. Cell Biochem Biophys *77*, 203-211.

281. Kumar, A.P., Nguyen, M.N., Verma, C., and Lukman, S. (2018). Structural analysis of protein tyrosine phosphatase 1B reveals potentially druggable allosteric binding sites. Proteins *86*, 301-321.

282. Asante-Appiah, E., Patel, S., Dufresne, C., Roy, P., Wang, Q., Patel, V., Friesen, R.W., Ramachandran, C., Becker, J.W., Leblanc, Y., et al. (2002). The structure of PTP-1B in complex with a peptide inhibitor reveals an alternative binding mode for bisphosphonates. Biochemistry *41*, 9043-9051.

283. Zhang, Z.Y., Maclean, D., McNamara, D.J., Sawyer, T.K., and Dixon, J.E. (1994). Protein tyrosine phosphatase substrate specificity: size and phosphotyrosine positioning requirements in peptide substrates. Biochemistry *33*, 2285-2290.

284. Zhang, Z.Y., Thieme-Sefler, A.M., Maclean, D., McNamara, D.J., Dobrusin, E.M., Sawyer, T.K., and Dixon, J.E. (1993). Substrate specificity of the protein tyrosine phosphatases. Proceedings of the National Academy of Sciences of the United States of America *90*, 4446-4450.

285. Bilwes, A.M., den Hertog, J., Hunter, T., and Noel, J.P. (1996). Structural basis for inhibition of receptor protein-tyrosine phosphatase-alpha by dimerization. Nature *382*, 555-559.

286. Crooke, S.T. (2017). Molecular Mechanisms of Antisense Oligonucleotides. Nucleic Acid Ther *27*, 70-77.

287. Zinker, B.A., Rondinone, C.M., Trevillyan, J.M., Gum, R.J., Clampit, J.E., Waring, J.F., Xie, N., Wilcox, D., Jacobson, P., Frost, L., et al. (2002). PTP1B antisense oligonucleotide lowers PTP1B protein, normalizes blood glucose, and improves insulin sensitivity in diabetic mice. Proceedings of the National Academy of Sciences of the United States of America *99*, 11357-11362.

288. Monia, B.P., Lesnik, E.A., Gonzalez, C., Lima, W.F., McGee, D., Guinosso, C.J., Kawasaki, A.M., Cook, P.D., and Freier, S.M. (1993). Evaluation of 2'-modified oligonucleotides containing 2'-deoxy gaps as antisense inhibitors of gene expression. J Biol Chem *268*, 14514-14522.

289. Digenio, A., Pham, N.C., Watts, L.M., Morgan, E.S., Jung, S.W., Baker, B.F., Geary, R.S., and Bhanot, S. (2018). Antisense Inhibition of Protein Tyrosine Phosphatase 1B With IONIS-PTP-1BRx Improves Insulin Sensitivity and Reduces Weight in Overweight Patients With Type 2 Diabetes. Diabetes Care *41*, 807-814.

290. Koizumi, M., Takagi-Sato, M., Okuyama, R., Araki, K., Sun, W., and Nakai, D. (2007). In vivo antisense activity of ENA oligonucleotides targeting PTP1B mRNA in comparison of that of 2'-MOE-modified oligonucleotides. Nucleic Acids Symp Ser (Oxf), 111-112.

291. LaRochelle, J.R., Fodor, M., Xu, X., Durzynska, I., Fan, L., Stams, T., Chan, H.M., LaMarche, M.J., Chopra, R., Wang, P., et al. (2016). Structural and Functional Consequences of Three Cancer-Associated Mutations of the Oncogenic Phosphatase SHP2. Biochemistry *55*, 2269-2277.

6. PUBLICATIONS

Free Radical Biology and Medicine 162 (2021) 27–37

Contents lists available at ScienceDirect

Free Radical Biology and Medicine

journal homepage: www.elsevier.com/locate/freeradbiomed

Human CREBBP acetyltransferase is impaired by etoposide quinone, an oxidative and leukemogenic metabolite of the anticancer drug etoposide through modification of redox-sensitive zinc-finger cysteine residues

Wenchao Zhang [a], Jérémy Berthelet [a,b], Christina Michail [a], Linh-Chi Bui [a], Panhong Gou [c], Rongxing Liu [a], Romain Duval [d], Justine Renault [a], Jean-Marie Dupret [a], Fabien Guidez [c], Christine Chomienne [c,e], Fernando Rodrigues Lima [a,*]

[a] Université de Paris, BFA, UMR 8251, CNRS, F-75013, Paris, France
[b] Université de Paris, CEDC, UMR 7216, CNRS, F-75013, Paris, France
[c] Université de Paris, Institut de Recherche Saint-Louis, UMRS 1131, INSERM, F-75010, Paris, France
[d] Université de Paris, BIGR, UMRS 1134, INSERM, F-75015, Paris, France
[e] Service de Biologie Cellulaire, Assistance Publique des Hôpitaux de Paris (AP-HP), Hôpital Saint Louis, Paris, France

ARTICLE INFO

Keywords:
CREBBP
Quinone
Oxidative metabolite
Inhibition
Zinc-finger cysteines
Histone acetylation

ABSTRACT

Etoposide is an extensively prescribed anticancer drug that, unfortunately, causes therapy-related leukemia. The mechanisms by which etoposide induces secondary hematopoietic malignancies are poorly documented. However, etoposide-related leukemogenesis is known to depend on oxidative metabolites of etoposide, notably etoposide quinone, that can react with protein cysteine residues such as in topoisomerases II. CREBBP is a major histone acetyltransferase that functions mainly as a transcriptional co-activator. This epigenetic enzyme is considered as a tumor suppressor that plays a major role in hematopoiesis. Genetic alterations affecting CREBBP activity are highly common in hematopoietic malignancies. We report here that CREBBP is impaired by etoposide quinone. Molecular and kinetic analyses show that this inhibition occurs through the rapid and covalent (k_{inhib} = 16.10^2 $M^{-1}.s^{-1}$) adduction of etoposide quinone with redox sensitive cysteine residues within the RING and PHD Zn^{2+}-fingers of CREBBP catalytic core leading to subsequent release of Zn^{2+}. In agreement with these findings, experiments conducted in cells and in mice treated with etoposide showed irreversible inhibition of endogenous CREBBP activity and decreased H3K18 and H3K27 acetylation. As shown for topoisomerases II, our work thus suggests that the leukemogenic metabolite etoposide quinone can impair the epigenetic CREBBP acetyltransferase through reaction with redox sensitive cysteine residues.

1. Introduction

Lysine acetyltransferase (KAT) enzymes acetylate histone and non-histone proteins through the transfer of an acetyl group from acetyl-coenzyme A (AcCoA) to specific lysine residues [1,2]. CREB binding protein (CREBBP, also known as CBP or KAT3A) is a major mammalian KAT enzyme that functions as a transcriptional co-activator notably through acetylation of histones (in particular H3K18 and H3K27) and transcription factors (such as p53) [3–5]. CREBBP is a tumor suppressor that is important in normal development. Germline loss-of-function mutations in *CREBBP* cause Rubinstein-Taybi syndrome, a developmental disorder that includes predisposition for leukemia [6]. CREBBP is a critical regulator of normal hematopoiesis and alteration of the acetyltransferase activity of the enzyme contributes to lymphomagenesis and leukemogenesis [7–11]. Moreover, loss of function mutations in *CREBBP* are indeed common in lymphoma and leukemia and are associated with aberrant acetylation of histone H3 (and non-histone proteins [9,10,12–14]. Multiple chromosomal translocations associated with hematological malignancies involve the KAT domain of CREBBP resulting in fusion proteins that contribute to leukemogenesis through abnormal histone acetylation [7,15,16]. The crucial role of CREBBP in normal and malignant hematopoiesis is further underlined

Abbreviations: CREBBP, CREB Binding Protein; KAT, lysine acetyltransferase; NBT, nitroblue tetrazolium; IAF, iodoacetamide-fluorescein.

* Corresponding author.
E-mail address: fernando.rodrigues-lima@u-paris.fr (F.R. Lima).

https://doi.org/10.1016/j.freeradbiomed.2020.11.027
Received 20 October 2020; Received in revised form 22 November 2020; Accepted 23 November 2020
Available online 2 December 2020
0891-5849/© 2020 Elsevier Inc. All rights reserved.

by different mouse models that show that lack of functional CREBBP leads to serious hematological defects [17–19].

Etoposide is a semi-synthetic podophyllotoxin derivative widely used for the treatment of many types of cancer. This chemotherapeutic drug acts as a topoisomerase II poison that inhibits the enzyme's ability to ligate DNA, resulting in an accumulation of double-strand breaks and subsequent apoptosis [20]. Although etoposide is commonly prescribed as a front-line treatment of a variety of human malignancies, this chemotherapeutic drug is also known to cause secondary leukemia [21–23]. However, the molecular basis underlying etoposide-induced leukemogenesis is not well-defined. In humans, etoposide is readily metabolized by CYP3A4 into etoposide catechol which is further oxidized by cellular oxidases/peroxidases into the reactive metabolite etoposide quinone [24–26]. Several studies have implicated oxidative etoposide metabolites, in particular etoposide quinone, as the primary contributors to the leukemogenic process [27–31]. Notably, etoposide quinone has been shown to react with redox sensitive cysteine residues of topoisomerase II enzymes [28–30]. In addition, efficacy of etoposide quinone against type II topoisomerases was found to be considerably higher than that of etoposide thus emphasizing the key role of this oxidative metabolite in the biological effects of etoposide and putting forward impairment of topoisomerase II functions by etoposide quinone as a major mechanism in etoposide-induced leukemia [28–30]. Nevertheless, reaction of etoposide quinone with additional cellular proteins besides topoisomerase II inhibition have been suggested [32–36]. In particular, recent studies indicate that exposure to etoposide may have epigenetic effects unrelated to topoisomerases II [37–40]. In line with these observations, we report herein molecular and kinetic evidence showing that the histone acetyltransferase CREBBP is irreversibly impaired by etoposide quinone, the major oxidative metabolite of etoposide. We found that this inhibition occurs through the rapid adduction by etoposide quinone of redox-sensitive cysteine residues located in the PHD/RING Zn^{2+}-fingers of CREBBP and known to be crucial for its acetyltransferase activity [41–43]. Experiments in hematopoietic cells and in mice further confirm that exposure to etoposide irreversibly impairs CREBBP acetyltransferase activity with concomitant decrease in cellular histone H3 acetylation. Overall, our data indicate that, in addition to the alteration of topoisomerase II functions, etoposide quinone can impair CREBBP acetyltransferase by reacting with key cysteine residues within the catalytic core of the enzyme. Inhibition of a key epigenetic enzyme such as CREBBP by etoposide quinone may be an additional mechanism contributing to etoposide-dependent leukemogenesis.

2. Materials and methods

2.1. Chemicals and reagents

Etoposide and etoposide quinone were from Toronto Research Chemicals (Canada). Recombinant human H3.1 histone was from Actif Motif (Belgium). Antibodies used in this paper are: H3K18Ac (9675S, Cell Signaling), H3K27Ac (ab4729, Abcam, UK), H3 (3638S, Cell Signaling, France), CREBBP (A22, Santa Cruz, Germany), 6xHis (H1029, Sigma-Aldrich, France), secondary anti-rabbit (A1949, Sigma-Aldrich, France) and secondary anti-mouse (31430, ThermoFisher, France). All other chemicals, reagents and cells were from Sigma-Aldrich (France) otherwise noted.

2.2. Protein expression and purification

cDNA sequences from human CREBBP encoding residues 1096–1751 (CREBBP catalytic core), 1205–1279 (CREBBP RING domain) and 1280–1321 (CREBBP PHD domain) were cloned into pET28a expression vector and transformed into competent *E.coli* C41 (DE3). Bacteria were grown in Luria-Broth (LB) medium containing 30 μg/ml kanamycin and 20 μg/ml chloramphenicol. Recombinant protein expressions were induced by 0.5 mM of IPTG and the cultures were shaken overnight at 16 °C. Bacteria pellets were resuspended in buffer A (20 mM Tris-HCl, 300 mM NaCl, 1% Triton X-100, 0.2 mM β-mercaptoethanol (β-ME), 1 mg/ml lysozyme, protease inhibitors, pH 8.0) and lysed for 30 min at 4 °C under agitation. The lysate was then sonicated for 10 min (10 s ON, 20 s OFF, 20% power) and the soluble fraction was clarified by centrifugation (15000 g, 4 °C, 30 min). The supernatant was incubated with His-Select Nickel Affinity Gel beads for 2 h on ice under agitation in presence of 10 mM imidazole. The proteins were eluted with buffer B (20 mM Tris-HCl, 300 mM NaCl, pH 8.0) containing 300 mM imidazole and buffer exchanged with a desalting column (PD-10) to buffer C (Tris-HCl 20 mM, NaCl 150 mM, 10% glycerol pH 8.0). Protein purity was assessed by SDS PAGE followed by Coomassie staining. Proteins were stored at −80 °C.

2.3. CREBBP acetyltransferase activity assay

CREBBP acetyltransferase activity was assayed as previously described [44]. CREBBP catalytic core was incubated with 100 μM AcCoA, 30 μM H3K18 or H3K27 peptide, 1 mM DTT in 100 μl of assay buffer (25 mM Tris-HCl pH 8.0) for 20 min at room temperature. The reaction was stopped with 100 μl of $HClO_4$ (15% v/v in water) and 20 μl aliquots of the mixture were injected in a reverse phase ultra-fast liquid chromatography system (RP-UFLC, Shimadzu, France). Peptides were separated under isocratic conditions (80% acetonitrile, 20% water, 0.12% TFA, flow rate of 0.6 ml/min) on a Shim-pack XR-ODS column at 40 °C. H3K18 and H3K27 substrate peptides and their acetylated product were detected by fluorescence (excitation: 485 nm, emission: 530 nm) and quantified by integration of the peak fluorescence areas.

2.4. Effects of etoposide quinone on CREBBP acetyltransferase activity

CREBBP catalytic core (500 nM) was incubated for 10 min at room temperature in the presence of different concentrations (0, 5, 10, 20, 40 μM) of etoposide quinone (EQ) or the parent drug (ET) in 20 μl assay buffer. Then, 80 μl of assay buffer (100 μM AcCoA, 30 μM H3K18 or H3K27 peptide, final concentrations) were added to the treated enzyme mixture and CREBBP acetyltransferase activity was assayed for 20 min at room temperature as described above.

2.5. Effects of reducing agents and buffer exchange on etoposide quinone-inhibited CREBBP

CREBBP catalytic core (500 nM) was first incubated with etoposide quinone (40 μM) or etoposide (ET) for 10 min at room temperature. Samples were either buffer exchanged using a desalting column (PD SpinTrap G-25, GE Healthcare, France) to remove free etoposide quinone in solution or further incubated with 10 mM DTT. Protein concentration was assessed after buffer exchange using Bradford assay (Bio-Rad, France). Residual acetyltransferase activity of CREBBP was assayed as described above.

2.6. Kinetic analysis of CREBBP inhibition by etoposide quinone

CREBBP catalytic core (500 nM) was incubated in the presence of different concentrations of etoposide quinone (0, 1, 2.5, 5, 7.5, 10 μM) in assay buffer. Every 30 s, an aliquot of the solution was taken and diluted 10 times in assay buffer to stop the reaction. Residual activity of CREBBP was then measured by UFLC as described above. The data were analyzed as described previously for irreversible inhibitors under pseudo first order conditions using Prism Graphpad and Excel softwares [45]. The rate of inhibition of CREBBP by etoposide quinone can be described as follows:

Ln (% residual CREBBP activity) = $-k_{obs}$ x t, where k_{obs} is apparent first-order inhibition rate constant, and t is time). For each etoposide concentration, the k_{obs} values can be extracted from the slopes of the

natural logarithm of the percentage of CREBBP activity as a function of time. The second order rate constant (k_{inhib}) was obtained from the slope of k_{obs} values plotted as a function of etoposide concentration ($k_{inhib} = k_{obs}$/[etoposide quinone]).

2.7. Fluorescein-conjugated iodoacetamide (IAF) labeling and nitro blue tetrazolium (NBT) staining

CREBBP catalytic core (10 μg), CREBBP RING (10 μg) or CREBBP PHD (10 μg) domains were incubated in the presence of increasing concentrations (0, 5, 10, 20, 40 μM) of etoposide quinone for 10 min at room temperature in assay buffer. For IAF labelling of free CREBBP protein cysteines, aliquots were incubated in the presence of 50 μM fluorescein-conjugated iodoacetamide (IAF) for 10 min at 37 °C. The labelling reaction was stopped by the addition of 10 μl sample buffer containing 200 mM β-mercaptoethanol prior to SDS-PAGE and transfer onto a nitrocellulose membrane. IAF fluorescence was detected using a Fujifilm LAS 4000 detection system ($\lambda_{exc} = 485$ nm, $\lambda_{em} = 530$ nm). For detection of etoposide quinone adducts on CREBBP proteins, NBT staining was carried out as reported by Ref. [46]. Briefly, aliquots of proteins were first separated by SDS-PAGE and transferred onto a nitrocellulose membrane prior to incubation with 2 M potassium glycinate, 0.6 mg/ml NBT, pH 10.0 at room temperature for 30 min in the dark.

2.8. Zn^{2+} release analysis

CREBBP RING (5 μM) or CREBBP PHD (5 μM) domains were incubated in the presence or absence of etoposide quinone (40 μM) in assay buffer containing 100 μM 4-(2-pyridylazo) resorcinol (PAR). PAR reacts with free Zn^{2+} in solution according to the scheme:

$$2PAR + Zn^{2+} \rightarrow PAR(2)\text{-}Zn^{2+}$$

The PAR(2)-Zn^{2+} complex has an absorption peak around 490 nm. The reaction was initiated by addition of etoposide quinone and monitored by reading the absorbance of the solution at 490 nm using a microplate reader (Biotek Instruments, France).

2.9. Mass spectrometry analysis

CREBBP catalytic core (10 μM) was incubated with 40 μM EQ for 20 min at room temperature in assay buffer. The reaction was stopped with 10 mM DTT and diluted 20 times in assay buffer. Samples were then incubated overnight at 37 °C with trypsin (Promega, France) at 12.5 ng/μl in 25 mM ammonium bicarbonate pH 8.0. The supernatant containing peptides was acidified with formic acid (FA), desalted on C18 tips (Pierce C18 tips, Thermo Scientific, France), and eluted in 10 μl 70% ACN, 0.1% FA. Desalted samples were evaporated using a SpeedVac then taken up in 10 μl of buffer A (water, 0.1% FA) and 5 μl were injected on a nanoLC HPLC system (Thermo Scientific, France) coupled to a hybrid quadrupole-Orbitrap mass spectrometer (Thermo Scientific, France). Peptides were loaded on a reverse phase C18 μ-precolumn (C18 PepMap100, 5 μm, 100A, 300 μm i.d.x5 mm) and separated on a C18 column (EASY-spray C18 column, 75 μm i.d.x50 cm) at a constant flow rate of 300 nl/min, with a 120 min gradient of 2–40% buffer B (buffer B: 20% water, 80% ACN, 0.1% FA). MS analyses were performed by the Orbitrap cell with a resolution of 120.000 (at m/z 200). MS/MS fragments were obtained by HCD activation (collisional energy of 28%) and acquired in the ion trap in top-speed mode with a total cycle of 3 s. The database search was performed against the Swissprot database and the *Homo sapiens* taxonomy with Mascot v2.5.1 software with the following parameters: tryptic peptides only with up to 2 missed cleavages, variable modifications: cysteine etoposide quinone and methionine oxidation. MS and MS/MS error tolerances were set respectively to 7 ppm and 0.5 Da. Peptide identifications were validated using a 1% False Discovery Rate (FDR) threshold obtained by Proteome Discoverer (version 2.2, Thermo Scientific, France) and the percolator algorithm. The candidate sequences modified by etoposide quinone were manually inspected for *de novo* sequencing.

2.10. Bioactivation of etoposide into etoposide quinone by a myeloperoxidase (MPO)/H_2O_2 system

Etoposide was bioactivated into etoposide quinone *in vitro* using a myeloperoxidase/H_2O_2 system as described previously [31]. Briefly, etoposide (100 μM), H_2O_2 (200 μM) and myeloperoxidase (MPO) (5 units/ml) were co-incubated in 1 ml of 100 mM sodium acetate (pH 6.5) for 30 min at 37 °C. Etoposide quinone formation was detected by spectrophotometry (UV–1650PC, Shimadzu, France). Inactive MPO (heated for 30 min at 95 °C) was used as a negative control. 20 μl of bioactivated etoposide were mixed with 30 μl CREBBP (0.5 μM final) in assay buffer and incubated 20 min at room temperature. Then, 50 μl of assay buffer containing 30 μM H3K18 peptide, 100 μM AcCoA and 1 mM DTT (final concentrations) were added to the solution and CREBBP activity was assessed by UFLC as described above.

2.11. Detection of H3 acetylation by dot blot

CREBBP (500 nM) was first incubated with etoposide quinone or etoposide (40 μM) in 20 μl assay buffer for 10 min at room temperature. Then, 80 μl of assay mix (100 μM AcCoA, 300 ng recombinant human H3) were added and further incubated for 20 min at room temperature. Samples (corresponding to 200 and 100 ng H3) were dot-blotted using a Dot-Blot apparatus (Bio-Rad, France) onto nitrocellulose membranes (0.1 μm). Detection of H3K18 and H3K27 acetylation was carried out by western blotting using specific antibodies. The membranes were then stripped and reprobed with anti-H3 antibody.

2.12. Western blot

Samples were separated by SDS-PAGE prior to transfer onto a nitrocellulose membrane (0.45 μm, GE Healthcare, France) for 2 h 30 min at 4 °C. Membranes were blocked in 5% non-fat milk in PBS 0.05% Tween-20 (PBST) for 2 h and incubated overnight with primary antibody in 1% non-fat milk PBST at 4 °C. The next day, membranes were washed 5 times with PBST and incubated with secondary antibody for 2 h at room temperature. Membranes were then washed 5 more times and the signal was detected by chemiluminescence using ECL Prime on an Amersham Imager 600 detection system (GE Healthcare, France).

2.13. Cellular culture and treatment with etoposide

K562 cells were cultured in RPMI 1640 medium supplemented with 10% fetal bovine serum (FBS) and 1 mM L-glutamine at 37 °C, 5% CO_2. K562 cells (10.10^6 cells) were washed 3 times with RPMI 1640 medium and then treated with 40 μM etoposide in RPMI 1640 medium containing 1 mM L-glutamine for 24 h at 37 °C, 5% CO_2. Cells were then washed with PBS before use.

2.14. Acid extraction of histones

K562 cells in 100 mm petri dishes or bone marrow from mice hind limb long bones were lysed for 30 min at 4 °C with 400 μl lysis buffer (PBS pH 7.5, 0.5% Triton X-100, 3.3 μM trichostatin A (TSA) and protease inhibitors) and then centrifuged (15000 g) for 10 min at 4 °C. The pellet (nucleus enriched fraction) was incubated overnight at 4 °C in 400 μl 0.2 M HCl. The next day, the acid extract was centrifuged (10 min at 6500 g, 4 °C) and the supernatant (histone enriched fraction) was taken. Protein concentration was determined using Bradford reagent (Bio-Rad, France). 10 μg of histone extract were separated by SDS-PAGE (18%), transferred onto a nitrocellulose membrane and detected by

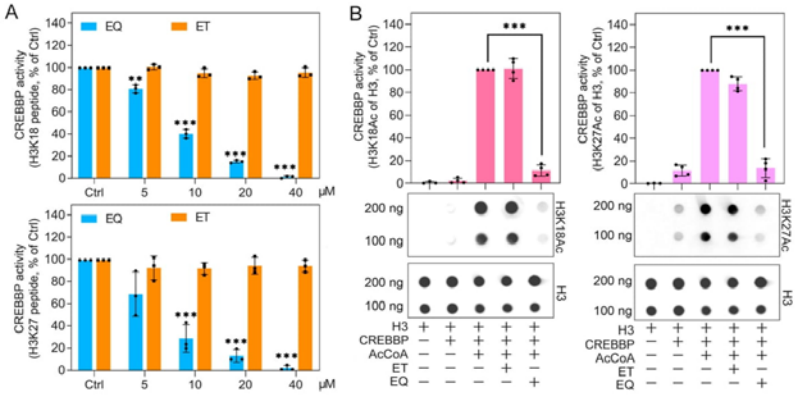

Fig. 1. Etoposide quinone inhibits CREBBP acetyltransferase activity
(A) Purified CREBBP catalytic core (aa 1096–1700) was incubated with increasing concentrations of etoposide quinone (EQ), etoposide (ET) or vehicle (Ctrl) for 20 min at room temperature. Residual CREBBP acetyltransferase activity was then measured by UFLC using H3K18 and H3K27 fluorescent peptides. Results are means of three independent experiments. Error bars indicate S.D. values. $^{**}p < 0.05$ or $^{***}p < 0.001$ compared with control (Ctrl).
(B) CREBBP catalytic core was first pre-incubated with 40 μM etoposide quinone (EQ) or etoposide (ET) for 20 min at room temperature prior to further incubation with recombinant histone H3 and acetyl-Coenzyme A (AcCoA) for another 20 min at room temperature. Samples were dot-blotted and H3K18 (left panel) and H3K27 (right panel) acetylation was detected using specific antibodies. Dot-blots were quantified using ImageJ software. Results are means of three independent experiments. Error bars indicate S.D. values. $^{***}p < 0.001$ compared with control (no EQ or ET).

western-blot using H3K18Ac, H3K27Ac or H3 antibodies. Grayscale quantitative analysis of Western blots was performed using ImageJ software.

2.15. Immunoprecipitation of endogenous CREBBP

K562 cells (10.10^6 cells) or mice bone marrow from hind limb long bones were lysed with lysis buffer (PBS pH 7.5, 1% Triton X-100, 3.3 μM trichostatin A, 100 μM DTT and protease inhibitors) for 30 min on ice and then centrifuged for 15 min (15000 g) at 4 °C. The supernatant was taken and the concentration of proteins in the extracts was determined by the Bradford reagent (Bio Rad, France). CREBBP was immunoprecipitated from 2.5 mg total protein extracts by an overnight incubation (under rocking conditions) with 1 μg of anti-CREBBP antibody (Santa Cruz, Germany) at 4 °C. The following day, samples were rocked for 2 h at 4 °C with 25 μl protein A agarose beads (Santa Cruz, Germany). The beads were washed 3 times with assay buffer and then incubated at room temperature with 60 μl of assay buffer containing 30 μM H3K18 fluorescent peptide, 100 μM AcCoA and 1 mM DTT. After 1 h of incubation, beads were sedimented by centrifugation and 50 μl of the supernatant were taken and mixed with 50 μl of $HClO_4$ (15% v/v in water) to determine CREBBP activity by UFLC. Beads were then washed with PBS and incubated with sample buffer containing 200 mM β-ME for 5 min at 100 °C prior to SDS-PAGE and Western-blot analysis. Grayscale quantitative analysis of Western blots was performed using ImageJ software.

2.16. Treatment of mice with etoposide

C57BL/6 mice (12 weeks old female) were obtained from Janvier (Le Genest, France) and bred in pathogen-free conditions in the animal facility of the Institut de Recherche Saint-Louis IRSL (Hôpital Saint-Louis, Université de Paris). Mice (n = 6) were treated overnight by intraperitoneal injection of 100 mg/kg etoposide in DMSO. Controls (n = 6) were carried out with vehicle only. The following day, the hind limb long bones were taken and washed 3 times with cold PBS. Bone marrow was flushed from the bones with PBS and the bone marrow cells (5.10^7 cells/mice) were lysed with lysis buffer (PBS pH 7.5, 1% Triton X-100, 3.3 μM TSA, 1 mM DTT and protease inhibitors) for 30 min on ice under agitation. The supernatant was then used for immunoprecipitation of CREBBP and the pellet for histone extraction as described above. ChIP qPCR experiments were carried out as described below. All the animal procedures performed were approved by the local Committee on the use and care of Animal.

2.17. Chromatin immunoprecipitation (ChIP)

K562 cells (10.10^6 cells) or bone marrow cells (5.10^7 cells/mice) were fixed with 1% formaldehyde for 10 min at 37 °C. The reaction was stopped with the addition of 0.125 M glycine for 5 min at room temperature. Cells were then proceeded for ChIP using ChIP-IT® Express Chromatin Immunoprecipitation Kit (Active Motif, USA) according to manufacturer instructions. Anti-H3K18Ac, anti-H3K27Ac, and anti-H3 were used. Rabbit IgG were used as a control. Immunocomplexes were isolated with protein-A-agarose beads (Santa Cruz, Germany). DNA was isolated by phenol/chloroform extraction followed by ethanol precipitation. The primers used for qPCR were:

Human IL6_F: CAGCAGCCAACCTCCTCTAA
Human IL6_R: CTGTGAGCGGCTGTTGTAGA
Human MDM2_F: CGGAAAGATGGAGCAAGAAG
Human MDM2_R: CCCTCAAGACTCCCCAGTTT
Mouse MDM2_F: AGATCTGACGCCCTCTTCTG
Mouse MDM2_R: GCAGCTTCAGTCCCGATTTA
Mouse COPS2_F: CATCGCACATGAAATCATCC
Mouse COPS2_R: CACAAACTGTCGCTCAGGAA

2.18. Statistical analysis

Values are presented as mean ± standard deviation (SD) and analyzed by either *t*-test or one-way analysis of variance (ANOVA) using

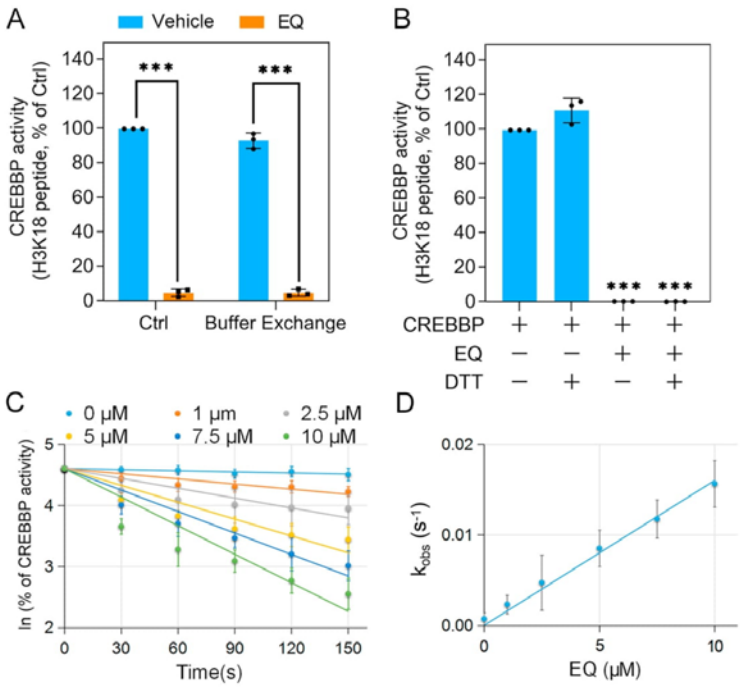

Fig. 2. Inhibition of CREBBP acetyltransferase activity by etoposide quinone is irreversible and fast
(A) CREBBP catalytic core was incubated with 40 μM etoposide quinone (EQ) or vehicle (Ctrl) for 20 min at room temperature. Samples were then buffer exchanged using PD-10 columns and CREBBP residual activity assayed by UFLC using H3K18 fluorescent peptide. Results are means of three independent experiments. Error bars indicate S.D. values. ***$p < 0.001$ compared with control.
(B) CREBBP catalytic core was pre-incubated with 40 μM etoposide quinone (EQ) for 20 min at room temperature followed by incubation with 10 mM DTT for 20 min at room temperature. Samples were then assayed for CREBBP activity by UFLC using H3K18 fluorescent peptide. Results are means of three independent experiments. Error bars indicate S.D. values. ***$p < 0.001$ compared with control.
(C) CREBBP catalytic core was incubated with different concentrations of etoposide quinone (0–10 μM). Aliquots were taken every 30s and residual acetyltransferase activity was measured by UFLC using H3K18 fluorescent peptide. For each etoposide quinone concentration the natural logarithm (ln) of the percentage (%) of CREBBP residual activity was plotted as a function of time. The apparent first order inhibition constants (k_{obs}) were calculated from the linear regressions (slopes). Results are means of three independent experiments. Error bars indicate S.D. values.
(D) The k_{obs} values were plotted against etoposide quinone (EQ) concentrations and the second order inhibition constant (k_{Inhib}) was extracted from the slope. Results are means of three independent experiments. Error bars indicate S.D. values.

Prism GraphPad 5 followed by two-tailed Tukey test. A threshold of $p < 0.05$ was used to consider differences as statistically significant.

3. Results

3.1. Etoposide quinone impairs the acetylation of H3K18 and H3K27 by CREBBP in vitro

The leukemogenic properties of etoposide resides, at least in part, on its metabolic bioactivation in hematopoietic cells into oxidative quinone metabolites, most notably etoposide quinone which is known to react with cysteine residues and be a strong inhibitor of nuclear topoisomerases II [24,28,29,47]. We asked whether etoposide quinone could affect other nuclear enzymes whose alteration could contribute to leukemogenesis. Interestingly, the histone acetyltransferase CREBBP is known to be a major regulator of hematopoiesis and impairment of its activity is linked to the development of hematological malignancies [7]. In addition, CREBBP activity is known to rely on redox-sensitive cysteine zinc finger within the catalytic core of the enzyme [41–43]. To test the effects of etoposide quinone on human CREBBP HAT activity, the purified recombinant catalytic core domain of the enzyme (residues 1096 to 1700) [48] (Supplementary Fig. 1) was incubated with increasing concentrations of the metabolite or the parent drug prior to measurement of the HAT activity of CREBBP using fluorescent histone H3 peptides as substrates [44]. We found that contrary to etoposide, etoposide quinone was able to inhibit CREBBP HAT activity in a dose-dependent manner with IC_{50} values in the low micromolar ranges (below 10 μM) for both H3K18 and H3K27 peptides (Fig. 1A and Supplementary Fig. 2). Consistently, assays carried out with recombinant histone H3 confirmed that etoposide quinone but not etoposide inhibits CREBBP HAT activity (Fig. 1B). No significant effects of etoposide on CREBBP activity were observed (even at concentrations of etoposide >200 μM (data not shown) further confirming that CREBBP HAT activity is more sensitive to etoposide quinone than to the parent drug etoposide.

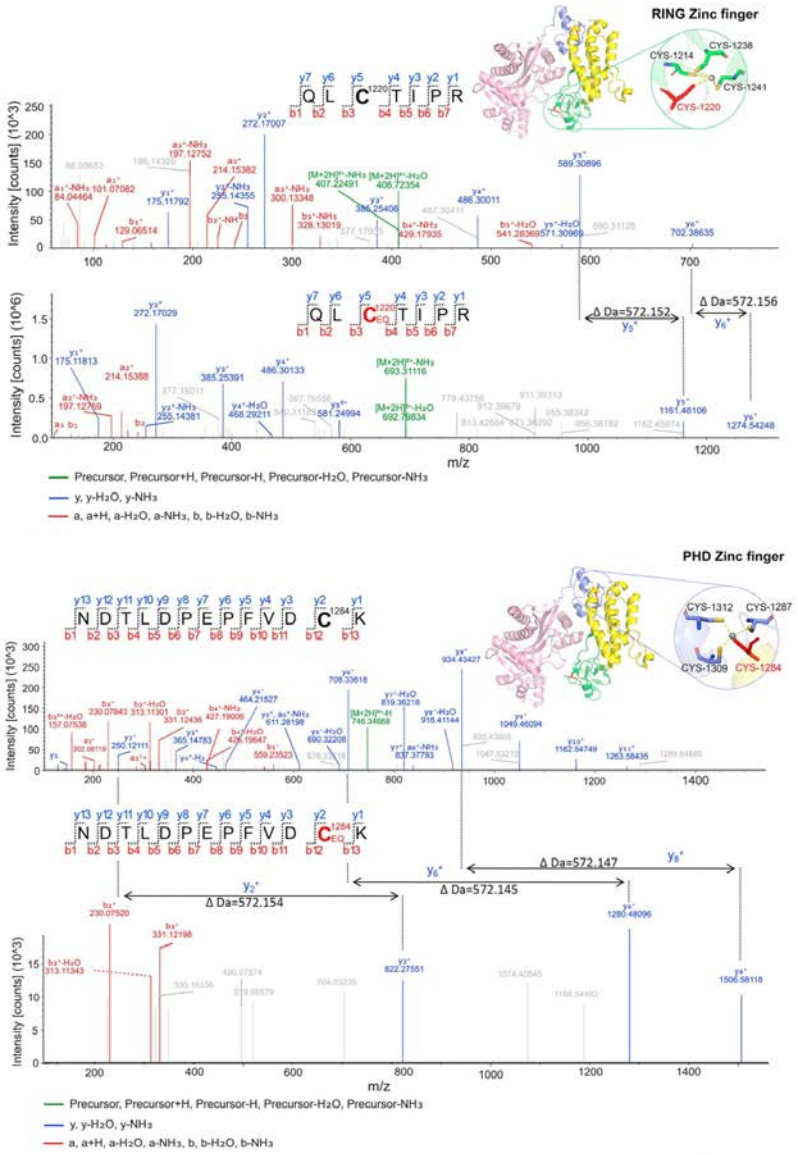

Fig. 3. Mass spectrometry analyses of etoposide quinone adducts on CREBBP catalytic core CREBBP catalytic core was incubated with etoposide quinone (40 μM) for 20 min at room temperature. The samples were reduced with DTT and alkylated with NEM prior to trypsin digestion and liquid chromatography-MS/MS analysis. A control without etoposide quinone was done in the same conditions. Mass spectra showing presence of an etoposide quinone adduct on cysteine 1220 of the RING Zn^{2+}-finger (Upper panels) and on cysteine 1284 of the PHD Zn^{2+}-finger (Lower panels) are shown. The sequences of the peptides are displayed on each panel in addition to the etoposide quinone adducts (EQ) on the cysteine residues.

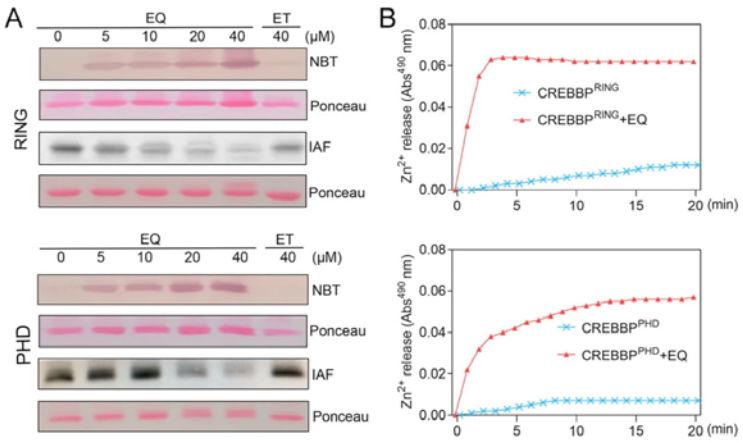

Fig. 4. Modification of cysteine residues of the RING and PHD domains of CREBBP by etoposide quinone and subsequent Zn^{2+} release

(A) Purified RING (aa 1205–1279) (top panel) and PHD (aa 1280–1321) (bottom panel) domains were incubated with increasing concentrations of etoposide quinone (EQ, 0–40 μM) or 40 μM etoposide (ET) for 20 min at room temperature. For the quinone-specific nitro blue tetrazolium (NBT) staining, samples were separated by SDS-PAGE and transferred onto nitrocellulose membranes. Etoposide quinone adducts on the RING and PHD proteins were then detected using NBT as described in Materials and Methods. Ponceau red staining is shown as a loading control. For the iodoacetamide-fluorescein (IAF) labelling, samples were incubated with 10 μM IAF for 10 min at room temperature, separated by SDS-PAGE and transferred onto nitrocellulose membranes. Cysteine residues labelled by IAF were detected by fluorescence (λ_{exc} = 485 nm, λ_{em} = 530 nm). Ponceau red staining is showed as a loading control

(B) Purified RING and PHD domains were incubated with or without etoposide quinone (40 μM) in the presence of 100 μM PAR. The absorbance of PAR-Zn^{2}-complexes (490 nm) was followed as a function of time at room temperature using a plate reader. Etoposide quinone had no effect on PAR absorbance (data not shown). . (For interpretation of the references to colour in this figure legend, the reader is referred to the Web version of this article.)

3.2. Inhibition of CREBBP by etoposide quinone is fast and irreversible

Etoposide quinone has been shown to be an irreversible and fast inhibitor of human topoisomerases II at micromolar concentrations [29,30]. To further analyze the inhibition mechanism of CREBBP by etoposide quinone, the enzyme was incubated with etoposide quinone and subsequently subjected to buffer exchange prior to measurement of residual HAT activity. As shown in Fig. 2A, the activity of CREBBP could not be recovered by buffer exchange after inhibition by etoposide quinone. Neither could the activity be restored by addition of the reducing agent DTT (Fig. 2B). To further analyze the inhibition mechanism of CREBBP by etoposide quinone, we performed kinetic experiments under pseudo-first order conditions (Fig. 2C and D) [45]. As shown in Fig. 2C, the semilogarithmic plots of percentage of residual activity against time for various concentrations of etoposide quinone indicated that the enzyme was inhibited in a time- and dose-dependent manner thus confirming the irreversible nature of the inhibition. The second-order rate constant of inhibition (k_{inhib}) was determined by plotting the k_{obs} values obtained from the semilogarithmic plots against etoposide quinone concentration and was found to be equal to 16.10^{2} $M^{-1}.s^{-1}$ (Fig. 2D). Overall, these data show that etoposide quinone inhibits CREBBP rapidly and irreversibly similar to etoposide quinone-dependent inhibition of human topoisomerases II [29,30].

3.3. Etoposide quinone forms covalent adducts with PHD/RING Zn^{2+}-finger cysteines of the catalytic core of CREBBP

Etoposide quinone has been previously shown to covalently inhibit human topoisomerases II by reaction with cysteine residues [30]. Moreover, quinone species, such as etoposide quinone, are known to be electrophilic chemicals that can readily react covalently with nucleophilic amino acids in proteins, most notably redox-sensitive cysteine residues [36,49–51]. The formation of these covalent quinone-protein adducts is considered as a major mechanism for the biological and toxicological effects of quinone species [51–54]. We carried out mass spectrometry analyses to investigate whether amino acids found within the catalytic core of human CREBBP could react with etoposide quinone and form such covalent adducts. LC-MS/MS analysis of tryptic digests of etoposide quinone-inhibited CREBBP allowed the identification of two peptides derived from the RING and PHD Zn^{2+}-finger domains with mass increases of 572.15 Da (corresponding to the mass of an etoposide quinone molecule) at cysteine residues 1220 and 1284, respectively (Fig. 3, upper and lower panel for RING and PHD sequences, respectively). To further confirm that etoposide quinone can react covalently with cysteine residues within the RING and PHD domains of the enzyme, we incubated purified recombinant RING and PHD proteins (aa 1205–1279 and 1280–1321, respectively; Supplementary Fig. 1) with etoposide quinone prior to quinone-specific nitro blue tetrazolium (NBT) staining and protein cysteine labeling by fluorescein-iodoacetamide (IAF) [34,46,55]. As shown in Fig. 4A, etoposide-quinone was able to form covalent adducts with both RING and PHD domains as evidenced by NBT staining of RING and PHD proteins treated with etoposide quinone. Covalent adduction of etoposide quinone on the two protein domains was accompanied with the concomitant loss of cysteine labeling by IAF thus supporting that quinone adducts occurred on reactive cysteine residues in these two domains. Zn^{2+}-bound cysteines found in Zn^{2+}-fingers are known to be redox sensitive and to readily react with electrophilic agents such as quinone species leading to covalent modification of these residues and to subsequent ejection of Zn^{2+} [56,57]. We thus used the metallochromic indicator 4-(2-pyridylazo)resorcinol (PAR) to monitor the release of Zn^{2+} from RING and PHD Zn^{2+}-fingers upon exposure to etoposide quinone [58]. As shown in Fig. 4B, exposure to etoposide quinone led to the rapid ejection of Zn^{2+} from both RING and PHD domains.

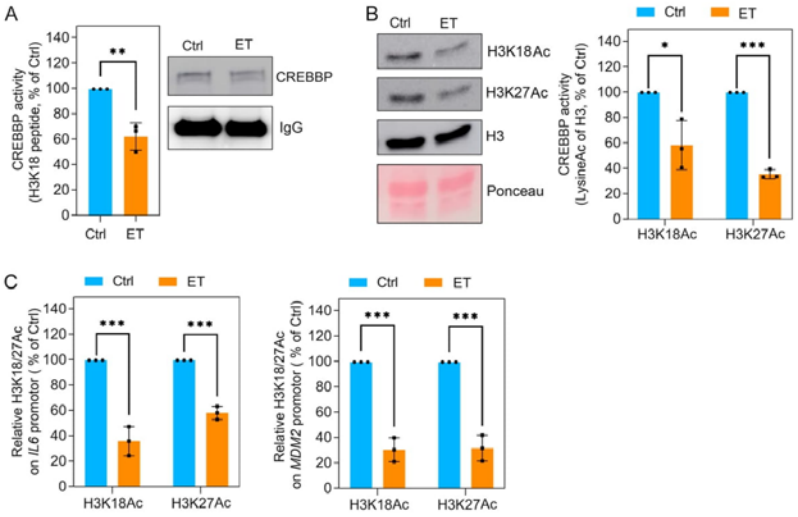

Fig. 5. Exposure of K562 cells to etoposide leads to inhibition of CREBBP and to the loss of H3K18 and H3K27 acetylation

(A) K562 cells were exposed to 40 μM etoposide (ET) or vehicle (Ctrl) for 24 h, cells were lysed and cellular CREBBP was isolated by immunoprecipitation. Immunoprecipitated CREBBP activity was measured by UFLC. In parallel, CREBBP protein content in immunoprecipitates was determined by Western-blot (Right panel). Results are means of three independent experiments. Western blot is representative of three independent experiments. Error bars indicate S.D. values. $^{**}p <$ 0.01 compared with control (Ctrl).

(B) Histones were extracted from the cell lysates and H3K18 and H3K27 acetylation was detected by Western blot. Quantification of H3 acetylation in Western blots was carried out using ImageJ software. Results are means of three independent experiments. Western blot is representative of three independent experiments. Error bars indicate S.D. values.$^{*}p < 0.05$ compared with control (Ctrl), $^{***}p < 0.001$.

(C) Chromatin immunoprecipitation (ChIP) was conducted on cells chromatin using anti-H3K18ac and H3K27ac histone marks as described in *Materials and Methods*. RT-qPCR experiments were subsequently carried out on *IL6* and *MDM2* genes using primers specific for their promotors. Results are means of three independent experiments. Error bars indicate S.D. values.$^{***}p < 0.001$ compared with control (Ctrl).

Altogether, the data reported above indicate that etoposide quinone covalently reacts with CREBBP catalytic core forming adducts with cysteine residues found within the RING and PHD Zn^{2+}-fingers, leading to the subsequent release of Zn^{2+}.

3.4. CREBBP activity is irreversibly inhibited in human hematopoietic cells and in mice exposed to etoposide

Upon administration, etoposide is readily metabolized into reactive oxidative compounds in cells, most notably etoposide quinone, that covalently binds to redox sensitive cysteine residues of proteins [25,59–62]. The biotransformation of etoposide into etoposide quinone is mainly due to cellular oxidative enzymes such as CYP3A4 or peroxidases [24,63]. To confirm that etoposide quinone generated from biotransformation of etoposide can indeed inhibit CREBBP, we took advantage of the previously described *in vitro* peroxidase/H_2O_2 system, that mimics the cellular oxidative bioactivation of etoposide into etoposide quinone [31,47]. As shown in Supplementary Fig. 3, etoposide oxidized by a functional peroxidase/H_2O_2 system was able to irreversibly inhibit CREBBP activity and lead to the formation of protein-quinone adducts (NBT staining) as well as loss of cysteine thiol labeling by IAF. In contrast, when a non-functional peroxidase/H_2O_2 system was used to metabolize etoposide, we did not observe inhibition nor formation of quinone adducts on cysteine residues were observed (Supplementary Fig. 3). These findings are in agreement with our results described above and confirm that, contrary to etoposide, its quinone metabolite can readily impair CREBBP HAT activity through formation of irreversible covalent adducts on redox sensitive cysteine residues.

As we mentioned above, metabolization of etoposide into oxidative metabolites, such as etoposide quinone, is prominent in hematopoietic cells treated with this chemotherapeutic drug and has been implicated in the leukemogenic processes [24,59,63]. We thus tested whether the inhibition of CREBBP HAT activity could occur in a cellular context. To this end, K562 cells were exposed to etoposide at concentrations that do not significantly impact cell viability (Supplementary Fig. 4) [64]. The endogenous CREBBP enzyme was then immunoprecipitated and assayed for HAT activity. As shown in Fig. 5A, endogenous CREBBP HAT activity was irreversibly inhibited in cells exposed to etoposide (~60% residual activity). Remarkably, we also found that the acetylation of histone H3 (H3K18Ac and H3K27Ac) in cells was also reduced upon etoposide treatment (Fig. 5B). Consistent with the loss of acetylation mark on histone H3, ChIP-qPCR experiments revealed decreased levels of H3K18Ac and H3K27Ac on the promoters of *IL6* and *MDM2* genes (known to be acetylated and regulated by CREBBP [10,65–67], (Fig. 5C). Further investigations carried out on mice (C57BL/6J, n = 6) treated with a clinically-relevant dose of etoposide *via* intraperitoneal injection (100 mg/kg) [68] revealed a decrease in H3K18 and H3K27 acetylation levels in histones isolated from the bone marrow cells of treated mice (Fig. 6A). In line with these data, the intrinsic HAT activity of immunoprecipitated CREBBP was significantly reduced in etoposide-treated mice (Fig. 6A and B). Furthermore, ChIP-qPCR experiments performed on chromatin extracted from mice bone marrow cells were in agreement with the previous results showing that H3K18 and H3K27 acetylation was decreased on the promoters of *COPS2* and

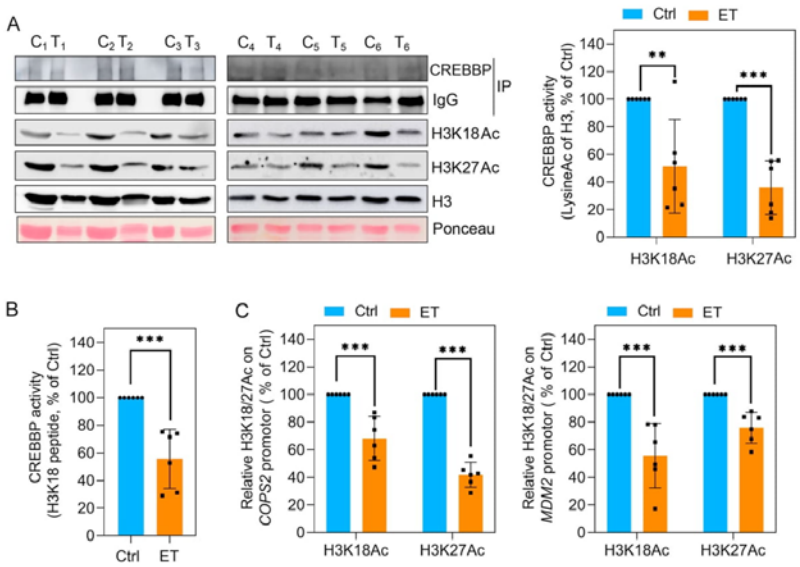

Fig. 6. Exposure of mice to etoposide inhibits CREBBP activity and H3K18 and H3K27 acetylation in bone marrow cells.
(A) C57BL/6J mice (n = 6) were treated with 100 mg/kg etoposide (Tn) or vehicle (Cn) for 24 h. Bone marrow was isolated from hind limb long bone. Histones were extracted from cell lysates and H3K18 and H3K27 acetylation was detected by Western blot (Left panels). Quantification of H3 acetylation in Western blots was carried out using ImageJ software (Right panel). Results are means of the six treated (Tn) and non-treated (Cn) mice. Error bars indicate S.D. $^{**}p < 0.01$ compared with control (Ctrl), $^{***}p < 0.001$ compared with Ctrl.
(B) CREBBP was first immunoprecipitated from the bone marrow cell lysates and its acetyltransferase activity of the immunoprecipates was measured by UFLC. In parallel, CREBBP protein content in the immunoprecipitates was determined by Western-blot (Fig. 6A, Left panel). Results are means of the six treated (Tn) and non-treated (Cn) mice. Error bars indicate S.D. $^{***}p < 0.01$ compared with control (Ctrl)
(C) Chromatin immunoprecipitation (ChIP) was carried on bone marrow cells chromatin using antibodies against the H3K18Ac and H3K27Ac histone marks as described in *Materials and Methods*. RT-qPCR experiments were subsequently carried out on murine *COPS2* and *MDM2* genes using primers specific for their promotors. Results are means of the six treated (Tn) and non-treated (Cn) mice. Error bars indicate S.D. values. $^{**}p < 0.01$ compared with control (Ctrl), $^{***}p < 0.001$ compared with Ctrl.

MDM2 genes of etoposide-treated mice (Fig. 6C). Taken together, these results are consistent with the data obtained with recombinant CREBBP and support the notion that metabolic activation of etoposide into oxidative reactive metabolites, notably etoposide quinone, leads to impairment of CREBBP HAT activity with subsequent aberrant histone acetylation.

4. Discussion

Despite its strong potential as a chemotherapeutic drug, etoposide is well-known to be associated with the development of treatment-related hematopoietic malignancies [22]. The molecular events underlying etoposide-dependent leukemogenesis remain poorly understood, recent studies suggest nonetheless that etoposide quinone, a reactive oxidative metabolite of etoposide, could be a major player in the leukemogenic process, notably through interactions with topoisomerase II enzymes [28–30]. However, as a reactive electrophilic species etoposide quinone likely exerts its toxic effects through alteration of other cellular protein targets [24,32,34,35,50,51]. In addition, recent studies suggest that exposure to etoposide could lead to epigenetic alterations, notably affecting histones, that may contribute to the deleterious effects of the drug [37,38]. In this work, we show that the leukemogenic oxidative metabolite of etoposide, etoposide quinone, is able to impair the activity of the histone acetyltransferase CREBBP. Remarkably, this histone acetyltransferase is recognized as a tumor suppressor that plays a crucial role in the homeostasis of the hematopoietic system [7,11,17,19,69]. Moreover, mutations and other molecular genetic abnormalities of CREBBP that alter its acetyltransferase activity are commonly observed in leukemia and lymphoma [7,9,10,14]. Interestingly, it has been shown that the histone acetyltransferase p300, the close homologue of CREBBP, is irreversibly inhibited by quinone species such as hydroxynaphthoquinones [70,71]. Our in depth enzymatic analyses indicate that the inhibition of CREBBP by etoposide quinone is irreversible and takes places rapidly with a second-order inhibition rate constant of 16.10^2 $M^{-1}.s^{-1}$ consistent with the value found for the irreversible inhibition of topoisomerase IIα by etoposide quinone (28.10^2 M^{-1} s^{-1}) [29]. Interestingly, topoisomerases II are known biological targets of etoposide quinone and impairment of these nuclear enzymes by etoposide quinone have been suggested to contribute to etoposide-related leukemogenesis [28–30]. The biological and toxicological effects of numerous quinone species, such as etoposide quinone, are known to depend on their capacity to react rapidly and covalently with protein cysteine residues, to form irreversible adducts that impact protein structure and/or functions [50,51]. Consistently, the irreversible inhibition of topoisomerase IIα by etoposide quinone has been suggested to rely on quinone adduction of several reactive cysteine residues of the enzyme [29,72]. In a similar manner, our mass spectrometry and labeling experiments showed that etoposide quinone was indeed able to form covalent adducts with two

cysteine residues within the RING and PHD domains of the CREBBP catalytic core (Figs. 3 and 4). The RING and PHD domains are each constituted of a redox sensitive C4 Zn^{2+}-fingers (4 cysteines coordinating the Zn^{2+} atom) that are known to be an integral part of the CREBBP catalytic core and to be essential for its acetyltransferase activity [41,42,48]. Of importance, the two cysteines we identified (Cys1220 and Cys1284) belong, to the RING and PHD Zn^{2+}-fingers, respectively where they coordinate the Zn^{2+} atom. Importantly, it was previously shown that mutation of Cys1284 to Ala results in CREBBP inactivation, thus supporting our findings [41]. Moreover, comparatively to our findings, it has been shown that Zn^{2+}-bound cysteines in Zn^{2+}-fingers readily react with quinone species to form covalent adducts that can lead to Zn^{2+} ejection and subsequent alteration of protein function [56,57]. More generally, release of Zn^{2+} from C4 Zn^{2+}-fingers (such as those in the RING and PHD domains of CREBBP) and their subsequent structural alterations are commonly observed when Zn^{2+}-finger cysteines are adducted by electrophilic chemicals [56,57]. We indeed observed that reaction of etoposide-quinone with RING and PHD Zn^{2+}-finger cysteines of CREBBP led to Zn^{2+} ejection (Fig. 4). Interestingly, it has been reported recently that certain quinones species, were able to react with a Zn^{2+}-finger in the catalytic domain of the histone demethylase KDM4A and to induce similar Zn^{2+} ejection [73]. In line with these observations, our results strongly suggest that impairment of CREBBP activity is likely due to the adduction of the bulky etoposide quinone molecule on these critical RING and PHD Zn^{2+}-finger cysteine residues, resulting in subsequent release of Zn^{2+} and alteration of the RING/PHD structures.

As shown for other well-known chemical leukemogens such as benzene, the leukemogenic effects of etoposide are increasingly recognized as relying on the metabolic activation of etoposide into reactive oxidative metabolites in the bone marrow, in particular etoposide quinone [24–26,30,31]. Recent studies indicate that etoposide quinone is more potent at impairing topoisomerase II functions than the parent drug etoposide, thus supporting a major role for this quinone metabolite on the topoisomerase II-dependent leukemogenic process of etoposide [28,30]. In accordance with these observations, we were unable to find any significant effect of etoposide on purified recombinant CREBBP activity *in vitro* in contrast to etoposide quinone. This is in agreement with the electrophilic properties of the quinone metabolite which prompt this species to react covalently with redox sensitive Zn^{2+}-finger cysteines [50,51,56]. As stated above, etoposide is readily oxidized in hematopoietic cells into etoposide quinone by cellular cytochromes P450 and peroxidases [24,25,63]. In line with the data obtained with recombinant purified CREBBP, exposure of hematopoietic cells to etoposide led to the inhibition of the endogenous enzyme with concomitant decrease in histone H3K18 and H3K27 acetylation (Fig. 5). Further experiments with mice exposed to etoposide confirmed inhibition of CREBBP acetyltransferase activity and decreased H3K18 and H3K27 acetylation (Fig. 6). Interestingly, a similar decrease in histone H3 acetylation was recently reported in a human neuroblastoma cell line exposed to etoposide [39].

Overall, our study shows that, in addition to the alteration of topoisomerase II functions, etoposide quinone, a leukemogenic oxidative metabolite of etoposide can impair CREBBP acetyltransferase by reacting with key cysteine residues within the catalytic core of the enzyme.

Declaration of competing interest

None declared.

Acknowledgments

This work was supported by running grants from Université de Paris and CNRS, and by grants from ANSES (Agence Nationale de Sécurité Sanitaire de l'Alimentation, de l'Environnement et du Travail) and ITMO Cancer (plan Cancer-Environnement). WZ, PG and RL are supported by China Scholarship Council PhD fellowships. CM is supported by a PhD fellowship from Université de Paris (ED BioSPC). We thank the technical platform "BioProfiler" (BFA, CNRS UMR 8251 Unit, Université de Paris) for provision of UFLC facilities. We thank Dr. O. Brookes and Dr. C. Mathieu for English language proofreading and comments. We thank Dr. F. Busi for help with PCR primers design and ordering.

Appendix A. Supplementary data

Supplementary data to this article can be found online at https://doi.org/10.1016/j.freeradbiomed.2020.11.027.

References

[1] P. Chi, C.D. Allis, G.G. Wang, Covalent histone modifications–miswritten, misinterpreted and mis-erased in human cancers, Nat. Rev. Canc. 10 (2010) 457–469.
[2] E. Verdin, M. Ott, 50 years of protein acetylation: from gene regulation to epigenetics, metabolism and beyond, Nat. Rev. Mol. Cell Biol. 16 (2015) 258–264.
[3] W. Gu, R.G. Roeder, Activation of p53 sequence-specific DNA binding by acetylation of the p53 C-terminal domain, Cell 90 (1997) 595–606.
[4] V.V. Ogryzko, R.L. Schiltz, V. Russanova, B.H. Howard, Y. Nakatani, The transcriptional coactivators p300 and CBP are histone acetyltransferases, Cell 87 (1996) 953–959.
[5] B.M. Dancy, P.A. Cole, Protein lysine acetylation by p300/CBP, Chem. Rev. 115 (2015) 2419–2452.
[6] J.H. Roelfsema, D.J. Peters, Rubinstein-Taybi syndrome: clinical and molecular overview, Expet Rev. Mol. Med. 9 (2007) 1–16.
[7] R. Dutta, B. Tiu, K.M. Sakamoto, CBP/p300 acetyltransferase activity in hematologic malignancies, Mol. Genet. Metabol. 119 (2016) 37–43.
[8] I. Garcia-Ramirez, S. Tadros, I. Gonzalez-Herrero, A. Martin-Lorenzo, G. Rodriguez-Hernandez, D. Moore, L. Ruiz-Roca, O. Blanco, D. Alonso-Lopez, J.L. Rivas, et al., Crebbp loss cooperates with Bcl2 overexpression to promote lymphoma in mice, Blood 129 (2017) 2645–2656.
[9] C.G. Mullighan, J. Zhang, L.H. Kasper, S. Lerach, D. Payne-Turner, L.A. Phillips, S. L. Heatley, L. Holmfeldt, J.R. Collins-Underwood, J. Ma, et al., CREBBP mutations in relapsed acute lymphoblastic leukaemia, Nature 471 (2011) 235–239.
[10] L. Pasqualucci, V. Trifonov, G. Fabbri, J. Ma, D. Rossi, A. Chiarenza, V.A. Wells, A. Grunn, M. Messina, O. Elliot, et al., Analysis of the coding genome of diffuse large B-cell lymphoma, Nat. Genet. 43 (2011) 830–837.
[11] J. Zhang, S. Vlasevska, V.A. Wells, S. Nataraj, A.B. Holmes, R. Duval, S.N. Meyer, T. Mo, K. Basso, P.K. Brindle, et al., The CREBBP acetyltransferase is a haploinsufficient tumor suppressor in B-cell lymphoma, Canc. Discov. 7 (2017) 322–337.
[12] H. Hashwah, C.A. Schmid, S. Kasser, K. Bertram, A. Stelling, M.G. Manz, A. Muller, Inactivation of CREBBP expands the germinal center B cell compartment, down-regulates MHCII expression and promotes DLBCL growth, Proc. Natl. Acad. Sci. U. S. A 114 (2017) 9701–9706.
[13] S.J. Horton, G. Giotopoulos, H. Yun, S. Vohra, O. Sheppard, R. Bashford-Rogers, M. Rashid, A. Clipson, W.I. Chan, D. Sasca, et al., Early loss of Crebbp confers malignant stem cell properties on lymphoid progenitors, Nat. Cell Biol. 19 (2017) 1093–1104.
[14] A. Inthal, P. Zeitlhofer, M. Zeginigg, M. Morak, R. Grausenburger, E. Fronkova, B. Fahrner, G. Mann, O.A. Haas, R. Panzer-Grumayer, CREBBP HAT domain mutations prevail in relapse cases of high hyperdiploid childhood acute lymphoblastic leukemia, Leukemia 26 (2012) 1797–1803.
[15] M. Qian, H. Zhang, S.K. Kham, S. Liu, C. Jiang, X. Zhao, Y. Lu, C. Goodings, T. N. Lin, R. Zhang, et al., Whole-transcriptome sequencing identifies a distinct subtype of acute lymphoblastic leukemia with predominant genomic abnormalities of EP300 and CREBBP, Genome Res. 27 (2017) 185–195.
[16] X.J. Yang, Lysine acetylation and the bromodomain: a new partnership for signaling, Bioessays : news and reviews in molecular, cellular and developmental biology 26 (2004) 1076–1087.
[17] A.L. Kung, V.I. Rebel, R.T. Bronson, L.E. Ch'ng, C.A. Sieff, D.M. Livingston, T. P. Yao, Gene dose-dependent control of hematopoiesis and hematologic tumor suppression by CBP, Genes Dev. 14 (2000) 272–277.
[18] V.I. Rebel, A.L. Kung, E.A. Tanner, H. Yang, R.T. Bronson, D.M. Livingston, Distinct roles for CREB-binding protein and p300 in hematopoietic stem cell self-renewal, Proc. Natl. Acad. Sci. U. S. A 99 (2002) 14789–14794.
[19] S.N. Zimmer, Q. Zhou, T. Zhou, Z. Cheng, S.L. Abboud-Werner, D. Horn, M. Lecocke, R. White, A.V. Krivtsov, S.A. Armstrong, et al., Crebbp haploinsufficiency in mice alters the bone marrow microenvironment, leading to loss of stem cells and excessive myelopoiesis, Blood 118 (2011) 69–79.
[20] E.L. Baldwin, N. Osheroff, Etoposide, topoisomerase II and cancer. *Current medicinal chemistry*, Anti-cancer agents 5 (2005) 363–372.
[21] A.R. Mistry, C.A. Felix, R.J. Whitmarsh, A. Mason, A. Reiter, B. Cassinat, A. Parry, C. Walz, J.L. Wiemels, M.R. Segal, et al., DNA topoisomerase II in therapy-related acute promyelocytic leukemia, N. Engl. J. Med. 352 (2005) 1529–1538.
[22] M. Pendleton, R.H. Lindsey Jr., C.A. Felix, D. Grimwade, N. Osheroff, Topoisomerase II and leukemia, Ann. N. Y. Acad. Sci. 1310 (2014) 98–110.

[23] M.A. Smith, L. Rubinstein, J.R. Anderson, D. Arthur, P.J. Catalano, B. Freidlin, R. Heyn, A. Khayat, M. Kraïlo, V.J. Land, et al., Secondary leukemia or myelodysplastic syndrome after treatment with epipodophyllotoxins, J. Clin. Oncol. : official journal of the American Society of Clinical Oncology 17 (1999) 569–577.
[24] M. Atwal, E.L. Lishman, C.A. Austin, I.G. Cowell, Myeloperoxidase enhances etoposide and mitoxantrone-mediated DNA damage: a target for myeloprotection in cancer chemotherapy, Mol. Pharmacol. 91 (2017) 49–57.
[25] V.E. Kagan, A.I. Kuzmenko, Y.Y. Tyurina, A.A. Shvedova, T. Matsura, J. C. Yalowich, Pro-oxidant and antioxidant mechanisms of etoposide in HL-60 cells: role of myeloperoxidase, Canc. Res. 61 (2001) 7777–7784.
[26] M.V. Relling, H.L. McLeod, L.C. Bowman, V.M. Santana, Etoposide pharmacokinetics and pharmacodynamics after acute and chronic exposure to cisplatin, Clin. Pharmacol. Ther. 56 (1994) 503–511.
[27] C.A. Felix, A.H. Walker, B.J. Lange, T.M. Williams, N.J. Winick, N.K. Cheung, B. D. Lovett, P.C. Nowell, I.A. Blair, T.R. Rebbeck, Association of CYP3A4 genotype with treatment-related leukemia, Proc. Natl. Acad. Sci. U. S. A 95 (1998) 13176–13181.
[28] E.G. Gibson, M.M. King, S.L. Mercer, J.E. Deweese, Two-mechanism model for the interaction of etoposide quinone with topoisomerase IIalpha, Chem. Res. Toxicol. 29 (2016) 1541–1548.
[29] D.A. Jacob, S.L. Mercer, N. Osheroff, J.E. Deweese, Etoposide quinone is a redox-dependent topoisomerase II poison, Biochemistry 50 (2011) 5660–5667.
[30] N.A. Smith, J.A. Byl, S.L. Mercer, J.E. Deweese, N. Osheroff, Etoposide quinone is a covalent poison of human topoisomerase IIbeta, Biochemistry 53 (2014) 3229–3236.
[31] Vlasova II, W.H. Feng, J.P. Goff, A. Giorgianni, D. Do, S.M. Gollin, D.W. Lewis, V. E. Kagan, J.C. Yalowich, Myeloperoxidase-dependent oxidation of etoposide in human myeloid progenitor CD34+ cells, Mol. Pharmacol. 79 (2011) 479–487.
[32] A.E. Alegría, P. Sanchez-Cruz, A. Kumar, C. Garcia, F.A. Gonzalez, A. Orellano, B. Zayas, M. Gordaliza, Thiols oxidation and covalent binding of BSA by cyclolignanic quinones are enhanced by the magnesium cation, Free Radic. Res. 42 (2008) 70–81.
[33] A. Montecucco, F. Zanetta, G. Biamonti, Molecular mechanisms of etoposide, EXCLI journal 14 (2015) 95–108.
[34] Q. Nian, J. Berthelet, W. Zhang, L.C. Bui, R. Liu, X. Xu, R. Duval, S. Ganesan, T. Leger, C. Chomienne, et al., T-cell protein tyrosine phosphatase is irreversibly inhibited by etoposide-quinone, a reactive metabolite of the chemotherapy drug etoposide, Mol. Pharmacol. 96 (2019) 297–306.
[35] E. Rojas, P. Mussali, E. Tovar, M. Valverde, DNA-AP sites generation by etoposide in whole blood cells, BMC Canc. 9 (2009) 398.
[36] B.K. Sinha, C.E. Myers, Irreversible binding of etoposide (VP-16-213) to deoxyribonucleic acid and proteins, Biochem. Pharmacol. 33 (1984) 3725–3728.
[37] E. Chamani, A. Rabbani-Chadegani, Z. Zahraei, Spectroscopic detection of etoposide binding to chromatin components: the role of histone proteins, Spectrochim. Acta Mol. Biomol. Spectrosc. 133 (2014) 292–299.
[38] H.J. Gill Super, A role for epigenetics in the formation of chromosome translocations in acute leukemia, Cancer genetics 208 (2015) 230–236.
[39] T. Groh, J. Hrabeta, M.A. Khalil, H. Doktorova, T. Eckschlager, M. Stiborova, The synergistic effects of DNA-damaging drugs cisplatin and etoposide with a histone deacetylase inhibitor valproate in high-risk neuroblastoma cells, Int. J. Oncol. 47 (2015) 343–352.
[40] N. Bagheri-Sereshki, B.F. Hales, B. Robaire, The effects of chemotherapeutic agents, bleomycin, etoposide, and cisplatin, on chromatin remodeling in male rat germ cells, Biol. Reprod. 94 (2016) 81.
[41] E. Kalkhoven, H. Teunissen, A. Houweling, C.P. Verrijzer, A. Zantema, The PHD type zinc finger is an integral part of the CBP acetyltransferase domain, Mol. Cell Biol. 22 (2002) 1961–1970.
[42] E. Kalkhoven, J.H. Roelfsema, H. Teunissen, A. den Boer, Y. Ariyurek, A. Zantema, M.H. Breuning, R.C. Hennekam, D.J. Peters, Loss of CBP acetyltransferase activity by PHD finger mutations in Rubinstein-Taybi syndrome, Hum. Mol. Genet. 12 (2003) 441–450.
[43] M. Delvecchio, J. Gaucher, C. Aguilar-Gurrieri, E. Ortega, D. Panne, Structure of the p300 catalytic core and implications for chromatin targeting and HAT regulation, Nat. Struct. Mol. Biol. 20 (2013) 1040–1046.
[44] R. Duval, L. Fritsch, L.C. Bui, J. Berthelet, F. Guidez, C. Mathieu, J.M. Dupret, C. Chomienne, S. Ait-Si-Ali, F. Rodrigues-Lima, An acetyltransferase assay for CREB-binding protein based on reverse phase-ultra-fast liquid chromatography of fluorescent histone H3 peptides, Anal. Biochem. 486 (2015) 35–37.
[45] R.A. Copeland, Evaluation of enzyme inhibitors in drug discovery. A guide for medicinal chemists and pharmacologists, Methods Biochem. Anal. 46 (2005) 1–265.
[46] M.A. Paz, R. Fluckiger, A. Boak, H.M. Kagan, P.M. Gallop, Specific detection of quinoproteins by redox-cycling staining, J. Biol. Chem. 266 (1991) 689–692.
[47] V.E. Kagan, J.C. Yalowich, G.G. Borisenko, Y.Y. Tyurina, V.A. Tyurin, P. Thampatty, J.P. Fabisiak, Mechanism-based chemopreventive strategies against etoposide-induced acute myeloid leukemia: free radical/antioxidant approach, Mol. Pharmacol. 56 (1999) 494–506.
[48] S. Park, R.L. Stanfield, M.A. Martinez-Yamout, H.J. Dyson, I.A. Wilson, P.E. Wright, Role of the CBP catalytic core in intramolecular SUMOylation and control of histone H3 acetylation, Proc. Natl. Acad. Sci. U. S. A 114 (2017) E5335–E5342.
[49] M.S. Elgawish, N. Kishikawa, K. Ohyama, N. Kuroda, Characterization of quinone derived protein adducts and their selective identification using redox cycling based chemiluminescence assay, Journal of chromatography. A 1403 (2015) 96–103.
[50] J.L. Bolton, T. Dunlap, Formation and biological targets of quinones: cytotoxic versus cytoprotective effects, Chem. Res. Toxicol. 30 (2017) 13–37.
[51] N. Shu, L.G. Lorentzen, M.J. Davies, Reaction of quinones with proteins: kinetics of adduct formation, effects on enzymatic activity and protein structure, and potential reversibility of modifications, Free Radic. Biol. Med. 137 (2019) 169–180.
[52] J.L. Bolton, M.A. Trush, T.M. Penning, G. Dryhurst, T.J. Monks, Role of quinones in toxicology, Chem. Res. Toxicol. 13 (2000) 135–160.
[53] X. Wang, B. Thomas, R. Sachdeva, L. Arterburn, L. Frye, P.G. Hatcher, D. G. Cornwell, J. Ma, Mechanism of arylating quinone toxicity involving Michael adduct formation and induction of endoplasmic reticulum stress, Proc. Natl. Acad. Sci. U. S. A 103 (2006) 3604–3609.
[54] I. Klopcic, M.S. Dolenc, Chemicals and drugs forming reactive quinone and quinone imine metabolites, Chem. Res. Toxicol. 32 (2019) 1–34.
[55] Y. Wu, K.S. Kwon, S.G. Rhee, Probing cellular protein targets of H2O2 with fluorescein-conjugated iodoacetamide and antibodies to fluorescein, FEBS Lett. 440 (1998) 111–115.
[56] S.M. Quintal, Q.A. dePaula, N.P. Farrell, Zinc finger proteins as templates for metal ion exchange and ligand reactivity. Chemical and biological consequences, Metall : integrated biometal science 3 (2011) 121–139.
[57] H. Lee, J. Komano, Y. Saitoh, S. Yamaoka, T. Kozaki, T. Misawa, M. Takahama, T. Satoh, O. Takeuchi, N. Yamamoto, et al., Zinc-finger antiviral protein mediates retinoic acid inducible gene I-like receptor-independent antiviral response to murine leukemia virus, Proc. Natl. Acad. Sci. U. S. A 110 (2013) 12379–12384.
[58] K. Miyamoto, K. Togiya, The creation of the artificial RING finger from the cross-brace zinc finger by alpha-helical region substitution, Biochem. Biophys. Res. Commun. 394 (2010) 972–975.
[59] N. Haim, J. Nemec, J. Roman, B.K. Sinha, Peroxidase-catalyzed metabolism of etoposide (VP-16-213) and covalent binding of reactive intermediates to cellular macromolecules, Canc. Res. 47 (1987) 5835–5840.
[60] N. Zheng, C.A. Felix, S. Pang, R. Boston, P. Moate, J. Scavuzzo, I.A. Blair, Plasma etoposide catechol increases in pediatric patients undergoing multiple-day chemotherapy with etoposide, Clin. Canc. Res. : an official journal of the American Association for Cancer Research 10 (2004) 2977–2985.
[61] Y. Fan, E.M. Schreiber, A. Giorgianni, J.C. Yalowich, B.W. Day, Myeloperoxidase-catalyzed metabolism of etoposide to its quinone and glutathione adduct forms in HL60 cells, Chem. Res. Toxicol. 19 (2006) 937–943.
[62] B.D. Lovett, L. Lo Nigro, E.F. Rappaport, I.A. Blair, N. Osheroff, N. Zheng, M. D. Megonigal, W.R. Williams, P.C. Nowell, C.A. Felix, Near-precise interchromosomal recombination and functional DNA topoisomerase II cleavage sites at MLL and AF-4 genomic breakpoints in treatment-related acute lymphoblastic leukemia with t(4;11) translocation, Proc. Natl. Acad. Sci. U. S. A 98 (2001) 9802–9807.
[63] X. Zhuo, N. Zheng, C.A. Felix, I.A. Blair, Kinetics and regulation of cytochrome P450-mediated etoposide metabolism, Drug Metabol. Dispos.: the biological fate of chemicals 32 (2004) 993–1000.
[64] M.M. Mc Gee, G. Campiani, A. Ramunno, C. Fattorusso, V. Nacci, M. Lawler, D. C. Williams, D.M. Zisterer, Pyrrolo-1,5-benzoxazepines induce apoptosis in chronic myelogenous leukemia (CML) cells by bypassing the apoptotic suppressor bcr-abl, J. Pharmacol. Exp. Therapeut. 296 (2001) 31–40.
[65] M.F. Barber, E. Michishita-Kioi, Y. Xi, L. Tasselli, M. Kioi, Z. Moqtaderi, R. I. Tennen, S. Paredes, N.L. Young, K. Chen, et al., SIRT7 links H3K18 deacetylation to maintenance of oncogenic transformation, Nature 487 (2012) 114–118.
[66] Y. Liu, Z.B. Xing, J.H. Zhang, Y. Fang, Akt kinase targets the association of CBP with histone H3 to regulate the acetylation of lysine K18, FEBS Lett. 587 (2013) 847–853.
[67] A. Sriraman, A. Dickmanns, Z. Najafova, S.A. Johnsen, M. Dobbelstein, CDK4 inhibition diminishes p53 activation by MDM2 antagonists, Cell Death Dis. 9 (2018) 918.
[68] F. Marchetti, J.B. Bishop, X. Lowe, W.M. Generoso, J. Hozier, A.J. Wyrobek, Etoposide induces heritable chromosomal aberrations and aneuploidy during male meiosis in the mouse, Proc. Natl. Acad. Sci. U. S. A 98 (2001) 3952–3957.
[69] W.I. Chan, R.L. Hannah, M.A. Dawson, C. Pridans, D. Foster, A. Joshi, B. Gottgens, J.M. Van Deursen, B.J. Huntly, The transcriptional coactivator Cbp regulates self-renewal and differentiation in adult hematopoietic stem cells, Mol. Cell Biol. 31 (2011) 5046–5060.
[70] K.C. Ravindra, B.R. Selvi, M. Arif, B.A. Reddy, G.R. Thanuja, S. Agrawal, S. K. Pradhan, N. Nagashayana, D. Dasgupta, T.K. Kundu, Inhibition of lysine acetyltransferase KAT3B/p300 activity by a naturally occurring hydroxynaphthoquinone, plumbagin, J. Biol. Chem. 284 (2009) 24453–24464.
[71] M.D. Vasudevarao, P. Mizar, S. Kumari, S. Mandal, S. Siddhanta, M.M. Swamy, S. Kaypee, R.C. Kodihalli, A. Banerjee, C. Naryana, et al., Naphthoquinone-mediated inhibition of lysine acetyltransferase KAT3B/p300, basis for non-toxic inhibitor synthesis, J. Biol. Chem. 289 (2014) 7702–7717.
[72] R.P. Bender, A.J. Ham, N. Osheroff, Quinone-induced enhancement of DNA cleavage by human topoisomerase IIalpha: adduction of cysteine residues 392 and 405, Biochemistry 46 (2007) 2856–2864.
[73] M.K. Jayatunga, S. Thompson, T.C. McKee, M.C. Chan, K.M. Reece, A.P. Hardy, R. Sekirnik, P.T. Seden, K.M. Cook, J.B. McMahon, et al., Inhibition of the HIF1alpha-p300 interaction by quinone- and indandione-mediated ejection of structural Zn(II), Eur. J. Med. Chem. 94 (2015) 509–516.

Biochemical and Biophysical Research Communications xxx (xxxx) xxx

Contents lists available at ScienceDirect

Biochemical and Biophysical Research Communications

journal homepage: www.elsevier.com/locate/ybbrc

From transglutaminases (TGs) to arylamine *N*-acetyltransferases (NATs): Insight into the role of a spatially conserved aromatic amino acid position in the active site of these two families of enzymes

Ximing Xu [a, b, 1], Wenchao Zhang [a, 1], Jérémy Berthelet [a], Rongxing Liu [a], Christina Michail [a], Alain F. Chaffotte [c], Jean-Marie Dupret [a], Fernando Rodrigues-Lima [a, *]

[a] Université de Paris, BFA, UMR 8251, CNRS, 75013, Paris, France
[b] Key Laboratory of Marine Drugs, Chinese Ministry of Education, School of Medicine and Pharmacy, Ocean University of China, Qingdao, 266003, China
[c] Institut Pasteur, Unité de Résonance Magnétique Nucléaire des Biomolécules, 75015, Paris, France

ARTICLE INFO

Article history:
Received 10 February 2020
Accepted 12 February 2020
Available online xxx

Keywords:
Arylamine N-Acetyltransferases
Transglutaminases
Active site
Catalytic mechanism
Transition state

ABSTRACT

Transglutaminases (TG) and arylamine *N*-acetyltransferases (NAT) are important family of enzymes. Although they catalyze different reactions and have distinct structures, these two families of enzymes share a spatially conserved catalytic triad (Cys, His, Asp residues). In active TGs, a conserved Trp residue located close to the triad cysteine is crucial for catalysis through stabilization of transition states.

Here, we show that in addition to sharing a similar catalytic triad with TGs, functional NAT enzymes also possess in their active site an aromatic residue (Phe, Tyr or Trp) occupying a structural position similar to the Trp residue of active TGs. More importantly, as observed in active TGs, our data indicates that in functional NAT enzymes this conserved aromatic residue is also involved in stabilization of transition states. These results thus indicate that in addition to the three triad residues, these two families of enzymes also share a spatially conserved aromatic amino acid position important for catalysis. Identification of residues involved in the stabilization of transition states is important to develop potent inhibitors. Interestingly, NAT enzymes have been shown as potential targets of clinical interest.

© 2020 Elsevier Inc. All rights reserved.

1. Introduction

Transglutaminases (TGs) (EC 2.3.2.13) are a family of calcium-dependent enzymes that catalyze the formation of an isopeptide bond between glutamine side chains and the ε-amino groups of lysine residue side chains [1–3]. This process results in cross-linking of proteins involved in important biological processes such as coagulation. Crystal structures of TGs have shown that the catalytic center of these enzymes shares common structural properties with the papain-like family of cysteine protease, notably the presence of a catalytic triad of Cys-His-Asp [2,4].

Arylamine *N*-acetyltransferases (NATs) (EC 2.3.1.5) are an important family of xenobiotic-metabolizing enzymes that catalyze the acetyl-coenzyme A (AcCoA)-dependent acetylation of arylamines including drugs and carcinogens [5,6]. NAT enzymes are found in a range of eukaryotic and prokaryotic species where they may play diverse functions [6–9]. Several eukaryotic and prokaryotic NAT enzymes have been described at both functional and structural levels [9–16]. All these structural studies identified a common fold that comprises three domains and a Cys-His-Asp/Glu catalytic triad in the active site of NAT enzymes [9,14,16,17]. Although TG and NAT enzymes have otherwise distinct 3D structures, catalyze different reactions and assume different functions, the structural studies on TGs and NATs indicate that these two families of enzymes both share a catalytic center and notably a structurally conserved catalytic triad [2,18]. In addition, the catalytic reaction of TG and NAT enzymes relies on ping-pong mechanisms where the cysteine of the triad acts as the catalytic nucleophile residue [2,12,14,18,19]. Further studies on TGs identified a strictly conserved aromatic residue (corresponding to Trp 241 in human TG2) in the active site that is essential for activity of these enzymes [2,4]. This Trp residue is conserved in all enzymatically active TGs and has been shown to serve mainly on the stabilization of transition-states through interaction involving the side chain of

* Corresponding author.
E-mail address: fernando.rodrigues-lima@u-paris.fr (F. Rodrigues-Lima).
[1] These authors contributed equally and should be considered as co-first authors.

https://doi.org/10.1016/j.bbrc.2020.02.082
0006-291X/© 2020 Elsevier Inc. All rights reserved.

Please cite this article as: X. Xu et al., From transglutaminases (TGs) to arylamine *N*-acetyltransferases (NATs): Insight into the role of a spatially conserved aromatic amino acid position in the active site of these two families of enzymes, Biochemical and Biophysical Research Communications, https://doi.org/10.1016/j.bbrc.2020.02.082

the Trp residue [4]. By using different structural and enzymatic approaches, we show that in addition to sharing a similar catalytic triad with TGs, NAT enzymes also possess in their active site an aromatic residue (Phe, Tyr or Trp) occupying a structural position similar to the Trp residue of functional TGs. The identification in active site of NATs of a conserved position involved in stabilization of transition states is of importance to better understand the catalytic mechanisms of this family of enzymes and to design potent inhibitors [20].

2. Materials and methods

2.1. Materials

Acetyl coenzyme A (AcCoA), p-nitrophenylacetate (PNPA), p-dimethylaminobenzaldehyde (DMAB), p-aminosalicylate (PAS), 2-aminofluorene (2-AF) were from Sigma-Aldrich.

2.2. Expression and purification of wild-type Mesorhizobium loti NAT1 and mutant enzymes

The pET28a-*M. loti* NAT1 vector encodes the enzyme as a (6xHis) tagged fusion protein and was used as a template to make Phe42-Tyr, Phe42Trp, Phe42His, Phe42Ile and Phe42Ala mutants as described previously [21]. Expression of the NAT proteins in *E. coli* BL21(DE3) and purification was carried out as reported previously [21]. Protein concentrations were determined using the Bradford assay (Bio-rad). Proteins were also analyzed by SDS-PAGE and stained using Coomassie stain.

2.3. NATs activity assays

PNPA assays were carried out in 96-well plates as described previously [8]. Briefly, the mixtures contained NAT enzyme (5 μg/ml final) and p-AS or 2-AF (500 μM final) in a volume of 100 μl of 25 mM Tris-HCl pH 7.5. The reaction was initiated by addition of PNPA (2 mM final) dissolved in DMSO. The rates were determined by monitoring the increase in absorbance at 405 nm using a thermostated (37 °C) plate reader (BioTek, France). The data were corrected by substracting the non specific hydrolysis of PNPA in the absence of NAT enzyme. All assays were done in triplicates and are shown as mean ± SD.

DMAB assays were also carried out in 96-well plates as described previously [8]. Briefly, 50 μL reaction mixtures, containing NAT enzyme (10 μg/mL), *p-AS* (0–300 μM) and AcCoA (0–400 μM) in 25 mM Tris-HCl pH 7.5. The reaction was quenched by adding 40 μL of cold trichloroacetic acid (40%). Finally, 100 μL DMAB (2%) in 9:1 acetonitrile and water were added to the mixture Reaction rate was monitored according the decrease of absorbance at 450 nm. All assays were done in triplicates and are shown as mean ± SD.

NATs catalyze acetyl transfer using a ping pong bi-bi mechanism. Accordingly, kinetic constants for *M. loti* NAT1 (wild type) and mutants were determined by nonlinear fitting to equation (1) or equation (2) (in case of substrate inhibition behavior at high concentration of substrates) [22]:

$$v = \frac{V\mathrm{max}AB}{KAB + KBA + AB} \quad (1)$$

$$v = \frac{V\mathrm{max}AB}{KAB\left(1 + \frac{B}{KiB}\right) + KBA + AB} \quad (2)$$

where Vmax is the maximum velocity; A and B are the concentrations of the two substrates; K_A and K_B are Michaelis-Menten constants for substrate A and B, respectively. K_iB is the inhibition constant for *p*-AS. The overall rate constant k_{cat} was calculated by using $k_{cat} = V_{max}/[E_0]$, where $[E_0]$ is total enzyme concentration.

Thermodynamic parameters ($\Delta\Delta G_B$ and $\Delta\Delta G_{TS}$) were calculated as previously described [4,23](see equations (3) and (4)) and represent, respectively, the difference between WT and mutant enzymes in free energy required to form the enzyme-substrate complex (ES) from E + S, and the difference in free energy between WT and mutants to stabilize the transition-state complex.

$$\Delta\Delta GB = \Delta GBmut - \Delta GBwt = RT \ln\left(\frac{Kmmut}{Kmwt}\right) \quad (3)$$

$$\Delta\Delta GTS = \Delta GTSmut - \Delta GTSwt = RT \ln\left[\frac{(kcat/Km)wt}{(kcat/Km)mut}\right] \quad (4)$$

2.4. Circular dichroism (CD) spectroscopy

Circular dichroism analyzes were carried out at described previously [24]. *M. loti* NAT1 and mutants (0.5 mg/ml or 2 mg/ml) were dialyzed against 20 mM potassium phosphate buffer (pH 7.5).

2.5. Structural analyzes

Coordinates of the 3D structures of human tissue transglutaminase 2 (PDB: 1KV3), human tissue transglutaminase 3 (PDB: 1L9M), human factor XIII (PDB: 1QRK), human NAT2 (PDB: 2PFR), *Mycobacterium abscessus* NAT (PDB: 4GUZ) and *Mesorhizobium loti* NAT1 (PDB:2BSZ) were retrieved from the Protein Data Bank. Structure were aligned, analyzed and visualized using Chimera software [25].

2.6. Gaussian Network Model (GNM) calculation

The GNM of *M. loti* NAT1 structure (PDB: 2BSZ) and human TG2 (PDB: 1KV3) were analyzed by Prody program [26,27]. Kirchhoff matrix was built firstly, with cut-off distance of 7 Å, and gamma value of 1.0. The slowest mode was selected for square fluctuation analysis.

3. Results and discussion

Fig. 1A shows the conservation of the Cys-His-Asp catalytic triad residues of three different active transglutaminase enzymes (including human TG2) that have been structurally aligned. This alignment also clearly indicates the structural conservation of the Trp residue (Trp 241 for human TG2) in the active site of TGs in a position close to the catalytic cysteine side chain (a distance of 5.9 Å between the thiol group of the catalytic cysteine and the Trp side chain). We also aligned the 3D structures of three well characterized and enzymatically active NATs (human NAT2, *Mycobacterium abscessus* NAT and *Mesorhizobium loti* NAT1). As shown in Fig. 1B, a similar structural arrangement of the Cys-His-Asp catalytic triad and of a Phe residue (Phe42 for *M. loti* NAT1) in the active site of these enzymes was found. Moreover, in the aligned NAT structures, this Phe residue (or Trp residue for *M. abscessus* NAT) is also positioned very close to the catalytic cysteine (distance of 5.5 A between the thiol group of Cys73 and the Phe42 side chain in *M. loti* NAT1) as observed for the Trp residue in TGs structures (Fig. 1A and B). Further structural alignment of the catalytic center of TGs and NAT enzymes (for clarity only human TG2 and *M. loti* NAT1 are

Please cite this article as: X. Xu et al., From transglutaminases (TGs) to arylamine *N*-acetyltransferases (NATs): Insight into the role of a spatially conserved aromatic amino acid position in the active site of these two families of enzymes, Biochemical and Biophysical Research Communications, https://doi.org/10.1016/j.bbrc.2020.02.082

shown in Fig. 1C) supports the observation that the Phe and Trp residues occupy a very similar spatial position in the catalytic site of these two different enzymes (Fig. 1C). In NATs, the Phe residue is part of a highly conserved motif (known as the "PFEN" motif) which participates to the active site pocket of NAT enzymes and contributes to the stability of their structures [28]. Multiple sequence alignment of the amino acid sequences of 41 enzymatically active eukaryotic and prokaryotic NAT enzymes clearly shows the high degree of conservation of this motif (Supplementary Figure 1). More importantly, the alignment indicates that in active NATs, only a Phe, Tyr or Trp residue is present in the motif thus strongly suggesting that an aromatic residue is needed at this position for NAT activity (Fig. 1D and supplementary Figure 1). In active TG enzymes, so far, only a Trp residue has been found at this equivalent position [2,4]. However, it has been shown that Tyr could partially functionally compensate for Trp in catalysis [4]. As indicated in Fig. 1E, protein flexibility analysis using Gaussian Network Model (GNM) approaches further show that the catalytic triad amino acids and the Phe/Tyr/Trp residue (referred thereafter in the manuscript as "F/Y/W" residue) of the "PFEN" motif of *M. loti NAT1* display little flexibility (with square fluctuations below 0.1) as observed in TG enzymes (Fig. 1E; for clarity only human TG2 and/or *M. loti* NAT1 square fluctuations per residue number are shown). Reduced flexibility of these catalytic residues is consistent with the need to maintain their spatial arrangement for catalysis (notably for transition state stabilization) [4,12]. As shown previously, in active TG enzymes the conserved Trp residue has been shown to be crucial for stabilization of transition state intermediates [4]. Therefore, our results reported above strongly suggest that the "F/Y/W" residue of the "PFEN" motif of NAT enzymes fulfils a role in catalysis similar to that of the active site Trp residue of functional TGs.

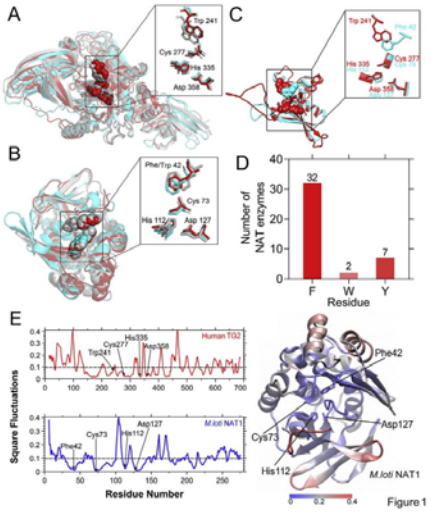

Fig. 1. Structural comparison of enzymatically active transglutaminases and arylamine N-acetyltransferases.
(A) Structural alignment of human TG2 (red color), human TG3 (grey color) and human factor XIII (cyan color). Catalytic triad residues (Cys-His-Asp) and the conserved Trp residue are shown. Numbering corresponds to amino acids of human TG2.
(B) Structural alignment of human *M. loti* NAT1 (red color), *M. abscessus* NAT (grey color) and human NAT2 (cyan color). Catalytic triad residues (Cys-His-Asp) and the conserved Phe42/Trp42 (*M. loti* NAT1 and *M. abscessus* NAT, respectively) are shown.
(C) Structural alignment of the catalytic center of human TG2 (amino acids 231–372, red color) and *M. loti* NAT1 (amino acids 38–138, cyan color). The catalytic triad residues and the Trp241 and Phe42 residues of human TG2 and *M. loti* NAT1 are shown in red and cyan colors, respectively.
(D) Residue type in the 'PFEN" motif of functional NAT enzymes. The numbers were calculated from the multiple alignment of the amino acid sequence of the 41 active NAT enzymes (see supplementary Fig. 1). Occurrence of Phe (F), Trp (W) and Tyr (Y) residue at the second position of the 'PFEN' motif of NAT enzymes is shown above each bar.
(E) Residue mobility of *M. loti* NAT1 and human TG2 were calculated using Gaussian Network Model (GNM) as described in Materials and Methods. Square fluctuations of human TG2 (PDB 1KV3) and *M. loti* NAT1 (PDB 2BSZ) were generated from the slowed mode of GNM and are shown for each residue. Mean value of all the residues for each protein is drawn in dashed line. The right panel shows a cartoon diagram of *M. loti* NAT1 with color scale of residue mobility (square fluctuations ranging from dark blue to red). . (For interpretation of the references to color in this figure legend, the reader is referred to the Web version of this article.)

Biochemical and enzymatic analyses were carried out using *M. loti* NAT1 as a model of active NAT enzymes. This NAT enzyme is well characterized both at the structural and functional level and is easily amenable to mutagenesis, heterologous expression in *E. coli*, purification to homogeneity and enzymatic assays [21,24]. In *M. loti* NAT1, the aromatic residue present in the "PFEN" motif is a Phe residue (supplementary Figure 1). Therefore, WT *M. loti* NAT1 and several mutants where the Phe42 residue was mutated to Tyr, Trp, His, Ala, or Ile were expressed in E. *Coli* as done previously with TG2 [4]. No differences in the growth and amount of *E. coli* cells were observed suggesting that no mutant was deleterious for the bacterium. All cultures (1 L of Luria-Berthani medium) yielded ~30 mg of pure and soluble proteins excepted for the F42A mutant (~5 mg protein) which was prone to aggregation at high concentrations (>0.5 mg/ml) (Fig. 2A). In order to evaluate possible structural changes due to the mutations of Phe42, far and near-UV circular dichroism (CD) spectroscopy analysis was carried out with the purified proteins. As shown in Fig. 2B, the mutations had no impact on the secondary structure of the enzyme. Similarly, near-UV CD spectroscopy showed no major differences between WT *M. loti* NAT1 and the mutants, excepted for the F42W for which a small difference in molar ellipticity was observed between 290 and 310 nm due to the introduction of the Trp residue was observed (Fig. 2C). Therefore, these experiments suggest that F42Y, F42W, F42H, and F42I mutant have an overall fold similar to the WT enzyme. This is in agreement with the crystal structure of the F42W *M. loti* NAT1 mutant which has been shown to fold exactly as the WT *M.loti* NAT1 enzyme [24]. As expected from the expression and purification experiments, analysis of the F42A mutant by CD gave inconsistent results due to its tendency to aggregate at high concentrations (>0,5 mg/ml). This further suggests that the presence at position 42 of a residue with a large side chain (larger than Ala) is needed for protein integrity. This is also consistent with data indicating that amino acids of the "PFEN" motif are involved in stabilizing the structure of NAT enzymes [28].

We next tested whether the different mutants were functional using two prototypic NAT arylamine substrates, 2-aminofluorene (2-AF) and *p*-aminosalicylate (*p*-AS). As shown in Fig. 2D, NAT activity was readily measured for WT enzyme (with a Phe at position 42), F42Y and F42W mutants. Conversely, F42H, F42I and F42A mutants displayed very poor activity. Moreover, while F42W mutant had activity similar to those of the WT enzyme, the F42Y mutant displayed activity higher than WT. These data clearly indicate that the presence of an aromatic residue at position 42 is crucial for NAT enzyme activity. This is in agreement with the strict conservation of an aromatic residue at this position in functional NAT enzymes characterized to date (Fig. 1D and supplementary Figure 1).

To better evaluate the role of the F/Y/W residue of the "PFEN"

Please cite this article as: X. Xu et al., From transglutaminases (TGs) to arylamine *N*-acetyltransferases (NATs): Insight into the role of a spatially conserved aromatic amino acid position in the active site of these two families of enzymes, Biochemical and Biophysical Research Communications, https://doi.org/10.1016/j.bbrc.2020.02.082

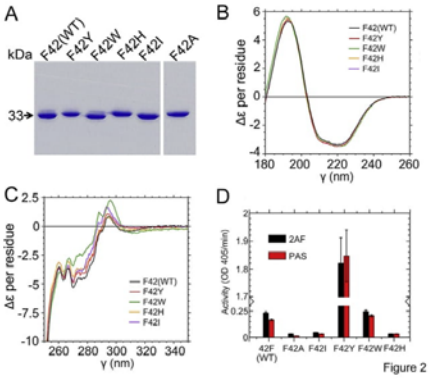

Figure 2

Fig. 2. Heterologous expression, purification and determination of NAT activity of WT M. loti NAT1 and F42Y, F42W, F42H, F42I and F42A mutants.
(A) Coomassie staining of 3 μg of WT *M. loti* NAT1, F42Y, F42W, F42H, F42I and F42A mutants.
(B) Far-UV CD spectra (180–260 nm) of WT *M. loti* NAT1, F42Y, F42W, F42H and F42I mutants.
(C) Near-UV CD spectra (250–350 nm) of WT *M. loti* NAT1, F42Y, F42W, F42H and F42I mutants.
(D) Enzymatic activity of WT *M. loti* NAT1, F42Y, F42W, F42H, F42I and F42A mutants towards 2-AF and p-AS substrates. Data are represented as means ± SD of triplicate experiments.

motif of NAT enzymes, notably in transition-state stabilization, kinetic parameters (K_m, k_{cat}, k_{cat}/K_m) were determined for the active *M. loti* NAT1 proteins (WT, F42W and F42Y) using AcCoA and PAS as model substrates. Activity of NAT enzymes occurs via a bi-bi ping pong mechanism, the initial rates were fitted to equation (1), which reflects this (see Materials and Methods and supplementary Figure 2). As substrate inhibition was observed for the F42Y mutant, the equation to which the initial rates for this mutant were fitted includes a substrate inhibition parameter (Equation (2), see Materials and Methods and supplementary Figure 2). Kinetic constants for the three M. *loti* NAT1 proteins are shown in Table 1. All enzymes were found to be highly active with k_{cat} values > 1 s^{-1}. Notably, the k_{cat} of the F42W and F42Y were 5 and 60 times higher than those of the WT enzyme. The K_m values for AcCoA and PAS were also moderately increased by the mutations (up to 13 times for K_m AcCoA of the F42Y compared to WT). Accordingly, $\Delta\Delta G_B$ values for AcCoA and PAS were also increased (values ranging from 0.57 to 1.86 kcal/mol). This is in agreement with different structural studies on *M. loti* NAT1, *P. aeruginosa* NAT, *M. Abscessus* NAT, *M. Marinum* NAT, *M. smegmatis* NAT and human NAT2 showing that the F/Y/W residue interacts with the cofactor CoA and/or aromatic substrates [10,24,28–30]. Our results are also in agreement with the data obtained in TG enzymes, where substitution of the Trp residue have a greater impact on the catalytic rate constant k_{cat} than on the Michaelis constant K_m parameter [4]. Taking into account the data reported above, the catalytic efficiencies (k_{cat}/K_{mAcCoA} and k_{cat}/K_{mPAS}) of F42W and F42Y were found to be increased compared to WT, notably for the F42Y mutant (k_{cat}/K_{mAcCoA} and k_{cat}/K_{mPAS} 5 and 24 times higher than WT, respectively (Table 1). These increases in catalytic efficiency are largely attributable to increases in k_{cat} rather than decreased in K_m and are associated with reduced $\Delta\Delta G_{TS}$ (−0.91 kcal/mol for the enzyme acetylation step and −1,53 kcal/mol for the PAS acetylation step by the F42Y mutant). Introduction of a hydroxyl and indole group in F42Y and F42W mutants may further contribute to stabilization of the transition state intermediate through hydrogen bonds as shown for TG enzymes [4]. Overall, our data indicate that the F/Y/W residue of the 'PFEN' motif of NAT enzymes is likely to be involved in transition state stabilization as shown for its counterpart in TG enzymes (Trp241 in human TG2) [4].

Table 1
Kinetic and thermodynamic parameters for PAS acetylation by (RHILO)NAT1 WT and F42W and F42Y mutants.

	WT	F42W	F42Y
k_{cat} (s^{-1})	1.36 ± 0.61	6.86 ± 1.22	82.12 ± 18.14
K_m(AcCoA) (μM)	94.11 ± 43.5	404.8 ± 125.2	1228.23 ± 252.4
K_m(PAS) (μM)	164.03 ± 49.05	665.72 ± 231.5	427.12 ± 150.3
k_{cat}/K_m(AcCoA) $(s^{-1}\mu M^{-1})$	0.014	0.017	0.067
k_{cat}/K_m(PAS) $(s^{-1}\mu M^{-1})$	0.008	0.010	0.192
$\Delta\Delta G_B$(AcCoA) (kcal/mol)		0.86	1.52
$\Delta\Delta G_B$(PAS) (kcal/mol)		0.83	0.57
$\Delta\Delta G_{TS}$(AcCoA) (kcal/mol)		−0.09	−0.91
$\Delta\Delta G_{TS}$(PAS) (kcal/mol)		−0.13	−1.53

Kinetic constants and ΔΔG values were determined as described in Materials and Methods. Values are mean ± SD of triplicate determinations.
$\Delta\Delta G_B$ = differences between WT and mutant enzymes in free energy required to form the Michaelis complex.
$\Delta\Delta G_{TS}$ = differences between WT and mutant enzymes in free energy required to stabilize the transition-state complexes.

Although more modest than its impact on catalysis, the conserved Trp residue of TG enzymes has also been shown to contribute to formation of the Michaelis complex [4]. Accordingly, we also confirmed that the F/Y/W residue of the 'PFEN' motif of NATs also contributes to substrate binding (Table 1) [10,24,29–31]. Identification of active site residues involved in the stabilization of transition state residues is important to understand catalytic mechanisms and to develop potent inhibitors [20]. As the inhibition of bacterial NAT enzymes has been shown to be of clinical interest, our data may thus be helpful in the design of NAT inhibitors [9,31,32].

Declaration of competing interest

The authors declare that they have no conflict of interest.

Acknowledgements

This work was supported by University Paris Diderot and CNRS. We thank the China Scholarship Council (CSC) for supporting the PhD of WZ, XX and RL. CM is supported by a PhD fellowship from Paris Diderot University (Ecole Doctorale BioSPC). All authors declare they have no conflict of interest.

Appendix A. Supplementary data

Supplementary data to this article can be found online at https://doi.org/10.1016/j.bbrc.2020.02.082.

References

[1] C.S. Lee, H.H. Park, Structural aspects of transglutaminase 2: functional, structural, and regulatory diversity, Apoptosis : Int. J. Program. Cell Death 22 (2017) 1057–1068, https://doi.org/10.1007/s10495-017-1396-9.
[2] S.N. Murthy, S. Iismaa, G. Begg, D.M. Freymann, R.M. Graham, L. Lorand, Conserved tryptophan in the core domain of transglutaminase is essential for catalytic activity, Proc. Natl. Acad. Sci. U.S.A. 99 (2002) 2738–2742, https://doi.org/10.1073/pnas.052715799.
[3] H. Sun, M.T. Kaartinen, Transglutaminases in monocytes and macrophages, Med. Sci. 6 (2018), https://doi.org/10.3390/medsci6040115.
[4] S.E. Iismaa, S. Holman, M.A. Wouters, L. Lorand, R.M. Graham, A. Husain, Evolutionary specialization of a tryptophan indole group for transition-state stabilization by eukaryotic transglutaminases, Proc. Natl. Acad. Sci. U.S.A.

Please cite this article as: X. Xu et al., From transglutaminases (TGs) to arylamine *N*-acetyltransferases (NATs): Insight into the role of a spatially conserved aromatic amino acid position in the active site of these two families of enzymes, Biochemical and Biophysical Research Communications, https://doi.org/10.1016/j.bbrc.2020.02.082

100 (2003) 12636–12641, https://doi.org/10.1073/pnas.1635052100.
[5] D.W. Hein, Molecular genetics and function of NAT1 and NAT2: role in aromatic amine metabolism and carcinogenesis, Mutat. Res. 506–507 (2002) 65–77, https://doi.org/10.1016/s0027-5107(02)00153-7.
[6] E. Sim, N. Lack, C.J. Wang, H. Long, I. Westwood, E. Fullam, A. Kawamura, Arylamine N-acetyltransferases: structural and functional implications of polymorphisms, Toxicology 254 (2008) 170–183, https://doi.org/10.1016/j.tox.2008.08.022.
[7] A.E. Glenn, E.P. Karagianni, A. Ulndreaj, S. Boukouvala, Comparative genomic and phylogenetic investigation of the xenobiotic metabolizing arylamine N-acetyltransferase enzyme family, FEBS Lett. 584 (2010) 3158–3164, https://doi.org/10.1016/j.febslet.2010.05.063.
[8] N. Laurieri, J. Dairou, J.E. Egleton, L.A. Stanley, A.J. Russell, J.M. Dupret, E. Sim, F. Rodrigues-Lima, From arylamine N-acetyltransferase to folate-dependent acetyl CoA hydrolase: impact of folic acid on the activity of (HUMAN)NAT1 and its homologue (MOUSE)NAT2, PloS One 9 (2014), e96370, https://doi.org/10.1371/journal.pone.0096370.
[9] E. Sim, G. Fakis, N. Laurieri, S. Boukouvala, Arylamine N-acetyltransferases–from drug metabolism and pharmacogenetics to identification of novel targets for pharmacological intervention, Adv. Pharmacol. 63 (2012) 169–205, https://doi.org/10.1016/B978-0-12-398339-8.00005-7.
[10] A.M. Abuhammad, E.D. Lowe, E. Fullam, M. Noble, E.F. Garman, E. Sim, Probing the architecture of the Mycobacterium marinum arylamine N-acetyltransferase active site, Protein Cell 1 (2010) 384–392, https://doi.org/10.1007/s13238-010-0037-7.
[11] S.J. Holton, J. Dairou, J. Sandy, F. Rodrigues-Lima, J.M. Dupret, M.E. Noble, E. Sim, Structure of Mesorhizobium loti arylamine N-acetyltransferase 1, Acta crystallogr. Section F, Struct. Biol. Cryst. Commun. 61 (2005) 14–16, https://doi.org/10.1107/S1744309104030659.
[12] X. Kubiak, I. Li de la Sierra-Gallay, A.F. Chaffotte, B. Pluvinage, P. Weber, A. Haouz, J.M. Dupret, F. Rodrigues-Lima, Structural and biochemical characterization of an active arylamine N-acetyltransferase possessing a non-canonical Cys-His-Glu catalytic triad, J. Biol. Chem. 288 (2013) 22493–22505, https://doi.org/10.1074/jbc.M113.468595.
[13] M. Martins, B. Pluvinage, I. Li de la Sierra-Gallay, F. Barbault, J. Dairou, J.M. Dupret, F. Rodrigues-Lima, Functional and structural characterization of the arylamine N-acetyltransferase from the opportunistic pathogen Nocardia farcinica, J. Mol. Biol. 383 (2008) 549–560, https://doi.org/10.1016/j.jmb.2008.08.035.
[14] J.C. Sinclair, J. Sandy, R. Delgoda, E. Sim, M.E. Noble, Structure of arylamine N-acetyltransferase reveals a catalytic triad, Nat. Struct. Biol. 7 (2000) 560–564, https://doi.org/10.1038/76783.
[15] I.M. Westwood, S.J. Holton, F. Rodrigues-Lima, J.M. Dupret, S. Bhakta, M.E. Noble, E. Sim, Expression, purification, characterization and structure of Pseudomonas aeruginosa arylamine N-acetyltransferase, Biochem. J. 385 (2005) 605–612, https://doi.org/10.1042/BJ20041330.
[16] H. Wu, L. Dombrovsky, W. Tempel, F. Martin, P. Loppnau, G.H. Goodfellow, D.M. Grant, A.N. Plotnikov, Structural basis of substrate-binding specificity of human arylamine N-acetyltransferases, J. Biol. Chem. 282 (2007) 30189–30197, https://doi.org/10.1074/jbc.M704138200.
[17] X. Xu, X. Kubiak, J.M. Dupret, F. Rodrigues-Lima, Arylamine N-acetyltransferases: a structural perspective. Comments regarding the BJP paper by Zhou et al. Br. J. Pharmacol. 171 (2013) 279–280, https://doi.org/10.1111/bph.12273, 2014.
[18] F. Rodrigues-Lima, C. Delomenie, G.H. Goodfellow, D.M. Grant, J.M. Dupret, Homology modelling and structural analysis of human arylamine N-acetyltransferase NAT1: evidence for the conservation of a cysteine protease catalytic domain and an active-site loop, Biochem. J. 356 (2001) 327–334, https://doi.org/10.1042/0264-6021:3560327.
[19] B. Riddle, W.P. Jencks, Acetyl-coenzyme A: arylamine N-acetyltransferase. Role of the acetyl-enzyme intermediate and the effects of substituents on the rate, J. Biol. Chem. 246 (1971) 3250–3258.
[20] R.A. Copeland, Evaluation of enzyme inhibitors in drug discovery. A guide for medicinal chemists and pharmacologists, Methods Biochem. Anal. 46 (2005), 1-265.
[21] N. Atmane, J. Dairou, D. Flatters, M. Martins, B. Pluvinage, P. Derreumaux, J.M. Dupret, F. Rodrigues-Lima, The conserved glycine/alanine residue of the active-site loop containing the putative acetylCoA-binding motif is essential for the overall structural integrity of Mesorhizobium loti arylamine N-acetyltransferase 1, Biochem. Biophys. Res. Commun. 361 (2007) 256–262, https://doi.org/10.1016/j.bbrc.2007.07.034.
[22] A. C.-B, Fundamentals of Enzyme Kinetics, second ed. ed., Portland Press, London, 1995.
[23] A.J. Wilkinson, A.R. Fersht, D.M. Blow, G. Winter, Site-directed mutagenesis as a probe of enzyme structure and catalysis: tyrosyl-tRNA synthetase cysteine-35 to glycine-35 mutation, Biochemistry 22 (1983) 3581–3586, https://doi.org/10.1021/bi00284a007.
[24] X. Xu, I. Li de la Sierra-Gallay, X. Kubiak, R. Duval, A.F. Chaffotte, J.M. Dupret, A. Haouz, F. Rodrigues-Lima, Insight into cofactor recognition in arylamine N-acetyltransferase enzymes: structure of Mesorhizobium loti arylamine N-acetyltransferase in complex with coenzyme A, Acta Crystallogr. Sect. D Biol. Crystallogr. 71 (2015) 266–273, https://doi.org/10.1107/S139900471402522X.
[25] E.F. Pettersen, T.D. Goddard, C.C. Huang, G.S. Couch, D.M. Greenblatt, E.C. Meng, T.E. Ferrin, UCSF Chimera–a visualization system for exploratory research and analysis, J. Comput. Chem. 25 (2004) 1605–1612, https://doi.org/10.1002/jcc.20084.
[26] A. Bakan, A. Dutta, W. Mao, Y. Liu, C. Chennubhotla, T.R. Lezon, I. Bahar, Evol and ProDy for bridging protein sequence evolution and structural dynamics, Bioinformatics 30 (2014) 2681–2683, https://doi.org/10.1093/bioinformatics/btu336.
[27] A. Bakan, L.M. Meireles, I. Bahar, ProDy: protein dynamics inferred from theory and experiments, Bioinformatics 27 (2011) 1575–1577, https://doi.org/10.1093/bioinformatics/btr168.
[28] J. Sandy, A. Mushtaq, S.J. Holton, P. Schartau, M.E. Noble, E. Sim, Investigation of the catalytic triad of arylamine N-acetyltransferases: essential residues required for acetyl transfer to arylamines, Biochem. J. 390 (2005) 115–123, https://doi.org/10.1042/BJ20050277.
[29] A. Cocaign, X. Kubiak, X. Xu, G. Garnier, I. Li de la Sierra-Gallay, L. Chi-Bui, J. Dairou, F. Busi, A. Abuhammad, A. Haouz, J.M. Dupret, J.L. Herrmann, F. Rodrigues-Lima, Structural and functional characterization of an arylamine N-acetyltransferase from the pathogen Mycobacterium abscessus: differences from other mycobacterial isoforms and implications for selective inhibition, Acta Crystallogr. Sect. D Biol. Crystallogr. 70 (2014) 3066–3079, https://doi.org/10.1107/S1399004714021282.
[30] E. Fullam, I.M. Westwood, M.C. Anderton, E.D. Lowe, E. Sim, M.E. Noble, Divergence of cofactor recognition across evolution: coenzyme A binding in a prokaryotic arylamine N-acetyltransferase, J. Mol. Biol. 375 (2008) 178–191, https://doi.org/10.1016/j.jmb.2007.10.019.
[31] J. Sandy, S. Holton, E. Fullam, E. Sim, M. Noble, Binding of the anti-tubercular drug isoniazid to the arylamine N-acetyltransferase protein from Mycobacterium smegmatis, Protein Sci. : Publ. Protein Soc. 14 (2005) 775–782, https://doi.org/10.1110/ps.041163505.
[32] B. Pluvinage, J. Dairou, O. Possot, M. Martins, A. Fouet, J.M. Dupret, F. Rodrigues-Lima, Cloning and molecular characterization of three arylamine N-acetyltransferase genes from Bacillus anthracis: identification of unusual enzymatic properties and their contribution to sulfamethoxazole resistance, Biochemistry 46 (23) (2007) 7069–7078.

Please cite this article as: X. Xu et al., From transglutaminases (TGs) to arylamine *N*-acetyltransferases (NATs): Insight into the role of a spatially conserved aromatic amino acid position in the active site of these two families of enzymes, Biochemical and Biophysical Research Communications, https://doi.org/10.1016/j.bbrc.2020.02.082

Supplemental material to this article can be found at:
http://molpharm.aspetjournals.org/content/suppl/2019/06/20/mol.119.116319.DC1

1521-0111/96/2/297–306$35.00
MOLECULAR PHARMACOLOGY
Copyright © 2019 by The American Society for Pharmacology and Experimental Therapeutics
https://doi.org/10.1124/mol.119.116319
Mol Pharmacol 96:297–306, August 2019

MOLECULAR PHARMACOLOGY

T-Cell Protein Tyrosine Phosphatase Is Irreversibly Inhibited by Etoposide-Quinone, a Reactive Metabolite of the Chemotherapy Drug Etoposide[S]

Qing Nian, Jérémy Berthelet, Wenchao Zhang, Linh-Chi Bui, Rongxing Liu, Ximing Xu, Romain Duval, Saravanan Ganesan, Thibaut Leger, Christine Chomienne, Florent Busi, Fabien Guidez, Jean-Marie Dupret, and Fernando Rodrigues Lima

Université de Paris, BFA, UMR 8251, CNRS, Paris, France (Q.N., J.B., W.Z., L.-C.B., R.L., F.B., J.-M.D., F.R.L.); Key Laboratory of Marine Drugs, Chinese Ministry of Education, School of Medicine and Pharmacy, Ocean University of China, Qingdao, China (X.X.); Université de Paris, BIGR, UMRS 1134, INSERM, Paris, France (R.D.); Université de Paris, Institut de Recherche Saint-Louis, UMRS 1131, INSERM, Paris, France (S.G., C.C., F.G.); Université de Paris, IJM, UMR 7592, CNRS, Paris, France (T.L.); and Service de Biologie Cellulaire, Assistance Publique des Hôpitaux de Paris, Hôpital Saint Louis, Paris, France (C.C.)

Received February 18, 2019; accepted June 7, 2019

ABSTRACT

Etoposide is a widely prescribed anticancer drug that is, however, associated with an increased risk of secondary leukemia. Although the molecular basis underlying the development of these leukemias remains poorly understood, increasing evidence implicates the interaction of etoposide metabolites [i.e., etoposide quinone (EQ)] with topoisomerase II enzymes. However, effects of etoposide quinone on other cellular targets could also be at play. We investigated whether T-cell protein tyrosine phosphatase (TCPTP), a protein tyrosine phosphatase that plays a key role in normal and malignant hematopoiesis through regulation of Janus kinase/signal transducer and activator of transcription signaling, could be a target of EQ. We report here that EQ is an irreversible inhibitor of TCPTP phosphatase (IC_{50} = ~7 μM, second-order rate inhibition constant of ~810 $M^{-1} \cdot min^{-1}$). No inhibition was observed with the parent drug. The inhibition by EQ was found to be due to the formation of a covalent adduct at the catalytic cysteine residue in the active site of TCPTP. Exposure of human hematopoietic cells (HL60 and Jurkat) to EQ led to inhibition of endogenous TCPTP and concomitant increase in STAT1 tyrosine phosphorylation. Our results suggest that in addition to alteration of topoisomerase II functions, EQ could also contribute to etoposide-dependent leukemogenesis through impairment of key hematopoietic signaling enzymes, such as TCPTP.

Introduction

Protein tyrosine phosphatases (PTPs) are important regulators of the activity of numerous signaling pathways involved in major cellular processes such as cell growth, proliferation, and differentiation (Tonks, 2006; Tiganis and Bennett, 2007; Pike and Tremblay, 2016). T-cell protein tyrosine phosphatase (TCPTP) is a cytosolic tyrosine phosphatase which is ubiquitously expressed. However, the highest levels of expression of TCPTP are found in hematopoietic cells, where this enzyme modulates growth factor and cytokine signaling pathways, thus contributing to immune and hematopoietic cell homeostasis (Wiede et al., 2012; Pike and Tremblay, 2016). In particular, TCPTP negatively regulates Janus kinase (JAK)/signal transducer and activator of transcription (STAT) signaling through the dephosphorylation of different tyrosine phosphorylated JAK/STAT proteins, such as STAT1 or JAK1 (ten Hoeve et al., 2002; Dorritie et al., 2014; Pike and Tremblay, 2016). In addition to STAT1, TCPTP also dephosphorylates STAT3 and STAT5 and negatively regulates their activation (Pike and Tremblay, 2016). The JAK/STAT pathway plays a crucial role in hematopoiesis, and aberrant activation of STAT signaling is involved in leukemogenesis (Dorritie et al., 2014; Pike and Tremblay, 2016). Interestingly, deletions or inactivating mutations of TCPTP were identified in T-cell leukemia and non-Hodgkin's lymphoma and associated with elevated STAT signaling and changes in gene expression (Kleppe et al., 2010, 2011a,b; Pike and Tremblay, 2016). In addition, it has been reported that TCPTP is overexpressed in MYC-driven mouse B-cell lymphoma (Young et al., 2009). The importance of TCPTP in hematopoiesis is further supported by knockout mouse models

This work was supported by University Paris Diderot and CNRS. Q.N., W.Z., and R.L. are supported by China Scholarship Council Ph.D. fellowships. J.B. was supported by a Ph.D. fellowship from Région Ile de France (Cancéropole 2015).
https://doi.org/10.1124/mol.119.116319.
[S] This article has supplemental material available at molpharm.aspetjournals.org.

ABBREVIATIONS: DTT, dithiothreitol; EQ, etoposide quinone; ETOP, etoposide; FA, formic acid; FAM, fluorescein amadite; 5-IAF, fluorescein 5-iodoacetamide; IFNγ, interferon γ; JAK, Janus kinase; MPO, myeloperoxidase; MS, mass spectrometry; MS/MS, tandem MS; NBT, nitroblue tetrazolium; pNPP, p-nitrophenyl phosphate; PTP, protein tyrosine phosphatase; RP-UFLC, reverse-phase ultrafast liquid chromatography; STAT, signal transducer and activator of transcription; TCPTP, T-cell protein tyrosine phosphatase.

Downloaded from molpharm.aspetjournals.org at ASPET Journals on May 8, 2022

(PTPN2−/−), where the absence of TCPTP induces severe hematopoietic defects (affecting lymphoid, myeloid, and erythroid lineages) and progressive systemic inflammation leading to death (You-Ten et al., 1997; Bourdeau et al., 2007; Heinonen et al., 2009; Wiede et al., 2012). These studies highlight the important role of TCPTP in normal and malignant hematopoiesis.

Etoposide (ETOP) is a widely used anticancer drug to treat a variety of human malignancies (Hande, 1998; Baldwin and Osheroff, 2005). The mechanisms of action proposed for its antitumor activity are based mainly on its interaction with topoisomerase II (Baldwin and Osheroff, 2005; Deweese and Osheroff, 2009). ETOP is indeed known to affect the catalytic cycle of these enzymes and to stabilize topoisomerase II–bound DNA strand breaks, which have the potential to activate cell death pathways (Jacob et al., 2011). Despite the wide clinical use of ETOP, this chemotherapeutic drug is known to induce treatment-related leukemias (Baldwin and Osheroff, 2005; Pendleton et al., 2014). In humans, ETOP can be oxidized by cytochrome P450 (CYP3A4) and myeloperoxidases into etoposide quinone (EQ), which was found to have an effect on topoisomerase II enzymes several times stronger than that of the parent drug (Zhuo et al., 2004; Fan et al., 2006; Jacob et al., 2011; Vlasova et al., 2011). Although the molecular basis for ETOP-induced leukemogenesis is not well understood, evidence increasingly indicates that EQ is a critical contributor to the development of ETOP-related secondary leukemia, in particular through alteration of topoisomerase II functions (Gantchev and Hunting, 1998; Kagan et al., 1999; Fan et al., 2006; Vlasova et al., 2011; Smith et al., 2014; Gibson et al., 2016). However, interactions of ETOP reactive metabolites with other cellular proteins and macromolecules may also contribute to ETOP-dependent leukemogenesis (Fan et al., 2006; Rojas et al., 2009).

We show here that EQ is an irreversible inhibitor of TCPTP phosphatase activity. Kinetic and molecular analyses using purified human TCPTP indicated that the irreversible inhibition of the enzyme by EQ is due to the formation of a covalent adduct with its catalytic cysteine. Accordingly, exposure of cultured hematopoietic cells to EQ leads to the irreversible inhibition of the endogenous TCPTP with a concomitant increase in cellular STAT1 phosphorylation. Interestingly, it is well known that dysregulation of the JAK/STAT signaling pathway is involved in leukemogenic processes (Benekli et al., 2009; Dorritie et al., 2014). Altogether, our data suggest that in addition to the disruption of topoisomerase II functions, EQ may also contribute to ETOP-related leukemia through alteration of important hematopoietic signaling enzymes, such as TCPTP.

Materials and Methods

Chemicals and Cells. ETOP and EQ were obtained from Toronto Research Chemicals (North York, Canada). Hydrogen peroxide, *N*-ethylmaleimide, fluorescein 5-iodoacetamide (5-IAF), myeloperoxidase (MPO), *p*-nitrophenyl phosphate (pNPP), sodium orthovanadate, nitroblue tetrazolium (NBT), and dimethylsulfoxide (DMSO) were purchased from Sigma-Aldrich (France). ETOP and EQ were diluted in DMSO at a stock concentration of 100 mM. HL60 (human acute promyelocytic leukemia) and Jurkat (human acute T-cell leukemia) cells were from Sigma-Aldrich.

Expression and Purification of Recombinant Human TCPTP Enzyme. Human TCPTP enzyme was expressed and purified as previously described (Duval et al., 2015), using BL21 (DE3) *Escherichia coli*, and transformed with a pET28a plasmid containing the cDNA of human PTNP2 (TC45 variant). The purified enzyme was reduced by incubation with 10 mM dithiothreitol (DTT) for 10 minutes in ice before buffer exchange with a PD-10 column (GE Healthcare, France) into 25 mM Tris-HCl, 150 mM NaCl, pH 7.5 (reaction buffer). The protein concentration was determined by the Bradford reagent (Bio-Rad, France), and purity was assessed by SDS-PAGE and Coomassie staining. Purified recombinant human TCPTP (1 mg/ml) was stored at −80°C until use.

Determination of TCPTP Activity Using pNPP Assay. The phosphatase activity was measured using pNPP as substrate as described previously (Montalibet et al., 2005). Typically, samples containing TCPTP were diluted 10 times with 100 mM sodium acetate buffer (pH 6, 1 mM DTT) containing 5 mM pNPP. The formation of the product (*p*-nitrophenol) was tracked by continuous measurement of the absorbance at 405 nm at 37°C using a thermostatic microplate reader (BioTek, France) in a total volume of 250 μl. The final concentration of TCPTP during the assay was 100 nM.

Determination of TCPTP Activity Using a Tyrosine-Phosphorylated STAT1 Peptide (Fluorescein Amadite-Phosphorylated STAT1). The tyrosine phosphatase activity of TCPTP was measured by reverse-phase ultrafast liquid chromatography (RP-UFLC) using a fluorescein amadite (FAM)-conjugated peptide derived from the sequence of human STAT1 ($_{697}$KGTGYIKTE$_{705}$, where the Y701 is phosphorylated) as described previously (Duval et al., 2015). In brief, samples containing TCPTP were diluted 100-fold with acetate buffer. Aliquots (100 μl) were incubated for 30 minutes at 37°C in the presence of 50 μM FAM–phosphorylated STAT1 peptide (final concentration of TCPTP was 10 nM). The reaction was stopped with 100 μl of 15% (v/v) $HClO_4$ prior to analysis by RP-UFLC using a Shim-pack XR ODS column (Shimadzu, France) connected to a Prominence Shimadzu UFLC system.

Effects of Etoposide and Etoposide Quinone on TCPTP Activity. Recombinant TCPTP (1 μM) was incubated with ETOP or different concentrations of EQ in 100 mM sodium acetate, pH 6, for 30 minutes at 37°C (total volume of 50 μl). Samples were diluted 10 times, then assayed for residual TCPTP activity using pNPP. To obtain the IC_{50} value, the dose-response curves were fitted with the Hill equation, $TCPTP_{activity} = 100/(1 + 10\text{^}((\log IC_{50} - [EQ]) \times Hillslope))$, where IC_{50} is the half-maximal inhibitory concentration of EQ. The effects of ETOP and EQ on the TCPTP tyrosine phosphatase activity were also assessed by an RP-UFLC approach using a tyrosine phosphorylated STAT1 peptide (see previous section).

Effects of Reducing Agents and Buffer Exchange on TCPTP Inhibited by EQ. TCPTP (1 μM) was first incubated with EQ (40 μM) or ETOP (100 μM) in 100 mM sodium acetate, pH 6, for 30 minutes at 37°C (total volume of 50 μl). Samples were either incubated with 1 or 10 mM DTT (10 minutes at room temperature) or buffer exchanged (PD Spin Trap G-25; GE Healthcare) to 100 mM sodium acetate, pH 6, prior to measurement of residual TCPTP activity using pNPP.

Fluorescein-Conjugated Iodoacetamide Labeling, Nitroblue Tetrazolium Staining, and Detection of Oxidized TCPTP Catalytic Cysteine. TCPTP (1 μM) was first incubated with ETOP (100 μM) or EQ (40 μM) in 100 mM sodium acetate, pH 6, at 37°C for 30 minutes followed by the addition of 20 μM 5-IAF (total volume of 50 μl) and further incubation at 37°C for 10 minutes (in the dark). Samples were separated by SDS-PAGE and transferred onto nitrocellulose membranes. 5-IAF covalent labeling of TCPTP cysteine residues was detected by western blot using antifluorescein antibodies (reference number 11426346910; Sigma-Aldrich). Membranes were stripped and further probed with anti-TCPTP antibody (reference number SAB4200249; Sigma-Aldrich).

The formation of covalent adducts of EQ on TCPTP was detected by NBT redox-cycling staining as reported previously (Paz et al., 1991). In brief, TCPTP (1 μM) was incubated with ETOP (100 μM) or EQ (40 μM) in 100 mM sodium acetate, pH 6, at 37°C for 30 minutes (total

Downloaded from molpharm.aspetjournals.org at ASPET Journals on May 8, 2022

volume 50 μl). Samples were separated by SDS-PAGE and transferred onto nitrocellulose membranes. EQ-bound TCPTP on the membranes was stained by incubation with 0.6 mg/ml NBT in 2 M potassium glycinate, pH 10, for 30–45 minutes in the dark at room temperature. Next, membranes were washed thoroughly with PBS and further probed with anti-TCPTP antibody (reference number 11426346910; Sigma-Aldrich).

For the detection of oxidized TCPTP catalytic cysteine, TCPTP (1 μM) was treated with ETOP (100 μM), EQ (40 μM), or H_2O_2 (100 μM) in a total volume of 50 μl. Aliquots were then separated by SDS-PAGE and analyzed by western blot with a specific antioxidized PTP active site antibody (reference number MAB 2844; R&D Systems) as described previously (Duval et al., 2015).

Effects of MPO-Dependent Bioactivation of ETOP into EQ. Myeloperoxidase was used to bioactivate ETOP into EQ as described previously (Kagan et al., 1999; Fan et al., 2006; Vlasova et al., 2011). To this end, MPO (5 U) was incubated with ETOP (100 μM) and H_2O_2 (100 μM) in 100 mM sodium acetate, pH 6.5, for 30 minutes at room temperature (in a total volume of 1 ml). Heat-inactivated MPO (boiled for 30 minutes) was used as a negative control. Catalase (300 U/ml final concentration) was added to remove excess H_2O_2. Finally, reaction mix (48 μl) was added to recombinant TCPTP (1 μM final concentration) in 100 mM sodium acetate, pH 6, and incubated for 30 minutes at 37°C (total volume of 50 μl). After incubation, and a 10-times dilution, the residual activity of TCPTP was measured using the pNPP assay. IAF and NBT labeling and detection of oxidized TCPTP catalytic cysteine were also carried out on TCPTP treated with MPO as described earlier.

Kinetics of TCPTP Inhibition by EQ. The kinetic data were analyzed as reported by Copeland (2005) for irreversible inhibitors. The kinetic data were fitted and plotted using Qtiplot software (http://www.qtiplot.com/). In brief, TCPTP (3 μM) was incubated with different concentrations of EQ (pseudo first-order conditions) in 100 mM sodium acetate, pH 6, at 37°C. At different time points, aliquots were removed and assayed for residual TCPTP activity using pNPP assay. The rate of inhibition of TCPTP by EQ can be represented as follows: ln [% residual activity] = $k_{obs} \times t$ (where t is time and k_{obs} is the apparent first-order inhibition rate constant). The apparent first-order inhibition rate constants ($k_{obs} = k_{inact} \times [EQ]$) can be calculated for each EQ concentration from the slope of the natural log (ln) of percentage residual activity plotted against time. The second-order rate constant (k_{inact}) was determined from the slope of k_{obs} plotted against EQ concentrations.

Effects of EQ on TCPTP in the Presence of the Competitive PTP Inhibitor Orthovanadate (Na_3VO_4). TCPTP (1 μM) was incubated with 1 mM orthovanadate in the presence or absence of EQ (40 μM) in 100 mM sodium acetate, pH 6, at 37°C for 30 minutes. Samples were diluted 10 times in 100 mM sodium acetate, pH 6, containing 1 mM EDTA and residual TCPTP activity measured using pNPP assay.

Molecular Docking. TCPTP protein structure data were obtained from the RCSB Protein Data Bank database (Protein Data Bank ID 1L8K). The protein structure was prepared using the PrepWizard module in the Schrödinger suite (Schrödinger LLC, https://www.schrodinger.com). In brief, missing side chains or loops were completed. The pKa values of residues were predicted and hydrogens were added at pH 7. Water molecules were removed. Finally, the structure was optimized by a restrained energy minimization with the OPLS3 force field. The ligand (EQ) was constructed by a Maestro module and was also refined by the OPLS3 force field. Covalent docking was carried out with the catalytic residue Cys 216 selected as the docking center. Grid box size was set to $20 \times 20 \times 20$ Å^3. Michael addition reaction type was selected for the covalent docking. The final conformation was selected, and images were prepared with VMD program (Humphrey et al., 1996).

Mass Spectrometry Analysis. TCPTP (1 μM) was incubated with 100 μM EQ for 30 minutes at 37°C in 100 mM sodium acetate, pH 6. After reduction with DTT (10 mM), the samples were diluted 10 times in sodium acetate buffer, and unmodified thiol moieties of cysteines were blocked by addition of 10 mM *N*-ethylmaleimide for 10 minutes. Samples were then incubated overnight at 37°C with trypsin (Promega, France) at 12.5 ng/μl in 25 mM ammonium bicarbonate, pH 8.0. The supernatant containing peptides was acidified with formic acid (FA); desalted on C18 tips (Pierce C18 tips; Thermo Scientific, France); and eluted in 10 μl of 70% acetonitrile, 0.1% FA. Desalted samples were evaporated using a SpeedVac, then taken up in 10 μl of buffer A (buffer A: water, 0.1% FA), and 5 μl were injected on a nanoLC high-performance liquid chromatography system (Thermo Scientific) coupled to a hybrid quadrupole-Orbitrap mass spectrometer (Thermo Scientific). Peptides were loaded on a reverse-phase C18 μ-precolumn (C18 PepMap100, 5 μm, 100 A, 300 μm i.d. × 5 mm) (ThermoFischer, Paris France) and separated on a C18 column (EASY-spray C18 column, 75 μm i.d. × 50 cm) (ThermoFischer) at a constant flow rate of 300 nl/min, with a 120-minute gradient of 2%–40% buffer B (buffer B: 20% water, 80% acetonitrile, 0.1% FA). Mass spectrometry (MS) analyses were performed by the Orbitrap cell with a resolution of 120,000 (at *m/z* 200). Tandem MS (MS/MS) fragments were obtained by higher-energy collisional dissociation activation (collisional energy of 28%) and acquired in the ion trap in top-speed mode with a total cycle of 3 seconds. The database search was performed against the Swiss-Prot database (02/2017) and the *Homo sapiens* taxonomy with Mascot v2.5.1 software (Matrix Sciences, Boston, MA) with the following parameters: tryptic peptides only with up to two missed cleavages, variable modifications: cysteine EQ and methionine oxidation. MS and MS/MS error tolerances were set to 7 ppm and 0.5 Da, respectively. Peptide identifications were validated using a 1% false discovery rate threshold obtained by Proteome Discoverer (version 2.2; Thermo Scientific) and the percolator algorithm. The candidate sequences modified by EQ were manually inspected for de novo sequencing.

Cell Culture, TCPTP Immunoprecipitation, and STAT1 Phosphorylation Kinetics. HL60 and Jurkat cells were maintained in RPMI 1640 medium supplemented with 10% heat-inactivated fetal bovine serum and 1 mM L-glutamine in T-75 flasks. Cells (60 ml at 2×10^6 cells/ml) were washed with PBS prior to exposure to 50 μM EQ (or DMSO) for 30 minutes at 37°C (5% CO_2) in RPMI 1640 medium.

For immunoprecipitation of endogenous TCPTP, treated cells were washed with PBS and resuspended in lysis buffer (PBS, 1% Triton X-100, 1 mM sodium orthovanadate, phosphatase cocktail inhibitor 2, and protease inhibitor cocktail; Sigma-Aldrich) for 20 minutes. Cell lysates were centrifuged at 15,000*g* for 10 minutes at 4°C, and supernatants (whole cell extracts) were taken. TCPTP was immunoprecipitated by incubating 1 mg of whole cell extracts with 1 μg of polyclonal TCPTP antibody (reference number SAB4200249; Sigma-Aldrich) overnight at 4°C. Samples were then rocked for 1 hour at 4°C in the presence of 30 μl of protein A–Agarose (Santa Cruz, Germany). The immunobeads were harvested by centrifugation, washed three times with lysis buffer, and split into two portions. One part of the beads was incubated with 50 μM FAM–phosphorylated STAT1 peptide to measure residual immunoprecipitated-TCPTP activity by RP-UFLC as described earlier. The second part of immunobeads was incubated with nonreducing Laemmli sample buffer. Eluates were separated by SDS-PAGE and analyzed by western blot using an anti-TCPTP antibody (reference number MAB 1930; R&D Systems).

For the STAT1 phosphorylation kinetic analysis, cells treated with EQ or DMSO were washed with fresh medium and incubated for 20 minutes in medium supplemented with 10 ng/ml of human interferon γ (IFNγ). Cells were then washed in fresh medium, and aliquots (2×10^6 cells) were removed at different time points, washed with PBS, and lysed. STAT1 activation was then assayed in lysates by western blot using anti-phospho-STAT1 (phosphorylated tyrosine 701, reference number 9176; Cell Signaling Technology). Membranes were reprobed sequentially with anti-STAT1 (reference number 9167;

Downloaded from molpharm.aspetjournals.org at ASPET Journals on May 8, 2022

Cell Signaling Technology), anti-TCPTP (reference number SAB4200249; Sigma-Aldrich), and anti-β actin (reference number 3700; Cell Signaling Technology) antibodies. Quantification of STAT1 phosphorylation in western blots was carried out using ImageJ software (National Institutes of Health) (Schneider et al., 2012).

Statistical Analysis. The study was designed in such a manner that three independent replicates were conducted for each experiment prior to statistical analysis. All data are expressed as the mean ± S.D. All statistical analyses were then carried out using Prism 5.03 (GraphPad Software, La Jolla, CA) with a threshold of $P < 0.05$ to consider differences as statistically significant. For experiments where multiple groups were compared with control, a one-way analysis of variance (ANOVA) was used. If statistical significance was reached, data were further analyzed with Dunnett's post hoc test. For experiments between two groups, a two-tailed Student's t test was used. No experiment was removed from the final analysis. For quantitative polymerase chain reaction experiments (Supplemental Fig. 3), six experimental points were used in the data analysis, which consisted of a Student's t test to compare the effect of EQ versus control in cells induced with interferon γ.

Results

Effect of Etoposide Quinone on Activity of TCPTP. The effects of ETOP and EQ on the activity of recombinant human TCPTP expressed and purified from bacteria were assessed. As a first experiment, TCPTP was incubated in the presence of 100 μM ETOP or increasing concentrations of EQ prior to the measurement of the residual enzyme activity with the chromogenic pNPP phosphatase substrate. As shown in Fig. 1A, EQ inhibits the hydrolysis of this substrate in a dose-dependent manner with half-maximal inhibitory concentration (IC_{50}) values of 7.3 μM (Supplemental Fig. 1). Conversely, 100 μM ETOP did not display any inhibitory effect, therefore suggesting that inhibition of TCPTP activity could occur with EQ but not with the parent drug. These results were further validated with a UFLC-based enzyme assay using a more specific TCPTP substrate consisting of a phospho-STAT1 peptide derived from the sequence of human STAT1 ($_{697}$KGTGYIKTE$_{705}$, where the Y701 is phosphorylated) as described by Duval et al. (2015). UFLC quantification of the dephosphorylated STAT1 confirms that EQ, but not ETOP, inhibits TCPTP phosphatase activity (Fig. 1B).

Etoposide Quinone Covalently Reacts with TCPTP Cysteine Residues. As EQ, but not ETOP, inhibits TCPTP activity, we next hypothesized that this inhibition could result from the general chemical reactivity properties of quinone chemicals and, notably, the possibility that they react covalently with proteins (Bolton and Dunlap, 2017; Bolton et al., 2018). NBT can be used to stain proteins covalently modified by quinones to form quinone proteins. As shown in Fig. 2A, NBT reaction generated only a signal when TCPTP was treated with EQ, confirming the presence of covalent quinone adducts on TCPTP.

Knowing that protein cysteinyl residues are common nucleophilic targets of quinone electrophiles, we therefore strived to show whether TCPTP cysteinyl residues could be modified after exposure to EQ. TCPTP was treated with EQ and then incubated with fluorescein-conjugated iodoacetamide (IAF), a specific cysteinyl thiol reagent. Our results (Fig. 2B) show that EQ decreased IAF labeling of TCPTP, therefore indicating that EQ reacts with cysteine residues of TCPTP.

Quinone chemicals can also display redox-cycling properties that lead to generation of reactive oxygen species. In addition, it is known that TCPTP can be inhibited by reactive oxygen species through the oxidation of its catalytic cysteine residue (Ostman et al., 2011). We therefore evaluated whether EQ could oxidize the catalytic cysteine residue of TCPTP using an antibody specifically directed against the oxidized catalytic cysteine residue of protein tyrosine phosphatases (Duval et al., 2015). Figure 2C shows that EQ treatment does not lead to TCPTP active site cysteine oxidation, and that the basal oxidation of catalytic cysteine achieved during the experiment and observed in control and ETOP treatment is decreased with EQ. This is in agreement with the formation of an EQ adduct on the catalytic cysteine of the enzyme. Therefore, these data altogether suggest a loss of TCPTP activity due to EQ adduction of the catalytic cysteine.

When clinically administered to patients, ETOP is biochemically metabolized to EQ by different enzymes, notably myeloperoxidase, which is highly expressed in bone marrow hematopoietic cells (Fan et al., 2006; Atwal et al., 2017). To test if EQ generated from peroxidase/H_2O_2-dependent bioactivation of ETOP would yield similar TCPTP inhibition, we used an in vitro peroxidase activation system that mimics the

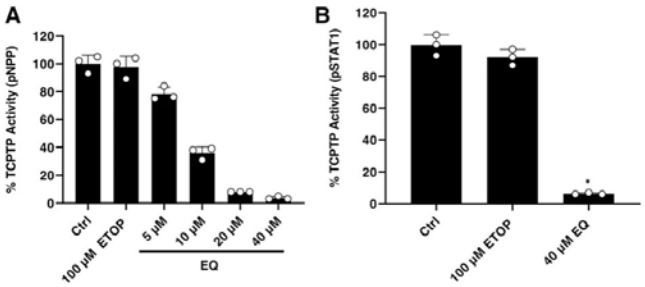

Fig. 1. Effect of ETOP and EQ on human TCPTP activity. (A) Effect of ETOP and EQ on TCPTP activity measured by pNPP dephosphorylation. One micromolar TCPTP was incubated with 100 μM ETOP and 5–40 μM EQ for 30 minutes at 37°C and diluted 10-fold prior to measurement of residual activity in the presence of 5 mM pNPP as described in the *Materials and Methods* section. Results are the mean of three independent experiments; error bars indicate S.D. (B) Measurements of TCPTP FAM–phosphorylated STAT1 peptide dephosphorylation activity. TCPTP was incubated with 100 μM ETOP and 40 μM EQ for 30 minutes at 37°C and residual TCPTP activity measured as described under *Materials and Methods*. Results are the mean of three independent experiments; error bars indicate S.D. *$P < 0.05$, determined using ANOVA followed by Dunnett's post hoc analysis. Ctrl, control.

Downloaded from molpharm.aspetjournals.org at ASPET Journals on May 8, 2022

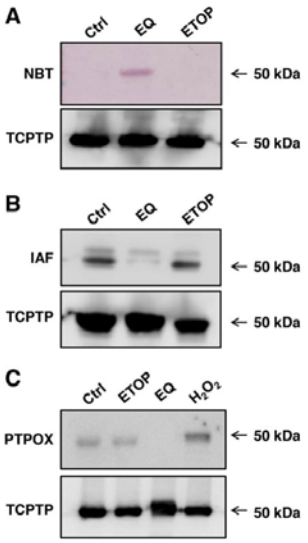

Fig. 2. Modification of TCPTP cysteine residues by EQ. (A) Detection of human TCPTP adducts by NBT staining. Human TCPTP was incubated with 40 μM EQ or 100 μM ETOP for 30 minutes. Samples were separated by SDS-PAGE and transferred onto a nitrocellulose membrane. Quinone adducts were detected by NBT staining as described in *Materials and Methods*. The membrane is representative of three independent experiments. (B) 5-IAF staining of human TCPTP to detect unmodified cysteines. Human TCPTP was incubated with 40 μM EQ or 100 μM ETOP for 30 minutes prior incubation for 10 minutes with 20 μM 5-IAF. SDS-PAGE was transferred onto a nitrocellulose membrane. IAF adducts were detected by fluorescence after SDS-PAGE as described in the *Materials and Methods* section. The membrane is representative of three independent experiments. (C) Detection of TCPTP protein oxidation. Human TCPTP was incubated with 100 μM ETOP, 40 μM EQ, or 100 μM H_2O_2 for 30 minutes prior to analysis with western blot using an antioxidized TCPTP active site antibody as described in *Materials and Methods*. The membrane is representative of three independent experiments. Ctrl, control.

bioactivation of ETOP into EQ in hematopoietic cells described previously (Kagan et al., 1999; Vlasova et al., 2011). As shown in Supplemental Fig. 2A, in the presence of a functional peroxidase/H_2O_2 enzymatic system, ETOP is capable of inhibiting TCPTP activity with concomitant quinone adduction (NBT labeling) and loss of IAF cysteine labeling of TCPTP protein (Supplemental Fig. 2, B and C). Conversely, when inactive peroxidase is used, no inhibition of TCPTP and quinone adduction on cysteine residues is observed (Supplemental Fig. 2). This confirms that EQ, but not the parent drug, can inhibit TCPTP activity through covalent adduction, a result which is consistent with the electrophilic nature of the quinone moiety of EQ which enables Michael addition with thiol groups (Fan et al., 2006; Bolton et al., 2018).

Identification of the Catalytic Cysteine Residue of TCPTP as a Target of EQ. Orthovanadate, a transition state analog generally used as a competitive protein phosphotyrosine phosphatase inhibitor, was used to evaluate whether EQ inhibition involves reactions at the active site of the enzyme as described previously (Seiner et al., 2007). Figure 3A shows that vanadate confers protection to TCPTP as the inhibition of the enzyme is significantly slowed by the competitive inhibitor, thereby providing evidence that the reaction is active site directed. Computational analysis using covalent docking approaches further indicated that the catalytic cysteine of TCPTP (cysteine 216) can form an adduct in the active site through the formation of a covalent bond between the sulfur atom and the carbon 6′ of the quinone moiety (Fig. 3B).

To ascertain that the catalytic cysteine residue of TCPTP can be covalently adducted by EQ, we analyzed recombinant protein treated with EQ using liquid chromatography–MS/MS. As shown in Fig. 3C, the $[M+3H]^{3+}$ molecular ion of the tryptic peptide harboring the catalytic cysteine displays a 190.9 *m/z* increase after treatment with EQ, corresponding to the mass of the EQ adduct. This mass of EQ adduct is also confirmed in the $a16^{2+}$, $y17^{2+}$, and $y20^{3+}$ ions of the fragmented peptide. It is well known that tyrosine phosphatases are readily inhibited by chemicals able to modify their catalytic cysteine (Seiner et al., 2007; Ostman et al., 2011). Altogether, these experiments indicate that EQ impairs TCPTP activity through the covalent adduction of its catalytic cysteine.

Characterization of Reversibility and Kinetics of TCPTP Inhibition by EQ. TCPTP inhibition by EQ was further evaluated for reversibility. To this end, TCPTP enzyme was inhibited by EQ and subsequently subjected to a buffer exchange experiment before measuring its residual activity. Consistent with the data described earlier, buffer exchange could not restore TCPTP activity (Fig. 4A). Depending on the chemical structure of the quinones, reversibility of cysteine adducts through reduction has already been described (Bolton and Dunlap, 2017; Bolton et al., 2018). We therefore examined the effect of two concentrations of the reducing agent DTT on the reversion of TCPTP inhibition by EQ. As shown in Fig. 4B, even at a 10 mM concentration, DTT was not successful at restoring the activity of EQ-inhibited TCPTP, thereby confirming the stable and covalent nature of the reaction between EQ and the catalytic cysteine of TCPTP. These observations are consistent with previously published data on the inhibition of topoisomerase II by EQ (Jacob et al., 2011; Smith et al., 2014; Gibson et al., 2016).

Finally, the kinetics of TCPTP inhibition by EQ were studied under pseudo first-order conditions, which allowed observation of time- and dose-dependent inhibition (Fig. 5A) and permitted the determination of the second-order inhibition kinetic constant, $k_{inact} = \sim 810 \pm 73\ M^{-1} \cdot min^{-1}$, derived from the slope of the graph with pseudo first-order kinetic constants plotted against EQ concentration (Fig. 5B). These kinetic data also confirm the irreversible nature of the inhibition of TCPTP by EQ.

EQ Alters TCPTP Activity and Enhances STAT1 Phosphorylation in HL60 and Jurkat Cells. Taking into consideration the in vitro effects of EQ observed with recombinant TCPTP protein, HL60 and Jurkat cell lines were treated with EQ to study its effect on cellular TCPTP. After 30-minute exposure, the cells were lysed and cellular TCPTP immunoprecipitated. The residual TCPTP activity was measured using the phospho-STAT1 peptide substrate dephosphorylation assay using UFLC detection (Duval et al., 2015) and immunoprecipitated-TCPTP protein content evaluated by western blot. Figure 6 shows that, upon exposure to EQ, the

Downloaded from molpharm.aspetjournals.org at ASPET Journals on May 8, 2022

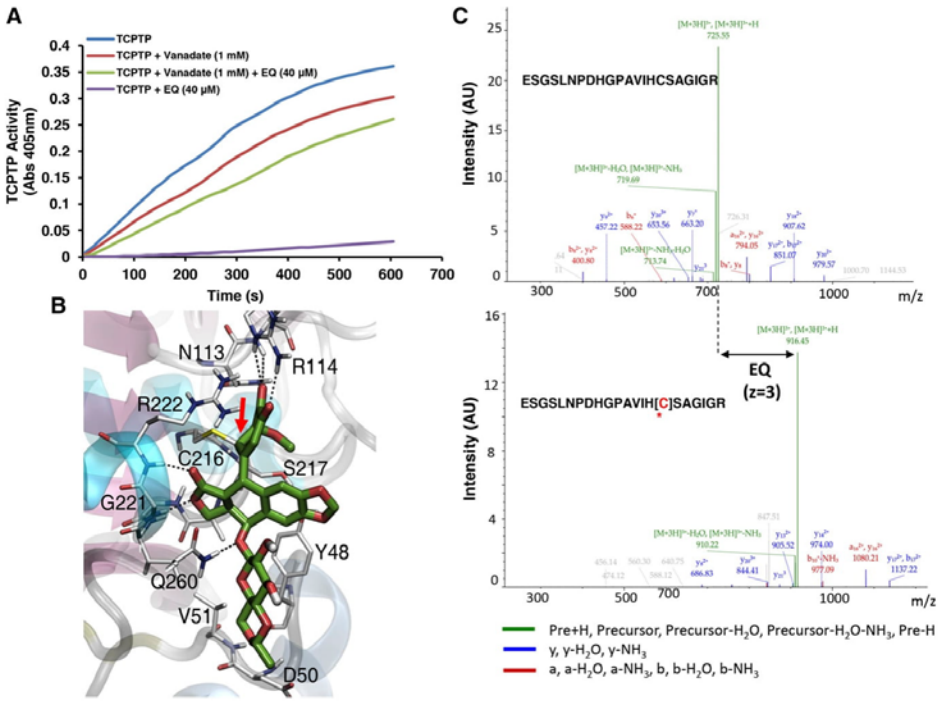

Fig. 3. Mapping of EQ adduct on TCPTP protein active site cysteine. (A) Effect of sodium orthovanadate on TCPTP inhibition by EQ. One micromolar human recombinant TCPTP was incubated with 40 μM EQ and/or 1 mM orthovanadate for 30 minutes at 37°C and residual activity measured as described in *Materials and Methods*. The experiment is representative of three independent experiments. (B) Molecular docking model of EQ bound in a human TCPTP protein structure. EQ molecule adduct atom coordinates were obtained inside the TCPTP active site pocket as described in the *Materials and Methods* section. EQ is displayed with green sticks and is covalently bonded to the C216 residue. (C) Mass spectrometry characterization of EQ adduct on the active site cysteine tryptic peptide. One micromolar TCPTP protein was incubated with 100 μM EQ for 30 minutes at 37°C prior to trypsine treatment and liquid chromatography–MS/MS analysis as described in *Materials and Methods*. The upper panel depicts the spectrum obtained with control, untreated TCPTP protein, whereas the lower panel shows data acquired with TCPTP samples treated with EQ. The sequence of the peptide is displayed on each panel in addition to the position of the EQ adduct on cysteine in the lower panel. Abs, absorbance; AU, arbitrary units.

cellular TCPTP activity decreased to roughly 30% and 50% that of the control cells in HL60 and Jurkat cells, respectively. These data are consistent with studies carried out on the inhibition of PTP1B (a tyrosine phosphatase related to TCPTP) by naphthoquinones (Iwamoto et al., 2007). These results indicate that EQ inhibits TCPTP in a cellular environment, and we therefore investigated whether, under such conditions, TCPTP-dependent intracellular signaling could be altered. Incubation of HL60 cells with IFNγ triggers STAT1 phosphorylation signaling. This signaling is sustained at a higher level (1.5-fold for 60 minutes) in cells exposed to EQ treatment as compared with untreated controls (Fig. 7A). Similar results were also obtained with Jurkat cells, with more than 2-fold phosphorylation after 1 hour (Fig. 7B). To further show that EQ increases STAT1 signaling, we measured the expression of three genes (*APOL1*, *GBP1*, and *IRF1*) known to be regulated by STAT1 (Hartman et al., 2005; Reardon and McKay, 2007). As shown in Supplemental Fig. 3, quantitative polymerase chain reaction analyses indicated that the expression of *APOL1*, *GBP1*, and *IRF1* is increased in Jurkat cells exposed to EQ. These results indicate that inhibition of TCPTP by EQ is associated with increased STAT1 phosphorylation and higher expression of STAT1-regulated genes in these cells upon stimulation with IFNγ.

Discussion

Etoposide is currently one of the most commonly used antitumor drugs. However, its use in clinics is associated with an increased risk of secondary leukemia (Pendleton et al., 2014). Several threads of experimental evidence indicate that EQ, a reactive metabolite of ETOP, is involved in ETOP-related leukemia through alteration of the topoisomerase II function (Gantchev and Hunting, 1998; Kagan et al., 1999; Fan et al., 2006; Jacob et al., 2011; Vlasova et al., 2011; Smith et al., 2014; Gibson et al., 2016). However, effects of EQ on other cellular targets could also contribute to ETOP-related leukemogenesis (Haim et al., 1987; Fan et al., 2006; Rojas et al., 2009).

Downloaded from molpharm.aspetjournals.org at ASPET Journals on May 8, 2022

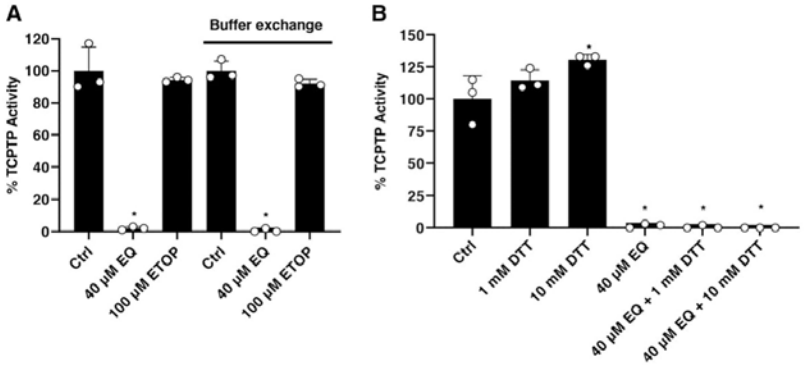

Fig. 4. Irreversibility of TCPTP inhibition by EQ. (A) Effect of buffer exchange on activity of TCPTP preincubated with EQ. Human TCPTP was incubated with 40 μM EQ or 100 μM ETOP for 30 minutes followed by buffer exchange or no buffer exchange prior to residual pNPP dephosphorylation activity determination as described in *Materials and Methods*. Results are the mean of three independent experiments; error bars indicate S.D. $^*P < 0.05$, determined using ANOVA followed by Dunnett's post hoc analysis. (B) Effect of DTT on activity of TCPTP preincubated with EQ. Human TCPTP was preincubated or not with 40 μM EQ for 30 minutes followed by treatment with 1 or 10 mM DTT. Residual pNPP dephosphorylation activity was determined as described in *Materials and Methods*. Results are the mean of three independent experiments; error bars indicate S.D. $^*P < 0.05$, determined using ANOVA followed by Dunnett's post hoc analysis. Ctrl, control.

We investigated the possibility of protein tyrosine phosphatase TCPTP being a target of EQ. TCPTP plays a pivotal role in normal and malignant hematopoiesis through the negative regulation of the JAK/STAT signaling pathway (Dorritie et al., 2014). Interestingly, ETOP was reported to activate STAT1 signaling in HeLa cells. In addition, it has been shown that protein tyrosine phosphatases similar to TCPTP could be inhibited by polyaromatic quinones (Wang et al., 2004; Iwamoto et al., 2007). In line with this, we found in this work that EQ, the quinone metabolite of ETOP, was able to inhibit cellular TCPTP activity with subsequent increase in tyrosine phosphorylation of STAT1 in hematopoietic cell lines. Using further molecular and kinetic approaches, we show that EQ is an irreversible inhibitor of TCPTP. The second-order rate constant (k_{inact}) for this inhibition was found to be ~810 $M^{-1}{\cdot}min^{-1}$ (Fig. 5B). This rate constant is close to values found for naphthoquinone-dependent inhibition of human protein tyrosine phosphatase 1B (420 $M^{-1}{\cdot}min^{-1}$), a tyrosine phosphatase structurally related to TCPTP (Wang et al., 2004). Interestingly, naphthoquinones have been shown to alter cell signaling, in particular through increased tyrosine phosphorylation (Iwamoto et al., 2007; Klotz et al., 2014). In addition, the k_{inact} value for the inhibition of TCPTP by EQ is comparable to that reported previously for hydrogen peroxide (600 $M^{-1}{\cdot}min^{-1}$), a known endogenous regulator of tyrosine protein phosphatases (Seiner et al., 2007; Ostman et al., 2011). Inhibition of TCPTP by EQ was not reversed by buffer exchange (Fig. 4A). This observation, along with the time-dependent nature of the reaction (Fig. 5A), indicates that the inhibition of TCPTP by EQ is irreversible. It is well known that the activity of protein tyrosine phosphatases such as TCPTP relies on a reactive active site cysteine that

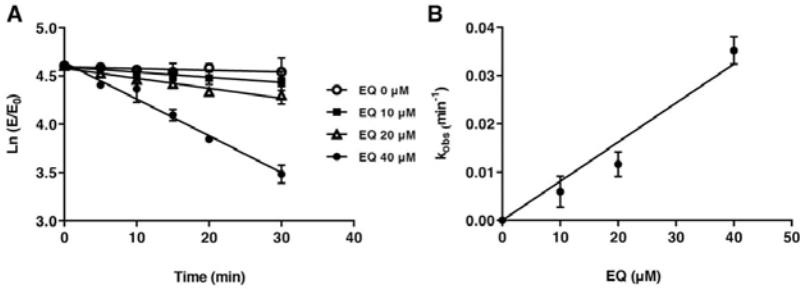

Fig. 5. Kinetics of TCPTP inhibition by EQ. (A) Determination of pseudo first-order inhibition rate constant for TCPTP inhibition by EQ. TCPTP (3 μM) was incubated with different concentrations (0, 10, 20, and 40 μM) of EQ and assayed for residual activity at different time points as described in *Materials and Methods*. The value of k_{obs} was determined as the slope of the linear regression of data expressed as the natural logarithm of the residual activity as a function of time. Results are the mean of three independent experiments; error bars indicate S.D. (B) Determination of the second-order inhibition rate constant for TCPTP inhibition by EQ. Values of k_{obs} were plotted as a function of EQ concentration, and k_{inact} was determined as the slope of the linear regression as described in *Materials and Methods*. Results are the mean of three independent experiments; error bars indicate S.D.

Downloaded from molpharm.aspetjournals.org at ASPET Journals on May 8, 2022

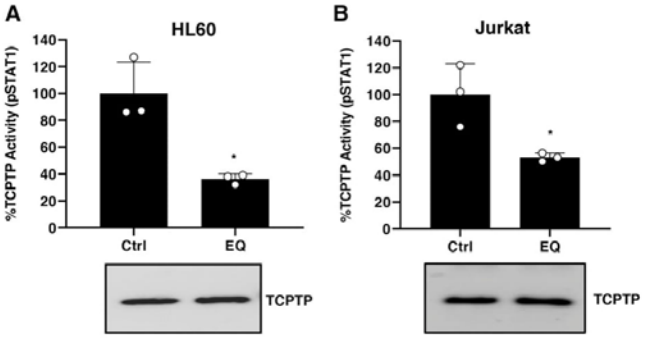

Fig. 6. Inhibition of TCPTP by EQ in HL60 and Jurkat cells. HL60 (A) and Jurkat cells (B) were treated or not [control (Ctrl)] with 50 μM EQ for 30 minutes at 37°C. Cells were lysed and cellular TCPTP protein was immunoprecipitated prior to residual activity determination and TCPTP protein content determination by western blotting as described in *Materials and Methods*. Results are the mean of three independent experiments; error bars indicate S.D. $^*P < 0.05$, determined using Student's t test as described under the *Materials and Methods* section. Western blot is representative of three independent experiments. pSTAT1, phosphorylated STAT1.

can be modified by oxidants or electrophilic chemicals with subsequent loss of activity and altered cell signaling (Ostman et al., 2011; Klotz et al., 2014). In addition, several quinones, such as EQ, are Michael acceptors that can covalently react with cysteine residues to form irreversible adducts (Fan et al., 2006; Li et al., 2016; Bolton et al., 2018). Accordingly, we found that the irreversible nature of the inhibition of TCPTP by EQ is due to formation of covalent adducts on the catalytic cysteine residue of the enzyme (cysteine 216). This was confirmed by the fact that the inhibition process of TCPTP by EQ was slowed by addition of the competitive TCPTP inhibitor orthovanadate and by computational docking approaches. More importantly, mass spectrometry analysis of TCPTP inhibited by EQ shows that the active site cysteine residue of the enzyme is indeed adducted by EQ (Fig. 3C). Interestingly, recent experimental data indicate that EQ poisons topoisomerase II enzymes through cysteine adduction mechanisms, and that this covalent modification of topoisomerase II by EQ is likely to contribute to ETOP-related leukemogenesis (Jacob et al., 2011;

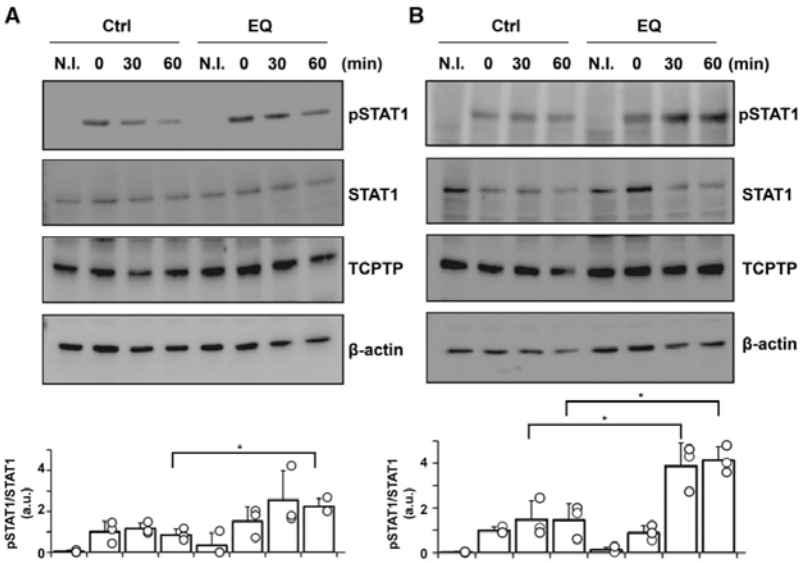

Fig. 7. STAT1 phosphorylation kinetic analysis in HL60 and Jurkat cells induced with IFNγ. HL60 (A) and Jurkat cells (B) were treated or not [control (Ctrl)] with 50 μM EQ for 30 minutes at 37°C, then washed prior to incubation for 20 minutes with IFNγ. Washed cells were then analyzed at different time points as described in *Materials and Methods*. Results are the mean of three independent experiments; error bars indicate S.D. $^*P < 0.05$, determined using Student's t test as described under the *Materials and Methods* section. Western blot is representative of three independent experiments. Quantification of STAT1 phosphorylation in western blots was carried out using ImageJ software. a.u., arbitrary unit; N.I., no interferon; pSTAT1, phosphorylated STAT1.

Downloaded from molpharm.aspetjournals.org at ASPET Journals on May 8, 2022

Smith et al., 2014). Of note, the activity of EQ against topoisomerase IIα was found to be considerably higher than that of ETOP. Indeed, EQ can inhibit DNA relaxation at 100-fold lower levels (1 vs. 100 μM) of drug when compared with ETOP (Gibson et al., 2016). In their study on the inhibition of topoisomerase IIβ by EQ and ETOP, Smith et al. (2014) reported that whereas 15 μM EQ inhibited DNA cleavage by Topo2β in 6 minutes, less than 15% inhibition was observed with the parent drug ETOP. In addition, EQ is able to inhibit ATP hydrolysis by topoisomerase IIα, whereas ETOP cannot (Gibson et al., 2016). Interestingly, while EQ was found to inhibit TCPTP, the parent drug did not. This is in agreement with the electrophilic nature of EQ, which enables it to covalently react with the catalytic cysteine of TCPTP through Michael addition (Fan et al., 2006; Bolton et al., 2018). Tyrosine phosphatases closely related to TCPTP, such as PTP1B, have been shown to be inhibited by naphthoquinones through active site cysteine covalent modification (Iwamoto et al., 2007; Klotz et al., 2014). We found that EQ was also able to inhibit the phosphatase activity of PTP1B (Supplemental Fig. 4). Although we cannot rule out that EQ may affect STAT1 tyrosine phosphorylation through effects on other tyrosine phosphatases, small interfering RNA–mediated knockout of TCPTP in Jurkat cells and knockout mice models clearly indicates that impairment of TCPTP activity strongly impacts STAT1 tyrosine phosphorylation (Simoncic et al., 2002; Kleppe et al., 2010). Increasing evidence indicates that cytochrome P450/myeloperoxidase-dependent oxidative activation of ETOP into reactive metabolites (notably EQ) in hematopoietic cells is a key contributor to ETOP-related leukemia (Zhuo et al., 2004; Fan et al., 2006; Jacob et al., 2011; Vlasova et al., 2011; Smith et al., 2014; Gibson et al., 2016; Atwal et al., 2017). We show here that in addition to disruption of topoisomerase II functions, EQ could also contribute to ETOP-related leukemia through interactions with TCPTP and subsequent cell signaling alteration.

Acknowledgments

We thank the technical platform "BioProfiler-UFLC" (BFA Unit, Paris Diderot University) for provision of UFLC facilities. We are grateful to Dr. Oliver Brookes for English language proofreading of this manuscript.

Authorship Contributions

Participated in research design: Nian, Berthelet, Rodrigues Lima.
Conducted experiments: Nian, Berthelet, Bui, Ganesan, Leger.
Performed data analysis: Nian, Berthelet, Zhang, Bui, Liu, Duval, Ganesan, Leger, Chomienne, Busi, Guidez, Dupret, Rodrigues Lima.
Wrote or contributed to the writing of the manuscript: Nian, Berthelet, Xu, Ganesan, Leger, Busi, Rodrigues Lima.

References

Atwal M, Lishman EL, Austin CA, and Cowell IG (2017) Myeloperoxidase enhances etoposide and mitoxantrone-mediated DNA damage: a target for myeloprotection in cancer chemotherapy. *Mol Pharmacol* **91**:49–57.
Baldwin EL and Osheroff N (2005) Etoposide, topoisomerase II and cancer. *Curr Med Chem Anticancer Agents* **5**:363–372.
Benekli M, Baumann H, and Wetzler M (2009) Targeting signal transducer and activator of transcription signaling pathway in leukemias. *J Clin Oncol* **27**: 4422–4432.
Bolton JL and Dunlap T (2017) Formation and biological targets of quinones: cytotoxic versus cytoprotective effects. *Chem Res Toxicol* **30**:13–37.
Bolton JL, Dunlap TL, and Dietz BM (2018) Formation and biological targets of botanical o-quinones. *Food Chem Toxicol* **120**:700–707.
Bourdeau A, Dubé N, Heinonen KM, Théberge JF, Doody KM, and Tremblay ML (2007) TC-PTP-deficient bone marrow stromal cells fail to support normal B lymphopoiesis due to abnormal secretion of interferon-gamma. *Blood* **109**:4220–4228.
Copeland RA (2005) *Evaluation of enzyme inhibitors in drug discovery*, Wiley-Interscience, Hoboken.
Deweese JE and Osheroff N (2009) Coordinating the two protomer active sites of human topoisomerase IIalpha: nicks as topoisomerase II poisons. *Biochemistry* **48**: 1439–1441.
Dorritie KA, McCubrey JA, and Johnson DE (2014) STAT transcription factors in hematopoiesis and leukemogenesis: opportunities for therapeutic intervention. *Leukemia* **28**:248–257.
Duval R, Bui LC, Berthelet J, Dairou J, Mathieu C, Guidez F, Dupret JM, Cools J, Chomienne C, and Rodrigues-Lima F (2015) A RP-UFLC assay for protein tyrosine phosphatases: focus on protein tyrosine phosphatase non-receptor type 2 (PTPN2). *Sci Rep* **5**:10750.
Fan Y, Schreiber EM, Giorgianni A, Yalowich JC, and Day BW (2006) Myeloperoxidase-catalyzed metabolism of etoposide to its quinone and glutathione adduct forms in HL60 cells. *Chem Res Toxicol* **19**:937–943.
Gantchev TG and Hunting DJ (1998) The ortho-quinone metabolite of the anticancer drug etoposide (VP-16) is a potent inhibitor of the topoisomerase II/DNA cleavable complex. *Mol Pharmacol* **53**:422–428.
Gibson EG, King MM, Mercer SL, and Deweese JE (2016) Two-mechanism model for the interaction of etoposide quinone with topoisomerase IIα. *Chem Res Toxicol* **29**: 1541–1548.
Haim N, Nemec J, Roman J, and Sinha BK (1987) Peroxidase-catalyzed metabolism of etoposide (VP-16-213) and covalent binding of reactive intermediates to cellular macromolecules. *Cancer Res* **47**:5835–5840.
Hande KR (1998) Etoposide: four decades of development of a topoisomerase II inhibitor. *Eur J Cancer* **34**:1514–1521.
Hartman SE, Bertone P, Nath AK, Royce TE, Gerstein M, Weissman S, and Snyder M (2005) Global changes in STAT target selection and transcription regulation upon interferon treatments. *Genes Dev* **19**:2953–2968.
Heinonen KM, Bourdeau A, Doody KM, and Tremblay ML (2009) Protein tyrosine phosphatases PTP-1B and TC-PTP play nonredundant roles in macrophage development and IFN-gamma signaling. *Proc Natl Acad Sci USA* **106**:9368–9372.
Humphrey W, Dalke A, and Schulten K (1996) VMD: visual molecular dynamics. *J Mol Graph* **14**:33–38, 27–38.
Iwamoto N, Sumi D, Ishii T, Uchida K, Cho AK, Froines JR, and Kumagai Y (2007) Chemical knockdown of protein-tyrosine phosphatase 1B by 1,2-naphthoquinone through covalent modification causes persistent transactivation of epidermal growth factor receptor. *J Biol Chem* **282**:33396–33404.
Jacob DA, Mercer SL, Osheroff N, and Deweese JE (2011) Etoposide quinone is a redox-dependent topoisomerase II poison. *Biochemistry* **50**:5660–5667.
Kagan VE, Yalowich JC, Borisenko GG, Tyurina YY, Tyurin VA, Thampatty P, and Fabisiak JP (1999) Mechanism-based chemopreventive strategies against etoposide-induced acute myeloid leukemia: free radical/antioxidant approach. *Mol Pharmacol* **56**:494–506.
Kleppe M, Lahortiga I, El Chaar T, De Keersmaecker K, Mentens N, Graux C, Van Roosbroeck K, Ferrando AA, Langerak AW, Meijerink JP, et al. (2010) Deletion of the protein tyrosine phosphatase gene PTPN2 in T-cell acute lymphoblastic leukemia. *Nat Genet* **42**:530–535.
Kleppe M, Soulier J, Asnafi V, Mentens N, Hornakova T, Knoops L, Constantinescu S, Sigaux F, Meijerink JP, Vandenberghe P, et al. (2011a) PTPN2 negatively regulates oncogenic JAK1 in T-cell acute lymphoblastic leukemia. *Blood* **117**: 7090–7098.
Kleppe M, Tousseyn T, Geissinger E, Kalender Atak Z, Aerts S, Rosenwald A, Wlodarska I, and Cools J (2011b) Mutation analysis of the tyrosine phosphatase PTPN2 in Hodgkin's lymphoma and T-cell non-Hodgkin's lymphoma. *Haematologica* **96**:1723–1727.
Klotz LO, Hou X, and Jacob C (2014) 1,4-naphthoquinones: from oxidative damage to cellular and inter-cellular signaling. *Molecules* **19**:14902–14918.
Li Y, Jongberg S, Andersen ML, Davies MJ, and Lund MN (2016) Quinone-induced protein modifications: kinetic preference for reaction of 1,2-benzoquinones with thiol groups in proteins. *Free Radic Biol Med* **97**:148–157.
Montalibet J, Skorey KI, and Kennedy BP (2005) Protein tyrosine phosphatase: enzymatic assays. *Methods* **35**:2–8.
Ostman A, Frijhoff J, Sandin A, and Böhmer FD (2011) Regulation of protein tyrosine phosphatases by reversible oxidation. *J Biochem* **150**:345–356.
Paz MA, Flückiger R, Boak A, Kagan HM, and Gallop PM (1991) Specific detection of quinoproteins by redox-cycling staining. *J Biol Chem* **266**:689–692.
Pendleton M, Lindsey RH Jr, Felix CA, Grimwade D, and Osheroff N (2014) Topoisomerase II and leukemia. *Ann N Y Acad Sci* **1310**:98–110.
Pike KA and Tremblay ML (2016) TC-PTP and PTP1B: regulating JAK-STAT signaling, controlling lymphoid malignancies. *Cytokine* **82**:52–57.
Reardon C and McKay DM (2007) TGF-beta suppresses IFN-gamma-STAT1-dependent gene transcription by enhancing STAT1-PIAS1 interactions in epithelia but not monocytes/macrophages. *J Immunol* **178**:4284–4295.
Rojas E, Mussali P, Tovar E, and Valverde M (2009) DNA-AP sites generation by etoposide in whole blood cells. *BMC Cancer* **9**:398.
Schneider CA, Rasband WS, and Eliceiri KW (2012) NIH Image to ImageJ: 25 years of image analysis. *Nat Methods* **9**:671–675.
Seiner DR, LaButti JN, and Gates KS (2007) Kinetics and mechanism of protein tyrosine phosphatase 1B inactivation by acrolein. *Chem Res Toxicol* **20**:1315–1320.
Simoncic PD, Lee-Loy A, Barber DL, Tremblay ML, and McGlade CJ (2002) The T cell protein tyrosine phosphatase is a negative regulator of janus family kinases 1 and 3. *Curr Biol* **12**:446–453.
Smith NA, Byl JA, Mercer SL, Deweese JE, and Osheroff N (2014) Etoposide quinone is a covalent poison of human topoisomerase IIβ. *Biochemistry* **53**:3229–3236.
ten Hoeve J, de Jesus Ibarra-Sanchez M, Fu Y, Zhu W, Tremblay M, David M, and Shuai K (2002) Identification of a nuclear Stat1 protein tyrosine phosphatase. *Mol Cell Biol* **22**:5662–5668.
Tiganis T and Bennett AM (2007) Protein tyrosine phosphatase function: the substrate perspective. *Biochem J* **402**:1–15.
Tonks NK (2006) Protein tyrosine phosphatases: from genes, to function, to disease. *Nat Rev Mol Cell Biol* **7**:833–846.

Downloaded from molpharm.aspetjournals.org at ASPET Journals on May 8, 2022

Vlasova II, Feng WH, Goff JP, Giorgianni A, Do D, Gollin SM, Lewis DW, Kagan VE, and Yalowich JC (2011) Myeloperoxidase-dependent oxidation of etoposide in human myeloid progenitor CD34+ cells. *Mol Pharmacol* **79**:479–487.
Wang Q, Dubé D, Friesen RW, LeRiche TG, Bateman KP, Trimble L, Sanghara J, Pollex R, Ramachandran C, Gresser MJ, et al. (2004) Catalytic inactivation of protein tyrosine phosphatase CD45 and protein tyrosine phosphatase 1B by polyaromatic quinones. *Biochemistry* **43**:4294–4303.
Wiede F, Chew SH, van Vliet C, Poulton IJ, Kyparissoudis K, Sasmono T, Loh K, Tremblay ML, Godfrey DI, Sims NA, et al. (2012) Strain-dependent differences in bone development, myeloid hyperplasia, morbidity and mortality in ptpn2-deficient mice. *PLoS One* **7**:e36703.
Young RM, Polsky A, and Refaeli Y (2009) TC-PTP is required for the maintenance of MYC-driven B-cell lymphomas. *Blood* **114**:5016–5023.
You-Ten KE, Muise ES, Itié A, Michaliszyn E, Wagner J, Jothy S, Lapp WS, and Tremblay ML (1997) Impaired bone marrow microenvironment and immune function in T cell protein tyrosine phosphatase-deficient mice. *J Exp Med* **186**: 683–693.
Zhuo X, Zheng N, Felix CA, and Blair IA (2004) Kinetics and regulation of cytochrome P450-mediated etoposide metabolism. *Drug Metab Dispos* **32**: 993–1000.

Address correspondence to: Fernando Rodrigues Lima, Université de Paris, BFA, UMR 8251, CNRS, F-75013 Paris, France. E-mail: fernando.rodrigues-lima@univ-paris-diderot.fr

Downloaded from molpharm.aspetjournals.org at ASPET Journals on May 8, 2022

Check for updates

Received: 22 October 2021 | Revised: 14 November 2021 | Accepted: 16 November 2021

DOI: 10.1002/pro.4246

PROTEIN STRUCTURE REPORTS

THE PROTEIN SOCIETY WILEY

Structural characterization of a pathogenic mutant of human protein tyrosine phosphatase PTPN2 (Cys216Gly) that causes very early onset autoimmune enteropathy

Qing Nian[1,2] | Jérémy Berthelet[2] | Marianna Parlato[3] | Ariel E. Mechaly[4] | Rongxing Liu[2] | Jean-Marie Dupret[2] | Nadine Cerf-Bensussan[3] | Ahmed Haouz[4] | Fernando Rodrigues Lima[2]

[1]Department of Blood Transfusion, Sichuan Provincial People's Hospital, University of Electronic Science and Technology of China and Chinese Academy of Sciences Sichuan Translational Medicine Research Hospital, Chengdu, China

[2]Université de Paris, CNRS, Unité de Biologie Fonctionnelle et Adaptative, Paris, France

[3]Université de Paris, INSERM, Institut Imagine, Paris, France

[4]Institut Pasteur, Plate-forme de Cristallographie-C2RT, CNRS UMR 3528, Paris, France

Correspondence
Fernando Rodrigues Lima, Université de Paris, BFA, UMR 8251, CNRS, 75013 Paris, France.
Email: fernando.rodrigues-lima@u-paris.fr

Present address
Jérémy Berthelet, Université de Paris, CNRS, Centre Epigénétique et Destin Cellulaire, Paris, France

Funding information
Centre National de la Recherche Scientifique; Institut Pasteur; Université de Paris; Région Ile de France (Cancéropole); China Scholarship Council (CSC)

Abstract

PTPN2 is an important protein tyrosine phosphatase (PTP) that plays a key role in cell signaling. Deletions or inactivating mutations of PTPN2 have been described in different pathologies and underline its critical role in hematopoiesis, autoimmunity, and inflammation. Surprisingly, despite the major pathophysiological implications of PTPN2, the structural analysis of this PTP and notably of its pathogenic mutants remains poorly documented. Contrary to other human PTP enzymes, to date, only one structure of PTPN2 (wild-type form) has been reported. Here, we report the first crystal structure of a pathogenic mutant of PTPN2 (Cys216Gly) that causes an autoimmune enteropathy. We show in particular that this mutant adopts a classical PTP fold. More importantly, albeit inactive, the mutant retains its ability to bind substrates and to adopt the characteristic catalytically competent closed form of PTP enzymes. This novel PTPN2 structure may serve as a new tool to better understand PTP structures and the structural impacts of pathogenic mutations. Moreover, the C216G PTPN2 structure could also be helpful to design specific ligands/inhibitors.

KEYWORDS

crystal structure, pathogenic mutation, protein tyrosine phosphatase, PTPN2

1 | INTRODUCTION

PTPN2 is a ubiquitous protein tyrosine phosphatase (PTP) that serves as negative regulator of cytokines and

Abbreviations: PTP, protein tyrosine phosphatase; PTPN2, PTP non-receptor type 2.

Qing Nian and Jérémy Berthelet contributed equally to this work.

 © 2021 The Protein Society.

growths factors signaling.[1] PTPN2 is known to act as a tumor suppressor in T-cell leukemia and lymphoma.[2] Moreover, several studies have implicated PTPN2 in diabetes, autoimmune, and inflammatory diseases.[3–5] Knock-out mice models further support the key role of PTPN2 in hematopoiesis and inflammation.[6,7] More recently, PTPN2 was identified as a major target for cancer immunotherapy.[8–11] Despite the physiological and pathophysiological importance of PTPN2, this tyrosine phosphatase and its disease-associated mutated forms remain poorly studied at both molecular and structural levels.[1]

We have recently reported a germline de novo missense variant (C216G) in human PTPN2 as a novel cause of autoimmune enteropathy due to PTPN2-dependent aberrant activation of the JAK/STAT pathway.[12] Cys216 in PTPN2 corresponds to an evolutionarily conserved active site residue in PTPs that makes the nucleophilic attack on the phosphor-tyrosyl residue of the substrates (Figure 1a,b). Although mutations of this active site Cys residue are known to affect the activity of PTP enzymes, they can also convert them into inactive enzymatic forms that however retain the ability to bind substrates.[13–15]

Numerous structures of PTP enzymes (mostly their catalytic domains) have been described.[16] Notably, more than 200 structures of human PTP1B (including mutants and ligand bound forms), the closest homolog of PTPN2 (75% amino acid sequence identity between their catalytic domains, that is, residues 1–314), are available in the Protein Data Bank (PDB). Surprisingly, to date, only one PTPN2 structure (catalytic domain of WT PTPN2, residues 1–314) has been reported thus limiting the structural knowledge of this key PTP enzyme.[17] Therefore, to understand the structural bases of the pathogenic C216G mutation of PTPN2 and, more broadly, to better characterize the structure of this PTP, we carried out crystal structure studies of the C216G mutant.

2 | RESULTS AND DISCUSSION

As observed for other PTP enzymes, the full length PTPN2 (415 amino acids) is not easily amenable to crystallization, therefore we used the truncated form of C216G PTPN2 corresponding to the PTP catalytic domain (residues 1–314) that has been used previously to crystalize WT PTPN2.[17] Similar truncated forms have also been commonly used for the determination of the crystal structures of the catalytic domain of other PTPs, notably human PTP1B the closest homolog of PTPN2.[16] As shown in Figure 1c, both catalytic domains of WT and C216G PTPN2 (residues 1–314) were readily expressed and purified to homogeneity from *Escherichia coli* thus indicating that the C216G mutation has no gross impact on the quality of expression and solubility of the protein. Purified WT PTPN2 (catalytic domain, residues 1–314) was found to be active toward a tyrosine-phosphorylated peptide substrate (SAAPYLKTK) derived from human STAT3, whereas the C216G PTPN2 mutant was inactive (Figure 1d, left panel). Similar results were obtained with a generic nonpeptide phosphatase substrate (pNPP) (Figure 1d, right panel). In addition, upon transfection in HEK293 cells, the C216G PTPN2 mutant failed to dephosphorylate cellular tyrosine-phosphorylated proteins in contrast to the WT form (Figure 1e). Overall, these results are in agreement with our previous studies obtained with the full forms of WT and C216G PTPN2.[12] We next crystallized the C216G PTPN2 protein, which allowed us to determine the structure of this PTPN2 mutant at a resolution of 2.4 Å (Table 1; coordinates are deposited in the PDB under the PDB ID 6ZZ4). C216G PTPN2 was found as a dimer in the crystal as observed previously for other PTPs structures including human PTP1B (Figure 2a).[18–20] This contrasts with the unusual packing reported for WT PTPN2 (PDB code 1L8K), where one molecule of the enzyme (via its the DDQ loop) is inserted in the active site of a neighboring molecule, resulting in a continuous row of WT PTPN2 molecules.[17] The mechanism underlying this unusual crystal packing of WT PTPN2 structure (with multimerization of PTPN2 molecules) remains unclear and might point to crystal packing artifacts, suggesting that the WT PTPN2 structure reported so far might not reflect, at least in part, a biologically relevant structure of the enzyme.[17]

As observed for WT PTPN2, the overall structure of C216G PTPN2 adopts the characteristic PTP fold with, notably, the important structural/functional loops that are found in PTP enzymes (Figures 1a and 2b). The structure of the mutant clearly shows the replacement within the P-loop of the evolutionary conserved catalytic cysteine residue by a glycine and further supports that the mutation has no major effect on the overall structure of the enzyme as underlined by the RMSD value of 0.54 Å (over 254 Cα) between WT and C216G PTPN2 structures (Figure 2b,c). More in depth comparison shows nonetheless significant structural differences in the WPD and K122 loops (Figure 2c), whereas other important loops, including the P-loop that harbors the C216G mutated residue (and two other essential catalytic residues Arg221 and Ser223) have highly similar conformations (Figure 2c,d: P-loop panel; Figure S1). While in WT PTPN2, the WPD loop adopts a classical "open" conformation,[17] in C216G PTPN2 this loop is in a "closed" form (Figure 2d: WPD loop panel). In PTP enzymes, notably PTPN2 or PTP1B, the WPD loop acts as a flexible gate that upon substrate binding makes a

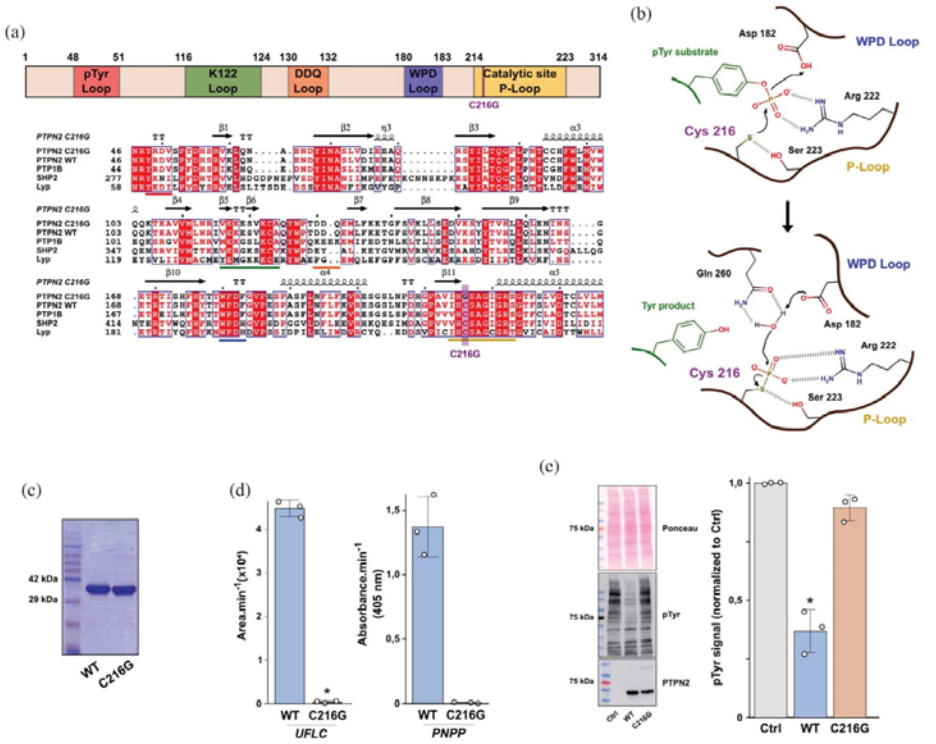

FIGURE 1 Expression, purification, and enzymatic characterization of C216G PTPN2 catalytic domain (residues 1–314). (a) Top panel: Schematic representation of the different key domains of PTPN2 1–314. Location of the C216G mutation is highlighted in purple. pTyr loop is shown in red, K122 loop in green, DDQ loop in orange, WPD loop in blue, and P-loop (catalytic site) in yellow. Bottom panel: Sequence alignment of human PTPN2, PTP1B, SHP2 (PTPN11), and Lyp (PTPN22) enzymes (Uniprot database). Key domains of PTPN2 are underlined using the same color scheme as top panel. Location of the conserved C216 residue is highlighted in purple. (b) Two step mechanism of PTPN2 phosphatase activity. C216 residue is essential for the phosphatase activity: the thiolate anion will perform a nucleophilic attack on the phosphate group of the phosphorylated tyrosine substrate, and this phosphate group will later react with a molecule of water to regenerate the catalytic cysteine. Catalytic residues are labeled in black and the phosphorylated tyrosine is displayed in green. Location of the WPD loop and P-loop are depicted in blue and yellow, respectively. (c) 3 μg of purified recombinant WT or C216G 1–314 PTPN2 were analyzed by SDS-PAGE and stained by Coomassie blue. The migration of the molecular weight markers are displayed in Lane 1. (d) Left panel: Recombinant WT or C216G 1–314 PTPN2 (10 nM) activity was assessed by UFLC using a pSTAT3 fluorescent peptide. Barplots and error bars represent the means and the *SD* of three independent experiments. *: *p*.value < .05 compared with control (WT). Right panel: recombinant WT or C216G 1–314 PTPN2 (400 nM) activity was assessed by absorbance (405 nm) using pNPP, a chromogenic phosphatase substrate. Barplots and error bars represent the means and the *SD* of three independent experiments. *: *p*.value < .05 compared with control (WT). (e) HEK293T cells transfected with WT or C216G Flag-PTPN2 plasmids and 50 μg of cellular protein extracts were separated by SDS-PAGE and transferred onto a nitrocellulose membrane. Flag-PTPN2 protein was detected using an anti-Flag antibody and the global level of tyrosine phosphorylation using an anti-Pan-pTyr antibody. Ponceau staining was carried out to ensure equal protein loading. pTyr signal was then normalized by Ponceau staining, and the resulting ratio normalized by control (Ctrl). Barplots and error bars represent the means and the *SD* of three independent experiments, respectively. *: *p*.value < .05 compared with control (Ctrl)

conformational switch movement of around 10 Å from an "open" to a catalytically competent "closed" form (Figure 2d: WPD loop panel).[16] This is consistent with the presence in the active site pocket of the C216G PTPN2 structure of a phosphate group that mimics a phosphorylated tyrosine substrate (in particular through

TABLE 1 Data collection and refinement statistics

Resolution range	43.59–2.432 (2.519–2.432)
Space group	C 1 2 1
Unit cell	142.89, 55.98, 101.42, 90, 120.74, 90
Total reflections	178,268 (16,822)
Unique reflections	25,796 (2,475)
Multiplicity	6.9 (6.8)
Completeness (%)	98.25 (94.49)
Mean I/sigma(I)	10.97 (2.38)
Wilson B-factor	45.48
R-merge	0.1178 (0.6409)
R-meas	0.1276 (0.6941)
R-pim	0.04844 (0.2634)
CC1/2	0.996 (0.878)
CC*	0.999 (0.967)
Reflections used in refinement	25,770 (2,468)
Reflections used for R-free	1,288 (123)
R-work	0.2087 (0.2559)
R-free	0.2531 (0.3338)
CC (work)	0.931 (0.860)
CC (free)	0.921 (0.753)
Number of non-hydrogen atoms	4,760
Macromolecules	4,557
Ligands	30
Solvent	173
Protein residues	556
RMS (bonds)	0.009
RMS (angles)	1.24
Ramachandran favored (%)	97.10
Ramachandran allowed (%)	2.90
Ramachandran outliers (%)	0.00
Rotamer outliers (%)	0.00
Clashscore	6.20
Average B-factor	50.48
Macromolecules	50.51
Ligands	60.60
Solvent	47.84
Number of TLS groups	2

contacts with the side chains of the important catalytic residues Arg222 and Asp182) (Figure S1b). Other PTP structures with a phosphate group in the active site have been previously reported and showed evidence of a closed WPD-loop.[21] Further structural comparison between C216G PTPN2 and the structures of PTP1B in its closed (RMSD 0.52 Å over 264 Cα) and open (RMSD 0.6 Å over 260 Cα) forms (PDB codes 15AY and 1T4J, respectively) further support that the C216G PTPN2 structure is in a "closed" form while WT PTPN2 structure was obtained in an open form (Figure S1c: WPD loop panel).[17] This further indicates that the C216G mutation does not impair binding of ligands in the active site that induce closure of the WPD loop and make the enzyme adopt a "catalytically competent" conformation.[16] Accordingly, it is known that inactive PTP enzymes which are mutated on their catalytic cysteine (equivalent to Cys216 in PTPN2) may retain the ability to bind substrates.[14,19] In addition, protein tyrosine pseudophosphatases have been described.[15] These proteins are atypical PTPs that are catalytically inactive through mutations within their active site (notably the catalytic cysteine residue) and/or important domains required for catalysis.[22] These inactive PTPs maintain a classical 3D fold and the ability to bind phosphorylated proteins and have been suggested to act as signaling regulators.[15] Thermal shift assay experiments with a tyrosine-phosphorylated peptide substrate (SAAPYLKTK) derived from human STAT3 further supported that albeit inactive, C216G PTPN2 was able to bind substrates (Figure S1g). This suggests that C216G PTPN2 could function as tyrosine pseudophosphatase.

The most striking structural difference between WT PTPN2 and C216G mutant form is observed in the K122 loop (also known as E-loop) (Figure 2d: E117-R222 salt bridge panel and K122 loop panel; Figure S1c: K122 loop panel). In PTPs structures, the K122 loop (residues 116–123 in PTPN2) adopts a conformation that allows the conserved Glu119 residue to form a salt bridge with the side chain of the invariant catalytic residue Arg222 of the P-loop (Figure 2d: E117-R222 salt bridge panel). This ionic bond is observed in all classical PTPs structures and serves to stabilize the structure of the P-loop in a position that favors binding of the tyrosine phosphate to the P-loop.[16,17] The C216G PTPN2 structure shows that the conformation of the K122 loop adopts a conformation that allows the formation of the key Glu117-Arg222 salt bridge (Figure 2d: E117-R222 salt bridge panel). This is in sharp contrast with the conformation of the K122 loop in the WT PTPN2 form, where the Glu117 residue is at a distance of 13 Å of the Arg222 residue thus impairing the formation of the Glu117-Arg222 ionic bond (Figure 2d: E117-R222 salt bridge panel). Moreover, the overall conformation of the K122 loop in WT PTPN2 is significantly different from the one of C216G mutant with the side chains of Lys118, Lys122, and Glu119 moving more than 10 Å between the two PTPN2 structures (Figure 2d: K122

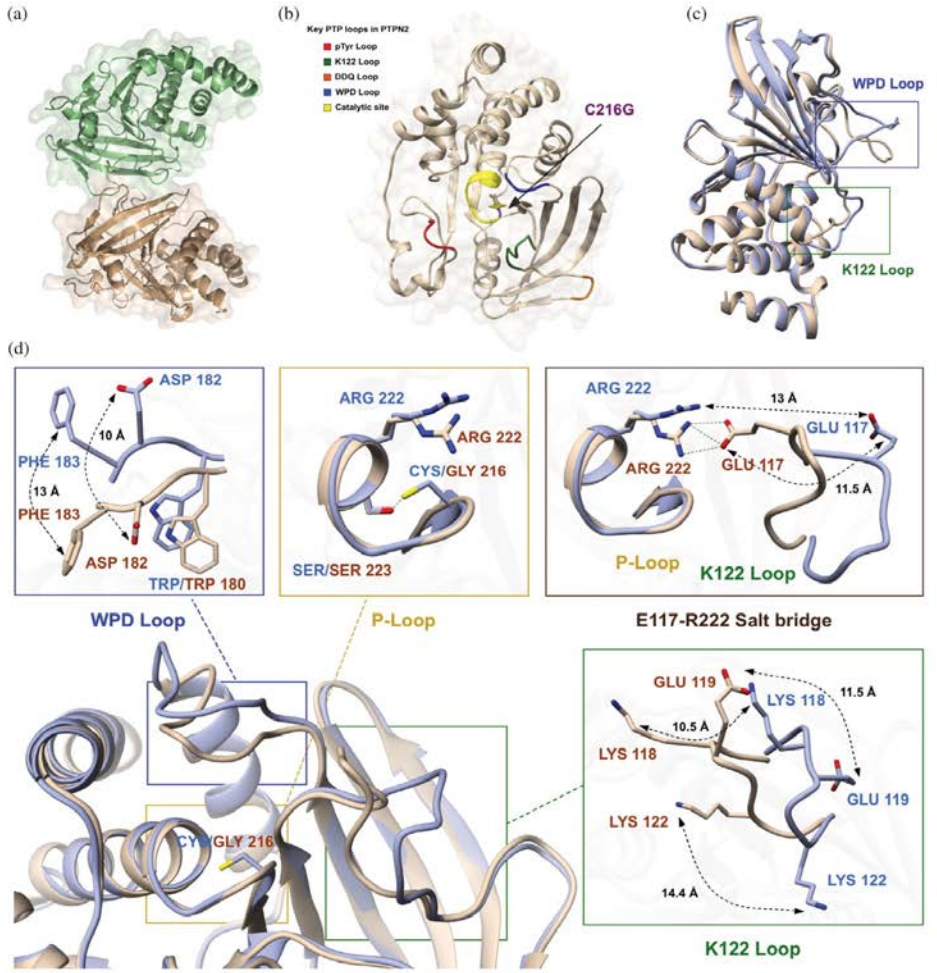

FIGURE 2 Overall structure and comparison of C216G PTPN2 and WT PTPN2. (a) Ribbon representation of the dimer of C216G PTPN2. Each monomer is represented with a different color. Protein surface is represented by transparency. (b) Ribbon representation of the Cα trace of C216G PTPN2. The positioning of each key domain of PTPN2 is displayed as follows: pTyr loop is shown in red, K122 loop in green, DDQ loop in orange, WPD loop in blue, and P-loop (catalytic site) in yellow. Location of the C216G mutation is shown with a purple arrow. Protein surface is represented by transparency. (c) Structural alignment of WT (blue) and C216G (beige) PTPN2 monomers. Regions of interest where differences are significant between the two structures are highlighted by boxes (K122 loop is displayed in green and WPD loop in blue). (d) Close-up view of the structural alignment between WT (blue) and C216G (beige) PTPN2. Each region of interest is zoomed in to have a more detailed view of the differences in the involved residues (P-loop [catalytic site] is shown in yellow, K122 loop in green, WPD loop in blue, and the interaction between the P-loop and the K122 loop is displayed in brown). Hydrogen bonds between Arg 222 and Glu 117 residues are depicted with green dashed lines. Distances between residues are represented with black double-heads dashed arrows. Residues are labeled in blue for WT PTPN2 and in brown for C216G mutant

loop panel). These significant differences of the structure of the K122 loop between the WT and mutant PTPN2 forms and the absence of the key Glu117-Arg222 salt bridge in WT PTPN2 are not because the two PTPN2 structures are in the closed (C216G PTPN2) or in the open form (WT PTPN2). Indeed, the conformation of the K122 loop in PTPs is not related to their closed or open state status.[16] This is further illustrated in Figure S1c (K122 loop panel) where the conformation of the K122 loop of C216G PTPN2 and PTP1B in its closed or open form are highly similar (with the side chains of the Glu117 and Lys122 of C216G PTPN2 and their PTP1B counterparts displaying positions), whereas the K122 loop of WT PTPN2 adopts a completely different conformation. As stated above, this unusual conformation of the K122 loop of WT PTPN2 compared to other PTPs (notably human PTP1B) could be due to crystallization artifacts that impacted the packing of the PTPN2 molecules in the crystal.[17]

In this work, we determined the first structure of an inactive mutant of PTPN2 (C216G PTPN2) which causes an intestinal autoimmune disorder.[12] We show that the overall structure of the C216G mutant is similar to WT PTPN2 structure and displays the characteristic PTP fold. More importantly, we found that, albeit inactive, the C216G PTPN2 mutant retains the ability to bind substrates and can adopt the characteristic catalytically competent PTP closed form.[16] This suggests that the C216G PTPN2 mutant could, at least partially, act as a pseudophosphatase.[22] Comparison of the C216G PTPN2 and WT PTPN2 structures also pointed out conformational differences in the K122 loop between the two forms of the enzyme that supports that the WT PTPN2 structure deposited in the PDB may not correspond (at least in part) to a biologically relevant structure of WT PTPN2.[17] While additional work will be needed to ascertain this point, we believe that this novel PTPN2 structure may help to understand the impact of pathogenic variants on PTPN2 conformation and may serve as a new tool for the study of PTP structures and design of specific ligands/inhibitors.

3 | MATERIALS AND METHODS

Detailed materials and methods can be found as supplementary material file.

ACKNOWLEDGMENTS

This work was supported by institutional grants from Université de Paris, Institut Pasteur and CNRS. Q. N. and R. L. were supported by a PhD fellowship from the China Scholarship Council (CSC). J. B. was supported by a PhD fellowship from Région Ile de France (Cancéropole). The authors thank the staff of the crystallography platform at Institut Pasteur for carrying out robot-driven crystallization screening. The authors acknowledge synchroton SOLEIL (Saint-Aubin, France) for granting access to their facility and the staff of Proxima1 for helpful assistance during the data collection. The authors also thank the technical platform "Bioprofiler" from the BFA Unit for provision of UFLC facilities.

CONFLICT OF INTEREST

The authors declare no potential conflict of interest.

AUTHOR CONTRIBUTIONS

Nadine Cerf-Bensussan, **Ahmed Haouz**, and **Fernando Rodrigues Lima**: Conceived the project. All authors performed experiments or/and analyzed the data. **Jérémy Berthelet** and **Fernando Rodrigues Lima**: Wrote the manuscript with input from all authors.

ORCID

Fernando Rodrigues Lima https://orcid.org/0000-0002-1081-4767

REFERENCES

1. Pike KA, Tremblay ML. TC-PTP and PTP1B: Regulating JAK-STAT signaling, controlling lymphoid malignancies. Cytokine. 2016;82:52–57.
2. Kleppe M, Lahortiga I, El Chaar T, et al. Deletion of the protein tyrosine phosphatase gene PTPN2 in T-cell acute lymphoblastic leukemia. Nat Genet. 2010;42:530–535.
3. Wiede F, Ziegler A, Zehn D, Tiganis T. PTPN2 restrains CD8+ T cell responses after antigen cross-presentation for the maintenance of peripheral tolerance in mice. J Autoimmun. 2014;53:105–114.
4. Grohmann M, Wiede F, Dodd GT, et al. Obesity drives STAT-1-dependent NASH and STAT-3-dependent HCC. Cell. 2018;175:1289–1306.
5. Svensson MND, Doody KM, Schmiedel BJ, et al. Reduced expression of phosphatase PTPN2 promotes pathogenic conversion of Tregs in autoimmunity. J Clin Invest. 2019;129:1193–1210.
6. You-Ten KE, Muise ES, Itié A, et al. Impaired bone marrow microenvironment and immune function in T cell protein tyrosine phosphatase-deficient mice. J Exp Med. 1997;186:683–693.
7. Heinonen KM, Bourdeau A, Doody KM, Tremblay ML. Protein tyrosine phosphatases PTP-1B and TC-PTP play nonredundant roles in macrophage development and IFN-γ signaling. Proc Natl Acad Sci U S A. 2009;106:9368–9372.
8. Manguso RT, Pope HW, Zimmer MD, et al. In vivo CRISPR screening identifies Ptpn2 as a cancer immunotherapy target. Nature. 2017;547:413–418.
9. LaFleur MW, Nguyen TH, Coxe MA, et al. PTPN2 regulates the generation of exhausted CD8+ T cell subpopulations and restrains tumor immunity. Nat Immunol. 2019;20:1335–1347.

10. Wei J, Long L, Zheng W, et al. Targeting REGNASE-1 programs long-lived effector T cells for cancer therapy. Nature. 2019;576:471–476.
11. Wiede F, Lu K, Du X, et al. PTPN 2 phosphatase deletion in T cells promotes anti-tumour immunity and CAR T-cell efficacy in solid tumours. EMBO J. 2020;39:e103637.
12. Parlato M, Nian Q, Charbit-Henrion F, et al. Loss-of-function mutation in PTPN2 causes aberrant activation of JAK signaling via STAT and very early onset intestinal inflammation. Gastroenterology. 2020;159:1968–1971.
13. Flint AJ, Tiganis T, Barford D, Tonks NK. Development of "substrate-trapping" mutants to identify physiological substrates of protein tyrosine phosphatases. Proc Natl Acad Sci U S A. 1997;94:1680–1685.
14. Blanchetot C, Chagnon M, Dubé N, Hallé M, Tremblay ML. Substrate-trapping techniques in the identification of cellular PTP targets. Methods. 2005;35:44–53.
15. Reiterer V, Pawłowski K, Desrochers G, Pause A, Sharpe HJ, Farhan H. The dead phosphatases society: A review of the emerging roles of pseudophosphatases. FEBS J. 2020;287:4198–4220.
16. Tautz L, Critton DA, Grotegut S. Protein tyrosine phosphatases: Structure, function, and implication in human disease. Methods Mol Biol. 2013;1053:179–221.
17. Iversen LF, Møller KB, Pedersen AK, et al. Structure determination of T cell protein-tyrosine phosphatase. J Biol Chem. 2002;277:19982–19990.
18. Stuckey JA, Schubert HL, Fauman EB, Zhang ZY, Dixon JE, Saper MA. Crystal structure of Yersinia protein tyrosine phosphatase at 2.5 Å and the complex with tungstate. Nature. 1994;370:571–575.
19. Jia Z, Barford D, Flint AJ, Tonks NK. Structural basis for phosphotyrosine peptide recognition by protein tyrosine phosphatase 1B. Science. 1995;268:1754–1758.
20. Almo SC, Bonanno JB, Sauder JM, et al. Structural genomics of protein phosphatases. J Struct Funct Genomics. 2007;8:121–140.
21. Tabernero L, Aricescu AR, Jones EY, Szedlacsek SE. Protein tyrosine phosphatases: Structure-function relationships. FEBS J. 2008;275:867–882.
22. Mattei AM, Smailys JD, Hepworth EMW, Hinton SD. The roles of pseudophosphatases in disease. Int J Mol Sci. 2021;22:6924.

SUPPORTING INFORMATION

Additional supporting information may be found in the online version of the article at the publisher's website.

How to cite this article: Nian Q, Berthelet J, Parlato M, Mechaly AE, Liu R, Dupret J-M, et al. Structural characterization of a pathogenic mutant of human protein tyrosine phosphatase PTPN2 (Cys216Gly) that causes very early onset autoimmune enteropathy. Protein Science. 2021; 1–7. https://doi.org/10.1002/pro.4246